
بسم الله الرحمن الرحيم

"THE INVESTIGATION OF CITRULLINATED PROTEIN, B-CELLS AND THEIR SURVIVAL NICHES IN ATHEROSCLEROSIS WITH COEXISTING RHEUMATOID ARTHRITIS"

Ammad Ahmed

Thesis submitted to the University of Glasgow for the degree of

Doctor of Philosophy

The research programme was carried out at Glasgow University
Division of Immunology, Infection and Inflammation

Faculty of Medicine
University of Glasgow
May, 2010

Dedication

This thesis is dedicated to the living memory of my father Fazal Manan may Almighty ALLAH bless him.

Abstract

Rheumatoid arthritis (RA) is an autoimmune disease that primarily affects the joints and is characterized by bone and cartilage erosion. These patients have an increased risk of developing co-morbid cardiovascular disease (CVD). In this study the vascular adventitia from patients with coexisting RA and CVD was investigated to identify factors in the vascular environment that could affect the immune component of RA. This included the histological evaluation of aortic adventitial sections for known RA-associated autoantigens; B cells their survival factors and associated cytokines. In addition, these human studies were the impetus for the initiation of a study to investigate the effect of B cell depletion on atherosclerosis.

Citrullinated proteins (CP), RA associated antigens, are an inflammation specific entity. These modified proteins are processed by (PADI), a calcium dependent enzyme expressed by inflammatory cells and some microbial species. The presence of RA specific autoantibodies (ACPA) suggests a role for citrullinated proteins in RA pathogenesis. The aim of the present study was to determine whether the inflammatory milieu in the vascular adventitia of RA patients had any association with CP. The expression of CP was confirmed in the vascular adventitia, and CVD patients with coexisting RA were found to have increased levels of CP compared to non-RA CVD patients. In addition, ACPA levels were detectable in serum samples of only RA patients. When ACPA positive RA patients were sub grouped (CP>5.5), a strong association was observed between ACPA levels and C-reactive protein (CRP) in this subgroup (CP>5.5). This is suggestive of a CP and ACPA link in vascular inflammation in patients with coexisting RA.

The presence of B-lymphocytes has been shown in both murine and human vascular adventitia. In this study we demonstrated that the presence of B cell aggregates is tissue specific, since matched internal mammary artery (IMA) had no detectable B cells in the adventitia. Furthermore, BAFF and APRIL are present in the aortic adventitia and support the conclusion that a survival niche is present in the aortic adventitia; cytokine expression was demonstrated in

lymphocytes, adipocytes and vascular endothelial cells. Interestingly, smoking resulted in higher levels of BAFF expression in the aortic adventitia of CVD patients. Previous studies have shown that smoking induces vasoconstriction of small vessels (vasa vasorum), and hence hypoxia of the vascular endothelial cells. We hypothesised that hypoxia would induce the increased expression of BAFF and APRIL in vascular endothelial cells. Using murine vascular endothelial cells we investigated the effect of hypoxia on BAFF and APRIL mRNA transcript levels. However, hypoxia did not have any effect on transcript levels. In addition, significant correlations were observed in RA patients only, between B cells and APRIL, B cells and CP, APRIL and CP. This part of my thesis demonstrates that the aortic adventitia of RA patients with coronary heart disease is associated with an environment that is conducive to B cell survival and harbours a known RA-associated self-antigen. Importantly, these insights provide a rationale for the perpetuation of B cell auto-reactivity outside of both lymphoid tissue and the joint in RA.

Previous studies have shown that atherosclerosis is a T cell mediated disease with an imbalance in Th1 and Th2 responses. Macrophages and interleukin 18 (IL-18, proatherogenic) cytokine have been demonstrated in aortic adventitia of humans in previous studies. However, their expression in the vascular adventitia of RA patients has not been investigated. The present study confirmed macrophage IL-18 expression in vascular adventitia, which is similar among the Subgroups (RA vs. non RA) and (smokers vs. non smokers).
Furthermore, a Th2 phenotype has been proposed as atheroprotective, mediated by anti oxLDL antibody producing B cells. Interestingly, recent studies have demonstrated interleukin 33 (IL-33) a Th2 cytokine to reduce the atherosclerotic lesion in an experimental model of atherosclerosis. However, it's expression and significance in human vessels has not been extensively investigated. In this study, using immunohistochemistry, IL-33 was localised to vascular endothelial cells of vasa vasorum in aortic adventitia and lining layer of IMA. Importantly, IL-33 was down regulated in smoker's AA suggestive of failed protective mechanism of this Th2 cytokine. In contrast, IL-33 expression was not affected by smoking in the matched IMA tissue.

In the past B-lymphocytes have been shown as an atheroprotective pathway; whereas the use of B cells depletion therapy (Rituximab) suggests a proinflammatory role of these cells in RA. Could B cell depletion therefore mediate unexpected deficit on vascular lesions in RA? My thesis revealed expression of B cells and their survival factors in the aortic adventitia. Therefore to investigate the impact of B cell depletion therapy on atherosclerosis, a mouse model (huCD20/ApoE$^{-/-}$) was generated. The preliminary data are suggestive of reduction in atherosclerotic plaques with B cells depletion. These studies will be extended in future to formally test the above hypothesis.

In summary I have shown for the first time the cytokine and cellular niche that exists in human aorta in RA patients. Such data will in due course inform the mechanism of accelerated vascular pathogenesis in RA.

Acknowledgements

I thank all of you who have made last three years of my PhD an enjoyable and exciting journey.

First of all, I would like to thank Prof. Iain B McInnes, for giving me this opportunity and whose continued support, guidance and willingness to allow me independence have been invaluable. He helped me to believe in my self and in possibilities to reach my goals. I would like to express my sincere gratitude to Dr Carl Goodyear whose enthusiasm, research skills and positive attitude are outstanding. I have not only learned material facts, but also focus and organisation. Together, their supervision has provided an ideal intellectual environment to learn science for which I will always be grateful and their enthusiasm and encouragement have persisted and sustained me over the last three years. I am thankful to Dr Lindsay Maclellan for her encouragement, advice and assistance with the animal model. I am grateful to Fujimi Sugiyama whose patience; generosity and friendship have been most valuable.

The staff in the Dept. of immunology, university of Glasgow the Centre for Rheumatic Disease, deserve my thanks for their patience and support as I have slowly acquired the practical art of laboratory science. In particular James. H Reilly, who was kind and generous in providing invaluable assistance for immunohistology. I also thank Susan Kitson for help and support and for performing ACPA (ELISA). I would like to thank Dr Ivana Hollan (The feiring heart clinic, Norway) for providing precious tissue samples. I thank all the patients who generously donated samples.

I thank all friends, especially Alistair Eston, Mousa komai-koma ,Denngao yao, Derek Gilchrist for their encouragement and help.

My parents have for many years offered me every opportunity in pursuit of education. I thank all my family members for their love and support especially, Chachagul, Mahgul ammi, Trorbibi, Aghaamu Chandamu, Nazaunty, Nanokhala, Danyal, Haroon, Sani, Rabia, Saima, faisal, Mariam and Azra. Most important has

been blessings, encouragement, patience, enthusiasm and love of my mother, without whom, it would not have been written.

Table of Contents

Dedication iii
Abstract iv
Acknowledgements vii
Table of Contents ix
List of Tables xiii
List of Figures xiv
Author's declaration xvi
List of Abbreviations xvii
1 Introduction 1
1.1 Rheumatoid Arthritis 1
1.1.1 Aetiology and Pathogenesis 2
1.1.2 Joint inflammation 2
1.1.3 Disease progression and Treatment 8
1.1.3.1 Treatment 8
1.2 B lymphocytes in RA 9
1.2.1 Murine B lymphocytes 10
1.2.2 Factors affecting B cell differentiation and survival 13
1.2.2.1 B cell activation factor 13
1.2.2.2 A Proliferation inducing ligand (APRIL) 14
1.3 Rheumatoid Arthritis and vascular risk 17
1.3.1 Atherosclerosis (a priori) 18
1.3.1.1 Structure of a normal Blood vessel 19
1.3.2 The inside out phenomenon 20
1.3.3 The outside in phenomenon 21
1.3.4 Inflammation in Atherosclerosis 22
1.3.5 Oxidized LDL triggers an inflammatory response 23
1.3.6 Monocyte recruitment to Macrophage activation 23
1.3.7 B-lymphocyte “A good guy” in Atherosclerosis? 24
1.3.7.1 Lamina adventitia and B cells in vascular inflammation 24
1.3.8 Different T cell subsets in Atherosclerosis 25
1.3.8.1 CD4+ T Lymphocytes 25
1.3.9 Mast cells in atherosclerosis 27
1.4 Interleukin-1 (IL-1) superfamily cytokines in RA and Atherosclerosis 27
1.4.1 Interleukin 18 (IL-18) 28
1.4.2 Interleukin 33 (IL-33) 29
1.1.1.1 IL-33 in RA 31
1.1.1.2 IL-33 in CVD 31
1.2 Hypothesis and Aims 33
2 Methods and Material 35
2.1 Human Biopsy samples 36
2.1.1 Immunohistochemistry 36
2.1.1.1 Deparaffination and hydration 37
2.1.1.2 Antigen Retrieval 37
2.1.1.3 Non specific binding block 38

2.1.1.4 Secondary antibody and mounting of section 38
2.1.1.5 Additional steps performed for Pan specific Biotinylated secondary antibody 38
2.1.1.6 Sequence of major staining steps for all the stainings 39
2.1.2 Preparation of Modified fibrinogen 43
2.1.2.1 Biotinylation of native and modified fibrinogen 43
2.1.2.2 Preparation of "a citrulline rich sample" cornified skin cell lysates 44
2.1.3 Western Blotting 44
2.1.3.1 Sample preparation 44
2.1.3.2 Electrophoresis 44
2.1.3.3 Coomassie staining 45
2.1.3.4 Transfer of Proteins to PVDF membrane 45
2.1.3.5 Immunostaining for proteins 45
2.1.4 Double Fluorescent staining of RA synovium and Aortic adventitia 46
2.1.5 Scoring and statistical analysis 47
2.1.5.1 Scoring of stained tissues 47
2.1.5.2 Statistical analysis 48
2.2 Effects of Oxidized LDL on cultured cells 48
2.2.1 Human endothelial cell culture 48
2.2.2 Murine endothelial cell culture 49
2.2.2.1 Murine cell culture in T-25 flasks 49
2.3 Polymerase chain reaction (PCR) 49
2.3.1 RNA isolation 49
2.3.2 First strand cDNA synthesis 50
2.3.3 PCR 50
2.3.4 Quantitative PCR 51
2.3.4.1 Normalisation of cDNA samples 51
2.3.4.2 Primer Design 51
2.3.4.3 Generation of DNA standards for QPCR 52
2.3.4.4 SYBR QPCR protocol 53
2.3.4.5 Analysis of QPCR data and stats 54
2.4 Lipoprotein isolation and oxidative modification 54
2.4.1 Modified Lowry protein assay 55
2.4.2 Lipoprotein (Lipo) Electrophoresis 55
2.5 Animal study 56
2.5.1 Mouse Model 56
2.5.2 Mouse Genotyping 56
2.5.2.1 Mouse tail sample preparation 56
2.5.2.2 PCR reaction conditions for genotyping 56
2.5.3 Flow cytometric analysis of mouse blood samples 57
2.5.3.1 Blood sampling 57

2.5.3.2 PBMC staining 58
2.5.4 High-fat diet and B cell depletion 58
2.5.4.1 B cell depletion in huCD20^{+}/ApoE$^{-/-}$ mice 59
2.5.4.2 Animal euthanasia 59
2.5.4.3 Mouse dissection 59
2.5.4.4 Mouse tissue harvesting 60
2.5.4.5 Spleen 60
2.5.4.6 Lymph nodes 61
2.5.4.7 Bone marrow 61
2.5.4.8 Heart and aorta 62
3 The cellular composition of human aortic adventitia from coronary bypass patients with rheumatoid arthritis 65
3.1 Introduction 66
3.2 Results 70
3.2.1 Patients characteristics 70
3.2.2 Citrullinated proteins are increased in the aortic adventitia of patients with rheumatoid arthritis 71
3.2.2.1 CP staining established in RA synovium 71
3.2.3 B lymphocytes are present in the aortic adventitia from patients with CVD 75
3.2.4 B-cell aggregates in rheumatoid arthritis patients with advanced atherosclerosis 78
3.2.5 Detection of plasma cells in the aortic adventitia of patients with advanced cardiovascular disease. 78
3.2.6 Generation of citrullinated fibrinogen 80
3.2.7 Reactivity of modified fibrinogen confirmed with sera from RA patients 81
3.2.8 Plasma cells secreting antibodies to citrullinated protein in RA synovium 82
3.2.9 ACPA and CP together affect the cardiovascular outcome of RA patients 84
3.2.10 Dominant B-lymphocyte survival factor (BAFF) expression in the smokers aortic adventitia 87
3.2.11 A proliferation inducing ligand (APRIL) specific to aortic adventitia from CVD patients 89
3.3 Adventitial B-cells correlate with citrullinated protein and APRIL in patients with rheumatoid arthritis 91
3.3.1 Macrophages in aorta of patients with advanced atherosclerotic lesions 92
3.3.2 Interleukin 18 a proatherogenic cytokine of IL-1 family 95
3.3.3 BAFF and APRIL expressed by mouse vascular endothelial cell line (SVEC4-10) 97
3.4 Discussion 102
4 IL-33 in Vascular Biology 105
4.1 Introduction 106
4.2 Aims 108
4.3 Results 109
4.3.1 IL-33 expressed by vascular endothelial cells of AA and IMA 109

4.3.1.1 IL-33 is down regulated in aortic adventitia of smokers 111
4.3.2 IL-33/sST2 mRNA transcript under oxLDL and Hypoxic conditions . 114
4.3.2.1 Lipoprotein isolation and oxidative modification 117
4.3.2.2 The effect of ox-LDL on the level of IL-33 transcript in SVEC4-10 118
4.3.2.3 Synchronized SVEC4-10 and IL-33/sST2 mRNA 120
4.3.2.4 Confluence of cultured cells and IL-33 expression 121
4.3.2.5 Validation of generated lipoproteins 123
4.3.2.6 Hypoxia and IL-33/sST2 124
4.4 Discussion 129
5 The impact of B cell depletion therapy on Atherosclerosis 131
5.1 Introduction 132
5.1.1 Aims of the study 134
5.2 Result 135
5.2.1 Model system and plan of the study 135
5.2.2 Generating huCD20^{+}/ApoE$^{-/-}$ mice 135
5.2.3 Four huCD20^{+}/ApoE$^{-/-}$ mice on high fat diet 137
5.2.3.1 Monitoring of body weight 138
5.2.3.2 Circulating B lymphocytes and rituximab 139
5.2.3.3 Effects of B cell directed therapy on lymphocytes of spleen and lymph nodes 144
5.2.3.4 Effects of rituximab on B cell subsets in spleen 146
5.2.3.5 Analysis of Aortic lesions 149
5.3 Discussion 154
6 General Discussion 156
References 163
Appendix 186

List of Tables

Table 1.1. ACR criteria for rheumatoid arthritis 2
Table 1.2. Human isozymes of Peptidyl arginine deiminases 6
Table 1.3. Role of B cells in the regulation of immune responses 10
Table 2.1. Details of antibodies and antigen retrieval system used in staining of human biopsy samples.....36
Table 2.2. Sequence of major steps performed for all the different stainings. ..39
Table 3.1. Characteristics of patients in the group.....70
Table 3.2. Details of patients positive for plasma cells.....84

List of Figures

Figure 1.1 A possible Etiological model for ACPA positive subset of RA 8
Figure 1.2 Illustration of functions and receptors of BAFF and APRIL 15
Figure 1.3 The focal intimal thickening of a blood. 20
Figure 1.4 The development of atherogenesis beginning at the adventitial layer 22
Figure 1.5 A model for IL-33/ST2 signalling T1/ST2 Receptor 30
Figure 2.1 A guide to sectioning the heart for cross sectional analysis 64
Figure 3.1 CP staining using different antigen retrieval systems 72
Figure 3.2 Citrulline staining in aortic adventitia 73
Figure 3.3 Scores for CP staining in aortic adventitia and IMA. 74
Figure 3.4 CP in aortic adventitia of smokers and non-smokers 75
Figure 3.5 CD20 staining in aortic adventitia. 76
Figure 3.6 B cell presence limited to aortic adventitia 77
Figure 3.7 Scores for CD20 staining in aortic adventitia and IMA. 78
Figure 3.8 Plasma cell staining in RA synovium 79
Figure 3.9 Coomassie staining for citrullinated fibrinogen 81
Figure 3.10 Western blot analysis for citrullinated proteins 82
Figure 3.11 Plasma cell secreting antibodies to citrullinated fibrinogen 84
Figure 3.12 ACPA and CRP in RA patients 86
Figure 3.13 BAFF staining in human aortic adventitia 88
Figure 3.14 BAFF staining score in human aorta and IMA 89
Figure 3.15 APRIL staining in aortic adventitia 90
Figure 3.16 APRIL staining scores in human samples 91
Figure 3.17 Associations observed in RA patients between citrullinated proteins B cells and APRIL. 92
Figure 3.18 Macrophage staining in aortic adventitia 93
Figure 3.19 Macrophages in aortic adventitia 94
Figure 3.20 IL-18 staining in aortic adventitia 96
Figure 3.21 IL-18 staining scores in aortic adventitia and IMA 97
Figure 3.22 BAFF and APRIL expression 98
Figure 3.23 Mouse APRIL QPCR 100
Figure 3.24 Quantitative analysis of APRIL expression in vascular endothelial cells 101
Figure 4.1 IL-33 expressed by vasa vasorum of aortic adventitia 110
Figure 4.2 IL-33 expressed by vascular endothelial cells of IMA. 111
Figure 4.3 IL-33 expressions reduced in smokers AA 112
Figure 4.4 IL-33 expressions in Aortic adventitia and IMA 113
Figure 4.5 IL-33 expressions in RA and non-RA patients 114
Figure 4.6 PCR for IL-33 and sST2 in vascular endothelial cell line (SVEC4-10) 115
Figure 4.7 QPCR for IL-33 and house keeping gene (GAPDH) 116
Figure 4.8 Modified Lowry assay 117
Figure 4.9 QPCR analysis of IL-33 expression in mouse endothelial cell line (SVEC4-10). 118
Figure 4.10 IL-33 expression at earlier time points (6hr, 12hr, 24hr) 119
Figure 4.11 A) IL-33 mRNA expression at 6hr, 12hr and 24hr time point 120
Figure 4.12 IL-33 mRNA expression in synchronized mouse vascular endothelial cells 121
Figure 4.13 IL-33 mRNA upregulated with confluence 122
Figure 4.14 Gel electrophoresis for lipoproteins 123

Figure 4.15 Gel electrophoresis for lipoproteins 124
Figure 4.16 QPCR for IL-33 & sST2 gene expression under hypoxia 125
Figure 4.17 Hypoxia upregulates expression of house keeping gene GAPDH 126
Figure 4.18 IL-33 transcript levels, hypoxia and house keeping genes. 127
Figure 4.19 Fully confluent SVEC4-10 under hypoxia 128
Figure 5.1 Confirmation of $hCD20^{+}/ApoE^{-/-}$ mice 136
Figure 5.2 Model system planed for the study 137
Figure 5.3 Body weight chart 139
Figure 5.4 Circulating $huCD20^{+}$ cell at first week 140
Figure 5.5 Circulating B cells ($huCD20^{+}$) a week after the systemic treatment 141
Figure 5.6 B cells ($huCD20^{+}$) depletion one week before second treatment 142
Figure 5.7 B cells ($huCD20^{+}$) depletion one week after second treatment 143
Figure 5.8 Trend of Circulating B cells ($huCD20^{+}$) during the course of study .. 144
Figure 5.9 Depletion therapy and lymphocytes in spleen and lymph nodes..... 145
Figure 5.10 Marginal zone (MZ), follicular (Fo) and transitional type 2 (T2) B cells 147
Figure 5.11 B cells subsets in spleen and lymph nodes 148
Figure 5.12 B1a cells in spleen and lymph nodes 149
Figure 5.13 Schematic for dissection of mouse heart and aorta 150
Figure 5.14 Aortic lesions in $huCD20^{+}/ApoE^{-/-}$ mice 151
Figure 5.15 Atherosclerotic lesion areas in rituximab and IgG treated $CD20^{+}/ApoE^{-/-}$ mice 152
Figure 5.16 Percentage area of Aortic lesion in ($huCD20^{+}/ApoE^{-/-}$) mice 153

Author's declaration

I declare that the work presented in this thesis is my own unless specifically stated otherwise.

Ammad Ahmed

List of Abbreviations

AA	Aortic adventitia
ACR	American College of Rheumatology
ACPA	Anti citrullinated peptide antibody
$ApoE^{-/-}$	Apolipoprotein E knock out mice
APRIL	A proliferation inducing ligand
BAC	Bacterial artificial region
BCLL	B cell chronic lymphoid leukaemia
BCMA	B cell maturation antigen
BAFF	B cell activation factor
CIA	Collagen-Induced Arthritis
$CuSo_4$	Copper sulphate
CVD	Cardiovascular disease
CRP	C-reactive protein
DM	Diabetes Mellitus
DAS	Disease activity score
EDTA	Ethylene diamine tetracetic acid
ECs	Endothelial cells
FCM	Flow cytometric analysis
FACS	Fluorescent Activated Cell Sorter
HMGB-1	High Mobility Group Box chromosomal protein 1
$huCD20^{+}$	Human CD20 receptor positive transgenic mice
ICAM-1	Intercellular adhesion molecule 1
IL-1 RAcP	Interleukin 1 receptor accessory protein
IL 33	Interleukin 33
IL-18	Interleukin 18
IFNγ	Interferon gamma
IgG	Immunoglobulin G
IHD	Ischemic heart disease
IV	Intravenous
LSC	Laser scanning microscope
MEM	Minimum essential Medium Eagle
MES	2-(N-morpholino)ethanesulfonic acid

M	Molar
mM	millimolar
mg	milligram
ml	millilitre
nLDL	native LDL
ng	nanogram
nM	nanomolar
NTC	No template control
oxLDL	Oxidized Low density lipoproteins
PBMCs	Peripheral Blood Mononuclear Cells
PBS	Phosphate buffered Saline
PCR	Polymerase chain reaction
PE	Phycoerythrin
pg	picogram
PPRs	Pattern recognition receptors
PVDF	polyvinylidene difluoride
QDOT	Quantum dot
RA	Rheumatoid Arthritis
RBC	Red blood cells
RT PCR	Reverse transcription Polymerase chain reaction
RPMI	A cell culture medium produced at “Roswell Park Memorial Institute”
RPM	Revolution per minute
SDS	Sodium dodecyl sulphate
SRs	Scavenger receptors
SVEC4-10	Mouse lymphoid endothelial cell line Immortalized by simian virus 40
SCID	Severe combined immunodeficiency
SMCs	Smooth muscle cells
TACI	Transmembrane activator and cyclophilin ligand interactor
TGFβ	Transforming growth factor Beta
Th1	T helper lymphocyte type 1
Th2	T helper lymphocyte type 2
TNFα	Tumor necrosis factor alpha
TLRs	Toll like receptors

UTR	Untraslated region
μg	microgram
μl	microlitre
μm	micrometer
μM	micromolar
VCAM1	Vascular cell adhesion molecule 1

1 Introduction

1.1 Rheumatoid Arthritis

Rheumatoid arthritis (RA) is a chronic progressive systemic autoimmune disease, which is characterized by joint destruction. It affects 1% of the adult population and women have a three times greater risk of developing disease compared to men. People of any age group can be affected but most frequently the onset of the disease is between the age of 40-50 year [1].

In 1859 Garrod was the first to define Rheumatoid Arthritis (RA) as a disease and since then it has been recognised as a painful and disabling condition, which can lead to extensive compromise of function and mobility. The American Rheumatism Association set an initial criterion collection for clinically defining this disease, which have been a useful tool in the clinical diagnosis of disease and the selection of patients for the clinical trials [2]. However, even with defined criteria for the diagnosis of RA in patients (Table 1)[2] this is inadequate for the early diagnosis of patients, given that at least two of the seven criteria (nodules and erosions) are not present in the early stages of disease. One of the classical diagnostic criteria for RA is rheumatoid factor (RF), an autoantibody with specificity for the Fc region of immunoglobulin (IgG). However, the specificity of RF was argued and reported to be the result of secondary immune response during immune complex formation [3]. Importantly, experimental studies have failed to attribute a pathogenic role to RF in rheumatoid arthritis. Even with its undefined role in RA pathogenesis, the diagnostic utility of RF, in conjunction with the other criteria, is indisputable. Recently new criteria have been generated by a combined ACR / EULAR initiative. Although not yet generally available for publication in this thesis they will allow early attribution of the diagnosis of RA and in the long term improved outcomes as clinical alogrithms evolve.

Table 1.1. ACR criteria for rheumatoid arthritis

A patient is said to have rheumatoid arthritis if he or she meets at least four criteria.
1. Morning stiffness lasting at least 1 hr, present for at least 6 weeks
2. A least three joint areas simultaneously with soft-tissue swelling or fluid for at least 6 weeks
3. At least one area swollen in a wrist, metacarpophalangeal or proximal interphalangeal joint, for at least 6 weeks
4. Simultaneous involvement of the same joint areas on both sides of the body, for at least 6 weeks
5. Subcutaneous nodules seen by a doctor
6. Positive rheumatoid factor
7. Radiographic changes on hand and wrist radiographs (erosions or unequivocal bony decalcification)

1.1.1 Aetiology and Pathogenesis

1.1.2 Joint inflammation

The main feature of RA is joint damage, which is seen as a result of bone and cartilage erosion. The chronic progress in joint inflammation results in narrowing of joint spaces and severe deformity, which is associated with swelling, pain and loss of function.

The precise mechanism of RA is not clear, however, during the past three decades many susceptibility genes have been identified. Including the major

histocompatibility complex class II (MHC II), which is strongly associated with RA [4, 5]. More specifically, the HLA DRB1 shared epitope alleles (SE) were identified as a major genetic risk factor for RA, and a rationale for MHC class II mediated activation of T cell was put forward [6]. Around 80% of RA patients express DR4 and DR1, which share an epitope mapping to amino acids 70-74 (QKRAA) of the DRβ chain [6]. Many other gene associations have also been identified including for example PTPN22, C-type lectin and interferon regulatory factor-5 (IRF-5) [7-9]. Over the years epidemiological studies have highlighted a strong association between smoking and RA. Initially, smoking was not considered as an etiological factor in the pathogenesis of RA. However, a fascinating interaction was confirmed in RA patients between the shared epitope HLA-DRB1 and smoking [10, 11].

Although we do not conclusively know the initiating events that lead to chronic disease, studies have demonstrated that joint damage is a result of chronic inflammation of the synovial membrane. The synovial membrane becomes hyperplastic with cellular infiltrates, which include macrophages, mast cells, $CD4^+$ T cells, $CD8^+$ T cells, B cells, plasma cells, natural killer (NK) cells and NKT cells. Synovitis is associated with extensive cellular infiltrates - pathogenesis of disease is thought to driven by antigen specific responses. This can be partly thought to be due to antigen presenting cells (APC) interacting with T cells through their MHC and T cell receptor (TCR) receptor respectively. This results not only in T cell activation, via co-stimulatory signals mediated through CD80/86 or CD28-B.7 receptor [12], but also in the activation of the APC. In response to activation, T cells and APC (macrophages or dendritic cells, or potentially B cells) produce pro-inflammatory cytokines, such as TNFα, interleukin 6 (IL-6), IL-12, IL-23 and interleukin 1 (IL-1) [13-15]. This cytokine environment can promote the differentiation of naïve T cells to alternative phenotypes such as T helper 1 and Th 17, an IL-6 dependent T cell phenotype that produces amongst other things IL-17. Cytokines are implicated at every stage of RA pathogenesis from maintaining a chronic inflammatory synovitis to promoting articular destruction, through the subsequent activation of osteoclasts, chondrocytes and synovial fibroblasts [16]. In addition, to the

initiating autoimmunity it has also been proposed that chronic inflammation and articular damage can lead to the generation of neo-epitopes that promote further autoimmune responses. Finally, it should also be appreciated that inflamed joints are associated with a hypoxic environment, which supports angiogenesis [17].

Serological markers in RA

Rheumatoid factor (RF) has been widely used as a serological marker for the diagnosis of rheumatoid arthritis and is currently the only serological marker included in the ACR criteria, however, its specificity is limited as it can also be found in other diseases. More recently, an important addition in the clinician's diagnostic arsenal has emerged in the form of a new serological marker, anti-citrullinated peptide antibodies (ACPA). These antibodies are specific for citrullinated proteins, which will be discussed in detail (Section 1.1.2.1). ACPA are now recognised as a more specific diagnostic tool for RA patients and will be included in new EULAR / ACR criteria [18]. The sensitivity of ACPA is similar to RF ranging from 55% to 80%, however, ACPA are highly specific for RA (98%) [19]. They are also detectable in the early stage of the disease. The presence of these highly specific ACPA in 55-80% of patients does suggest that there are two distinct subsets of RA, an ACPA positive and an ACPA negative subset. Genetic associations in RA patients further support this RA sub-setting. The PTPN22 gene has a strong association with the ACPA positive RA patients [8], while other genes such as C-type lectin [7] and Interferon regulatory factor 5 (IRF-5) are exclusively associated with ACPA negative RA patients [9].

The presence of ACPA is strongly associated with the shared epitope gene HLADRB 1 within the major histocompatibility complex (MHC) in RA pathogenesis . This association between ACPA and HLADRB1 is true for 60% of RA patients; whereas, the remaining patients of the ACPA negative subset completely lack this genetic association [10 20-22]. It is established that smoking is a risk factor for ACPA positive subset of RA and no link existed between smoking and ACPA negative subset. In humans, a comparison of citrullinated protein in broncho-alveolar lavage (BLA) cells between smokers and non smokers revealed dominance of citrullinated protein among smokers [10].

Immunity to citrullinated Protein in RA

In the early 1960's it was demonstrated that RA serum contained an anti-perinuclear factor; by the end of the 1970's this reactivity was shown to be against keratin. This was further defined in the late 1990's by Schellekens et al who demonstrated that the actual reactivity of these autoantibodies was directed against self-proteins with citrullinated epitopes. Since then a number of proteins have been proposed as potential targets of ACPA. RA synovium harbours citrullinated fibrin as a target of anti-filaggrin auto-antibodies (AFA) [23] while, vimentin [24], collagen [25], Epstein-Barr virus nuclear antigen 1 [26] and alpha enolase [27] were also introduced as potential targets of the anti-citrulline antibodies.

Citrulline a product of deimination

Citrulline (cit) is an amino acid that can be formed as a result of a posttranslational modification, the deimination of the amino acid arginine (arg). This conversion of arginine to citrulline is performed by one of the five known enzymes in humans designated as peptidyl arginine deiminases (PADIs) [28, 29]. The isoenzymes of PADI listed in (Table 1.2) are all calcium dependent and tissue specific. The physiological role of these isozymes is unclear and still needs to be addressed. Cytoskeletal proteins reported to undergo citrullination include cytokeratin (intermediate filament in keratinocytes), filaggrin, vimentin, glial fibrillary acidic protein (specific to astrocytes), myelin basic protein (produced by oligodendrocytes), and histones [30]. Peptidyl arginine deiminase also catalyzes deimination of arginine under inflammatory conditions, as was demonstrated in the lining and sublining layer of RA synovium [31]. Other tissues have been shown to contain citrullinated proteins including; Stratum corneum of human epidermis [32], the deep cornified layer of human epidermis (citrullinated keratin, more specifically filaggirin) [33] and glial cells in the brain [34, 35]. Although, citrullinated proteins are found in different tissues constitutively, their functional significance is unclear. Perhaps, posttranslational modification of peptidylarginine a positively charged form to a neutral peptidylcitrulline makes

proteins vulnerable to proteolytic degradation, due to changes in the primary, secondary and tertiary structure of proteins [30]. Nevertheless, it cannot be assumed that citrullination is designated for physiological denaturation.

Peptidylarginine deiminases:

	PADI isozymes	**Expressed in Tissues**
1	PADI1	Epidermis
2	PADI2	Skeletal muscle, spleen, brain, secretory glands
3	PADI3	Hair follicle
4	PADI4	Neutrophils, Eosinophils, T cells, B-cells, FLS and endothelial cells.
5	PADI6	Eggs ovaries and embryos

Table 1.2. Human isozymes of Peptidyl arginine deiminases

There are factors that regulate these deiminases. For instance, the epidermal isozyme has been shown to be highly calcium dependent with special preference to specific pH in vitro [36]. The activation of these isozymes is optimal under high calcium concentrations. Interestingly, in physiological conditions calcium concentrations are low and these isozymes remain inactive. Takahara et al demonstrated that the PADI2 isoform is activated at Ca^{2+} concentration of 40-60 μM. This enzyme is inactive at intracellular calcium concentrations. Either it is calcium ion influx or release of PADI from the cells that ultimately exposes it to high calcium levels that cause its activation [37]. So this might support the argument that 'intense' conditions, like terminal differentiation occurring in the stratified layer of the skin, apoptosis and oxidative stress during inflammatory responses, triggers activation of these isozymes and ultimately citrullination of protein takes place.

The peptidylarginine deiminase isozymes 1-4 have been examined in the synovial tissue of RA patients; PADI2 and PADI4 were specifically found to be expressed in the RA synovium with a strong association with severity of inflammation [38]. In addition, at a pathophysiological level the presence of ACPA in around 80% of RA patients and the genetic association of PADI 4 in (Koreans and Japanese) with inflamed synovium supports the notion that PADI might have a critical role in RA pathogenesis [39]. As shown in table 2, PADI4 is expressed in neutrophils, eosinophils, natural killer (NK) cells, T cells and B cells. In addition, non-haemopoietic lineage cells e.g. fibroblast like synoviocytes (FLS), endothelial cells and sublining areas of RA synovium can also express this isoform. Importantly, citrullinated proteins were co localized with PADI4 around the lining and sublining layer of RA patients [37].

A model of RA pathogenesis

1 Klareskog et al presented an etiological model for disease pathogenesis in the ACPA positive subset of RA. It was proposed that smoking as an environmental factor triggers the citrullination of proteins in the lungs, which results in the generation of an immune response and production of ACPA in genetically susceptible individuals (HLA DRB1 shared epitope). In these individuals, any type of trauma or infection that leads to a non-specific inflammatory environment in joints could result in citrullination of proteins in the affected joints [40]. Pre-existing circulating ACPAs enter the joint and form immune complexes with the newly generated citrullinated proteins. The formation of these CP immune complexes leads to the recruitment of inflammatory cells, secretion of pro-inflammatory cytokines, and antibody production that eventually results in the development of chronic RA (Figure 1.1,Taken from Annual Review immunology)[6].

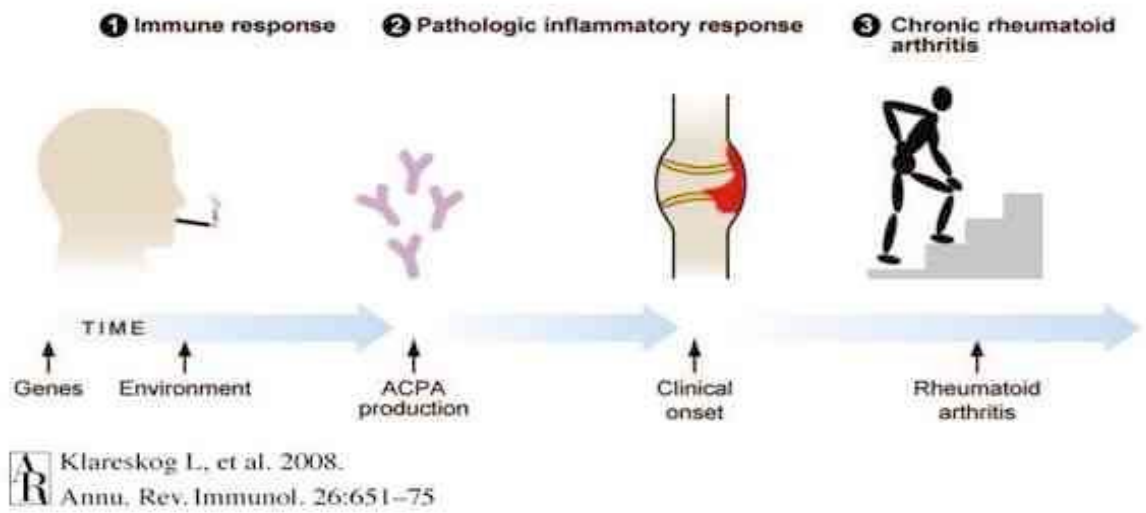

Figure 1.1 A possible Etiological model for ACPA positive subset of RA

1.1.3 Disease progression and Treatment

1.1.3.1 Treatment

There is no known cure for RA but many treatments are in place to stop the progression of this chronic ailment. Early and aggressive treatment of RA patients with disease modifying anti-rheumatic drugs, such as sulfasalzine, hydroxychloroquine, methotrexate, leflunomide and glucocorticoids is the first line of care. These small molecules, so called conventional disease modifying anti-rheumatic drugs (DMARD), are effective at controlling inflammatory activity [41]. Recently, a new powerful emerging therapeutic arsenal for the rheumatologist has changed practice namely the advent of biological agents. The first of these biological therapies was the anti-TNFα monoclonal antibody, infliximab [42]. Many different TNF blocking agents are now used in clinical practice; infliximab (chimeric anti TNF antibody), adalimumab (humanized anti TNF antibody) and etanercept (soluble TNF receptor). Two new agents will shortly be available, namely certolizumab (a pegylated Fab anti-TNF) and golimumab (a monoclonal antibody with monthly administration). TNF blockade provides approximately 60% improvement at the ACR20 level in MTX inadequate responder patients. However only around 25% of patients achieve a DAS29 low disease state or ACR70 level of improvement. Moreover, remission is not well maintained even if achieved in a majority of patients. Therefore new biologic

agents have emerged. Most recent in the cytokine blockade field, an alternative to the TNFα blocking agents is the anti-IL-6 receptor antibody, Tocilizumab [43]. This is now licenced and approved for use on a wide basis and delivers approximately similar responses to TNF blockade if used for first biologic in MTX-IR population but lower rates of responses in TNF blockade resistant patients. This initial trend for targeting biological agents to specific cytokines and their receptors, however, does not always prove to be efficacious. This was the case for the recombinant interleukin 1 receptor antagonist, anakinra, which although reduced erosion in RA patients did not match the effectiveness of TNF blocking agents [44].

Some of the most recent additions to the therapeutic armamentarium have been generated to specifically target T and B-lymphocytes [43]. Abatacept is a fusion protein that blocks the co-stimulatory signals necessary for T cell activation; it is composed of an immunoglobulin Fc region fused to the extracellular domain of CTLA4. This mechanism of action for this fusion protein relies on its ability to interact with B7 on APC and therefore inhibit this APC – T cell co-receptor interaction [43]. When it comes to refractory cases of rheumatoid arthritis, in particular those that are anti-TNFα non-responders, a further therapeutic option is B cell depletion therapy. This therapy utilises a monoclonal antibody (Rituximab) that binds to the CD20 receptor present on the surface of pre B and mature B cells resulting in the depletion of circulating B cells [45]. The therapeutic and pathogenetic clues offered by this approach formed an important part of my thinking in generating the data contained in my thesis.

1.2 B lymphocytes in RA

Thirty years ago research in RA was focused on B cells because of the importance of RF - with time trends changed and cytokines and T cells were seen as the more relevant aspect of RA immunopathology. More recently with the advent of B cell depleting agents it is now appreciated that the immunopathology is not restricted to one cell type or cytokine. In fact to understand the disease we have to have a thorough understanding of all the immune components. Researchers have also started to think outside of the box and investigate non-

traditional functions of cells demonstrating for example that B cells have additional immune functions (Table 1.3 Adapted from Martinez-Gamboa et al [46])

Table 1.3. Role of B cells in the regulation of immune responses

• As precursors of (auto) antibody-secreting plasma cells
• As antigen presenting cells
• In the differentiation of follicular dendritic cells in secondary lymphoid organs
• In lymphoid organogenesis
• In the initiation and regulation of T and B cell responses
• In the differentiation of effector T cells
• In the polarization into cytokine producing effector B cells
• In the expression of co-stimulatory molecules
• In the immune regulation (IL-10 positive B cells)

1.2.1 Murine B lymphocytes

Murine B cells can be divided into various subsets, some of which reside in specific anatomical locations e.g. B-1 B cell, which is a population primarily seen in the pleural and peritoneal body cavities. Another is the B-2 population, which is found in spleen, lymph nodes and blood. They are further classified on the basis of function, micro anatomical location and expression of surface receptors. Newly formed B cells are generated in the bone marrow and once they differentiate to an 'immature stage' they migrate to the spleen and can be identified based on surface expression of markers, IgM^{hi} IgD^{hi} $CD21^{-}$ $CD23^{-}$ $CD24^{hi}$

are termed transitional type-1 (T1). These cells further differentiate into transitional type-2 (T2) B cells IgM^{hi} IgD^{hi} CD21^{hi} CD23^{hi} CD24^{hi}. From these transitional cells marginal zone and mature follicular (B2) B cells are generated. Marginal zone B cells, IgM^{hi} IgD^{lo} CD21^{hi} CD23^{-} CD24^{hi} are a specialized population that reside in the marginal sinus of the spleen. Whilst B2 cells which reside in the main follicle (inside of the marginal sinus) and express IgM^{hi} IgD^{lo} CD21^{int} CD23^{hi} CD24^{int}. Interestingly, humans do not have exactly the same functional equivalent subsets compared to the murine B cell populations [47].

For a long time RA was regarded as a disease mediated by macrophages and T cells [48]. However, a case report for a 53 year old suffering from non-Hodgkin lymphoma (NHL) with coexistent RA, showed that after a course of B cell depletion therapy to treat the NHL, which in this instance was unresponsive, resulted in an enormous improvement in the patient's inflammatory synovitis. Importantly, this observation recognized a central role for B cells in RA pathogenesis [49]. This was further supported by another case of RA in association with chronic lymphocytic leukaemia (CLL). This patient had a significant decrease in the RA symptoms after the selective depletion of B cells by Rituximab a monoclonal antibody to CD20 receptor specific to B cells [50]. These findings were further confirmed by a randomized clinical trial, where selective depletion of B-lymphocytes in combination with methotrexate resulted in 50% improvement in clinical symptoms according to ACR criteria in 43% of RA patients at week 24 [45].

Many theories have been proposed to explain not only the mechanism behind the B cell depletion but also its efficacy in RA. It is currently assumed that the mechanism of action of B cell depleting agents could be through different pathways, one of them is antibody dependent cell mediated cytotoxicity (ADCC) or phagocytosis, which requires recognition of Fc portion of bound rituximab by Fcγ receptors and complement receptors 1 and 3 on macrophages [51, 52]. Studies have demonstrated that rituximab binding causes activation of the complement cascade, generating membrane attack complex that leads to lysis of B cells [53, 54]. Finally, rituximab bound B cells are recognised by natural killer cells via FcγRIII and complement receptor 3 that induces cytotoxicity of B cells [55].

Given that B cells are depleted it still remains for us to understand why the depletion of B cells actually leads to clinical improvement in RA patients. In explanation, B cells have various functions (Table 1.3), and various studies have been performed to investigate certain aspects of B cell biology is relation to RA. The autoantibody (Rheumatoid factor) secreting function of B cells in RA was recognised decades ago. Recently, the finding of autoantibodies to citrullinated peptide at an early stage of RA has resulted in enhanced diagnostic specificity [56]. These autoantibodies can form immune complexes that mediate activation of B cells and follicular dendritic cells (FDCs) through complement receptor (CR1 & CR2) and Fc receptors [57]. Cytokine production is a known effector response of T cells and macrophages. Studies have shown that B cells can secrete IL-6, lymphotoxin and TNFα, which then amplify immune responses [58]. However, further studies are required to properly characterize the cytokine producing ability of B cells in the synovium. Their ability as antigen presenting cells may also be important in the joints, as the B cell depletion therapy impaired ectopic germinal centre formation and the optimal activation of T cells [59].

Antigen specific B cells are known to have the capacity to internalize and process antigens to peptides. Thereafter, antigen presentation of these peptides is executed normally through presentation on the major histocompatibility complex (MHC) class II molecule. Importantly, the involvement of HLA-DR4 in this antigen presentation through B cells signifies a link between B lymphocytes and arthritis pathophysiology [46]. Adoptive transfer of $CD4^+$ T cells into SCID mice induced disease only in the presence of B cells, depletion of B cells with anti-CD20 mAb inhibited production of IFNγ and IL-1β suggesting a central role for viable B cells in the disease [59]. In the diseased synovium, cellular infiltrates include T lymphocytes, B cells and macrophages. In fact a non lymphoid tissue like synovial membrane in patients contains the presence of germinal centres closely resembling the germinal centre characteristic of secondary lymphoid organs [60]. Humby et al demonstrated that the ectopic germinal centres in RA synovium express activation induced cytidine deaminase (AID) an enzyme that influences somatic hypermutation and class switch recombination (CSR) of Ig genes. They also confirmed that these germinal centres are associated with ACPA producing plasma cells suggestive of functional aggregates of B cells in the inflamed synovium [61]. In another study B cell activating factor (BAFF or BLys) of

TNFα family is produced by fibroblast like synoviocytes (FLS) in the lining layer of synovial membrane, which then supports the survival of B cells in the disease membrane. In fact TNFα and INFγ could influence the release of BAFF [62].

1.2.2 Factors affecting B cell differentiation and survival

Like every proliferating cell, lymphocytes also seek appropriate support from the environment via elaboration of growth and survival factors. Lack of these signals can result in inefficient performance and some of the cells may die. B cell activation factor (BAFF) also known as Blys (B lymphocyte stimulator) is a member of Tumor necrosis factor (TNF) family. As the name implies it is a survival factor for transitional and mature B-lymphocytes. Another factor closely related to BAFF that shares some of its receptors and functional properties is a proliferation inducing ligand (APRIL).

1.2.2.1 B cell activation factor

A member of TNF family, known as a potent stimulator of B lymphocyte survival has many designations like (Blys, BAFF, zTNF4, TALL-1 and THANK) [63-65] Chromosomal mapping of BAFF gene revealed that it is located on chromosome 13q34 [66]. BAFF expression is seen in macrophages, monocytes, T-cells and dendritic cells. In addition, non haematopoietic cells like osteoclasts, fibroblast like synoviocytes and adipocytes produce BAFF as well [67, 68].

Structure:

BAFF is a type II membrane bound protein, which has three domains. An intracellular TNF homology domain (THD), one transmembrane domain with a furin processing site and an extracellular domain [69]. The extracellular domains of BAFF form a trimeric complex on the surface of cells and after proteolytic cleavage at the furin site a functional soluble trimeric complex. Unlike other TNF members, the BAFF trimer has an altered long loop conformation, a β strand and a long D-E loop, which is seen as negatively charged deep concave region [70]. Stability of the trimeric structure is ensured by the presence of the magnesium ions that binds along the three fold axis [71, 72].

BAFF Receptors:

BAFF has the ability to bind to three known receptors; B cell maturation antigen (BCMA) and transmembrane activator, cyclophilin ligand interactor (TACI) and BAFF-receptor. All of these receptors belong to the TNF receptor superfamily (Figure 1.2) [63]. BCMA and TACI have a cysteine rich extracellular domain, a signature of TNF receptors, which contains two to eight cysteine residues stabilized by disulphide bonds. BAFF-R differs from the other two receptors because it only contains four cysteine residues in the extracellular domain, which makes it the smallest cysteine rich domain (CRD) in TNF receptor superfamily. Importantly, BAFF-r also differs from BCMA and TACI because it only binds to BAFF [73], whilst the other two receptors also interact with APRIL. The ligand-binding region in these receptors normally requires the participation of only two cysteine residues. All these receptors are type III membrane proteins with multiple transmembrane domains that span the entire membrane. However, they do have a similar orientation to type I membrane protein [74].

As indicated above, BAFF shares the BCMA and TACI receptors with APRIL. BCMA was shown to be mainly expressed on mature B cells and was initially identified in cells of lymphoma patients with chromosomal translocation [75]. TACI expression was confirmed on B lymphocytes and non resting T cells, TACI stimulation triggers calcium dependent transcription factor i.e. nuclear factor of activated T cells (NF-AT) [76].

1.2.2.2 A Proliferation inducing ligand (APRIL)

APRIL, also known as TALL2, and is structurally related to BAFF i.e. a type II transmembrane protein with a trimeric assembly, with an extracelluar domain formed by 201 amino acids and a cytoplasmic domain consisting of 28 amino acids. APRIL has the unique ability to undergo maturation cleavage at the furin site inside the cell within the Golgi complex. This intracellular processing is carried out by furin convertase [77](Figure 4, adapted from Annual Review immunology[78]).

The unique furin processing site is located towards the NH2 terminal region of the protein and is common to both the BAFF and APRIL extracelluar domains.

However, the cleaved APRIL containing the short NH_2 consist of a unique cluster of amino acid (QKQKKQ) not found in BAFF. This unique sequence binds to glycosaminoglycan, which enables APRIL specifically bind to sydecan-1 on plasma cells and proteoglycan on non-haematopoietic cells [79].

There is a wide range of immune cells that express APRIL including monocyte, macrophages, dendritic cells and T cells. In addition to haematopoietic cells, other cell types produce APRIL i.e. osteoclasts and tumour cells [68]. In fact in breast cancer tissue APRIL and BAFF are expressed by infiltrating cells, epithelial cells and glands [67].

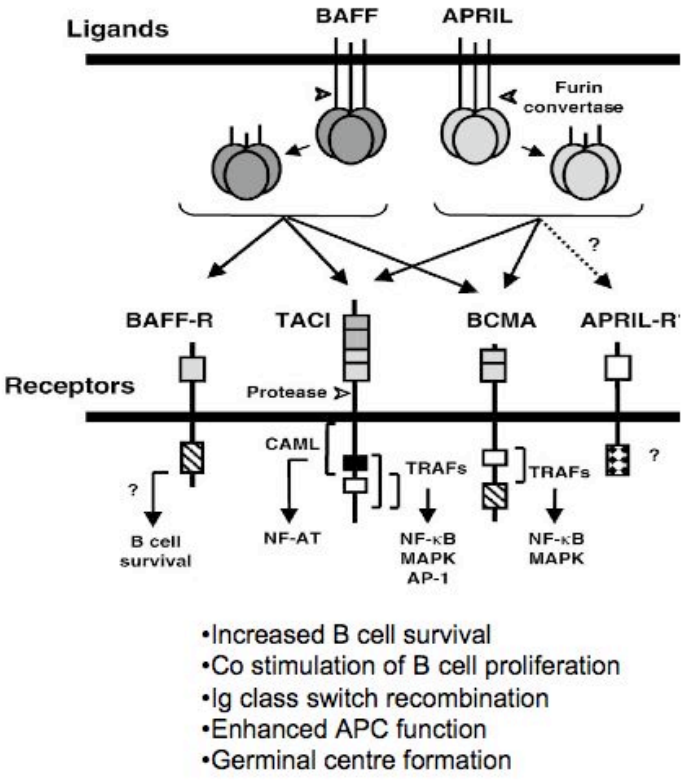

Figure 1.2 Illustration of functions and receptors of BAFF and APRIL

APRIL Receptors:

APRIL has a high affinity for the TNF receptors TACI and BCMA but does not interact with BAFF-R [68]. However, APRIL binds preferentially to B cell maturation antigen (BCMA). It has been proposed that an APRIL specific receptor exists but it currently has not been identified [80].

Different B cells at various stages express the receptors for APRIL and BAFF. Humans and mice both express BAFF-R on peripheral B cells and as B cells differentiation to plasma cells they lose the expression of BAFF-R. TACI is found on different B cell subsets like MZ, transitional T1 and T2 but not germinal centre B cells; whereas, BCMA is mainly expressed by the germinal centre B cells and plasma cells [81].

Biological functions

TNF receptors also called "Death receptor" have a signature death domain that contains TNF receptor associated factor (TRAFs) that upon stimulation can result in either apoptosis or survival. Receptors for BAFF and APRIL lack the death domains that are typical of TNF receptor family. It was established in BAFF deficient mice that secondary lymphoid organs lost 90% of marginal zone and follicular B-lymphocytes, which illustrates that BAFF plays a critical role as a survival factor [82]. Transgenic mice over expressing Bcl-2 with BAFF deficiency failed to rescue B cells and showed their lack of ability to have B cell maturation, which suggested that BAFF promote B cell differentiation and prevents them from apoptosis as well [83].

At a functional level, the antigen presentation ability of B cells is increased by APRIL. This is mediated through BCMA, whereby APRIL induces the up regulation of MHC class II and the co-stimulatory molecules CD80, CD86, CD40 and CD54. In addition APRIL binding to BCMA activates the NF-κB and JNK signalling pathways [84]. In another study lack of APRIL lead to an increased effector and memory T cells and impairment of IgA class switching recombination CSR [85]. In vitro data suggests that APRIL can also induce megakaryocytopoeisis, which implies

delineation of progenitor cells to megakaryoblasts, megakaryocytes and finally to platelet fragments [86]. Moreover, APRIL transgenic mice promote the formation of B-1 linked neoplasm, in fact high levels of APRIL in sera of patients suffering form B cell chronic lymphoid leukaemia (B-CLL) supported the notion [87].

1.3 Rheumatoid Arthritis and vascular risk

Rheumatoid arthritis primarily affects joints although around 15-20% of the patients exhibit extra-articular features; conventionally manifest as pericarditis, pleuritis, major cutaneous vasculitis, anemia, episcleritis and glomerulonephritis[88]. There is now extensive evidence based on observational cohort and case control studies that rheumatoid arthritis is strongly associated with cardiovascular morbidity and mortality [89-91].

Many autoimmune diseases including; RA, systemic lupus erythematosis (SLE), antiphospholipid syndrome, systemic sclerosis and primary systemic vasculitis are associated with increased risk of cardiovascular morbidity and mortality [92]. This can primarily be attributed to accelerated atherosclerosis [93]. As we have already discussed RA as a chronic autoimmune arthropathy manifested by cartilage and bone damage resulting in deterioration of both social and physical abilities of the patients. In fact reduced physical activity of RA patient significantly increased CVD risk profile as compared to physically active patients [94]. However, RA is associated with accelerated atherosclerosis and reduced life expectancy. This overt rise in mortality cannot be explained with the classical risk factors like diabetes mellitus, dyslipoproteinemia, tobacco smoking, high blood pressure, advanced age and genetic abnormalities [95]. In one study where RA patients were evaluated over a period of 20 years, it was revealed that the these patients had 50% mortality due to cardiovascular disease [96]. Similarly, in a prospective cohort of female patients with rheumatoid arthritis it was demonstrated that they had a relative risk for myocardial infarction (3.10, 95% CI) [97]. The cardiovascular events in RA patients equal that of DM2. This increased risk requires cardiovascular risk management as in DM2 [98].

In Northern Sweden a cohort of seropositive RA patients were followed for 15 years. This cohort showed that both sexes had an increased standardized mortality ratio of 1.46 in cardiovascular disease (CVD) and 1.54 in ischemic heart disease (IHD) [99]. In an additional study in North America, a cohort of 236 patients revealed an approximate 4-fold rise in cardiovascular events. Importantly, analysis of the patients follow up over this 8 year period excluded traditional risk factors like smoking, hypercholesterolemia and diabetes mellitus as the underlying mechanism of cardiovascular diseases. These findings suggested that systemic inflammation in RA patients is the culprit [100]. A similar observation was made in RA patients with a specific genetic constituent (HLADRB1) [101].

The chronic systemic inflammatory milieu associated with RA sets a stage that accelerates the atherosclerotic disease[102]. A meta-analysis of observational studies by Avina-Zubieta et al substantiated the increased cardiovascular risk in RA patients, concluding that in comparison to the general population RA patients have a 50% higher CVD mortality [103]. In a study to evaluate recent onset RA, patients were evaluated for sub-clinical atherosclerosis using ultrasonography to measure the carotid intima-media thickness (cIMT). The CRP level in these patients correlated with increased (cIMT) indicative of the presence of plaques in the vessel wall of the patients [104 105]. Vincenzo pasceri et al in an editorial discussed the similarities between atherosclerosis and rheumatoid arthritis and argued that various cell types ($CD3^+$, $CD4^+$ $CD28^{-)}$, adhesion molecules (VCAM-1, ICAM-1, E-selectin, P-selectin), cytokines (TNFα, IL-6, IL-2), metalloprotienases, and autoantibodies (OxLDL, HSP) show striking similarity between RA and unstable angina [106].

1.3.1 Atherosclerosis (a priori)

Atherosclerosis is a chronic inflammatory response characterized by asymmetric focal thickening of the intima, resulting in luminal narrowing of blood vessels. Atherosclerosis is one of the major causes of cardiovascular diseases (CVD) worldwide, which is a principal cause of death and illness in the developed countries [107-109]. CVD refers to a group of diseases that includes cerebrovascular accidents (stroke), coronary artery disease, myocardial infarction, congestive heart failure, angina, and aneurysms.

Atherosclerosis starts at an early age and gradually transforms into a complex structure. The atherosclerotic lesion undergoes transformation from an initial phase where lipid droplets and immune cells merely exist, to a state where lipid laden foam cells are dominant and called the fatty streak [110]. This is followed by a more complex phase of atheroma [111], in this mature phase the plaque is composed of endothelial cells (ECs), leukocytes, foam cells, smooth muscle cells (SMCs), a necrotic core, accumulated modified lipids and calcified regions [112]. All this takes place in the intimal layer of the vasculature and is accompanied by fibrous proliferation that marks the asymmetrical luminal narrowing of the blood vessels. Over a century ago two pathologists proposed contrasting ideas regarding the initiation of this complex disease. Carl von Rokitansky proposed atherosclerotic inflammation to be a result of endothelial dysfunction caused by mechanical injury and toxins. Whereas, Rudolf Virchow believed that changes of cells were critical in atherosclerosis and coined the term cellular pathology [113].

Almost two decades ago we started to appreciate a principal role for inflammation in atherosclerosis leading to major complications like myocardial infarction, stroke and vascular claudication. Steinberg postulated chemically modified lipoproteins to be the initiating factor, notably the oxidized low-density lipoproteins (OxLDL), leading to the primary formation of foam cells in the intima [114]. This was termed as the “altered lipoprotein hypothesis”. Alternatively, in 1993 Ross suggested “response to injury hypothesis”, which is an alteration of the endothelium and intima due to insults e.g. mechanical injury, toxins, and oxygen radicals that initiated the events leading to endothelial dysfunction [115]. These two processes favour the “inside-out” theory (see section 1.3.2), the traditional concept of vascular inflammation. However, the growing evidence for functional significance of vascular adventitia in the last decade has resulted in a new concept of “outside-in” hypothesis that will be discussed in a later section (1.3.3) [116].

1.3.1.1 Structure of a normal Blood vessel

It is important to know the basic structure of a normal blood vessel wall to understand the pathogenesis of atherosclerosis. A blood vessel is comprised of three layers, the intima, media and adventitia. The tunica intima is the inner most layer, which is comprised of a simple monolayer of endothelial cells

arranged on a basement membrane made of type IV collagen, laminin and sulphate proteoglycans. Finally, there is an internal elastic lamina made of insoluble protein polymer elastin that separates the tunica intima from media. The normal tunica media is the middle layer that contains exclusively vascular SMCs enclosed by basement membrane and embedded within an interstitial matrix. Whereas, the outer most layer is the tunica adventitia, a loose connective tissue comprised of fat cells, fibroblasts and capillaries separated from the tunica media by an external elastic lamina [117].

1.3.2 The inside out phenomenon

As the name implies the inside out theory begins at the tunica intima. An elevated level of lipid in the blood allows the low-density lipoproteins to diffuse into the tunica intima. This accumulation of LDL in the extracellular compartment leads to its modification, under the influence of enzymes and oxygen radicals, to OxLDL. This in turn results in the expression of vascular cell adhesion molecule 1 (VCAM1) and/or Intercellular adhesion molecule 1 (ICAM1) by endothelial cells, which promotes migration and invasion of monocytes and T cells into the intima [111].

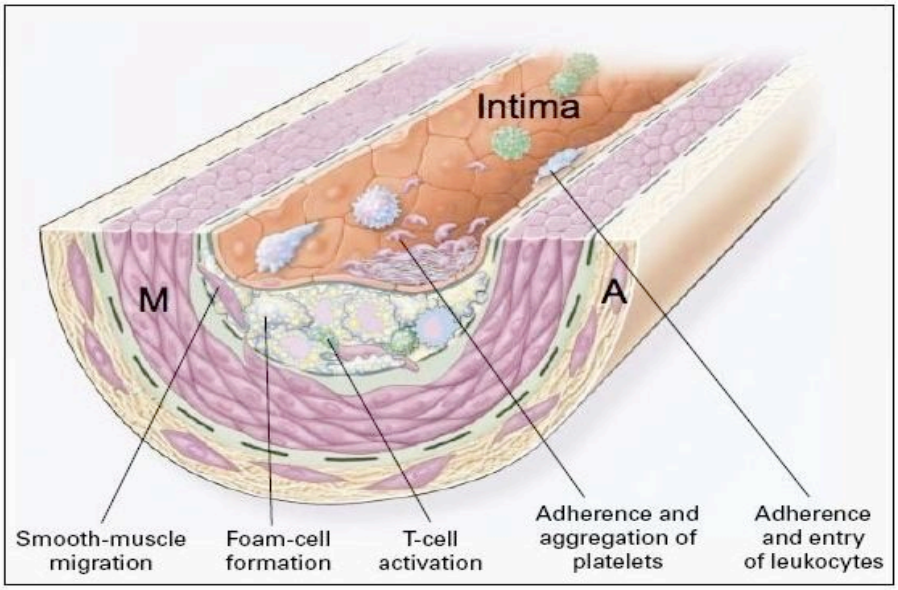

Figure 1.3 The focal intimal thickening of a blood.
Tunica intima with plaque shows smooth muscle cells, foam cells formation and activated T cells. Leukocytes and platelets can be seen attached to lining endothelium. Tunica media (M) is a thick layer of smooth muscle cells and tunica

adventitia (A) the outer most layers of adipocytes (adapted from Hannson at el. Nat Rev Immunol 2006).

The recruited monocytes, supported by the growth factor m-CSF, differentiate into macrophages. The resulting macrophages binds modified LDL through scavenger receptors (SR) that includes CD36, SR-A and SR-B1 [118-120]. Macrophages in human atherosclerotic lesions are shown to express TLR2 and TLR4 that can bind modified LDL whose uptake results in foam cell formation [121]. Antigen presented by macrophages and dendritic cells (antigen presenting cells) activate lymphocytes, which produce Th1 cytokines (IL-12, IL-18, INFγ and Tumor necrosis factor-alpha) [111]. The persistent inflammatory response is manifested as focal thickening of tunica intima with a core of cholesterol and cellular debris, surrounded by a fibrous cap of collagen fibre and smooth muscle cells, the set of events following the initiation of atherosclerosis at the tunica intima (Figure 1.3, taken form Ross, 1999).

1.3.3 The outside in phenomenon

The basic mechanism underlying the pathogenesis of atherosclerosis was revisited and an alternative hypothesis was proposed stating that the pathology of disease can be initiated at the outer most layer of a blood vessel (tunica adventitia). Maiellaro et al has attempted to elaborate this new paradigm, focusing on the role of the tunica adventitia in vascular inflammation. The theory is that a phenotypic switch of fibroblast to myofibroblast is caused by either (a) a tear of the elastic laminae or (b) by the products of chronic inflammation, i.e., cytokines, chemokines and leukotrienes (Figure 1.4, Adapted from Maiellaro et al) [116] shows the proposed order of events (from left to right) involved in the initiation of the vascular inflammation, starting with phenotypic switch of fibroblast to contractile myofibroblast, neovascularization, lipid oxidation leading to T cell and a humoral immune responses.

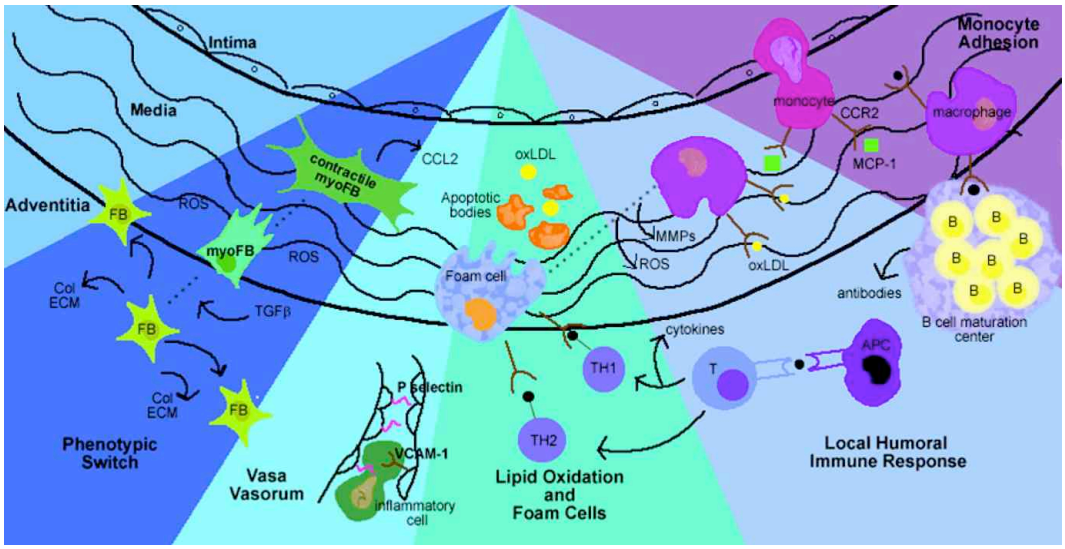

Figure 1.4 The development of atherogenesis beginning at the adventitial layer This begins in response to a tear in elastic lamina or as a result of chronic inflammatory cytokines, chemokines. These results in (from left to right) phenotypic switch of adventitial fibroblast to contractile myofibroblasts, neo-angiogenesis (vasa vasorum), lipid oxidation leads to T cell and humoral immune responses.

The myofibroblasts release MCP-1 that aids in the recruitment of cells into the adventitia. In addition to the myofibroblasts ability to recruit cells, the endothelium of the vasa vasorum starts to express molecules like P-selectin and VCAM-1 that assist in cellular trafficking towards the adventitia. To help perpetuate this disease process, un-switched fibroblasts in the adventitia secrete collagen thereby providing an extracelluar matrix for newly recruited cells. This is accompanied by neovascularization and modification and uptake of LDL by the macrophages leading to formation of foam cell [116]. Thereafter, foam cells activate T cells (Th1), which are followed by cytokines release, formation of ROS and apoptotic bodies at the site of lesion.

1.3.4 Inflammation in Atherosclerosis

A classical marker of inflammation is C-reactive protein (CRP), which is synthesized in the liver. Elevated levels of CRP in patients of unstable angina suggested that inflammation is critical in the pathogenesis of the disease [122]. Interestingly, significant levels of CRP in sub-clinical cases of myocardial infarction labelled it as an independent risk factor for this disease [123]. More

recently, the measurement of CRP level has been found to be useful in predicting diseases like stroke, peripheral vascular disease and myocardial infarction[124].

1.3.5 Oxidized LDL triggers an inflammatory response

Hyperlipidemia is defined as abnormally raised levels of lipids (LDL) in the blood and is thought to be the primary cause of atherosclerosis. The altered lipid levels are though to result in the transmigration of LDL across the vascular endothelial cells. Two decades ago, Witztum et al showed that in LDL receptor deficient rabbits atherosclerotic lesions contained modified oxLDL [125]. In ApoE knockout mice, an animal model of atherosclerosis, it has been shown that endothelial activation in response to modified LDL, either through oxidation or enzymatic process, results in the expression of ICAM-1 and VCAM-1 that in turn recruits inflammatory cells to the site of hemodynamic strain [126].

1.3.6 Monocyte recruitment to Macrophage activation

The recruitment of monocytes by the activated vascular endothelial cells was first demonstrated in the pre-lesional intima [127]. The differentiation of monocytes into long-lived macrophage takes place in the intima. The factor responsible for this differentiation is (MCSF), the osteopetrotic (op) deficient mice do not produce (MCSF), and in double knockout (op/ApoE$^{-/-}$) reduction in lesion size demonstrated (MCSF) significance in atherosclerosis [128].

Activated macrophages tend to express Pattern recognition receptor (PRRs), which includes scavenger receptors (SRs) and toll like receptors (TLRs). These SRs bind oxLDL, apoptotic particles, heat shock protein and bacterial endotoxins [129]. Accumulation of oxLDL in these macrophages results in the formation of foam cells, a classical feature of atherosclerosis. The atherosclerotic lesions also have a variety of immune cells including; T cells, macrophages, monocytes, vascular dendritic cells, mast cells and B cells [130, 131].

1.3.7 B-lymphocyte "A good guy" in Atherosclerosis?

Studies in atherosclerotic lesions of ApoE$^{-/-}$ mice have established that B cells are involved in the inflammatory component of this disease. Their location was reported in the base of the lesion, which was associated with high levels of Immunoglobulin M (IgM) and vascular cell adhesion molecule-1 (VCAM-1) [132]. B cell deficient LDL$^{-/-}$ mice on a western diet had a 30-40% increase in the lesion size, which imply an atheroprotective role for antibodies and B cells [133]. Caligiuri et al established a similar finding, where removal of the spleen in ApoE$^{-/-}$ resulted in enhancement of plaque size. To confirm the subset of cells responsible for this effect, B lymphocytes were adoptively transferred into these splenectomized mice and the conferred protection was associated with an increase in anti oxLDL antibodies [134]. Part of this protective effect stems from the production of natural antibodies by a specific set of innate-like B1 cells. These natural antibodies interact with both oxidized LDL and apoptotic cells and can protect mice from atherosclerosis [135, 136]. ApoE$^{-/-}$ mice in this chronic inflammatory disease exhibit high titres of antibodies against oxLDL [137]. In vitro data showed that IgM autoantibodies can recognise phosphorylcholine (PC) on oxLDL, and their binding prevents oxLDL uptake and degradation by macrophages [138]. These antibodies closely resemble the "natural" T15 antibodies to PC produced by B1 cells, and T15 IgM is known to protect against pneumococcal infection. Based on these facts pneumococcal immunization of LDL$^{-/-}$ resulted in reduced atherosclerosis [135]. Immunisation of mice with MDA-LDL an oxidation specific neo-epitope resulted in IL-5 dependent increased production of T15 IgM. This highlighted the fact that IL-5 can connect adaptive immunity to innate immunity [139]. So far, little is known about natural antibody production or presence of B1 cells in atherosclerotic aorta.

1.3.7.1 Lamina adventitia and B cells in vascular inflammation

Zohu x et al provided indirect evidence for the involvement of B cells in the presence of moderate hypercholesterolemia in ApoE$^{-/-}$ mice. This altered lipid environment resulted in high titres of oxLDL specific IgG2a antibodies, typical of the Th1 response seen in ApoE$^{-/-}$ mice. Interestingly severe hypercholesterolemia switched the T helper phenotype to Th2, which was evident from the increased presence of oxLDL specific IgG1 antibodies [140]. In a similar study increased levels

of IgG1 antibodies to malondialdehyde-modified low-density lipoprotein (MDA-LDL) and exogenous antigen keyhole limpet haemocyanin (KLH) were observed [141]. These observations, in an experimental model of atherosclerosis, made the link between the T lymphocyte dependent B cell responses and dyslipidemia. In more recent studies to further investigate dyslipidemia and B cell T cell interactions, $ApoE^{-/-}$ mice were fed a high fat chow for up to 78 weeks and the inflammatory response in tunica intima and adventitia were compared. This study demonstrated that not only were structures resembling tertiary lymphoid follicles present in the vessel wall but that they were predominantly present in the lamina adventitia. These lymphoid aggregates, formed under the influence of hyperlipidemia and old age, were comprised of dendritic cells, B cells, plasma cells and T cells [142].

In a separate study where angioplasty mediated overstretch injury to porcine coronary artery were performed, cellular proliferation of myofibroblasts and production of PDGF was observed in the adventitia, suggesting that adventitial changes lead to the recruitment of cells into the neointima that eventually leads to luminal narrowing [143]. Whereas, human adventitia were shown to have nodular aggregates, and these aggregates showed organised B cell dominance with few T cells, dendritic cells and macrophages suggesting resemblance to Mucosa associated lymphoid tissue (MALT) [144]. Human coronary arteries examined for contributions from intima and adventitia in plaque stability revealed that inflammation in tunica adventitia is significantly responsible for the plaque rupture [145].

1.3.8 Different T cell subsets in Atherosclerosis

1.3.8.1 CD4+ T Lymphocytes

Animal studies made it clear that immunocompetence was fundamental in atherosclerosis development. The lack of an immune component resulted in a dramatic 70% reduction in lesion size. Whereas, adoptive transfer of CD4+ T cells from atherosclerotic prone donors to immunodeficient mice aggravated the disease [146]. Moreover, to confirm a link between CD4+ T lymphocytes and disease associated antigen oxLDL in atherosclerosis, CD4+ T cells from mice immunized

with oxLDL transferred to ApoE$^{-/-}$/ SCID mice confirmed the proatherogenic potential of CD4+ T cells in aggravating the disease [147].

In support of these murine studies and the importance of T cells in atherosclerosis, human studies have demonstrated that atherosclerotic plaques contain CD4+ T cells that recognise antigens presented through major-histocompatibility-complex (MHC) class II molecules. These CD4+ T cells are reactive to antigens like oxidized LDL, heat shock protein 60 and Chlamydia [148].

Helper T cells subsets

T lymphocytes have different functional subsets and these include Th1, Th2 and a more recent addition the Th17 subset. It should also be appreciated that the role of B cells is not only related to their ability to produce antibodies but also their ability to present antigen and secrete cytokines that could potentially regulate the Th1/Th2 balance. Advanced atherosclerotic plaques in humans were reported to have a predominance of Th1 cells. This was based on the Immunohistochemical analysis of advance plaques showing the presence of increased levels of the Th1 cytokines, IFNγ and TNFα [149, 150].

The proatherogenic potential of Th1 cells was demonstrated in the double knockout ApoE$^{-/-}$/IFN$\gamma^{-/-}$ mouse. These mice were placed on a high fat diet and analysis of the model illustrated that the loss of IFNγ reduced lesion burden in male mice in particular [151]. Furthermore, administration of exogenous IFNγ into ApoE$^{-/-}$ resulted in increased plaque formation [152].

Different animal models have been used to show that atherosclerosis is an immune mediated response. In ApoE$^{-/-}$ mice pharmacological down regulation of Type 1 helper cell (Th1) with pentoxiphylline resulted in marked reduction in atherosclerosis [153]. Conversely, the Type 2 helper cell subset (Th2) producing IL-5, IL-4 and IL-13 have an ambiguous role in atherosclerosis. IL-5 has been shown to trigger B-cells to produce natural antibodies. These IgM antibodies have been shown to have an inverse relationship with carotid artery lesions suggestive of a protective role for these antibodies [154]. However, this relation needs to be further investigated. In addition the idea that the spleen is a vital organ, where development of an immune response against atherogenesis takes place was

introduced in late 1970s, when splenectomized war injured patients were found to be at increased risk of ischemic heart disease [155].

1.3.9 Mast cells in atherosclerosis

Mast cells are granulocytes that are known major effector cells in allergy and anaphylaxis. They are known to release a wide range of vasoactive substances (histamine & serotinin), proteolytic enzymes (tryptase & chymase), granulocyte monocyte colony stimulating factor (GM-CSF) and cytokines like TNFα, INFγ and IL-6 upon activation. Usually mast cells are rare in blood vessel walls, however, they are present in the tunica adventitia and rupture prone shoulder region of the atherosclerotic plaque [156].

In an animal study, activation of perivascular mast cells resulted in weakened plaque, marked by vascular leakage, macrophage apoptosis, intraplaque haemorrhage and leukocyte recruitment [157]. The mast cell deficient Ldlr-/-Kit(W-sh)(/W-sh) mice, show reduced lesions formation, which was associated with reduced T cells and macrophages. Moreover, introduction of wild type mast cells to mast cell deficient mice restored atherosclerosis progression, suggesting that IL-6 and IFNγ are provided by mast cells to promote atherogenesis [158]. Apolipoprotein E and ApoA-II dependent cellular cholesterol efflux is effectively incapacitated by mast cell chymase, therefore apolipoprotien mediated removal of cholesterol from mouse macrophages promote foam cell formation and atherogenesis [159].

1.4 Interleukin-1 (IL-1) superfamily cytokines in RA and Atherosclerosis

Cytokines comprise a class of proinflammatory proteins implicated in the pathogenesis of many autoimmune diseases. Some known autoimmune diseases like RA, psoriatic arthritis (PsA) and some other spondyloarthropathies have responded well to cytokines blocking therapies as noted above. Many cytokine families have been described, including the IL-12 superfamily (IL-27 and IL-35), the IL-2 superfamily (IL-15 and IL-21) and one in which I became particularly interested namely the IL-1 superfamily - specifically (IL-18 and IL-33). IL-1 family members share homology of sequence, gene location, structural dimensions and binding to their receptors [160].

1.4.1 Interleukin 18 (IL-18)

IL-18 is recognised as a cytokine of IL-1 superfamily, but was initially identified as an IFNγ inducing factor produced by murine splenocytes upon endotoxin stimulation. Within the family it has closest sequence homology to IL-33 [161]. A wide range of cells of both non haemopoietic or haemopoietic lineages express IL-18; these include dendritic cells, macrophages, kupffer cells, osteoblasts, adrenal cortex, intestinal epithelial cells, microglia, keratinocytes and synovial fibroblasts [161-166]. IL-18 is synthesized as a 24-kDa inactive precursor, which is cleaved to a mature active 18-kDa form by IL-1β converting enzyme also know as caspase-1 [167]. Active mature IL-18 signals via heterodimer receptor complex, which includes IL-18Rα (IL-1RcP) the chain that has an extracellular binding site for IL-18; whereas, the non-binding IL-1Rβ (AcPL) is a signal transducing chain with an accessory cell surface protein and both these chains are vital for IL-18 signalling [168].

IL-18 receptor (IL-18R) is expressed on a variety of cells, including macrophages, natural killer (NK) cells, neutrophils, smooth muscles and endothelial cells. Stimulation by IL-12 up regulates IL-18R on Th1 cells and B cells; in fact IL-18Rα is a marker for Th1 cells. The IL-18 ligand binding to its receptor result in engagement of adaptor proteins like MyD88 and IL-1 receptor associated kinase (IRAK), to promote the NF-κB nuclear translocation [161]. In vivo activity of IL-18 is regulated by a high affinity binding protein (IL-18BP) and also by a naturally occurring soluble IL-18Rα chain.

IL-18 is present in synovial membrane of patients with rheumatoid arthritis as both precursor (24-kDa) and mature (18-kDa) forms. Its expression is seen in macrophages and fibroblast like synoviocytes (FLS) in situ and along with IL-12 showed a synergistic property in supporting a Th1 inflammatory response [162, 169]. IL-18 induces monocyte maturation and activation resulting in the release of cytokines; it also causes degranulation of neutrophils and enhances the release of chemokines and cytokines by them. In concert with IL-12 it inhibits osteoclasts maturation, which then retards bone erosion [170]. IL-18 deficient mice are resistant to the development of collagen-induced arthritis; these mice exhibit both a reduction in inflammation and bone erosion.

To establish the proinflammatory role of IL-18 in the context of rheumatoid arthritis, patients were treated with the recombinant IL-18BP in phase I study; this trial did not show clinical efficacy. The lack of efficacy in this study could be due to redundant downstream signalling of IL-18 in the synovium or perhaps the intrinsic properties of the blocking agent employed [171].

In the experimental model of atherosclerosis i.e. $ApoE^{-/-}$ mice administration of IL-18 antibodies accelerated plaque formation. However, IL-18BP inhibits the proinflammatory effects of the IL-18 and not only resulted in a stable phenotype of the lesion but also caused reduction in size of the plaque [172]. In another study atherosclerotic lesion size were markedly reduced in double knock out mice (IL-18 and $Apo^{-/-}E$) that further elaborated the proinflammatory role of IL-18; whereas, Immunoglobulin subclass analysis revealed a Th2 phenotype dominance and reduced INFγ production. Interestingly, the lipid profile established that IL-18 somehow reduces the serum cholesterol [173]. To establish a mechanism for proatherogenic role of IL-18 in $ApoE^{-/-}$ exogenous administration exaggerated lesion formation and lack of INFγ in the same mice attenuated the response generated by IL-18; which strongly suggests that this is an INFγ dependent response [174].

1.4.2 Interleukin 33 (IL-33)

IL-33 a novel addition to the IL-1 superfamily (also abbreviated as IL-1F11) is a ligand for the IL-1 family receptor T1/ST2 found on mast cells and Th2 cells. IL-33 is produced as a 30-kDa protein that can induce production of Th2 cytokines like IL-4, IL-5 and IL-13[175]. It was proposed initially that IL-33 has a full-length form that can be processed to a more active form like IL-1β and IL-18. Interestingly, it was subsequently shown that caspase-1 mediated cleavage caused inactivation of IL-33 [176]. A similar in vitro observation has demonstrated that it is actually the full length form which is biologically active [177]. Moreover, apoptosis associated caspases like 3 and 7 caused inactivation of IL-33, which was seen as a reduction in NFκB activation [178]. However, it should be appreciated that full length IL-33 is released from necrotic cells by damage through infection or trauma and this probably mediates its most important effector physiologic function.

The biological effects of this cytokine are mediated when it binds to both the T1/ST2 and it's co receptor IL-1 receptor accessory protein (RAcP) - both of them form a receptor complex [179]. Interestingly, this co-receptor is common to other members of the IL-1 superfamily like IL-1α, IL-1β and IL-1F6 to IL-1 F9 for downstream signalling [180]. Like other IL-1 family cytokines IL-33 upon binding to its receptor results in ERK, P38, mitogen activated protein kinase (MAPK), NF-κB and JKN activation [181] (Figure 1.5). IL-33 has the properties of a cytokine; however, the nuclear localization and transcriptional properties exhibited by this cytokine suggested a close link to IL-1α and High mobility group box 1 (HMGB1) [182].

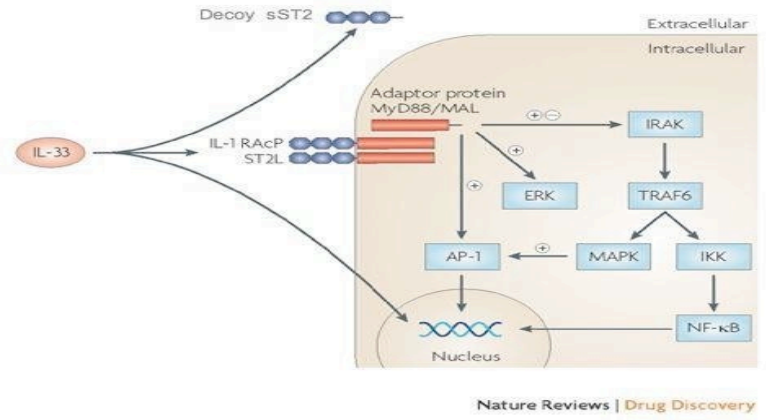

Figure 1.5 A model for IL-33/ST2 signalling T1/ST2 Receptor

ST2 is a member of toll like/IL-1 superfamily with several designations like IL1RL1, DER4, FIT-1 and T1). The IL-1 family receptors share a unique intracellular domain termed as Toll/Interleukin-1 receptor (TIR) domain, which comprises of a central core of five stranded β-sheets surrounded by 5 alpha helices. Beside the intracellular cellular TIR domain these receptors have a transmembrane fragment and an extracellular domain that contains three immunoglobulin like motifs. Since the initial discovery of ST2 in 1989 four isoforms of ST2 (sST2, ST2L, ST2V and ST2LV) have been identified [183-187]. The membrane bound form ST2L (IL1RL1-b) has all three basic components i.e.

extracellular, transmembrane and intracellular domains (Figure 1.5, (modified from therapeutic targets and novel biomarkers) [188]. The soluble form sST2 (also known as IL1R1-a) lack the intracellular domain and it has a unique nine amino acid sequence at the C-terminal [184, 189]. Interestingly, the expression of both these variants differs from the membrane bound form ST2L that is constitutively expressed on surface of mast cells and Th2 cells. The sST2 is more of an inducible form expressed upon appropriate stimulation of fibroblasts, mammary tissue, retina and osteogenic tissue. Moreover, the human gastrointestinal organs like stomach, spleen, small and large intestine predominantly express the ST2V; whereas, ST2LV is found on various tissues like cerebral, ocular, pulmonary and cardiac in the second half of embryogenesis [188].

1.4.2.1 IL-33 in RA

Different experimental models have revealed that IL-33/ST2 signalling can have both inflammatory and protective properties, for example soluble ST2 (sST2) administration in mice reduces the mortality caused by LPS challenge by down regulating the proinflammatory cytokines [190]. Yin H et al demonstrated a protective role for sST2 in a TLR4 mediated hepatic ischemic reperfusion injury [191]. The administration of sST2 in mice cause reduction in joint erosions, synovial hyperplasia and cellular infiltration in a model of collagen-induced arthritis (CIA) supporting this notion [192]. In addition, lack of ST2 receptor in mice attenuated disease in CIA; moreover, administration of IL-33 in ST2 deficient mice engrafted with wild type mast cells resulted in joint inflammation suggestive of IL-33 mediated mast cells activation [193]. Mast cells are implicated in the pathogenesis of RA in fact mast cell deficient mice are resistant to the development of disease and implanting mast cells restored joint inflammation [194], which might suggest that mast cell activation occurred through IL-33 activity.

1.4.2.2 IL-33 in CVD

Human and animal data suggest that IL-33/ST2 signalling has an imperative role in the pathophysiology of cardiovascular diseases. Serum concentration of sST2 are elevated in patients with acute heart failure [195]. High levels of serum sST2 were strongly correlated with increased future mortality in patients of acute

destabilized heart failure [196]. The potential of ST2 as a biomarker was highlighted when myocardial injury caused ST2 release in the patients; both the transmembrane form and the soluble form was induced, with soluble form dominating [197]. Therefore serum sST2 levels were analyzed in about 800 patients presenting with acute myocardial infarction, which predicted mortality and heart failure in the patients [198].

In an experimental model of atherosclerosis mice on high fat diet were treated with IL-33, which markedly reduced the plaque size through Th2 cytokines like IL-5; whereas, the administration of sST2 blocked this regulatory loop and increased atherosclerotic plaque [199]. In fact immunisation of mice with MDA-LDL an oxidation specific neo epitope resulted in an IL-5 dependent increased production of T15 IgM natural antibodies. This highlighted the fact that IL-5 can connect adaptive immunity to innate immunity [139]. So if IL-33 is mediating its cardioprotective effects through IL-5 then there seems to be a link between IL-33 and natural antibodies, which need to be investigated. Sanada et al demonstrated that biomechanical stress induced IL-33 release by cardiac fibroblasts resulted in reduced cardiac hypertrophy and fibrosis. In contrast ST2 deficient mice observed ventricular hypertrophy and impaired survival, in a volume overload model with aortic constriction compared with untreated controls [200].

1.5 Hypothesis and Aims

The immunopathological process in RA is characterised by ongoing immune responses that result in joint destruction. This autoimmune condition is strongly linked with cardiovascular morbidity. How the vascular environment influences the RA immune response and vice versa, contributing to high cardiovascular risk in RA, remains unclear. Some of the questions to be addressed in this thesis are detailed below.

a) Citrullinated protein is an RA associated self-antigen. Due to the high specificity (>98%) of ACPA in diagnosing RA patients, we must consider the significance of CP in the aortic adventitia.

- Does the inflammatory environment associated with CVD and RA alter the level of RA associated self-antigens in the aortic adventitia?

b) B lymphocytes have been documented in the aortic adventitia but we do not know whether the presence of B cells is different between CVD patients with or without RA. In addition, the factors mediating B cells survival in this disease-associated site remain obscure.

- Is the presence of B cells altered in RA vs. non-RA and are survival niches present in the aortic adventitia?

C) Atherosclerotic plaques contain inflammatory cells and cytokines (predominantly T cells, macrophages, IL-18) that appear to contribute to lesion formation.

- What is the difference in macrophages and IL-18 expression between RA and non-RA patient's vascular adventitia?

d) The IL-1 family cytokine IL-33 is reported to reduce lesion size in the experimental model of atherosclerosis.

- Which cells express IL-33 in human atherosclerotic lesions, and how is it different in RA patients?

e) B lymphocytes are atheroprotective, whereas, the clinical efficacy of B cell depletion therapy in RA identifies a pro-inflammatory role for B-lymphocytes.

- What will be the impact of B cells depletion therapy on atherosclerosis?

The aims of the study were to

- Examine the presence of citrullinated protein, a potential auto-antigen of rheumatoid arthritis, in human aortic adventitial biopsies and correlate this to B-lymphocytes and their survival niches (BAFF & APRIL) in rheumatoid patients.

- To investigate the effects of hypoxia and oxLDL on BAFF and APRIL in cultured vascular endothelial cells.

- To establish the expression of Interleukin 33 (IL-33) in human aortic adventitia and murine vascular endothelial cells and explore the impact of Oxidized LDL and hypoxia on its protein and gene expression.

- To investigate the impact of B cells depletion therapy with Rituximab (a monoclonal antibody against CD20 receptor) on lesion development in the experimental model of Atherosclerosis.

2 Methods and Material

2.1 Human Biopsy samples

The human aortic adventitia and Internal mammary artery (IMA) samples were from the Feiring Heart Biopsy study; biopsies were obtained from Patients undergoing coronary artery bypass graft (CABG) surgery. On the ventral aspect of the ascending aorta 1–3 punch holes were made from areas with less atherosclerotic lesions through the vessel wall; these areas were selected for proximal aortico-coronary anastamoses. Subsequently, part of the adventitia covered by the epicardium was removed from the biopsies, fixed in formalin and paraffin embedded. A total of 40 aortic adventitia and 33-matched internal mammary artery biopsies were used in the present study. All the patients gave written informed consent. Regional Ethics committee for Medical Research Norway approved the Feiring Heart Biopsy study.

2.1.1 Immunohistochemistry

The architecture of AA is primarily composed of adipocytes; which are signet rings shaped fat cells. The issue with these tissue samples was there limited number and they would pick lot of back ground staining. Therefore, the stainings were first established on RA synovium or human tonsil using different antigen retrievals, secondary antibodies and blocking systems and then the adventitias were stained with established protocols. These biopsies were stained for different cytokines, proteins and receptors; details of the primary antibodies, retrieval system and secondary antibodies are listed (Table 2.1).

Table 2.1. Details of antibodies and antigen retrieval system used in staining of human biopsy samples

Antibody	Clone	Source	Antigen Retrieval	Staining system
Citrullinated peptide	07-377	Upstate, Lake placid, NY, USA	Trypsin, 37C, 15 min	Horse anti Rabbit ImmPRESS
CD20	L-26	DAKO Cytomation	MW* 500w 15 min	Horse anti mouse ImmPRESS

Plasma cells	Vs38c	DAKO	MW* 500w 15 min	Horse anti mouse labeled with FITC
BAFF	Buffy-2	Alexis Biochemical	MW* 500w 15 min	ABC§
APRIL	Aprily-8	Alexis Biochemical	MW* 500w 15 min	Horse anti mouse ImmPRESS
CD68	MO 876	DAKO Cytomation	MW*, 500w 15 min	ABC§
IL-18	11.51 E3E1		MW*, 500w 15 min	ABC§
IL-33	Nessy-1	Alexis Biochemical	MW* 500w 15 min	Horse anti mouse ImmPRESS

MW*: microwave citrate buffer, pH 6.0 for antigen retrieval
ABC§: Biotinylated horse Pan-specific secondary antibody (Avidin biotin complex staining system)
Impress: Peroxidase linked secondary antibody, Vector laboratories.

The RA synovium, human tonsil and biopsy samples were stained using the following steps.

2.1.1.1 Deparaffination and hydration

Paraffin embedded sections cut 4-5 μm thick were mounted on electrostatically or Polysine coated microscope slides (BDH), which were then used for immunohistochemistry. Initially, the slides were incubated at 65^0C for 1 hour to soften the wax. Then the sections were deparaffinised in Xylene for about 10 minutes. After this the tissues were hydrated by sequential incubations at 100%, 90%, 70% ethanol 3 minutes each and then into distilled water for 5 minutes. The endogenous peroxidase activity was blocked with 0.5% hydrogen peroxide (Appendix 1, a) for 30 minutes at room temperature.

2.1.1.2 Antigen Retrieval

Two antigen retrieval methods (citrate or trypsin) were used depending on the stainings performed. Antigen retrieval by citrate buffer (Appendix 1, b), was performed by microwaving 500-600ml of buffer into a suitable container for 5

minutes. The slides were added to the container with buffer already heated to boiling. The sections were heated further in the microwave at high power for 8 minutes. Then they were allowed to cool down for another 15 minutes. (2) the antigen retrieval used for citrullinated peptide staining was done with the enzyme trypsin. In trypsin retrieval the sections are covered with the trypsin working solution (Appendix 1, e) and incubated for 15 minutes at $37^{O}C$ and then left for 5 minutes at room temperature. This was followed by 5 minutes wash twice in the TBS buffer (Appendix 1, c).

2.1.1.3 Non specific binding block

Subsequently, for every staining procedure non-specific binding was blocked with 5% normal horse serum for 30 minutes at room temperature. The optimum concentrations of primary antibodies and subtle changes in the order of the steps explained so far and different retrieval systems adapted are listed in (table 2.1 & 2.2). However, the incubation period for the primary antibodies for all the stainings performed was at 4 ^{O}C overnight.

2.1.1.4 Secondary antibody and mounting of section

On the second day the sections were brought to room temperature. After washing the sections in the TBS buffer (Appendix 1, c) they were incubated for half an hour with an appropriate secondary antibody. The secondary staining system mostly used (table 2.2) was an antibody coupled to peroxidase (Immpress kit, Vector laboratories). Finally, the staining was developed with Impact DAB (Diaminobenzidine) and after washing the slides in running water the sections were counter stained with hematoxylin and after the final wash in TBS buffer (Appendix 1, C) sections were mounted with a cover slip using DPX (Di-N-Butyle Phthalate in xylene).

2.1.1.5 Additional steps performed for Pan specific Biotinylated secondary antibody

Whenever the secondary antibody was not conjugated directly to HRP, a biotinylated antibody was used as a secondary; this was associated with additional steps, including the blocking of endogenous avidin, and a 30 minutes

incubation with avidin biotinylated horseradish peroxidase macromolecular complex (ABC Vector labs) was performed after application of secondary antibody for some of the stainings as listed in (Table 2.1).

2.1.1.6 Sequence of major staining steps for all the stainings

All the immunohistochemistry as well as the immunofluorescent staining performed on the human AA and IMA was slightly different depending on the stainings done. As their antibody dilutions, antigen retrieval and the staining systems were specific for each staining. The sequence of major steps was specific with subtle differences; details of the order of steps, antibody dilutions, Isotype control and positive tissue used for all the stainings performed are listed in (table 2.2).

Table 2.2. Sequence of major steps performed for all the different stainings.

Antibody dilution	Isotype control	Order of primary steps	Positive tissues
Citrullinated peptide/Protein 1/500	Monoclonal rabbit anti human	a) Antigen retrieval with Trypsin. b) Non-specific binding block with horse serum. c) Overnight primary antibody incubation at $4^{O}C$. d) Endogenous peroxidase block. e) Incubation with peroxidase linked secondary antibody. f) Staining developed with Impact DAB.	RA synovium

CD20 1/100	Monoclonal mouse IgG2a	a) Endogenous peroxidase block. b) Antigen retrieval with citrate buffer. c) Non specific binding block with horse serum. d) Overnight primary antibody incubation at $4^{O}C$. e) Incubation with peroxidase linked secondary antibody. f) Staining developed with Impact DAB.	RA synovium
Plasma cells 1/75	Monoclonal mouse antihuman IgG1	a) Endogenous peroxidase block. b) Antigen retrieval with citrate buffer. c) Non specific binding blocked with horse serum. d) Primary antibody incubation for one hour at room temperature. e) Incubation with peroxidase linked secondary antibody. f) Staining developed with Impact DAB.	RA synovium

BAFF 1/500	Monoclonal Rat anti human IgG	a) Antigen retrieval with citrate. b) Endogenous peroxidase block. c) Non specific binding blocked with horse serum. d) Overnight primary antibody incubation at $4^{O}C$. e) Secondary antibody incubation with biotinylated rabbit anti rat immunoglobulin. f) Avidin/Biotin complex. g) Staining developed with Impact DAB.	RA synovium
APRIL 1/500	Monoclonal mouse antihuman IgG1	a) Antigen retrieval with citrate buffer. b) Endogenous peroxidase block. c) Non specific binding blocked with horse serum. d) Overnight primary antibody incubation at $4^{O}C$. e) Incubation with peroxidase linked secondary antibody. f) Staining developed with Impact DAB.	Human Tonsil

CD68 1/100	Monoclonal mouse IgG1	a) Endogenous peroxidase block b) Antigen retrieval with citrate. c) Incubation with non-specific binding block plus Avidin. d) Incubation with primary antibody and the biotin block. d) Secondary antibody incubation with Biotinylated Pan specific horse immunoglobulin e) Incubation with Avidin/Biotin complex. f) Staining developed with impact DAB	RA synovium
IL-18 1/500	Monoclonal mouse IgG1	a) Endogenous peroxidase block. b) Antigen retrieval with citrate. c) Incubation for non-specific binding block plus Avidin. d) Incubation with primary antibody and the biotin. d) Secondary antibody incubation with Biotinylated Pan specific horse immunoglobulin e) Avidin/Biotin complex. f) Staining developed with Impact DAB.	RA synovium

IL-33 1/200	Monoclonal mouse antihuman IgG1	a) Endogenous peroxidase block. b) Antigen retrieval with citrate buffer. c) Non specific binding blocked with horse serum. d) Primary antibody incubation for one hour at room temperature. e) Incubation with peroxidase linked secondary antibody. f) Staining developed with Impact DAB.	Human Tonsil

2.1.2 Preparation of Modified fibrinogen

Human fibrinogen was modified to citrullinated protein as previously described [23, 201]. Plasminogen depleted human fibrinogen (calbiochem; EMD Biosciences) was incubated at 0.86mg/ml with 10U/ml of rabbit skeletal muscle peptidyl arginine deiminase (sigma Aldrich) in 0.1 M Tris-HCl (pH 7.4), 10mM $CaCl_2$, and 5mM DTT for 2 hours at 50°C. The reaction was stopped by adding 2% SDS and finally heated to 100°C for 3 minutes. Citrullinated fibrinogen was washed with 0.01 M carbonate buffer in Amicon spin column (millipore); this column had a molecular cut off (100kDa) and was centrifuged at 2500g for 10 minutes.

2.1.2.1 Biotinylation of native and modified fibrinogen

Citrullinated fibrinogen and native fibrinogen were both biotinylated using the NHS-LC biotinylation kit (Pierce Biotechnology). A concentration of 10mM sulpho-NHS-LC-Biotin was prepared by dissolving 2.2mg in 400µl ultra pure water. Then as per manufacturer's guidelines, the correct volume of biotin solution was added to the citrullinated fibrinogen and native fibrinogen and they were

incubated on ice for two hours. Biotinylated fibrinogen was later used as negative control in staining of antibodies to citrullinated protein.

2.1.2.2 Preparation of "a citrulline rich sample" cornified skin cell lysates

Human cornified skin is known to have CP; to generate a positive control for western blot analysis of citrullinated fibrinogen, we processed cornified skin cells that were collected from the forearm using a 12.5cm long scotch tap. Scotch tape was pasted on the forearm and rubbed 3-5 times along the length. The tape was placed in a Petri dish with both ends secured, cells were lysed by addition of 200µl of SDS-PAGE lysis buffer (Appendix 1, f). The cells were rubbed with a cell scraper. Cell lysates were collected into an eppendorf and heated at 95^{o}C for 5 minutes; this was then allowed to cool down. The lysates were centrifuged at 10,000rpm for 5 minutes to get rid of the cell debris. Finally, protein concentration was determined with the nano drop (Thermo scientific) and stored at -20 ^{o}C.

2.1.3 Western Blotting

2.1.3.1 Sample preparation

The cell lysates or proteins prepared as explained above were quantified using nanodrop (Thermo scientific) and equal concentrations of each protein sample were then used in the later stages. The samples were made by mixing LDS sample buffer (Appendix 2, c), reducing agent (Nupage, Invitrogen) as per manufacturer instructions and then heated for 10 minutes at 70^{o}C.

2.1.3.2 Electrophoresis

The Novex 4-12% Bis-Tris gels (Invitrogen) were used for the electrophoresis. After setting the gel cassette in the cell, both the upper and outer buffer chambers of cell were filled with appropriate volume of the running buffer (Appendix 2, a). Then an appropriate molecular weight marker for proteins and similar concentrations of the sample proteins were loaded onto the gel. The gel was run for 35 minutes at 200 volts.

2.1.3.3 Coomassie staining

To confirm the electrophoresis of different proteins used; coomassie staining was done to see various bands for each protein. After electrophoresis the gel was put in a fixative solution (Appendix 2, d) for 10 minutes. The gel was then stained with Coomassie blue (invitrogen) for 10 minutes with gentle shaking. A series of washing was carried out using destain solution (Appendix 4, f). This was followed by an overnight destain; which resulted in visualization of distinct bands for a variety of proteins. The solutions mentioned were prepared using the recipes stated in the appendix.

2.1.3.4 Transfer of Proteins to PVDF membrane

The western transfer followed the electrophoresis; which is completed using the invitrogen Blot module (as per manufacturers instructions). After carefully removing the gel from cassette, the gel and methanol soaked PVDF membrane was put together. It was ensured that there were no bubbles between the gel and membrane. Subsequently, the gel membrane was sandwiched between filter paper and blotting pads. The gel-membrane assembly within the blot module was tightly locked in the cell. The inner buffer chamber was filled with transfer buffer (Appendix 2, b); whereas, the outer chamber was filled with distilled water. Finally, the transfer of protein was carried out at a continuous 30 volts for 1 hour.

2.1.3.5 Immunostaining for proteins

The Immunostaining of the proteins on the PVDF membrane was started with a non-specific binding block. An incubation of one hour at room temperature with a blocking buffer; which was prepared by adding 5% non-fat milk marvel (premier International Foods, Lincs, UK) in TBST buffer (Appendix 1, c) The blocking buffer was removed and the detection antibody (pooled sera from RF positive RA patients) was added to the membrane. Patients sera was diluted to 1:100 in 5% dried skimmed milk/TBS plus 0.05% Tween; the PVDF membrane was incubated with patient's serum for overnight at 4^0C with gentle agitation. Next day the PVDF membrane was washed thrice with TBS plus 0.05% Tween for 5 minutes; then an HRP conjugated goat anti-human IgG (Southern biotech) was

used as a secondary antibody. This antibody was used at a dilution of 1:8000 in 5% dried skimmed milk/TBS plus 0.1% Tween and incubated for one-hour at room temperature. This was followed by a 3 times wash with TBS plus 0.05% Tween. Finally, the staining was developed for 5 minutes with chemiluminescent super signal (Pierce) and visualized by developing x-ray film (Kodak) using the developer (Konica Minolta, SRX101).

2.1.4 Double Fluorescent staining of RA synovium and Aortic adventitia

To establish the presence of plasma cells secreting antibodies to citrullinated proteins a double fluorescent staining was performed on paraffin embedded RA synovium. Initially the slides were incubated in the oven at 65^0C for one hour to soften the wax. The sections were deparaffinised in xylene and serially passed through graded alcohol i.e. 100%, 90%, 70% and finally to distilled water for properly hydrating the samples. Explained in detail (section 2.1.1).

The antigen retrieval was performed using citrate buffer (Appendix 1, b), which was done by microwaving 500-600ml of buffer into a suitable container for 5 minutes. After heating the buffer, sections were added to it. The slides were heated further in the microwave at high power for 8 minutes. Then the sections were allowed to cool down for about 15 minutes, slides were then washed in TBST twice for 5 minutes.

Subsequently, the sections were blocked for non-specific binding by incubating them with 2.5% goat serum for 30 minutes at room temperature. This was followed by a two-step Avidin/biotin block of 15 minutes each. After this the tissues were incubated with biotinylated-modified citrulline (10μg/ml) overnight at 4^oC.

The following day slides were left at 25^0C for half an hour to bring them to room temperature. To identify the binding of biotinylated modified citrulline in the tissues, staining was performed using a straptavidin conjugated QDOT 605 (invitrogen) at a 1:250 dilution. After this the tissues were blocked again but this time with 2.5% horse serum for 30 minutes at room temperature. This was followed by a two times wash in TBS plus 0.05% Tween for 5 minutes each.

Sections were further incubated with monoclonal anti-plasma cell antibody (Vs38c, DAKO) for 2 hours at a concentration of 2μg/ml in a humidified chamber (Table 2.1). The secondary antibody was selected carefully to make sure that the spectra of the fluorophore used in the double staining do not overlap, which might complicate the analysis. Therefore, slides were incubated with FITC labeled anti mouse IgG (15μg/ml, Vector); this resulted in green colored staining of the plasma cells. To stain the nuclei sections were mounted with medium containing 1.5μg/ml DAPI (Vectashield).

Finally, the staining was analyzed with the laser scanning cytometer (LSC, Compucyte). First the antibodies reactive to citrulline (red color) were located in the stained sections and images were captured. Then the plasma cells staining (green color) and nuclear staining with DAPI (blue color) was confirmed. Subsequently, all the images were merged to establish antibodies secreting plasma cells in the tissues. A similar sequence was followed for the Isotype controls; importantly, the exposure time and contrast enhancement were kept constant for both the positive and Isotype controls.

2.1.5 Scoring and statistical analysis

2.1.5.1 Scoring of stained tissues

A blinded observer scored all the stainings performed on 40 human aortic adventitia and 33 paired IMA. Visually counting number of cells per high power field for stainings of surface markers or intracellular staining; whereas, if staining was not only confined to cell surface and involved extracellular compartment then scores were recorded as percentage area per high power field. The raw data for scores was analyzed for normality. The normally distributed data (Citrullinated protein) staining in Aortic adventitia was further analyzed by calculating the mean percentage area. However, for all other stainings i.e. CD20, APRIL, BAFF, IL-18 and CD68 there was a non normal distribution so a median percentage area/HPF was calculated to complete the analysis.

2.1.5.2 Statistical analysis

The data was statistically analyzed by student's t-test to determine the statistical significance, when comparing two groups for normally distributed data. However, the data not following a normal distribution were analyzed for differences in quantitative variables by Non parametric Mann Whitney U test to determine the statistical significance, with a P value of <0.05 considered significant. Graphs are displayed as dot plots to clearly illustrate the details of scores for individual specimen. Finally, the associations between CRP vs. ACPA were analyzed using Fisher's exact test. All the statistical analyses were performed using GraphPad Prism version 4 for Mac (GraphPad Software).

2.2 Effects of Oxidized LDL on cultured cells

2.2.1 Human endothelial cell culture

Primary cultures of human sephenous vein endothelial cells HSVEC passages 3 were kindly provided by Professor Andrew Baker, University of Glasgow. Cells were maintained in T-75 flasks in endothelial cell basal medium MV2 and supplement pack (Promocell) included; Fetal Calf Serum 5%, Epidermal Growth Factor 5.0ng/ml, Hydrocortisone 0.2µg/ml, Vascular Endothelial Growth Factor 0.5ng/ml, basic Fibroblast Factor 10ng/ml, R3 IGF-1 20ng/ml, Ascorbic Acid 1µg/ml. The endothelial cells were cultured to full confluence, as checked by light microscopy and were then split; the media was taken off and cell monolayer was rinsed with 1x PBS (Sigma) at room temperature. The monolayer was trypsinized with 5ml of 1x of 0.5% trypsin EDTA (Sigma) at 37^0C for 5 minutes. The flask was banged a couple of times and 10 ml of media MV2 was added to stop the enzymatic action of Trypsin EDTA. To wash the collected trypsinzed cells they were put in a universal and spun at 1500rpm for 10 minutes. Cells were washed again in fresh media. Media was again taken off and cells were resuspended in 10ml of media MV2. Approximately 20% of the cells were used to seed a T-75 flask. Cells were used for experiments between passage 3 and 5.

2.2.2 Murine endothelial cell culture

A mouse lymphoid vascular endothelial Cell line SVEC4-10 [202] was also generously provided by Professor Andrew Baker, University of Glasgow. The Mouse lymphoid endothelial cell line, Immortalized by simian virus 40, were grown in T-75 flasks in Minimum essential medium Eagle MEM (Sigma) supplemented with 200 mM L-Glutamine (GIBCO), Pen-strep 10,000 units (GIBCO), sodium pyruvate (Sigma) 100mM and 10% FCS (Sigma). Media was changed twice a week. Cells were split as required and passaged as discussed above for human endothelial cells.

2.2.2.1 Murine cell culture in T-25 flasks

To look for the effects of OxLDL on IL-33/sST2 expression, cells were grown in vented T-25 flasks (Corning); for all the treatment groups T-25 flasks were seeded with equal number of cells and the confluence of monolayer was confirmed under light microscopy. After taking off the media the cells were washed 1xPBS at room temperature. This was followed by the monolayer harvest using the cell scraper (Corning). The scraped cell were washed with media and collected in a 15ml tube. They were then used to extract RNA as described in the following section.

2.3 Polymerase chain reaction (PCR)

2.3.1 RNA isolation

Human saphenous vein endothelial cells (HSVEC) and mouse endothelial cell line SVEC4-10 were grown in Endothelial cell basal medium MV2 and MEM respectively. They were exposed to oxLDL and nLDL at a concentration of 80 μg/ml in the relevant media for different time points i.e. 6hrs, 12hrs, 18hrs and 24hrs in T-25 flasks; cells were harvested from these tissue culture flasks as explained earlier in (section 2.2.2) and transferred to RNAase free 1.5 ml eppendorf. They were spun for 5 minutes at 1000 rpm and supernatant was discarded. To isolate intact RNA from HSVEC and SVEC4-10, 350 μl RLT buffer (supplied with RNeasy mini column kit by QIAGEN) was added to cells pellet in the eppendorf. RLT buffer is used for lysis and homogenisation of biological samples in the presence of highly denaturing guanidine isothiocyanate [GITC]

containing buffer that immediately inactivates RNases to ensure isolation of intact RNA. To purify RNA from the samples, the protocol of RNeasy minicolumn kit (QIAGEN) was followed as per manufacturer instructions.

Purified RNA samples were quantified on an eppendorf biophotometer. Uniform RNA concentration in each sample was confirmed by agarose gel electrophoresis. Samples were loaded on 1% agarose gel stained with Ethidium Bromide. Gel scanning with alphaimager Mitsubishi P91D (FujiFilm) was performed to ensure that all samples were similar in terms of intensity of fluorescent signals from each band.

2.3.2 First strand cDNA synthesis

The complementary DNA (cDNA) was synthesised according to the protocol described by manufacturer (Invitrogen) using reagents supplied with the Superscript™ III First-Strand Synthesis System. 1µl of RNA was diluted in 4µl of RNase-free H_2O and was adjusted to 2µg/µl RNA by mixing calculated volumes of diluted RNA and RNase-free H_2O. 1µM oligo dt and 1µl dNTP were added to each sample. Samples were placed in the thermocycler (BIO-RAD) for 5 minutes at 65^0 C and then on ice for 1 minute. The cDNA synthesis mix was prepared on ice by mixing 2µl of 10x RT buffer, 4µl 25mM $MgCl_2$, 2µl 0.1M DTT, 1µl RNaseOUT and 1µl SuperScript III Reverse Transcriptase. 10µl of cDNA Synthesis mix was added to each sample. For the control samples Superscript III Reverse Transcriptase was replaced by equivalent volume of RNase-free H_2O.

Samples were placed in the thermocycler for 50 minutes at 50^0C. Afterwards, raising the temperature to 85^0C for 5 minutes terminated the reaction. 1µl RNase H was added to each cDNA sample to remove any RNA and finally placed at 37^0C for 20 minutes. cDNA was stored at -20°C.

2.3.3 PCR

The PCR amplification was carried by using 2µl of cDNA of different genes. The cDNA was added to each PCR reaction, containing 10µl of PCR master mix (promega), 1µl of forward and reverse primers, 2.5mM dNTP (Biolab) and 35µl of RNAase free H_2O.

The PCR reaction was initiated with 1 cycle of denaturation for 5 minutes at 94^0C. The reaction was further programmed to 94^0C for 30sec, 55^0C for 30 seconds and at 72^0C for 30 seconds. Finally, a single cycle for extension of the product was set for 10 min at 72^0C. This standard thermal profile was used for the PCR performed for different genes in the study; except for the annealing temperature that were specific for most of the genes and are listed in (Appendix 6).

2.3.4 Quantitative PCR

2.3.4.1 Normalisation of cDNA samples

To allow effective comparison of gene levels between samples, normalisation of cDNA levels was undertaken. The amount of cDNA between samples can inadvertently be varied by multiple factors including: variation introduced during RNA extraction, differential RNA degradation, the amount of RNA used in the reverse transcription reaction and the reaction efficiency of the reverse transcription. This variation was reduced by; 1) Using exactly 5 μg of non-degraded total RNA (as determined by OD); 2) All samples that were directly compared within a quantitative PCR were reverse transcribed using the same master mix to avoid inter-day and inter mixture variability in reverse transcriptase activity; and 3) Housekeeping genes like GAPDH and β actin were used to normalise samples.

The cDNA samples were diluted 1 in 5 in nuclease free water and used as template for QPCR. Samples that were to be directly compared within a quantitative PCR were reverse transcribed using the same master mix to avoid inter day and inter mixture variability in reverse transcription activity.

2.3.4.2 Primer Design

A set of “inner” primers was designed for use in the quantitative PCR machine and an “outer” set of primers was designed for creating PCR products to act as standard templates. All primers were designed using the Primer3 software (Steve Rozen and Helen J. Skaletsky).

QPCR Primer specification were as follows:

- between 18 and 23 base-pair (bp) in length
- between 40 and 65% GC content (50% optimal)
- Tm of primers within 59.5^{o}C and 61^{o}C (60^{o}C optimal)
- Maximum self complementarity: 2
- Maximum 3'self complementarity: 1 (most important)
- Amplicon size less than 150bp
- Not more than two G or C bases in last 5 at 3' end of each primer (i.e. don't include a GC clamp)
- Avoid stretches of 4 or more G or C bases in a row

If this did not generate any primers then the max self-complementarity was relaxed from 2 to 3 and the primer Tm down to 59^{o}C. The only condition that was never relaxed was maximum 3 self-complementarity.

Outer primers were then designed to amplify the region in which the QPCR primers bind. These primers were designed with similar parameters although they could possess higher self-complementarity levels if the software could not suggest suitable primers using the above criteria.

BLAST analysis was used to ensure primer that primer sequences were specific to gene of interest alone and that no splice variants exist that could complicate the analysis.

2.3.4.3 Generation of DNA standards for QPCR

The generation of a standard curve is essential for quantifying the levels of the gene of interest in the test samples. A standard DNA template for each gene assayed was generated by taking the PCR product using the "outer" primers,

purifying the PCR product on a PCR purification column as per manufacturer's instructions (Qiagen QIAquick columns) and diluting this product to generate serial dilutions. Each of these dilutions was used as a template for a QPCR using the "inner" QPCR primers for amplification. A range of standards dilutions was used in each QPCR assay. The standard was diluted in nuclease free water and serial dilutions were given arbitrary values that were later used for calculating copies of the target gene.

2.3.4.4 SYBR QPCR protocol

Each sample/standard was performed in triplicate on the QPCR machine. A master mix was prepared for the total number of samples per reaction contained:

- 10μl Power SYBR green mix (Applied Biosystems, or similar mix from Roche)
- 0.8μl of primer mix (each primer mixed together at 50pmol /μl)
- 8μl nuclease free water (Ambion)

6μl of cDNA or standard as appropriate was placed in a "mixing" well, along with 54.5 μl master-mix. This was mixed by pipetting (for the full 54μl); at least three times. Around 19.8μl of this resulting mix was placed in each of the three wells (triplicate) on the QPCR plate. A non-template control (NTC) was included to determine the level of contamination and show the detection limit of the assay. Plate was spun for 20 seconds at 400g to place all contents at bottom of well. Using the 9700HT QPCR machine a standard run was performed, which uses the following reaction conditions:

- Initial 10 minutes at 94^{o}C not repeated
- 3 seconds at 94^{0}C then 30 seconds at 60^{o}C repeated 40 times (measuring fluorescence at the end of each 60^{o}C elongation step)
- Melt/ dissociation stage*

*At the end of the PCR a melt curve analysis was always performed. This measured the fluorescence during an incremental increase in temperature from 65^{o}C to 94^{o}C. This was to establish whether the PCR was specific. At the end of the run to confirm whether the PCR was successful the following things were looked at, the standard curve should have a correlation of r^2>0.97, preferably > 0.98. Additionally, the slope should be equal to 3.3 (which means that the PCR product was amplified by a factor of 10 every 3.3 cycles, which implies that the reaction was 100% efficient).

2.3.4.5 Analysis of QPCR data and stats

Levels of a housekeeping/reference gene were assayed via QPCR to determine the level of cDNA present within a specific sample. Each sample was allocated a ratio of its GAPDH content in relation to the 75th percentile of GAPDH levels of all samples assayed. This ratio was subsequently used to normalise the levels of target gene.

2.4 Lipoprotein isolation and oxidative modification

Blood was taken from 8 healthy volunteers (50ml each) for lipoprotein isolation. The blood was collected in 0.4mmol/l EDTA after 12hrs of fasting. To obtain plasma, blood was centrifuged at 3000rpm at 10^{0}C for 30 minutes. LDL was isolated using density adjustment of plasma (Plasma volume 150 ml) with sodium bromide (NaBr. Alfa Aesr) and four days of discontinuous ultracentrifugation at 50,000rpm, 10^{0}C in a Beckmen L-80 ultracentrifuge, using a Ti 70 rotor. The first day the background density of plasma was assumed 1.006 and was adjusted to 1.022 by adding 1.0gm dry salt NaBr to 50ml of plasma. This adjusted plasma was centrifuged at 50,000rpm at 10^{0}C for 18hrs. On the second day plasma density was adjusted to 1.020 by adding 28.31gm/L solution of NaBr and again spun at 50,000rpm at 10^{0}C for 18 hrs. On third day plasma density was adjusted to 1.065 by adding 3.24gm of NaBr dry salt and again centrifuged at 50,000rpm at 10^{0}C for 24 hrs. On day four LDL was carefully taken off and 1gm of NaBr was added to it and finally centrifuged at 50,000rpm at 10^{0}C for 24hrs. LDL isolated as described, was dialysed against 5 litres of PBS (with 0.25mM EDTA to protect from oxidation) using a dialysing tube with a molecular cut off (12000-14000 KDa). It was dialysed overnight at 4^{0}C three times. After dialysis the preparation

was passed through an Acrodisc filter (0.45um pore size) to sterilize and remove aggregates. 100μl was set aside for a modified Lowry protein determination. To oxidize the LDL, a final concentration of 10uM $CUSO_4$ was added to LDL (w/o EDTA) at 1mg/ml and incubated for 16-18 hours; EDTA was then added at a final concentration of 0.25mM to stop and protect from re-oxidation. Oxidized LDL was sterilized by passing through Acrodisc filter (0.45mM pore size) and stored at 4^0C in the dark.

2.4.1 Modified Lowry protein assay

LDL was prepared as explained earlier and to measure its concentration we used the modified Lowry protein assay. A 2x Lowry concentrate was prepared by mixing 3 parts copper reagent (Appendix 3) 1 part (1% sodium dodecyl sulphate) and 1 part (1 M NaOH). Just prior to mixing of these three stock solutions. The LDL sample was diluted to an estimated 0.025-0.25mg/ml with a buffer. A standard was prepared from 0.25mg/ml bovine serum albumin (pierce). 400μl of 2x Lowry concentrate was added to every 100μl of sample and mixed thoroughly before incubating at room temperature for 10min. After this 200μl of 0.2N folin reagent (VWR) was added quickly and incubated for 30min. Finally, the samples were analysed using an ELISA plate reader at 500nm (DYNEX revelation 3.2) to obtain OD readings; a standard curve was prepared from the BSA samples and we extrapolated the concentration of LDL samples.

2.4.2 Lipoprotein (Lipo) Electrophoresis

The lipoproteins produced from fasting human blood from healthy donors was modified using copper sulphate. Electrophoresis was performed to confirm that the above-explained process resulted in two separate entities i.e. oxidised LDL and native LDL. A freshly drawn specimen from an overnight fasting individual was used as a control. Assuming that fasting human plasma will show distinct bands for LDL and HDL.

This Agarose electrophoresis was performed using the paragon LIPO Gel kit (Beckman). All the samples to be tested were loaded on to the Lipo gel, 3-5μl of each sample was applied and allowed to diffuse for 5 minutes. This paragon gel was then placed onto the Gel Bridge assembly, in the Paragon Electrophoresis

cell with 45ml of Barbital buffer (Appendix 4). The gel was run at a set voltage of 100 volts for 30 minutes.

The gel was fixed and stained with paragon lipo stain (Appendix 4) for 5 minutes. After serial destain steps the gel was finally dried in a fume hood. The gel was scanned with an alphaimager Mitsubishi P91D (FujiFilm).

2.5 Animal study

2.5.1 Mouse Model

Human CD20 (huCD20^{+}) transgenic mice were kindly provided by Professor Mark J Shlomchick (Yale University, New Haven) [203]. These mice were crossed with Apolipoprotein E knockout mice (ApoE$^{-/-}$) (Jackson laboratory) to produce "huCD20^{+}/ApoE$^{-/-}$ mice". The breeding and maintenance was done by Biological services at the University of Glasgow. Litters were weaned at 3 weeks and tissue samples (tail) were taken and used to determine the genomic expression of the huCD20^{+} and ApoE genes.

2.5.2 Mouse Genotyping

2.5.2.1 Mouse tail sample preparation

Mouse tissue samples (tails) were placed in thin walled 0.2ml PCR tubes. 75μl of alkaline lysis buffer (Appendix 5) was added and incubated at 95°C for 1 hour. To neutralise and stop the reaction 75μl of neutralizing buffer (Appendix 5) was added to the samples. The prepared DNA was used in Polymerase chain reaction (PCR) as described in (section 2.3.3) and stored at -20 °C.

2.5.2.2 PCR reaction conditions for genotyping

The PCR reaction was started with an initial incubation at 94^{0}C for 3 minutes. The reaction proceeded with 35 cycles of; 94°C for 20sec, 64^{0}C for 40 seconds and 72^{0}C for 2 minutes. Four set of PCR were done to ensure the presence of the entire bacterial chromosome in the transgenic mice. Two of these PCRs amplify

regions within the hCD20 gene (exon 2 and 3' untranslated region), and the other two amplify sequences near the two ends of the BAC (5' BAC and 3' BAC) [203]. The sequences of oligonucleotides are as follows: **exon 2**, F, 5'-CACAAGGTAAGACTG CCAAAAATC-3' and R, 5'-ATATACAAGCCCCAAAACCAAAAG-3'; **3' untranslated region**, F, 5'-GGCCTTTGCATGGAGTGAC-3' and R, 5'-AGCCCTGTAGAAAGATAA ATGGA-3'**; 5' BAC**, F, 5'-ATTGTTTGAGTGCTCAGCATG-3' and R, 5'-GGGAAAAACAAT ATTGCCTCC-3'; **3' BAC**, F, 5'-GTTGGAGGT TCTGGTTG CAT-3' and R, 5'-AATTGGCT TAGGATTGGGCT-3' conditions were similar for 3 UTR and 3 BAC; whereas, for Exon 2 and 5 BAC the annealing temperature was different i.e. 58^0C for 50 seconds x35 cylces. In addition 3 primers were used to confirm $ApoE^{-/-}$ and the sequences of oligonucleotides are as follows: **ApoE IMR0180** F 5' GCCTAGCC GAGGGAGAGCCG 3'; **ApoE IMR0181** R 5' TGTGACTTGGGAGCTCTGCAGC 3'; **ApoE IMR0182** R 5' GCCGCCCCGACTGCATCT 3'.

2.5.3 Flow cytometric analysis of mouse blood samples

2.5.3.1 Blood sampling

To determine B cells ($huCD20^+$) in Rituximab/IgG treated ($huCD20^+/ApoE^{-/-}$), mice were bled by venesectioning of the tail. This was performed by placing them in a heatbox maintained at 38°C for approximately 10 minutes to allow dilation of blood vessels in the tail. Mice were restrained; the tail sterilized with 70% ethanol and a sterile scalpel was used to make a small nick in the tail. 70-100μl of blood was obtained using heparinised capillary tubes (Hawksley) and transferred into 1.5ml eppendorf tubes. The whole blood was centrifuged at 4000rpm for 10 minutes and serum was recovered that was stored at -20 °C. The remaining pellet was resuspended in an equal volume of sterile PBS (Appendix 1, d) to compensate for the volume of serum taken from each sample. The blood pellet collected was used for extracting peripheral blood mononuclear cells; the pellet was first mixed with PBS and then with ammonium chloride solution (stem cell technology) at a 9:1 ratio. This RBC lysis solution is buffered and optimized for gentle lysis of erythrocytes, with minimal effect on leukocytes. The sample was mixed by vortexing and incubation for 10 minutes on ice. The remaining cells (PBMCs) were washed twice in FACS buffer (Appendix 1, g). These cells were resuspended in 100μl of FACS buffer with Fc Block (i.e. anti-Mouse

CD16/CD32 or FcγRIII/II, BD bioscience) added as 1μl per 100μl of FACS buffer and then incubated the cells for 5 minutes on ice.

2.5.3.2 PBMC staining

PBMCs from hCD20^{+}/ApoE$^{-/-}$ were stained for different cell surface antigens; CD19-APC (ID3, BD pharmingen), CD3-PE (145-2c11, BD pharmingen), B220-PerCP (RA3-6B2, BD pharmingen), CD21-FITC (7G6, BD pharmingen), CD23-PE (2G8, southern biotech), CD24-PE (BD pharmingen, M1.69), IgM-PE (BD pharmingen), CD11b-PerCP (BD pharmingen, M1.70), IgM-FITC (BD pharmingen, II/41), IgD-FITC (bioscience, 11-26c), CD43-FITC (BD pharmingen, S7) and huCD20-FITC (L-27, BD bioscience). All the staining antibody solutions were prepared by adding 1μl of antibody per 100μl of FACS buffer (Appendix 1, g) except for huCD20, which was made by adding 15μl per 100μl of the buffer. The cells from blood samples were resuspended in 50μl of FACS buffer and to stain these cells 50μl of the staining solution was added to every sample making the final concentration of antibody to be 1:200 and the cells were incubated with these antibodies for 20 minutes at 4^{o}C. After incubating the cells the buffer was decant off and cells were washed twice in 1ml of FACS buffer each time centrifuged at 1600rpm for 5 minutes. Cells were then fixed for later analysis with a 250μl of paraformaldehyde-containing buffer cytofix (BD Biosciences), for 15 minutes at 4^{o}C. Following fixation, 1ml of permeabilization buffer (BD Bioscience) was added to each sample, centrifuged at 1600rpm for 5 minutes, decanted and samples resuspended in 300μl of FACS buffer. Finally, these fixed and stained cells were resuspended in 300μl of FACS buffer and acquired on a FACS calibur (BD biosciences). The resulting data was analyzed using Flowjo (Treestar).

2.5.4 High-fat diet and B cell depletion

High Fat diet

The cardiovascular literature refers to high fat diet as a western diet. The individual components of the diet are; 17.3% protein, 48.5% carbohydrate and 21.1% fat by weight. When the high fat diet is given to genetically susceptible mice (ApoE$^{-/-}$) it results in atherosclerosis. In this study high fat diet (Harlan) was given to huCD20^{+}/ApoE$^{-/-}$ at 6-7 weeks of age until the animals were sacrificed 16

weeks later. The body weight of the mice was regularly monitored during the study to ensure that high fat diet resulted in increase in the body weight of these mice.

2.5.4.1 B cell depletion in huCD20^{+}/ApoE$^{-/-}$ mice

HuCD20^{+}/ApoE$^{-/-}$ mice were given 100μl of 100μg intravenous (iv) injections of Rituximab (Rituxan), or chromopure human IgG (Jackson Immunochemicals) every 4 weeks. To perform iv injections, mice were placed in a heat box at 38^{o}C to ensure dilation of tail vessels. Warmed mice were placed in a restrainer; tails were swabbed with 70% ethanol and injections given in the tail veins. Pressure was applied to the injection site for approximately a minute to prevent further bleeding.

2.5.4.2 Animal euthanasia

At the end of 16 weeks the huCD20^{+}/ApoE$^{-/-}$ mice on a high fat diet were euthanised by a rising concentration of carbon dioxide (CO_2), in accordance with UK Home Office regulations. Mice were transferred to the cleaned plastic chamber connected to a carbon dioxide cylinder. The CO_2 was turned on and the CO_2 concentration gradually increased over several minutes resulting in euthanasia. To ensure that mice were successfully euthanised, we carefully noted that there were no reflexes before doing dissection.

2.5.4.3 Mouse dissection

Euthanised mice were pinned on a dissection board in a supine position so that the ventral aspect of the mice was easily accessible. Their skin was sprayed with 70% ethanol and a small nick was made in the skin with a pair of scissors. The skin was carefully folded to the side to expose the thoracic and abdominal regions. The anterior abdominal muscles were cut using the scissors and the cut was further extended vertically upwards towards the sternum and on both the flanks as well. This resulted in a clean surgical field with all the abdominal organs exposed. A terminal bleed was obtained via the vena cava and the needle was left for perfusion and fixation. Blood samples were used to obtain serum and PBMCs for Flow cytometric analysis as already explained (section 2.5.3)

2.5.4.4 Mouse tissue harvesting

2.5.4.5 Spleen

Spleen was carefully removed by cutting the vessel at the hilum. A single cell suspension was achieved by passing the spleen through a 70-micron cell strainer into 3ml of complete RPMI. Cells suspensions were increased to 10ml with complete RPMI and centrifuged at 400g for 5 minutes. The media was decanted and red blood cells present in spleen samples lysed with 2ml of ACK lysis buffer (Lonza) and incubated for 2 minutes and the cell suspension was increased to a volume of 10ml with complete RPMI and centrifuged at 400g for 5 minutes. The media was decanted and the cell pellet was resuspended in 10ml with complete RPMI. To determine the number of total lymphocytes present in the sample, 50μl of the cell suspension was taken off and mixed with 200μl of media. 50μl of this mix was added to 50μl of trypan blue and placed on a heamocytometer. All together 16 squares were counted (8 from the top left and 8 from the bottom right) and the number of cells corresponded to the total number of million cells in the 10ml cell suspension. The cell suspensions were centrifuged at 400g for 5 minutes, media was decanted and the cell pellet resuspended in FACS buffer (Appendix X) so that cells were at a density of 20 x 10^6 cells/ml. Cells were stained for different cell surface antigens; CD19-APC (ID3, BD pharmingen), CD3-PE (145-2c11, BD pharmingen), B220-PerCP (RA3-6B2, BD pharmingen), CD21-FITC (7G6, BD pharmingen), CD23-PE (2G8, southern biotech), CD24-PE (BD pharmingen, M1.69), IgM-PE (BD pharmingen), IgM-FITC (BD pharmingen, II/41), IgD-FITC (bioscience, 11-26c), CD43-FITC (BD pharmingen, S7) and huCD20-FITC (L-27, BD bioscience). All the staining antibody solutions were prepared by adding 1μl of antibody per 100μl of FACS buffer (Appendix 1, g) except for huCD20, which was made by adding 15μl per 100μl of the buffer. The cells from blood samples were resuspended in 50μl of FACS buffer and to stain these cells 50μl of the staining solution was added to every sample making the final concentration of antibody to be 1:200 and the cells were incubated with these antibodies for 20 minutes at 4°C. After incubating the cells the buffer was decant off and cells were washed twice in 1ml of FACS buffer each time centrifuged at 1600rpm for 5 minutes. The cells were fixed for later analysis with a 250μl of paraformaldehyde-containing buffer cytofix (BD Bioscience), for

15 minutes at 4°C. Following fixation, 1ml of permeabilization buffer (BD Bioscience) was added to the each samples, centrifuged at 1600rpm for 5 minutes, decanted and samples resuspended in 300μl of FACS buffer. Finally, these fixed and stained cells were resuspended in 300μl of FACS buffer and acquired on a FACS calibur (BD biosciences). The resulting data was analyzed using Flowjo (Treestar).

2.5.4.6 Lymph nodes

Different pairs of regional lymph nodes were removed such as popliteal, axillary, mesenteric and cervical. A single cell suspension was achieved by passing the lymph node fragments through 40-micron cell strainer. Cells were resuspended with total of 10ml of complete RPMI and centrifuged at 400g for 5 minutes. Cell pellets were resuspended in 10ml of complete RPMI and aliquot of resuspended cells were taken and manually counted on a chamber slide. Finally, the cell densities were adjusted to 20 x 10^6 cells/ml in warm RPMI and were stained (see spleen details above).

2.5.4.7 Bone marrow

The long bone like femur and tibia of the hind limbs were used for extracting bone marrow. Bones were cleared of tissues completely to avoid contamination with other cells. Then bones were cut at both ends using sharp scissors. The bone marrow was extracted using hydrostatic pressure. In brief, 1ml of media in a syringe with a 25g needle is used to flush the bone marrow out of the bone. The needle and syringe are then used to create a single cell suspension. Cells were resuspended with total of 10ml of complete RPMI and centrifuged at 400g for 5 minutes. Cell pellets were resuspended in 10ml of complete RPMI and aliquot of resuspended cells were taken and manually counted on a chamber slide. Cells were then stained for; CD19-APC (ID3, BD pharmingen), CD3-PE (145-2c11, BD pharmingen), B220-PerCP (RA3-6B2, BD pharmingen), IgM-PE (BD pharmingen), CD11b-PerCP (BD pharmingen, M1.70), IgM-FITC (BD pharmingen, II/41), IgD-FITC (bioscience, 11-26c) FCM as described in (see spleen details above)

2.5.4.8 Heart and aorta

After removal of the spleen, lymph nodes and hind limbs the needle in the vena cava was used to perfuse the circulatory system with PBS for 5 minutes, followed by 10 minutes with paraformaldehyde. The organs like spleen, lymph nodes, bone marrow and blood were harvested for staining and FACS analysis. As the mice were already fixed they remained in the cold room for 6 days. Later, the diaphragm was carefully removed to access the thoracic cavity. The sternum was cut up the midline till the upper end; which is at the nape of the neck and the ribcage was pinned on sides. Viscera within the thoracic cavity were carefully removed to avoid damage to heart and aorta. The heart was firmly held at the base with a pair of forceps and by applying some tension to the aorta it was carefully dissected off its attachments with the posterior wall of the thoracic cage. The aorta was cut proximal to the branch of the brachiocephalic artery and then dissected out from above downwards, up to the bifurcation into the common iliac arteries. The dissected heart and aorta were fixed in formalin for 24 hours and then transfer to 70% alcohol prior to processing tissue (tissue processing machine Shandon); finally the tissues were paraffin embedded.

Sectioning of the heart

Dissected heart with the attached aorta was cut using a sharp blade in a plane parallel to the cross sectional plane of aortic lumen as shown in (figure 2.1). Paraffin embedded formalin fixed sections were cut, Tissue block was pared into the aorta with the microtome set to (20μm) until the tissue was visible at this point the cutting scale is changed to 7μm. Thereafter, sections are cut serially and two sections were placed on each slide. All the aortas were cut till the atria were clearly visible. The sections are heated on a hot plate 60^0C for an hour to dry the sections and then stored at 4^0C.

Haematoxylin & Eosin staining

Heart sections were selected for Haematoxylin & Eosin (H & E) staining; after every two sections a slide was stained. The selected slides were heated in an oven for 35 minutes at 60^0C. Heated slides were dewaxed twice in xylene for 3 minutes. Thereafter, sections were hydrated in graded alcohol (100%, 90% and 70%) 6 minutes each and finally to running cold water for 3 minutes.

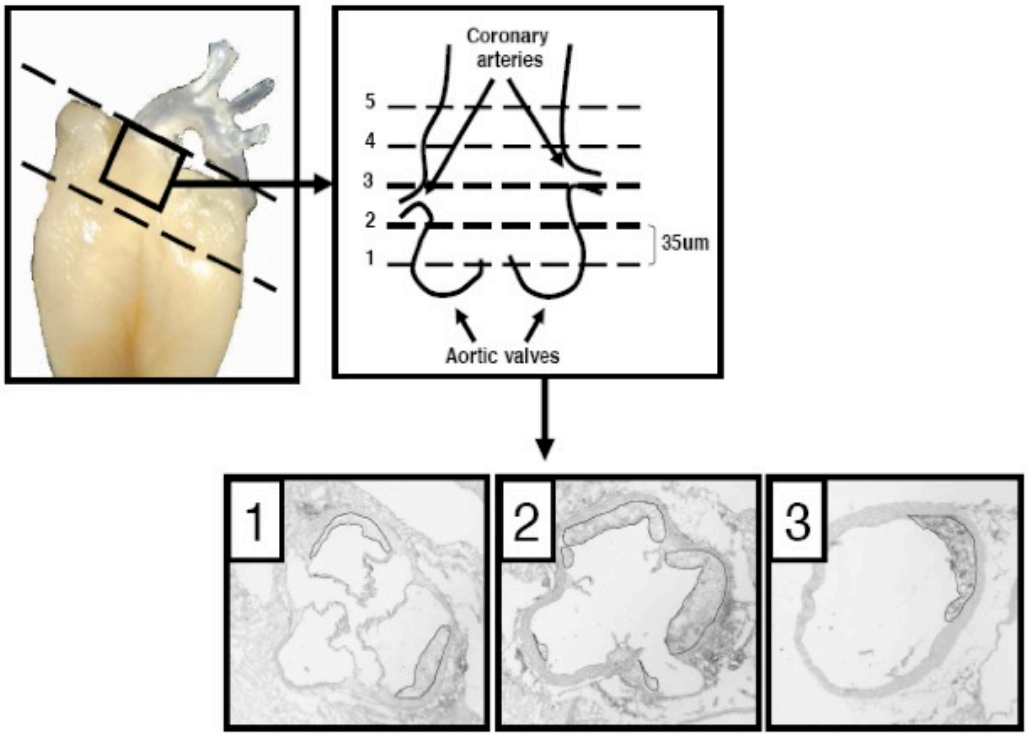

Figure 2.1 A guide to sectioning the heart for cross sectional analysis
The heart was cut at an angle of around 35 degree to the aortic origin as shown in the top left panel. Serial section (7μm) of formalin fixed paraffin embedded aorta were cut from the end where aortic valves were visible towards the ascending aorta as demonstrated in the top right panel. The aortic lumen with valves is demonstrated in (1) as more sections are cut the aortic valves starts to disappear. (2) Finally the aortic lumen can be seen without valves (3), the atherosclerotic lesion is marked

Dehydrated sections were stained with haematoxylin 2 minutes and then washed in running water for 3 minutes. To reduce background, sections were put in 1% acid/alcohol for few seconds and quickly rinsed in running water. Then the slides were placed in tap water for 30 seconds. Thereafter, sections were counterstained with 1% eosin for 2 minutes; excess stain was washed in running water. Tissues were dehydrated through (70%, 90% and 100%) alcohol 1 minute each. Sections were then placed in xylene for 3 minutes and finally mounted with DPX and a coverslip.

Quantification of lesion size

Heart sections stained with H & E were analysed using microscope (Carl Zeiss) mounted with a camera, and pictures were captured with the imaging system on 5x magnification. Lesions were examined in a blinded fashion. Morphometric analysis of the lesions was performed on cross sections through aortic origin by using image analysis software (Axio vision 4.4). The lesions were marked on top of the internal elastic lamina (see Figure 2.1). The aortic lumen and lesion area measurements from 5 sections were then used to calculate the percentage of luminal area obliterated by the lesion. This percentage area was than represented for demonstrating the extent of lesions longitudinally. Some lesions may have sheared off and be in the lumen, those were also measured and used in further analysis. The atherosclerotic lesion area is expressed as the mean of the lesion areas from 5 sections.

3 The cellular composition of human aortic adventitia from coronary bypass patients with rheumatoid arthritis

3.1 Introduction

Rheumatoid Arthritis (RA) is a chronic, progressive, systemic autoimmune disease characterized by joint destruction. This chronic inflammatory ailment results in poor quality of life and also an increase in the development of life-threatening outcomes, such as cardiovascular diseases (CVD). This is evident from the fact that RA patients have a strong association with cardiovascular morbidity and mortality [99, 204]. The underlying disease mechanism of RA is not known but post transitional modification of arginine to citrulline is proposed to be a potential auto antigen, which might be crucial in initiation of this chronic autoimmune disease. In fact the discovery of antibodies to citrullinated peptide/protein (ACPA) has augmented the diagnostic specificity of RA to 90-98% [56]. These disease specific antibodies can appear at early stages of the disease. Therefore, detection of ACPA has greatly improved early diagnosis of RA. However, the presence of ACPA alone is not enough to explain disease onset, therefore additional factors such as citrullinated protein, infections, genetic and environmental factor are all considered important for explaining the underlying disease mechanism. Klareskog et al proposed an etiological model, where an individual with genetic susceptibility and exposure to environmental factors are prone to develop ACPA. If at this point an unspecific stimulus such as trauma and infection leads to citrullination of proteins within the joints, then these target proteins are primed to be bound by circulating ACPA. As a result of this immune complexes are formed that aggravate joint inflammation. (reviewed [205])

Although ACPA antibodies are associated with RA, citrullinated proteins have been detected in disease-associated tissues in numerous inflammatory conditions [30, 206]. Citrullination is a posttranslational modification of arginine to citrulline that occurs under the influence of PADI a calcium dependent deiminating enzyme. This phenomenon is specific to apoptosis and inflammation. In fact there is evidence of PADI 2 and 4 associated with severity of inflammation in RA synovium; with activation of PADI occurring at calcium concentration 100 times more than physiological levels [207]. Nevertheless, to date the presence of citrullinated protein has not been reported in aortic adventitia of animals or humans.

The tunica intima, of the aorta, has been accepted as the classical site of initiation in atherosclerosis, however, there is supporting data that cellular infiltrates are present in both intima and adventitia. The pathological mechanisms that result in inflammatory infiltration of both the layers is unknown, perhaps there are disease-associated mechanisms in both the tunica intima and adventitia. Recent studies have demonstrated that inflammatory rheumatic disease patients undergoing coronary artery bypass graft (CABG) have more pronounced chronic inflammatory infiltration in the media and inner adventitia of the aorta[208].

In 1962 Schwartz et al established adventitial infiltrates in three different blood vessels i.e. iliac, cervical and coronary arteries; these infiltrates were mainly distributed around the vasa vasorum. Further analysis demonstrated that infiltrating cells in the adventitia strongly correlated to atheromatous lesions suggesting a role in the disease pathogenesis [209]. The type of cells present among the infiltrates are very important to know in order to understand the principal mechanism of the disease. The blood vessel of atherosclerotic patients were reported to have plasma cells with immunoglobulin IgM and IgD in the adventitial layer of the blood vessel[210]. Interestingly, B-cell presence is not only reported in human atherosclerotic lesions, in fact the aorta of $ApoE^{-/-}$ has been demonstrated to have B-lymphocytes even before the disease develops. Moreover, adoptively transferred lymphocytes homed to the aortic adventitia through a mechanism involving L-selectin[211]. Recently, Grabner et al established in $ApoE^{-/-}$ mice that lymphotoxin beta (LTβ) induces lymphoid aggregate formation and termed it adventitial aortic tertiary lymphoid organs (ATLOs); which contained B cell follicles, high endothelial venules (HEV), plasma cells and T cell areas[212]. Human aortic adventitia from patients with advanced atherosclerotic lesions showed lymphoid follicle like structures composed of macrophages, B cells and follicular dendritic cells[144]. A brief report on B lymphocytes in two patients with co existing RA and coronary artery disease (CAD) revealed a predominance of B cells in both the plaque and adventitia; this preliminary observation deviates from the dogma of T lymphocyte predominance in atherosclerotic lesions [213]. The presence of B cells in the aortic adventitia lead

us to hypothesize that the aortic adventitia of RA patients favours B cell proliferation and survival.

There is evidence that RA is strongly associated with cardiovascular morbidity and mortality [99, 204]. However, it is not clear how the vascular environment affects the immune component of RA. It has previously been shown that inflammatory rheumatic disease patients have more pronounced chronic inflammatory infiltration in the media and inner adventitia of the aorta [214]. To address whether vascular environment of diseased vessel in terms of cellular composition and cytokine expression differ, and whether this is affected by the immune component of RA, the aortic adventitia from patients with CVD and coexisting RA would be a good resource to explore. Aortic adventitial biopsy samples were obtained in the Feiring heart biopsy study from patients with advanced atherosclerosis of their coronary arteries who underwent CABG. A full medical history was taken from all patients and samples were sub-divided based on co-morbid diagnoses. During surgery, Internal mammary artery (IMA) was used as the grafting vessel, due to its decrease susceptibility to atherosclerosis; a biopsy sample of IMA was taken and used as internal control for our study.

The objective of this chapter was to compare the cellular composition and cytokine expression in 20 RA patients with coexisting CVD to CVD patients without RA. Importantly, the biopsy samples of IMA from 33 matched patients were considered non diseased and used as an internal control. The main aims of the study were:

1. To investigate the expression of an RA-associated self-antigen, citrullinated protein, in the aortic adventitia removed from patients with coexisting Rheumatoid arthritis and cardiovascular disease.

2. Investigate the presence of B cell aggregates and plasma cells in these lesions associated vessel and related them to expression of citrullinated protein.

3. Examine whether the aortic adventitia of RA patients with coronary artery disease had any association with B cell survival factors like BAFF and

APRIL, which might provide a supportive niche for the differentiation and survival of B cells.

3.2 Results

3.2.1 Patients characteristics

The human aortic adventitia and Internal mammary artery (IMA) samples were from the Feiring Heart Biopsy study; biopsies were obtained from Patients undergoing coronary artery bypass graft (CABG) surgery. A total of 40 AA and 33-matched IMA tissue samples were obtained. These 40 CVD patients had coexisting diseases and were divided into subgroups of RA (n=20) and non-RA (n=20). The demographic data and prevalence of traditional risk factors were similar in the RA and non-RA subgroups as shown below (Table 3.1).

Table 3.1. Characteristics of patients in the group

Characteristics	RA n=20 #	Non RA n=20 #
Age, years	70 ± 8.8	69 ± 9
Male sex, no. (%)	13 (20)	14 (20)
Duration of coronary artery disease, years	8 ± 10	9.4 ± 7.9
Time from angiography to CABG surgery, days	17 ± 29	32 ± 61 *
Acute coronary syndrome, no (%)	9 (20)	4 (20)
C- reactive protein mg/litre	12 ± 40	3 ± 3 *
Diabetes mellitus, no (%)	3 (20)	1 (20)
Smokers, no (%)	12 (20)	13 (20)
Hypertension, no (%)	14 (20)	9 (20)

Unless stated otherwise, values are mean ± SD. RA= rheumatoid arthritis; Non RA= non rheumatoid arthritis; CABG = coronary artery bypass graft. # Based on clinical diagnosis. ∗ P< 0.005 versus Non-RA

3.2.2 Citrullinated proteins are increased in the aortic adventitia of patients with rheumatoid arthritis

Citrullinated proteins have previously been detected in tissues (rheumatoid synovium, skin epithelium, glial fibrillary acidic protein, myelin basic protein) and in inflammatory conditions (RA, multiple sclerosis and Alzheimer's disease) [30, 206]. To investigate the presence of CP in the aortic adventitia of CABG patients with or without RA we first had to establish the technique for detection in our laboratory. The initial experiments were performed on sections from RA synovial biopsies, as we had a limited number of aortic adventitial sections. To determine the optimal antigen retrieval for citrulline staining we performed a series of standard antigen retrieval protocols.

3.2.2.1 CP staining established in RA synovium

RA biopsies that had previously been fixed (paraformaldehyde), embedded in paraffin, cut and placed on standard glass slides were subjected to different antigen retrieval procedures. After antigen retrieval the sections were stained with an anti-citrullinated protein antibody and the quality of staining determined. A citric acid retrieval (pH6) method was the first retrieval buffer used, due to a boiling step this retrieval method is known to be harsh. Our results demonstrated that under these retrieval conditions, the negative control staining was at a level that rendered this retrieval method unsuitable (figure 3.1A). The next retrieval method attempted was a milder system utilising Tris EDTA. Although, there was an improvement with decreased background staining, it was still not negligible and confounded any interpretation of positive control biopsies (Figure 3.1B). Finally, Trypsin retrieval was used and this did result in much cleaner negative controls. In addition, a further modification in the staining procedure was implemented; Instead of performing the peroxidase-blocking step prior to primary antibody incubation, it was performed before the secondary antibody incubation.

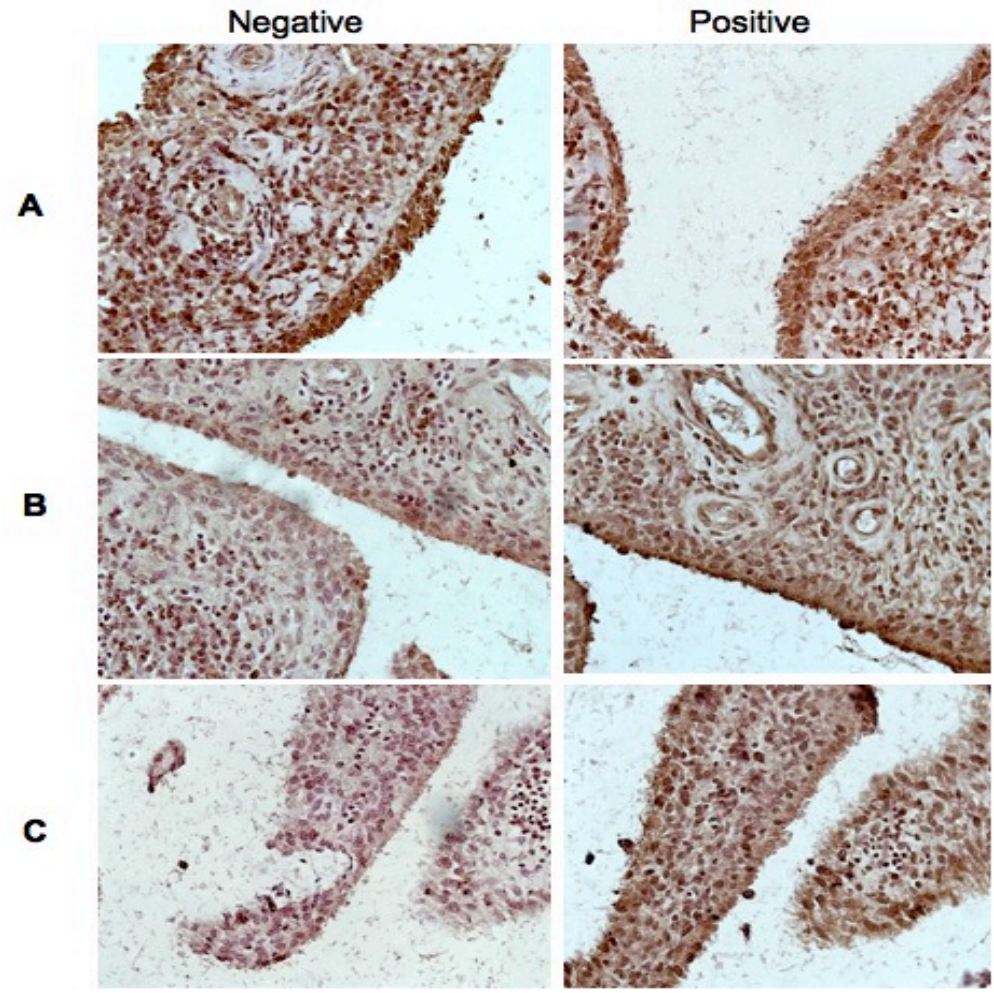

Figure 3.1 CP staining using different antigen retrieval systems

To establish CP staining different retrieval systems were used A) is the citric acid retrieval showing strong background (brown colour) of the Isotype control (top left panel). B) this staining was performed using EDTA, which is a mild retrieval system that resulted in some improvement in negative control but still there was a lot of background staining seen as (brown colour) in the middle left panel. C) Finally, trypsin was used as an antigen retrieval that resulted in clean negative (bottom left panel) and strong staining (brown colour) on the positive sections. The sections were counter stained with Haematoxylin to highlight the nuclei and cytoplasm. All the stainings both negative and positive were photographed at 40x magnification

In summary, trypsin retrieval and peroxidase block after primary antibody resulted in clean negative controls and the positive staining that was distinct and plausible based on prior publication and our expectations of expression (Figure 3.1, C). This optimised protocol was therefore used to stain all aortic

sections. All of the human aortic adventitia from patients with advanced CVD had observable levels of citrullinated proteins. It should also be noted that 9 out of 33 matched internal mammary arteries had moderate levels of citrulline staining. The CP stain was observable in mononuclear cells, interstitium and adventitial adipocytes (Figure 3.2, A-B).

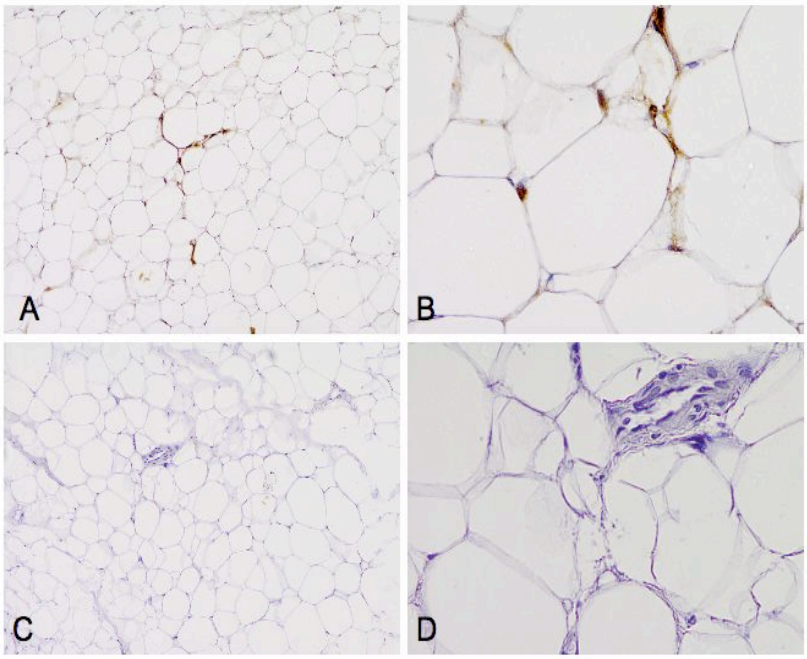

Figure 3.2 Citrulline staining in aortic adventitia

Citrullinated protein staining (brown) in the aortic adventitia can be noted in (A & B); especially the signet ring shaped fat cells of the tunica adventitia. The lower panel (C & D) represents the Isotype control for the CP staining. The sections were counter stained with haematoxylin to highlight nuclei and cell structure. A & C 10x magnification, B & D 40x magnification.

The level of CP staining was quantified in an observer-blinded manner; 5 high power fields per section were scored for the percentage area of positive staining. Since the raw data were normally distributed, mean of percentage area was analyzed as already explained (section 2.1.5). The results shown (Figure 3.3, A) clearly indicate that Aortic Adventitia has high levels of citrullinated protein as compared to matched IMA, the mean ± SD of AA vs. IMA were (3.81% ± 1.956%) and (0.35% ± 0.73%), respectively ($p = 0.0001$). As we confirmed that AA has more citrullinated protein the next objective was to see if the staining was

different in aortic adventitia of patients subgroups, with and without RA. Interestingly, we observed significantly more CP in RA patients, the mean ± SD in RA vs. non-RA were 4.78% ± 2.6% and 3.2% ± 1.4%, respectively (p = 0.017, T test; Figure 3.3B).

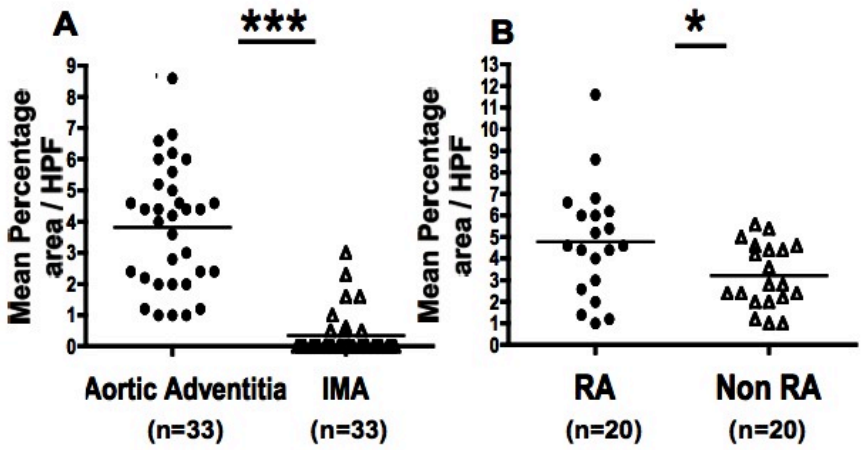

Figure 3.3 Scores for CP staining in aortic adventitia and IMA.
In each graph circles and triangles represents different groups that are compared with each other A) Matched samples of IMA were compared with aortic adventitia from the same patients stained for citrullinated proteins; a massive increase in CP was seen in comparison with the non diseased IMA. B) RA represented with a circle are shown to have significantly increased level of CP expression in comparison with Non RA patients. A p-value of <0.05 was considered statistically significant and was represented as an (*)

In addition, all the forty patients in the Feiring heart biopsy study were also subdivided into smokers (n=25) and non-smokers (n=15). As citrullination of proteins is associated with smoking and inflammation, we analysed CP in aortic adventitia of patients in this subgroup for any interesting associations. However, the analyses showed that smokers mean ± SD 4.47% ± 0.56% vs. non-smokers 5.15% ± 1.276%, was not significantly different (p = 0.086) as shown in the (Figure 3.4).

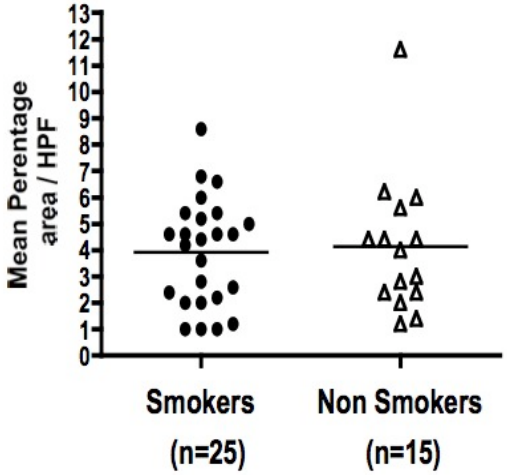

Figure 3.4 CP in aortic adventitia of smokers and non-smokers

In each graph circles and triangles represents different groups that are compared with each other. CP staining in smokers represented with a circle is shown to have almost similar level of CP as compared with Non-smokers

3.2.3 B lymphocytes are present in the aortic adventitia from patients with CVD

The literature on B cells presence in relation to atherosclerosis supports the fact that majority of their expression is in the AA rather than tunica intima in both humans and animals models[116, 142, 215]. Now that we confirmed the presence of CP an RA associated antigen in AA, we sought to further validate the presence and any possible link between B-lymphocytes and CP in RA. We set out to establish B cell staining in RA synovium and human tonsil with an antibody against CD20, which is a pan B cell marker. To optimise this staining we tried both citrate and Tris EDTA antigen retrieval methods. Citrate retrieval with a pan specific secondary antibody was not successful. Staining with both these retrieval systems had background staining of negative control. To optimize the staining method we tried an enzyme coupled secondary antibody system (Vector). This resulted in specific staining of the aortic adventitia with no background staining of the adipocytes in the Isotype control. Thereafter, the surgical biopsies of Aortic adventitia (n=40) and matched IMA (n=33) were stained for the presence of B-lymphocytes using the established protocol as discussed in (section 2.1.1). Discrete membrane staining of CD20 can be seen

among the infiltrating mononuclear cells in the aortic adventitia (Figure 3.5, A & B).

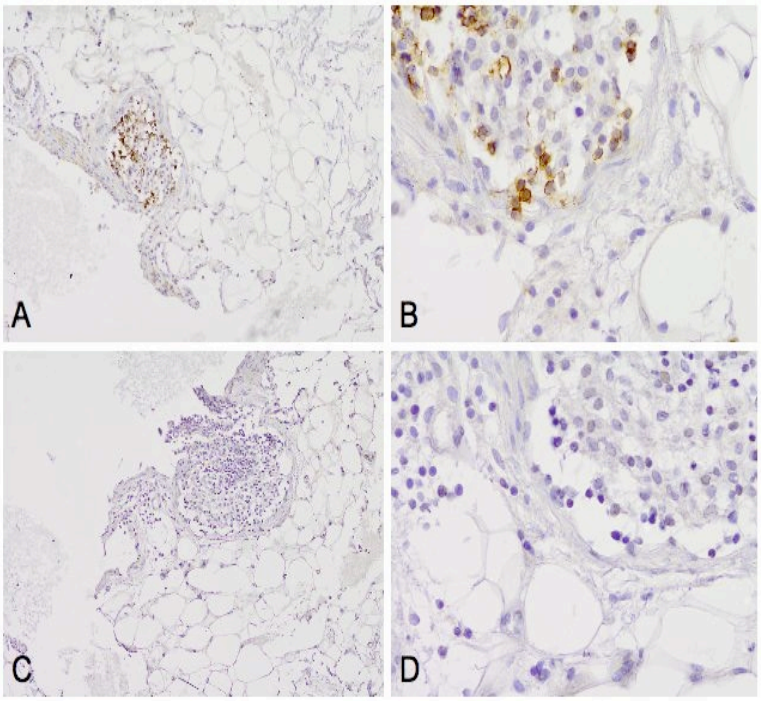

Figure 3.5 CD20 staining in aortic adventitia.

In these sections a small aggregate of inflammatory cells can be seen, surrounded by signet ring shaped fat cells. CD20 a B cells marker has a discrete membrane staining of cells seen within the small follicle (A & B). Sections were counter stained with haematoxylin that resulted in nice nuclear staining as seen in the lower panel, which is the negative control (C & D), original magnification 10x in A & C; 40x B & D

We were able to detect B-lymphocytes in 70% of the AA samples, whereas there were no B cells detected in IMA. In addition the aortic adventitial biopsies were sub grouped as RA (n=20) and non RA (n=20). When the percentage of B cell positive (72%) AA samples with coexisting RA were compared with non-RA samples (65%), a significant increase was seen in AA of RA patients (p value=0.03) (Figure, 3.6).

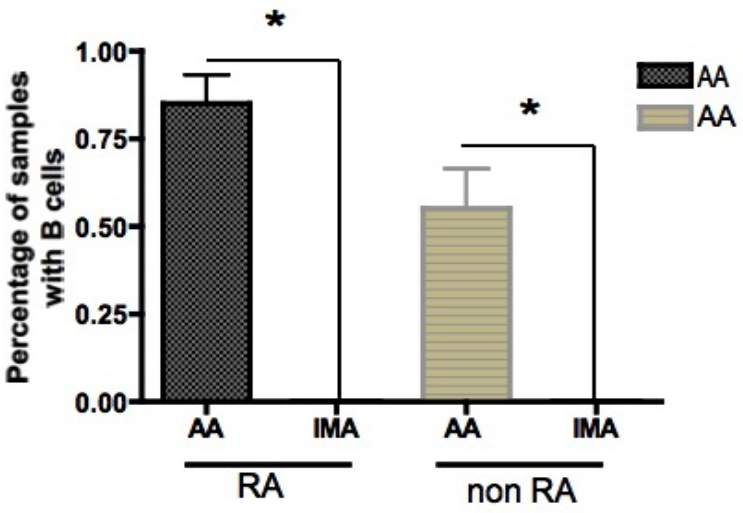

Figure 3.6 B cell presence limited to aortic adventitia
*The staining of all the biopsy samples for B cells (CD20) showed that their presence is limited to AA (both black and brown column), as none of the IMA had detectable B cells. The percentage of samples positive for B cells among RA patients (black column) were significantly more 75% vs. non RA around 60% (brown column) p value = 0.03 shown with an * asterisk*

Thereafter, the AA positive for B cells were scored in a blinded manner to determine level of B lymphocyte expression; CD20 positive cells were counted in a total of 5 HPF, as the raw data was non normally distributed it was therefore analysed by using median number of B lymphocytes/HPF already explained (section, 2.1.5).

We observed that only Aortic Adventitia had B lymphocytes, whereas, matched IMA adventitia had no B cells, the mean ± SD in AA vs. IMA were 0.65 ± 1.65 and (0), respectively ($p<0.05$, Wilcoxon rank test; Figure 3.7). Half of the aortic adventitia samples from these CVD patients had coexisting RA. Therefore, we also compared B cells positive aortic adventitia among the sub groups of RA vs. non-RA, the mean ± SD 0.65 ± 1.3 and 0.68 ± 1.91, respectively ($p = 0.816$). Furthermore, CVD patients (n=40) had another subgroup based on whether the patients smoked or not. We therefore also examined B cells staining scores between smokers and non-smokers, and the mean ± SD 6.8 ± 14 vs. 10 ± 22, was insignificant ($p = 0.58$).

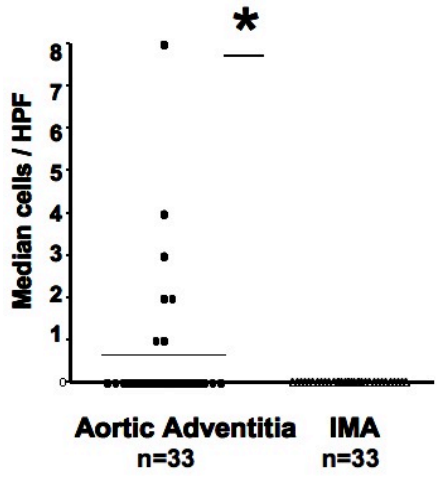

Figure 3.7 Scores for CD20 staining in aortic adventitia and IMA.
In the graph circles and triangles represents different groups, B cells were only seen in the aortic adventitia, the distribution of CD20 positive B cells between Aortic adventitial (n=33) and matched IMA (n=33) was statistically seen as (p-value of <0.05, Wilcoxon rank test).

3.2.4 B-cell aggregates in rheumatoid arthritis patients with advanced atherosclerosis

The aortic adventitia of patients with advanced atherosclerosis have follicle like structures composed primarily of B cells (Figure 3.5) Interestingly, in the adventitia of RA patients, 7 out of 20 had these follicles whilst in non-RA patients we only saw 3 out of 20, because of small sample size this interesting observation needs to be addressed in future studies.

3.2.5 Detection of plasma cells in the aortic adventitia of patients with advanced cardiovascular disease.

We have confirmed the presence of an RA associated auto-antigen i.e. citrullinated protein in adventitia of both RA and IMA. Predominance of B-lymphocyte and follicles in the diseased vessel made plasma cells an obvious choice for further investigation. Plasma cell staining has previously been demonstrated in RA synovium[61]. We used previously reported protocols to establish this staining not for in Immunohistochemistry by light microscopy, but also immunofluorescent staining of plasma cells. This was done so that we could

perform double staining of plasma cells secreting antibodies to modified citrulline (section 3.3.8). The plasma cells were stained for (p63) with a monoclonal antibody (Vs38c); this was detected as discrete membrane staining (Figure 3.8, A & B) of cells with characteristic phenotype (e.g. clock face nuclei and acentric nuclear distribution).

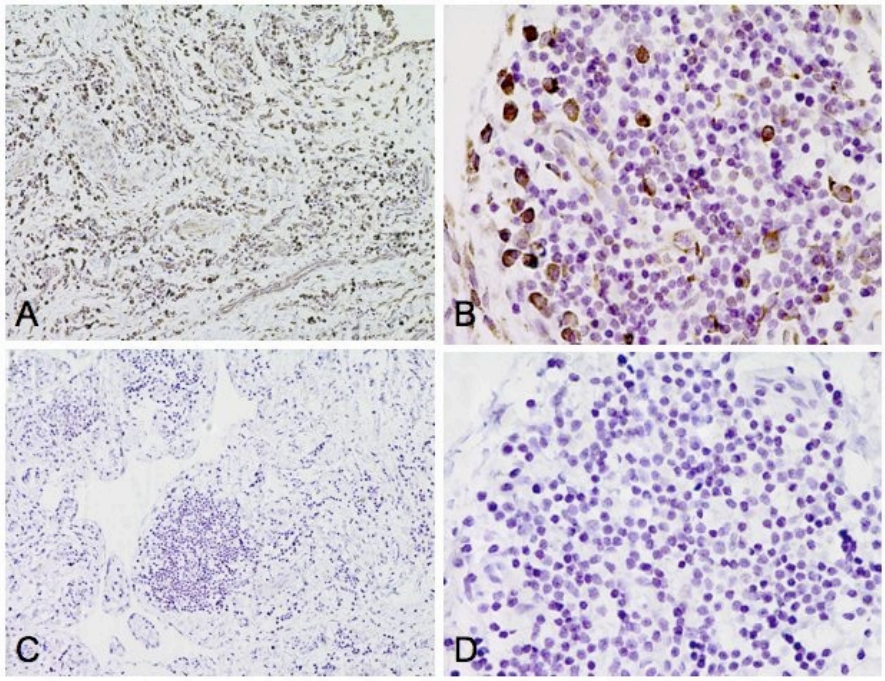

Figure 3.8 Plasma cell staining in RA synovium
The top panel shows a large number of plasma cells within the lymphocyte aggregates as intense discrete membrane staining (brown staining). The staining showed at different magnifications (A & B); while the lower panel (C & D) represents the Isotype control. The sections were counter stained with haematoxylin. Original magnification 10x A & C; 40x B & D

After establishing the plasma cell staining method on RA synovium, a number of adventitial biopsy tissues were stained for plasma cell presence. We found plasma cells presence in the aortic adventitia and next attempted to co localize these cells with citrulline reactive antibodies (Figure 3.11, A). This again required the generation of a novel tissue detection assay.

3.2.6 Generation of citrullinated fibrinogen

So far three important components of an immune response were identified in these biopsy tissues including citrullinated protein as a target antigen, B-lymphocytes along with aggregates as a source of plasma cells and presence of plasma cells seen in one biopsy sample. Now the next step was to generate citrullinated protein and then use it further as a ligand (bait) in the RA synovium to identify citrulline reactive antibodies secreted by plasma cells.

Human fibrinogen modified to citrullinated fibrinogen.

Human fibrinogen was modified based on enzymatic deimination using rabbit peptidyl arginine deiminase (PADI) as explained in the (section 2.1.2). The newly prepared citrullinated fibrinogen was run on an electrophoresis gel and then stained to confirm presence of the altered proteins (Figure 3.9)

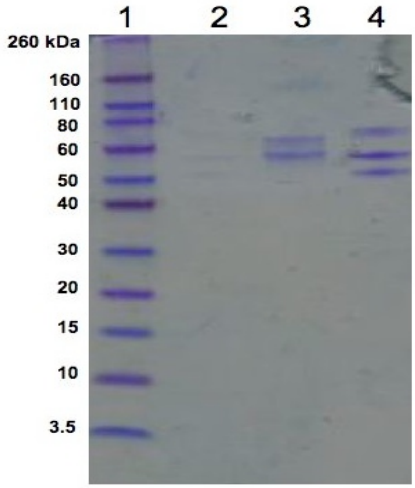

Figure 3.9 Coomassie staining for citrullinated fibrinogen
After electrophoresis of freshly prepared proteins, Coomassie staining confirmed all samples; lane 1 is a protein standard ladder, lane 2 is citrullinated fibrinogen, lane 3 is native fibrinogen and lane 4 is human cornified skin as a positive control. Multiple bands seen for all three proteins between 50-80 kDa

3.2.7 Reactivity of modified fibrinogen confirmed with sera from RA patients

To establish the reactivity of the freshly generated modified fibrinogen, fresh serum was collected from RA patients. Western blot membranes containing modified and non-modified fibrinogen and cornified skin extract were probed with sera from both Rheumatoid factor (RF) positive and negative Patients. The western blots probed with sera from healthy donors did not show any reactivity to citrullinated fibrinogen. However, the use of pooled sera from RA patients confirmed reactivity of citrullinated fibrinogen and skin (Figure 3.10, A).

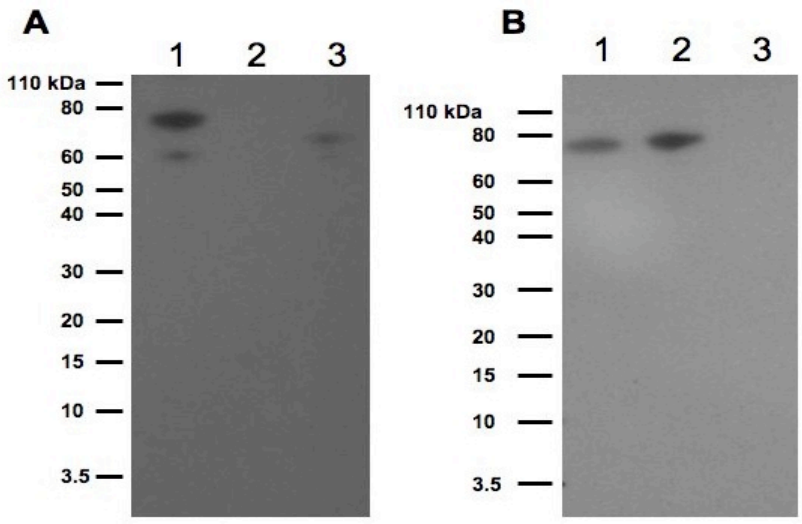

Figure 3.10 Western blot analysis for citrullinated proteins
A) Western blot using pooled sera from RF positive patients; Protein bands corresponding to molecular weight of 60-80 kDa represent citrullinated fibrinogen. Non-citrullinated fibrinogen was used as a negative control (lane 2) and human cornified skin as a positive control for citrullinated protein (lane 3). B) Western blot to confirm the biotinylation of proteins produced; lane 1 is citrullinated fibrinogen conjugated to biotin, lane 2 is biotinylated fibrinogen and lane 3 is skin, which was non-biotinylated and used as a negative control.

Citrullinated fibrinogen and native fibrinogen were biotinylated to be used as bait for ACPA antibodies and a western blot was performed to demonstrate that the proteins were biotinylated (Figure 3.10, B).

3.2.8 Plasma cells secreting antibodies to citrullinated protein in RA synovium

It has recently been established that plasma cells producing anticitrulline protein antibodies (ACPA) are present in the synovium of patients with RA[61]. We have reproduced this finding in RA synovial samples from patients by using citrullinated fibrinogen. As discussed above, the reactivity of newly prepared human citrullinated fibrinogen was confirmed on western blot. A biotinylated version of this reagent was used as a ligand to identify plasma cells secreting antibodies against citrullinated proteins. Autoantibody producing plasma cells were detected RA synovial samples by immunofluorescent staining. As can be seen in Figure 3.11 A-D, plasma cells (green) antibodies reactive to citrullinated

protein (fibrinogen in this case red) are co localized as (green & red) in the synovial tissue of RA patients.

Once the ACPA producing plasma cells were established in RA synovium the next step was to investigate their presence in the aortic adventitia. This was important because presence of RA associated antigen (CP) and presence of B cells foci make it highly likely that there might be antibody selection/maturation going on. A thorough analysis of all the aortic adventitial sections illustrated that although we could find plasma cells in the aortic adventitia (5 out of 40 samples) we could not detect any that exhibited citrullinated fibrinogen reactivity (figure 3.11, E & F).

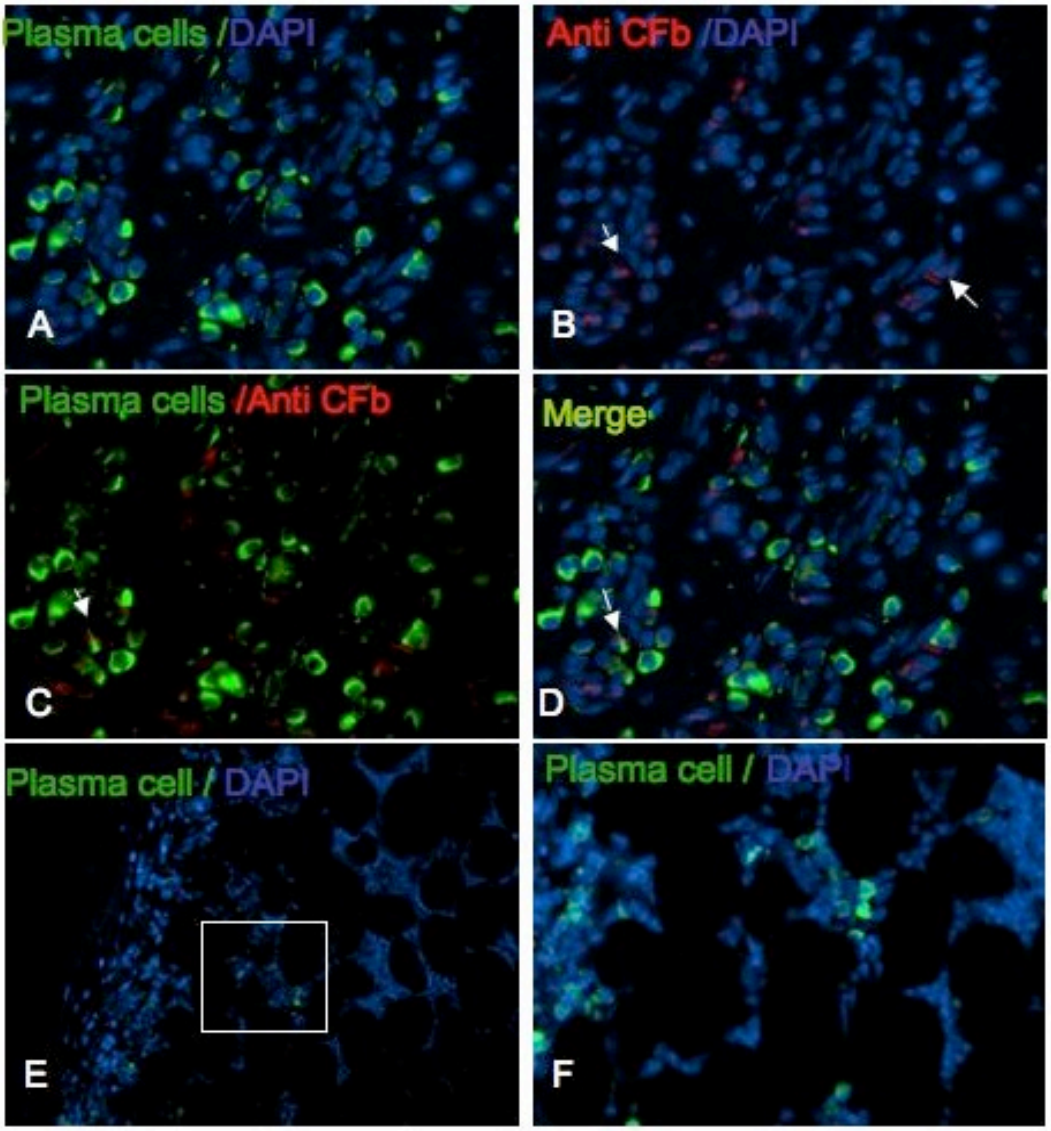

Figure 3.11 Plasma cell secreting antibodies to citrullinated fibrinogen
To confirm plasma cells producing antibodies to citrullinated proteins. RA synovial membrane was stained green with anti p63 for plasma cells green (A) biotinylated CFb was used to stain citrulline reactive antibodies shown with white arrows (red) (B) Double immunofluorescence staining for plasma cells with immunoreactive antibodies to citrullinated protein can be seen green & red together (D). Sections were countered stained with DAPI for nuclear staining. (original magnification 40x). Plasma cell stained (green) in aortic adventitia (E & F). 20x magnification

Details of the patients that were positive for plasma cells are given below (Table 3.2). Interestingly, these 5 patients have a mixed profile from age group to smoking. However, four out of five are females and are non-RA.

Table 3.2. Details of patients positive for plasma cells

SNo	Patient ID	Gender	Age	Smoker/Non smoker	Disease Profile
1.	3178	Male	81 years	Smoker	RA
2.	9897	Female	67 years	Smoker	Non RA
3.	2582	Female	78 years	Smoker	Non RA
4.	10508	Female	76 years	Non smoker	Non RA
5.	3183	Female	66 years	Non smoker	Non RA

3.2.9 ACPA and CP together affect the cardiovascular outcome of RA patients

The high specificity of ACPA in diagnosing RA patients at early stage, where patients do not have any overt signs of disease is an established fact. In fact ACPA expression persists at the end stage of disease and we wanted to validate any link between ACPA levels and CP in CVD patients with coexisting RA. Our data so far have demonstrated B cells and CP in the aortic adventitia of these

CVD patients (n=40), these patients also had coexisting RA (n=19) and remaining patients were considered non RA; however, the ACPA levels were not measured previously in this cohort. We therefore obtained the Axis Shield ELISA kit and determined the levels of ACPA in our RA cohort. The levels reported here for the RA cohort are from an ELISA kindly done by Susan Kitson in our lab. Out of 19 patients in our cohort that were diagnosed with RA, we were able to obtain serum samples from 17 patients. We were also able to obtain serum from CVD patients without RA as some of these patients had high CP staining in their aortic adventitia. Serum samples from controls (non-RA patient's) along with RA (n=17) were used in a standardized ELISA kit (Axis shield) to determine the levels of ACPA; 20U/ml is the cut off for a positive response in this assay. Importantly, we found that non-RA sera had no detectable levels of ACPA titres. However, ACPA levels were detectable in 70% of RA patients (12 out of 17), the mean ± SD (124.5 ± 61.89). The ACPA levels of patients examined are shown (Figure 3.12, A).

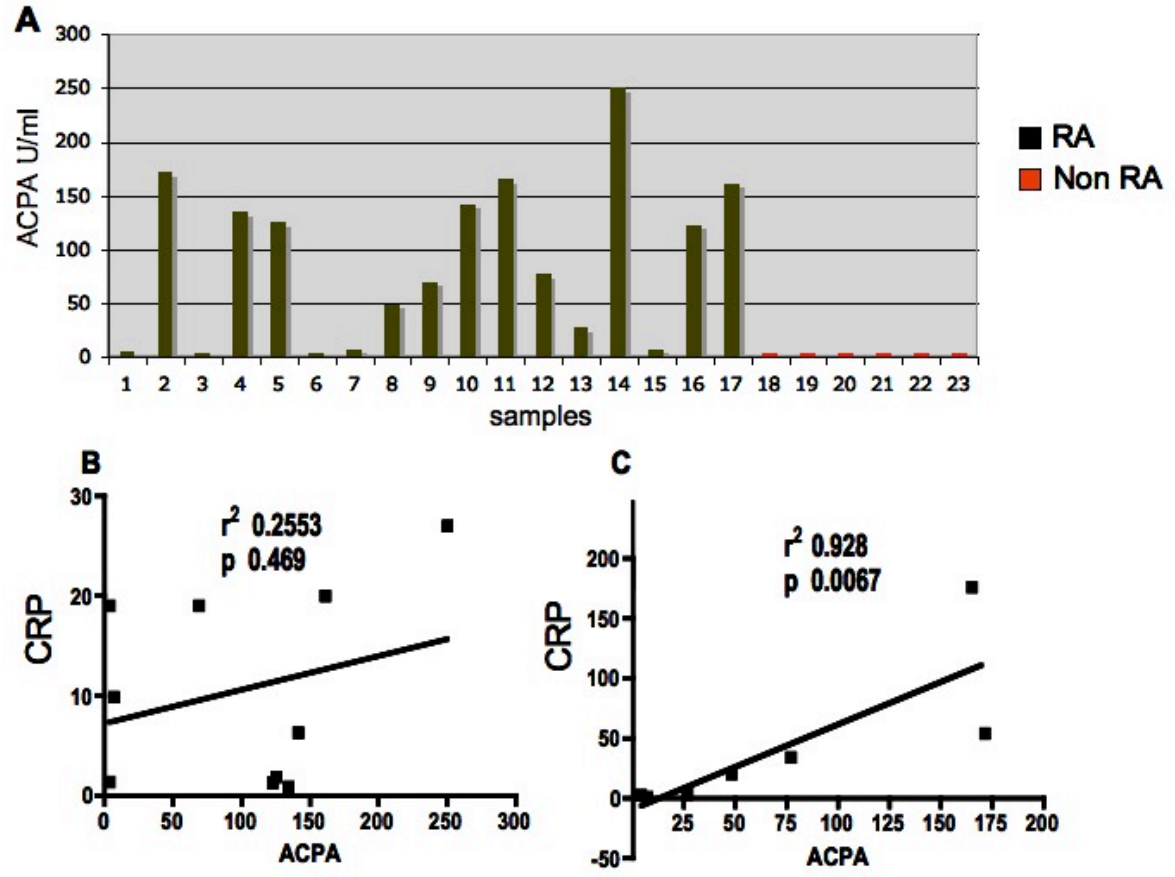

Figure 3.12 ACPA and CRP in RA patients

The ACPA levels were determined in the patients A) it was observed that all non-RA (red bars) had non-detectable levels of ACPA (ELISA). However, 12 out of 17 RA patients (brown bars) were found positive for ACPA levels, the mean ± SD (124.5 ± 61.89). The ACPA levels were further correlated with CRP and CP staining scores. To do the correlation subgroups were made, CP staining <5.5 was one group. B) the ACPA of these patients were correlated with their CRP levels, which was not significant (p=0.469) (C) Thereafter, ACPA level for the remaining patients (CP> 5.5) was correlated with the CRP, which resulted in a strong correlation (∗∗p value=0.0067 with r^2 0.9286).

All RA cohort samples were analysed for correlation between ACPA and CRP, this was because elevated levels of CRP are associated with increased incidence of ischemic heart disease[216]. In addition, the patient's characteristics for our cohort (Table 1) show that CRP is significantly increased in RA patients. When we examined all RA patients there was no-significant correlation seen between ACPA levels and CRP. Although in the present study we detected CP in the AA of non-RA patients similar to other inflammatory conditions. However ACPA was not detected in serum of non-RA patients, as this antibody reactivity is highly specific for RA.

To determine a relationship between patients with both (ACPA plus CP) vs. CRP levels we had to identify a subgroup based on the maximum CP staining scores in non-RA patients. When the cohort of RA patients was sub-divided based on CP expression level in the AA, we had two groups one with (CP<5.5) and the other (CP>5.5). The cut off point of (CP>5.5) was chosen, as this was the maximum seen in non-RA patients. This subgroup of RA patients with (CP>5.5) was correlated for ACPA vs. CRP levels. A linear regression analysis revealed no significant correlation for the RA patient's subset with (CP<5.5) (see Figure 3.12, B). As expected a strong correlation was confirmed for the subset with (CP>5.5), with a p value of 0.0067 and r^2= 0.9286 (Figure 3.12, C).

So far we have confirmed that both AA and IMA express CP, an RA associated autoantigen. Which is notably more in the AA as compared to IMA. In addition, CP the proposed RA autoantigen was expressed more in the CVD patients with coexisting RA (n=20) as compared to non-RA. Furthermore, B-lymphocytes were

only detected in AA and 75% of these tissues samples were from CVD patients with RA. B cell aggregates and autoantigen presence was an impetus to investigate plasma cells in the AA. Interestingly a total of 5 AA were positive for plasma cells. We then confirmed an anticipated association between CP expression and serum ACPA levels in CVD patients. The serum analysis of the patients showed that ACPA was detectable in RA subset of the CVD patients. Importantly, patients with CP>5.5 score showed a significant association between serum ACPA levels and CRP as anticipated.

3.2.10 Dominant B-lymphocyte survival factor (BAFF) expression in the smokers aortic adventitia

The aortic adventitia samples express a known auto-antigen, B cells and plasma cells. Assuming the fact that B cells survival in any tissue is dependent on B cell survival factors. The next step was to address whether there are any survival factors in these biopsy samples.

Unlike B cells BAFF staining was achieved using an avidin/biotin-based method. Using the established protocol BAFF was identified in the RA synovium. As explained in (section 2.1.1) it was seen that BAFF was expressed by infiltrating cells and non-haemopoietic cells like adipocytes and vascular endothelial cells. I then moved on staining AA and cytosolic staining of BAFF was prominent among mononuclear cells, adipocytes and vascular endothelial cells of vasa vasorum (Figure 3.13, A & B)

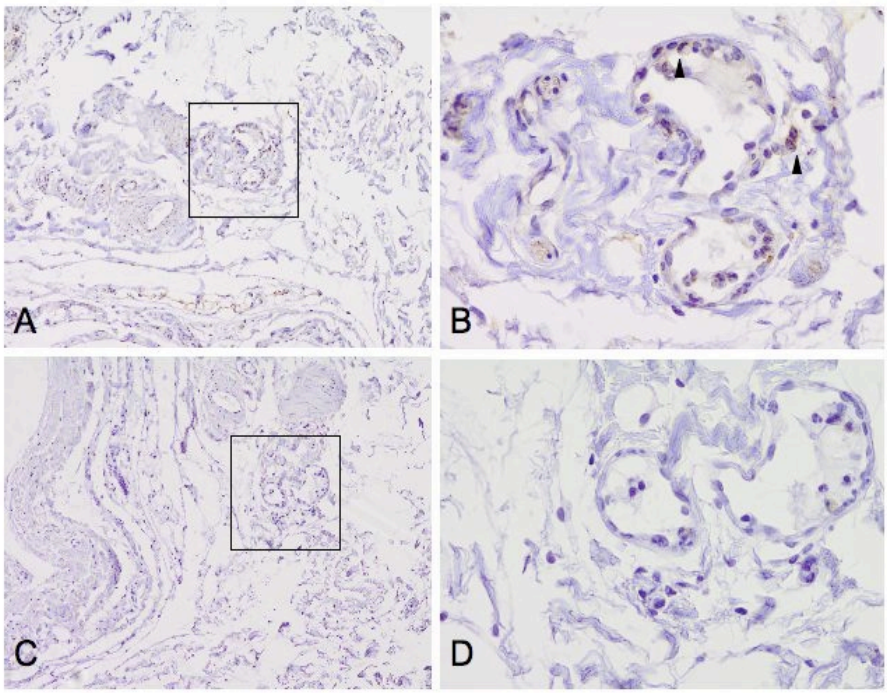

Figure 3.13 BAFF staining in human aortic adventitia
Lymphocytes in and around the vasa vasorum show cytoplasmic staining (brown colour) for BAFF (arrowheads) - in fact distinct staining of vascular endothelial cells of vasa vasorum is also shown (A & B); whereas, the lower panels represent the negative control for BAFF (C & D). The sections were counter stained with hematoxylin. Original magnification 10x in A & C; 40x B & D

Blinded observers scored the stained sections; these showed a non-normal distribution despite the fact that scoring was determined from 5 random high power fields. Therefore, the median percentage area was calculated for further analysis as already discussed (section 2.1.5). BAFF was present in 97% of AA vs. 27% of IMA ($p < 0.0001$, OR 85). The increased expression of BAFF in diseased adventitia suggests some interesting relation with the underlying disease. The data of matched AA vs. IMA revealed a mean ± SD 3.57 ± 3 and 0.63 ± 1.24 respectively, with a (p values<0.0001, Wilcoxon rank test; Figure 3.14, A). Interestingly, we also found a significantly higher expression of BAFF in the adventitia of the smoking patients, the mean ± SD for the subgroups are 4.8 ± 2.50 vs. 3.6 ± 2.93 and a (p value = 0.03, Mann-Whitney; Figure 3.14, B). These results suggests that the survival niche can be related with both smoking an independent risk factor for vascular diseases and underlying mechanism of

atherosclerosis. The staining score of BAFF were also analysed for another subgroup of RA vs. Non RA patient's, the mean ± SD 4.3 ± 3.17 vs. 4.4 ± 2.2 was not significant (p value = 0.81, Mann-Whitney)

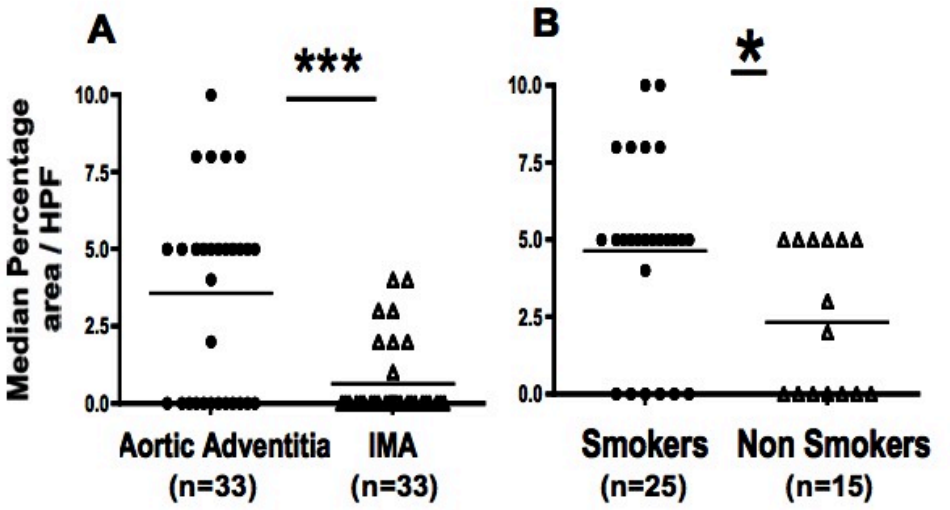

Figure 3.14 BAFF staining score in human aorta and IMA
In each graph circles and triangles represents different groups that are compared with each other (A) Scores for BAFF staining were significantly high in Aortic adventitia as compared to the matched IMA (p<0.0001, Wilcoxon rank test) B) Smoking patients had significantly more BAFF expression than non-smokers mean ± SD, 4.8 ± 2.50 vs. 3.6 ± 2.93 p = 0.03. A p-value of <0.05 is represented with an (∗).

3.2.11 A proliferation inducing ligand (APRIL) specific to aortic adventitia from CVD patients

We next probed the adventitia for another member of the TNF superfamily, APRIL, which also has potential role in B cell survival. Human tonsil was used to establish this staining protocol. Unlike BAFF in this staining method we used an enzyme coupled secondary antibody (Immpress vector). All the biopsy sections were stained for APRIL using the established protocol (section 2.1.1).

Staining for APRIL was observed in the adventitia, particularly in inflammatory cells resembling monocytes and lymphocytes in which discreet punctate staining was noted(figure 3.15, A & B). Importantly, non-haemopoietic cells were also observed to express APRIL. These cells include adipocytes and vascular

endothelial cells of the nutrient artery of aortic adventitia called vasa vasorum. Evaluating 5 high power fields for the percentage area of positive staining was done for scoring APRIL staining. Analysis was performed in both diseased aortic adventitia and the IMA specimens. Comparison of scores revealed that APRIL is extensively expressed in diseased vessels (figure 3.15, c); compared with IMA comparators.

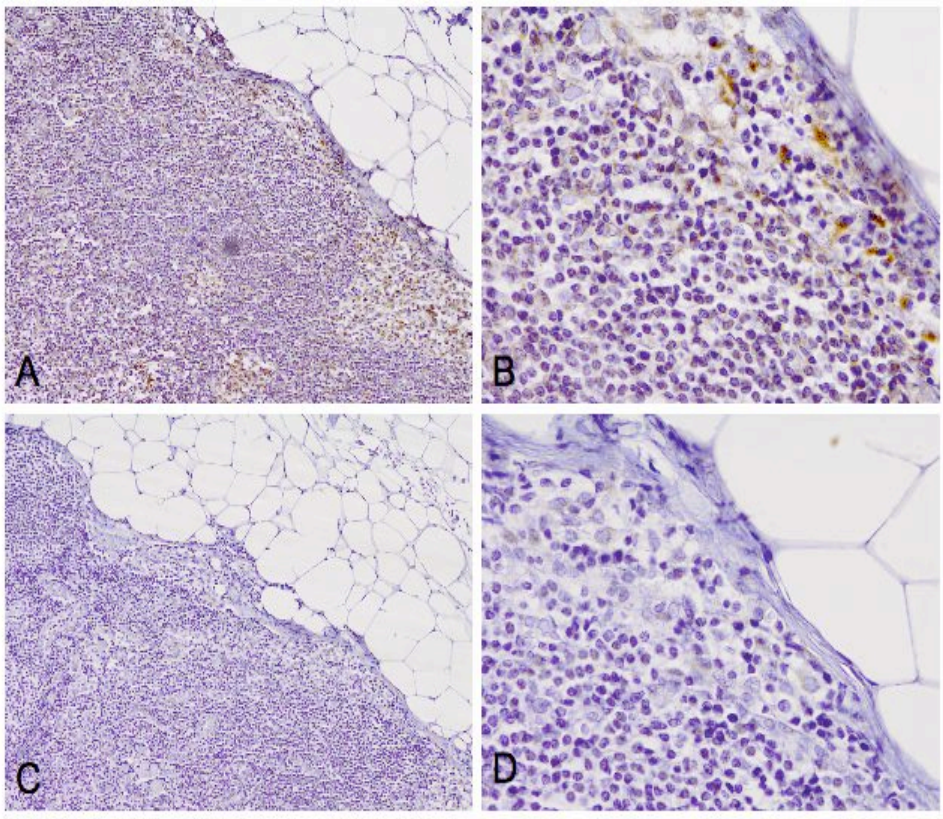

Figure 3.15 APRIL staining in aortic adventitia
The typical punctate and discreet APRIL staining is seen in this massive infiltrating area in the aortic adventitia (A & B), lower panel (C & D) are negative controls for the same area. Original magnification 10x & 40x respectively;

APRIL was present in 68% of AA vs 6.5% of IMA ($p < 0.0001$, OR 30.5; Figure 3.16). The staining pattern and level of expression did not completely mirror that of BAFF. For example, APRIL expression in smoking vs. non-smoking patients was not different, with the mean ± SD 1.4 ± 3.39 vs. 2 ± 5.2 (p value = 0.97,

Wilcoxon rank test). Similarly, comparison of RA vs. non-RA showed no difference as suggested by the figures for mean ± SD 2.5 ± 5.5 vs. 0.7 ± 1.8 p value = 0.52.

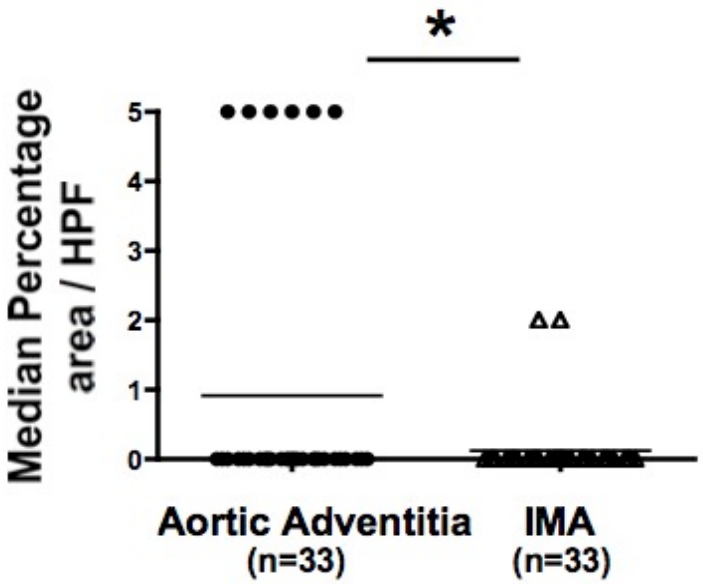

Figure 3.16 APRIL staining scores in human samples

In the graph circles and triangles represents AA compared with matched IMA. A significant difference was observed reflected by the mean ± SD 0.9 ± 1.9 vs. 0.12 ± 0.48 and a p value < 0.0006 (Wilcoxon rank test) represented (∗).

3.3 Adventitial B-cells correlate with citrullinated protein and APRIL in patients with rheumatoid arthritis

We next wished to explore further the possible role for these B cell survival niches in the context of RA pathogenesis. In RA patients, we noted a significant correlation between the presence of B cells and CP expression in AA tissues; r^2=0.56, p value = 0.0001 (Figure 3.17, A). As expected we also observed an

association between B cells and APRIL r^2=0.566, p value = 0.0017 (Figure 3.17, B). In addition, a significant correlation was noted for CP vs. APRIL, r^2=0.295, p value = 0.29 (Figure 3.17, C). Intriguingly, when we looked for similar correlations for CP, B cells and their survival factors in non-RA patients there were no significant correlation seen.

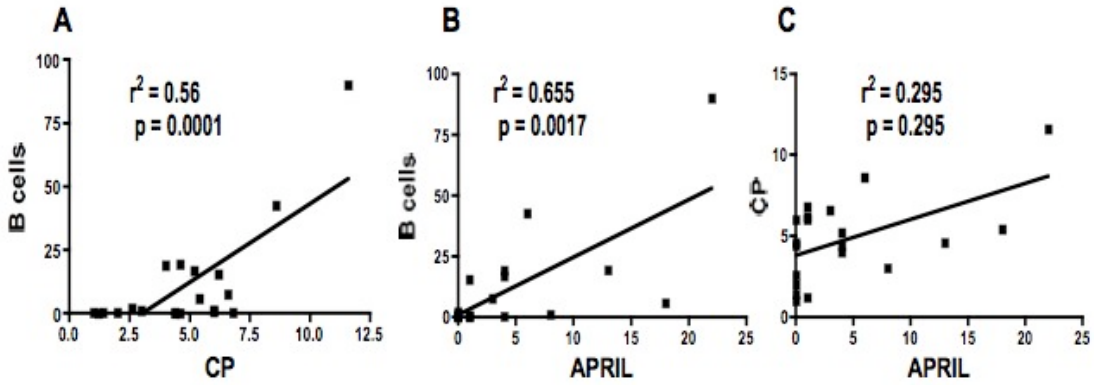

Figure 3.17 Associations observed in RA patients between citrullinated proteins B cells and APRIL.

The staining scores of RA patients were analyzed for any significant associations using fisher exact test. The significant associations observed were A) between B cells and CP (r^2 = 0.56; p = 0.0001), the second was B) among B cells and APRIL as (r^2 = 0.655; p = 0.0017), and C) APRIL and Citrullinated protein (r^2 = 0.29; p = 0.295) in RA patients. There was no significant association with smoking.

3.3.1 Macrophages in aorta of patients with advanced atherosclerotic lesions

Moving from B cells to macrophages and macrophage-derived cytokines AA were now probed for cytokine IL-18 and macrophages. Several prior studies have demonstrated the presence of macrophages in human atherosclerotic lesions.

Indeed, their presence is reported in aortic adventitia of human samples [13, 14, 21]. I elected therefore to perform a complete analysis of my AA samples cohort in order that I could examine potential cytokine expression of monokine derivation. Given the prominence of macrophages in RA pathogenesis it seemed reasonable to focus on macrophage biology particularly in trying to elucidate a contribution to accelerated vascular disease in RA. Therefore, we initially looked for the presence of macrophages in aortic adventitia of patients with coexisting rheumatoid arthritis, as their presence in the context of RA has not previously been reported. All the aortic adventitias were stained for CD68 a well-established macrophage marker; this demonstrated that these cells are present in the infiltrating areas and around the adipocytes (Figures 3.18, A&B).

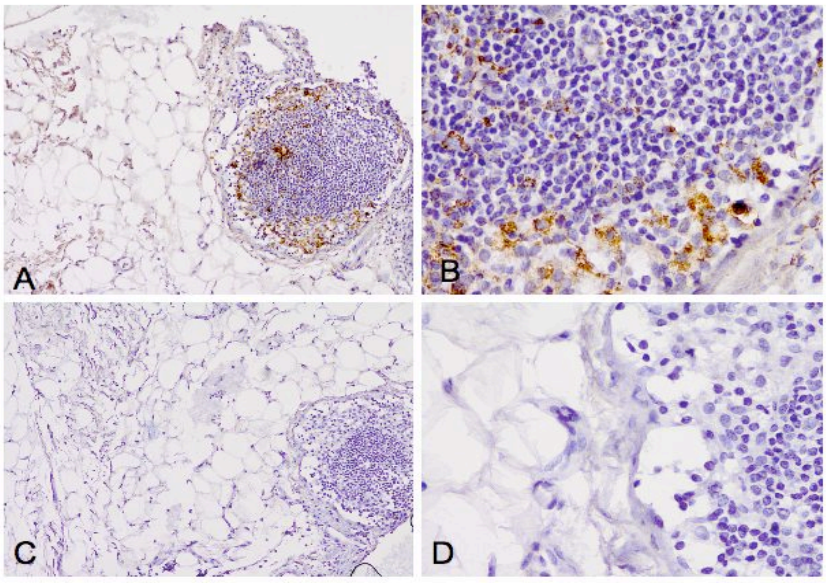

Figure 3.18 Macrophage staining in aortic adventitia

The aortic adventitial staining for macrophage marker CD68 can been seen (brown colour) in the periphery of this lymphocyte aggregate seen as a small follicle (A & B) and the Isotype control showed no background staining (C & D).

The sections were counter stained with hematoxylin. Original magnification 10x in A & C; 40x B & D

Analysis for the presence of macrophages in the aortic adventitia revealed similar representation in RA and non-RA patients, with mean ± SD 5.31 ± 4.36 and 4.1 ± 3.91 respectively (p value = 0.42, Mann-Whitney; Figure 3.19 A); comparison between smokers and non-smokers also showed no difference, the mean ± SD 4.17 ± 3.89 vs. 5.5 ± 4.4 and a (p value = 0.346, Mann-Whitney; Figure 3.18, B).

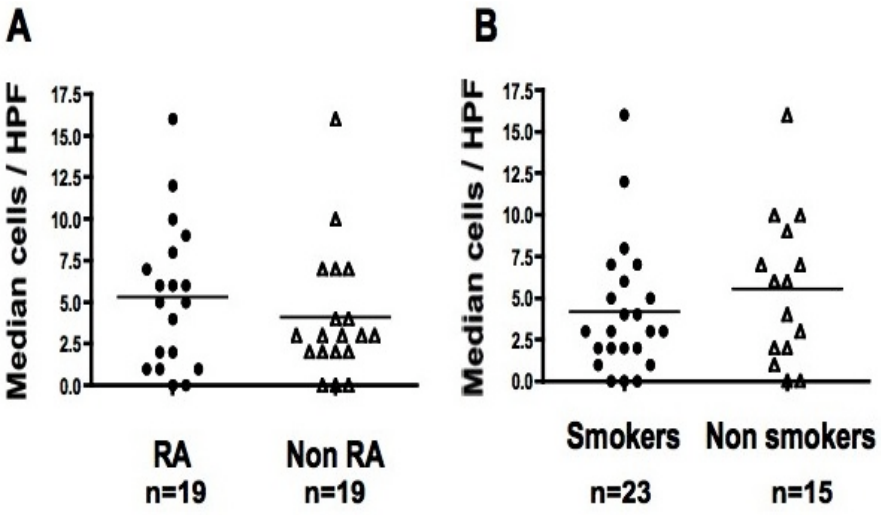

Figure 3.19 Macrophages in aortic adventitia

In each graph circles and triangles represents different subgroups that are compared with each other. A) The comparison between the RA and Non- RA group is not significantly different with mean ± SD 5.31 ± 4.36 and 4.1 ± 3.91 respectively (p value = 0.42, Mann-whitney). The other subgroup of the patient's cohort is that of smokers and non-smokers and there was no significant difference

observed B) smokers vs. non-smokers mean ± SD 4.17 ± 3.89 vs. 5.5 ± 4.4 and a p value = 0.346, Mann-Whitney.

The internal control (IMA) used through out the study was insufficient in quantity to examine macrophage staining. Therefore, we could not determine if there was any difference between the AA and matched IMA adventitia.

Given the presence of macrophage lineage cells, I next wished to examine the presence of pro-inflammatory monokine that might play a role in pathogenesis. I focused initially on the IL-1 superfamily member IL-18

3.3.2 Interleukin 18 a proatherogenic cytokine of IL-1 family

The proatherogenic potential of IL-18 has been demonstrated in experimental model of atherosclerosis.[22] IL-18 is known to have a synergistic effect with IL-12 and the combination of these cytokines is demonstrated to generate Th1 effector cells, which are known to accelerate the atherosclerosis. We investigated the presence of IL-18 in aortic adventitia and analyzed the difference between RA and non-RA patients. The staining of IL-18 was observed around the vasa vasorum as seen in (figure 3.20, A & B).

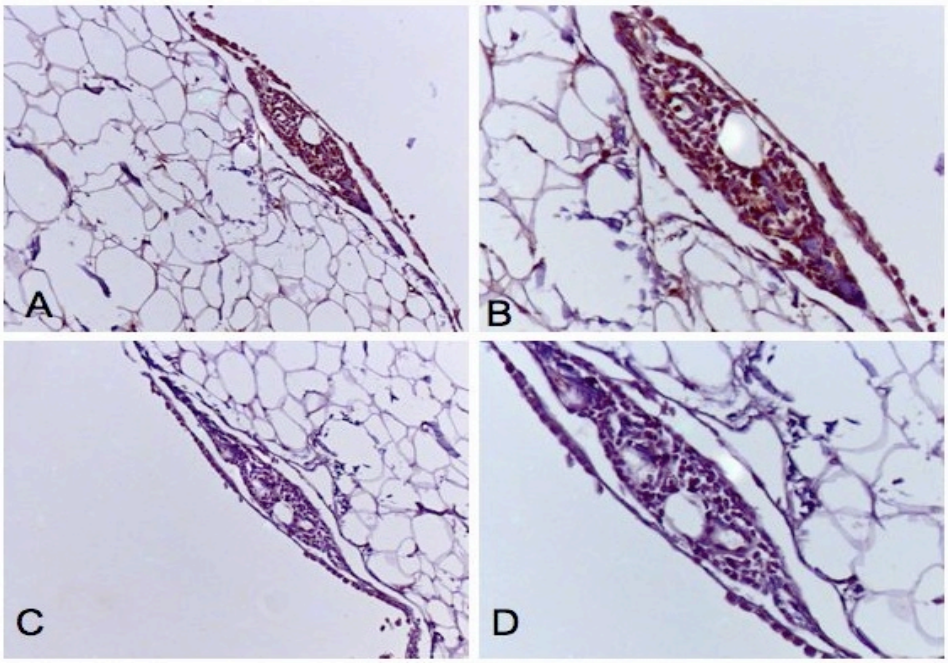

Figure 3.20 IL-18 staining in aortic adventitia

IL-18 positive cells can be seen in and around vasa vasorum expressed by infiltrating cells present at the margin of adventitial adipocytes (A & B); the lower panel represents the Isotype control with no staining of the infiltrating cells around the same vasa vasorum (C & D) sections were counter stained with hematoxylin original magnification 10x in A & C; magnification 40x B & D

The IL-18 staining was scored in the aortic adventitia in a blinded manner, number of cells was scored for 5 HPF and as the raw data was skewed therefore, median cells/HPF were used to analyse the data. IL-18 expression in these adventitial samples was different in RA and non-RA patients but statistically not, as the mean ± SD 8.3 ± 7.3 and 4.6 ± 3.9 respectively (p value = 0.10, Mann-Whitney; Figure 3.20, A). Whereas, the comparison of smokers vs. non-smokers showed a similar pattern, mean ± SD 7.1 ± 7 vs. 5.53 ± 4.2 respectively (p value = 0.91, Mann-Whitney; Figure 3.21, B). There was no control blood vessel (IMA)

available to stain for IL-18, therefore no data to shown differences between AA and IMA.

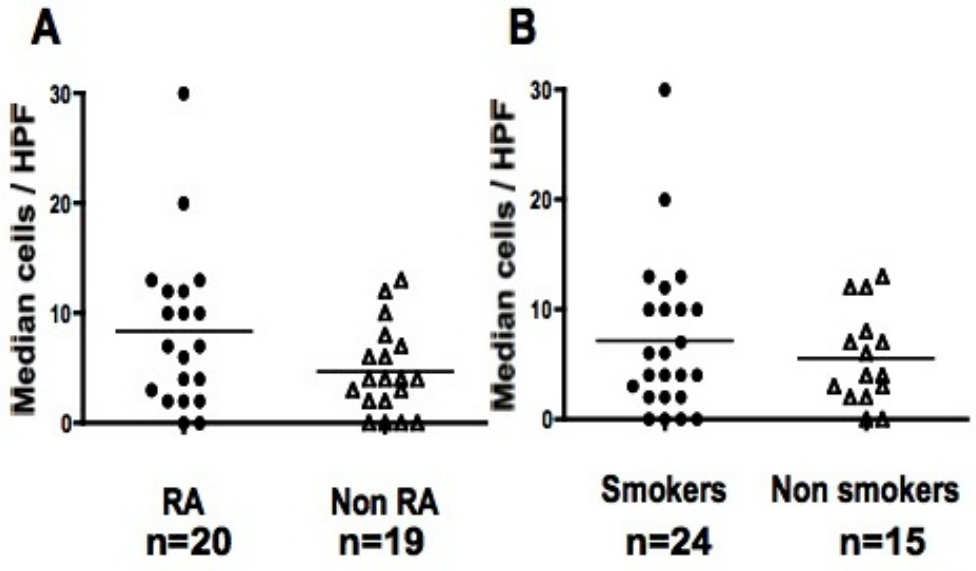

Figure 3.21 IL-18 staining scores in aortic adventitia and IMA

In each graph circles and triangles represents different subgroups that are compared with each other. A) The cytokine IL-18 was found in aortic adventitia and there was no significant difference seen between RA and Non RA patients, as the mean ± SD 8.3 ± 7.3 and 4.6 ± 3.9 respectively p value = 0.10; B). In fact smokers vs. non-smokers revealed no significant difference, as the with mean ± SD 7.1 ± 7 vs. 5.53 ± 4.2 respectively p value = 0.91

3.3.3 BAFF and APRIL expressed by mouse vascular endothelial cell line (SVEC4-10)

In human aortic adventitia we found that vascular endothelial cells of the vasa vasorum, which are the tiny nutrient artery of great vessels, expressed both

BAFF and APRIL. We established a culture system of mouse vascular endothelial cells to verify expression of APRIL and BAFF transcripts.

DNAase free RNA was extracted from mouse vascular endothelial cells and reverse transcribed to cDNA, which was further used to determine what the levels of these transcripts are in the samples as seen below. Vascular endothelial cell line (SVEC4-10) expresses both BAFF and APRIL transcripts (Figure 3.22).

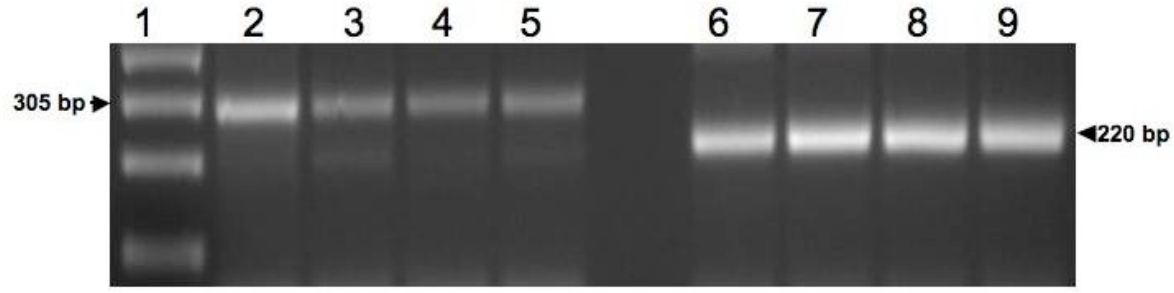

Figure 3.22 BAFF and APRIL expression

BAFF seen as (305 bp) band & APRIL as (220 bp) in vascular endothelial cell line (SVEC4-10) Lane 1 is 1 kb ladder, lane 2-3 represents the vascular endothelial cells expression of BAFF; where as lane 4-5 is BAFF expression in peritoneal macrophages, which were used as a positive control. Whereas, APRIL expression in mouse vascular endothelial cell is seen in lane (6-7) and mouse peritoneal macrophage expression of APRIL is lane 8-9.

The presence of these transcripts in the vascular endothelial cells supports our finding of their protein expression seen in AA and IMA. Moreover, vasa vasorum is present in the deeper layer i.e. the adventitial layer of large blood vessels; which is subject to hypoxic environment. As we confirmed the over expression of both the survival factors in the AA. In addition BAFF expression was found significantly more in the AA of smokers. It was intriguing to address the

expression levels of these transcripts under hypoxia because smoking is known to cause vasoconstriction of end arteries (vasa vasorum), which can induce hypoxia of vascular endothelial cells. To validate if, this phenomenon affects the transcripts of B cells survival factors experiments were carried out.

To initially investigate the effect of hypoxia on SVEC4-10 expression of BAFF and ARPIL transcripts we performed semi quantitative PCR. The expression of APRIL seemed to have some subtle changes when kept under hypoxic conditions. The subtle changes in the semi-quantitative analysis provided a rationale to perform quantitative PCR using SYBR green chemistry. The assay is shown by a product dissociation graph confirming the product specificity by a single peak and the standard curve was to extrapolate number of gene copies (Figure 3.23)

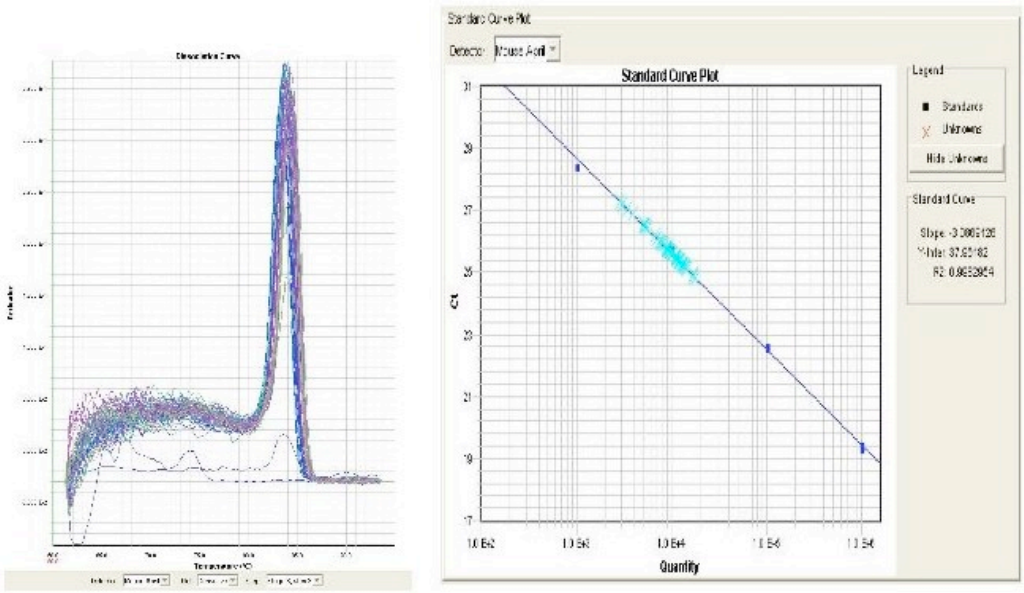

Figure 3.23 Mouse APRIL QPCR

The CDNA was used to quantify APRIL expression using the SYBR green; the dissociation curve on the left panel confirms product specificity and on the right is the standard curve generated using the outer primers to extrapolate the transcript copies.

We then went on and tried different set of conditions to establish the impact of hypoxia (1% oxygen) on transcript levels of APRIL. Cultured SVEC4-10 cells were seeded in T-25 flask and grown till confluence. Then each treatment was in triplicate and treated for 6 and 12 hours under both hypoxia and normoxia, which were compared with the base line APRIL expression at 0hr time point. Moreover, one set of cells were first kept in hypoxic for 6 hours and then brought to normoxia for another 6 hours to explore if reoxygenation effects the APRIL expression. After repeating the experiment several times it was confirmed that there was no effect of hypoxia or reoxygenation upon APRIL expression as shown in the (Figure 3.24)

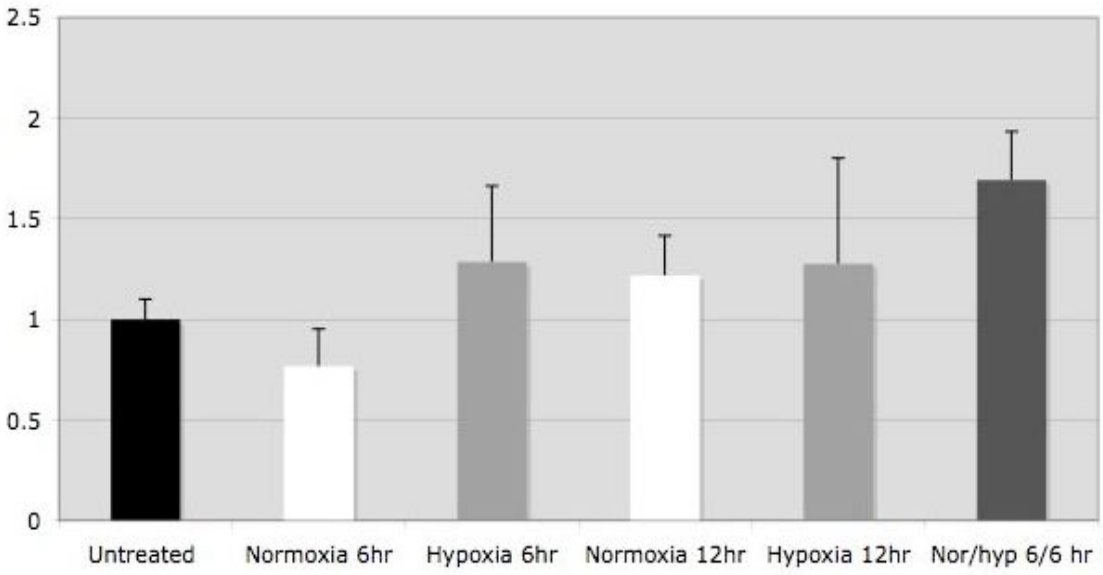

Figure 3.24 Quantitative analysis of APRIL expression in vascular endothelial cells Cultured cells were harvested untreated at 0hr shown as black column; there were cells that were kept under hypoxic conditions for 6 and 12hrs seen as grey columns and at similar time points cells were incubated under normoxia shown with white columns. The last group of cells was first incubated for 6hrs in hypoxia and then reoxygenated for another 6hrs. Every single group was as a biological triplicate. No significant differences were observed between the base line level and all the treatments.

3.4 Discussion

The salient findings of the present study are that the aortic adventitia of rheumatoid arthritis patients, with coronary heart disease, is associated with an environment that is conducive to B cell survival and harbours a known RA-associated self-antigen. Importantly, these insights provide a rationale for the perpetuation of B cell auto-reactivity outside of both lymphoid tissue and the joint in RA.

The presence of citrullinated protein is significantly more in RA aortic adventitia but a reasonable number of non-RA diseased vessels demonstrated CP presence as well, which confirms that citrullination is an inflammation-associated phenomenon rather than an RA specific. In addition the conversion of arginine to citrulline is Peptidylarginine deiminase (PADI) dependent deimination, which occurs under high calcium concentration; physiological calcium level does not support this enzymatic conversion [36]. However, under stress full conditions like apoptosis, terminal differentiation of skin cells and inflammatory responses the calcium concentrations are increased to levels that support citrullination.

These findings were broadened, as we correlated serum ACPA levels in our patients to the CP staining scores. To do this analysis we sub defined only RA patients on account of maximum CP staining score in non RA patients and therefore we had a group of patients with (CP>5.5) this was selected as a cut off because this was the maximum CP score observed in non RA patients. The serum ACPA levels of this subgroup (CP>5.5) of patient correlated to the CRP levels. A strong correlation was observed between ACPA levels and raised CRP levels. Which implies that CP and ACPA might be working synergistically in aggravating the inflammatory response in the blood vessels.

Our attempt to characterize plasma cells with citrulline reactive antibodies was ineffective, which may perhaps be because of inappropriate reactivity of the citrulline used but this is quite difficult to confirm as only one RA patient had plasma cells. In addition, Klareskog et al proposed two subtypes of RA patients APCA positive and ACPA negative patients [217]. If this stands true then even in suitable number of specimens we might have ACPA negative samples, as out of 5 patients positive for plasma cells 4 patient were non-RA; theoretically these samples should not be positive for citrulline reactive antibodies. At the time of

analysis the scorer was blinded to the samples and having noticed no citrulline reactive antibodies is genuine.

Studies to date have focused on intimal lesion in atherosclerosis and role of adventitial tissue has not yet been extensively elucidated. Lymphoid follicular structures in advanced atherosclerotic aortic adventitia were reported to have B cells [144] [215, 217]. More recently ApoE deficient mice were shown to have lymphoid follicle like structures with B cells, which were diet and age dependent [142]. However, we are showing for the first time that a B cell survival niche exist in the aortic adventitia that provide the microenvironment for B cell survival and maturation. Here we report not only CP presence in AA from CVD patients but also significantly increased levels in RA patients. In addition there were more macrophages, plasma cells and B cells in aortic adventitia then IMA along with its survival factors BAFF and APRIL. There were significant associations observed between CP, B cells and APRIL in RA patients.
BAFF expression was increased in smokers with CVD. The expression of both BAFF and APRIL was further confirmed at mRNA message level in vitro in a mouse vascular endothelial cell line (SVEC4-10). However, at a message level these survival factors were not affected with danger signal hypoxia.
There is increasing evidence to support the fact that cigarette smoking is an individual risk factor for both atherosclerosis and rheumatoid arthritis. Moreover, accumulating data from the past decade has indicated that citrullination is strongly associated with smoking and rheumatoid arthritis (RA). However, we could not observe any association between CP and smoking in patients of rheumatoid arthritis. Perhaps there are other unknown environmental factors involved in the citrullination of proteins that were not persistent within our groups.

Our study does have limitations as we have shown all the differences by comparing aortic adventitia from CVD patients and their matched IMA (non diseased vessel); which is not the best vessel to compare with aortic adventitia. Replacement of aortic adventitia with coronary artery with dimensions similar to IMA was one possible option. Secondly, matched saphenous vein adventitia is closer to aorta in size and calibre, so as a negative control it would have provided a better option for comparison. Moreover, the severity of inflammation

in these atherosclerotic plaques would have been underestimated as the specimens were selectively taken (for some surgical reasons) from areas with less severe disease.

The characteristic of IMA to resist atherosclerosis is established but it is not fully understood why it behaves different. However, Ferro et al showed that the lesions are ten times greater in coronary artery then the IMA. This was seen in the inner most layer i.e. intima but not in the tunica media [218]. The IMA have high antioxidant capacity compared to coronary artery SMC; IMA smooth muscle cells also express low tenascin and decorin that are involved in the LDL binding and SMC migration. Apart from these factors there are extrinsic features like axial stretch, sheer stress and small number of side branches that might play a role in the IMA resistance to atherosclerosis [219]. The underlying mechanism for resisting atherosclerosis might not be unfolded yet but there is some unknown attribute that makes IMA unique.

This study suggest that the aortic adventitia of rheumatoid arthritis patients, with coronary heart disease, is associated with an environment that is conducive to B cell survival and harbours a known RA-associated self antigen. Importantly, these insights provide a rationale for the perpetuation of vascular inflammation in RA patients with presence of both CP and ACPA in these patients.

4 IL-33 in Vascular Biology

4.1 Introduction

In atherosclerosis the balance between the Th1 and Th2 immune response is altered and studies have demonstrated that atherosclerosis is predominately a Th1 mediated disease. In fact, atherosclerotic lesions from patients with cardiovascular disease show a predominance of the Th1 cytokines IFNγ and IL-2 [149]. Moreover, the pharmacological down regulation of the Th1 response with pentoxiphylline, in a murine model of atherosclerosis, significantly reduces atherosclerotic burden [153].

One cytokine and its receptor that was recently hypothesized to have a role in the pathophysiology of cardiovascular diseases was IL-33, a novel cytokine of the IL-1 family and a mediator of Th2 responses [175]. It is expressed by synovial fibroblasts, macrophages, endothelial cells and cardiac fibroblasts [200, 220].The receptor for IL-33 is ST2 and this membrane bound form is constitutively expressed on mast cells, fibroblasts and Th2 cells. The secreted form (sST2) is a soluble inhibitory receptor also known as IL1R1-a. This is induced upon appropriate stimulation of fibroblasts, mammary tissue, retina and osteogenic tissue (reviewed [188]). IL-33 has dual properties that of a cytokine and a chromatin associated transcription repressor suggesting its close link to IL-1α and high mobility group box 1 (HMGB1) [182]. The release of this cytokine from the cells has not been convincingly shown. However, apoptosis associated caspases like 3 and 7 cause inactivation of IL-33, which was seen as a reduction in NFκB activation [178]. Interestingly, in our lab some unpublished work has shown that necrotic damage to cells with UV light cause release of full length IL-33; Gerard et al have reported a similar observation in endothelial cells [176].

Human and murine studies have suggested that the levels of soluble ST2 (sST2) are indicative of a role for it in cardiovascular disease. In support of this role, serum concentration of sST2 were found to be elevated in patients with acute heart failure [195] and the levels of serum sST2 strongly correlated with increased future mortality in patients of acute destabilized heart failure [196]. The potential of ST2 as a cardiovascular biomarker was highlighted when it was observed that myocardial injury induced the release of both sST2 and transmembrane ST2. sST2 was demonstrated to be increased one day after myocardial infarction and

was associated with creatine kinase (standard marker for myocardial infarction) and had an inverse association with ventricular function [197]. In addition the potential of sST2 as a biomarker of mechanical overload was investigated in a larger patient cohort where 800 patients presenting with acute myocardial infarction were tested for serum sST2. The serum levels of sST2 at the time of presentation in hospital correlated with 30 day mortality [198].

In juxtaposition to the detrimental role of ST2 in cardiovascular disease, Sanada et al demonstrated that biomechanical stress induced the production of IL-33 by cardiac fibroblasts, which resulted in reduced cardiac hypertrophy and fibrosis [200]. The beneficial role of increased levels of IL-33 was further demonstrated in vivo in an experimental model of atherosclerosis. The supplementation of recombinant IL-33 in ApoE knockout mice, fed on a high fat diet, resulted in a significant reduction in plaque size. This protective effect was specifically inhibited by the administration of sST2 [199]. The underlying mechanism of this IL-33-mediated protective effect was a shift from a predominantly Th1 mediated response to a Th2, which was associated with increased levels of atheroprotective anti-oxLDL IgM antibodies [139]. In support of this mechanism, the protective effects of IL-33 were lost upon inhibition of IL-5 with a blocking antibody.

The great vessels have thick muscular wall and the adventitia of these vessels need continuous supply of nutrients, which is achieved by tiny vessels called vasa vasorum (a single layer of vascular endothelium). Vasoconstriction (due to smoking) of this nutrient supply can result in hypoxia and increased wall thickness, which can further deteriorate the metabolic supply to the adventitia [221, 222]. Endothelium from blood vessels of chronically inflammed tissues like RA synovium and Crohn's disease intestine has marked expression of the cytokine IL-33 [182]. In addition IL-33 expression is demonstrated to be more in the resting endothelium and down regulated upon angiogenic stimulation. Therefore, it is hypothesised that vascular endothelial cells of the vasa vasorum in the aortic adventitia might express IL-33. An interesting question is whether or not co-morbid RA, smoking or levels of oxLDL will modulate this expression. It would be interesting to examine IL-33 expression in AA of smoking patients with that of non-smokers. Moreover, IL-33 is regarded as a novel alarmin, which can respond to danger signals and can function as an extracellular cytokine by mediating Th2

response through IL-4, IL-5, IL-13 and IL-33 also has nuclear repressor properties [223]. Cytokines like IL-5 can induce IgM production that can neutralize oxLDL. We proposed that if IL-33 expressing cells were subjected to danger signals (oxLDL and hypoxia) that are thought to play fundamental role in the progression of atherosclerosis, then we might be able to show interesting association between IL-33/sST2 system and risk factors of atherosclerosis.

4.2 Aims

In view of the role of IL-33 and ST2 in cardiovascular disease the aims of the present study are

1. Examine IL-33 expression in AA and IMA.

2. Verify IL-33 expression in mouse vascular endothelial cell line.

3. Investigate the effects of danger signals (oxLDL and hypoxia) on IL-33 expression in vascular endothelial cell line.

4.3 Results

4.3.1 IL-33 expressed by vascular endothelial cells of AA and IMA

To investigate the expression of IL-33 in the aortic adventitia of patients with advanced atherosclerosis, with or without coexisting RA, we performed immunohistochemistry on paraffin embedded sections from our cohort of 40 aortic adventitia and 33 matched internal mammary artery (IMA). Analysis of staining by light microscopy revealed that IL-33 was detectable in both aortic adventitia and IMA (Figure 4.1 and 4.2). We were able to detect pronounced staining of IL-33 in the vascular endothelial cells of the vasa vasorum of aortic adventitia (Figure 4.1). The staining observed in the vascular endothelial cells of the vasa vasorum had a distinct nuclear localisation pattern (figure 4.1B), implying that IL-33 is synthesised in these cells and transported to the nucleus as a transcriptional regulator. This pattern of staining was also observed in the IMA, where the predominantly positive cells were endothelial cells (lining monolayer) of IMA (figure 4.2B). The semi-quantitative scoring was performed to determine the mean number of IL-33 positive cells per high power field (40x) in the aortic adventitia mean ± SD (2.80 ± 2.5) vs. IMA (4.1 ± 4.36) demonstrated that there was no significant difference in their IL-33 staining ($p=0.36$, paired t test). The presence of IL-33 expressing endothelial cells is not necessarily a feature of cardiovascular disease but rather a component of normal physiology (Figure 4.1 and 4.2).

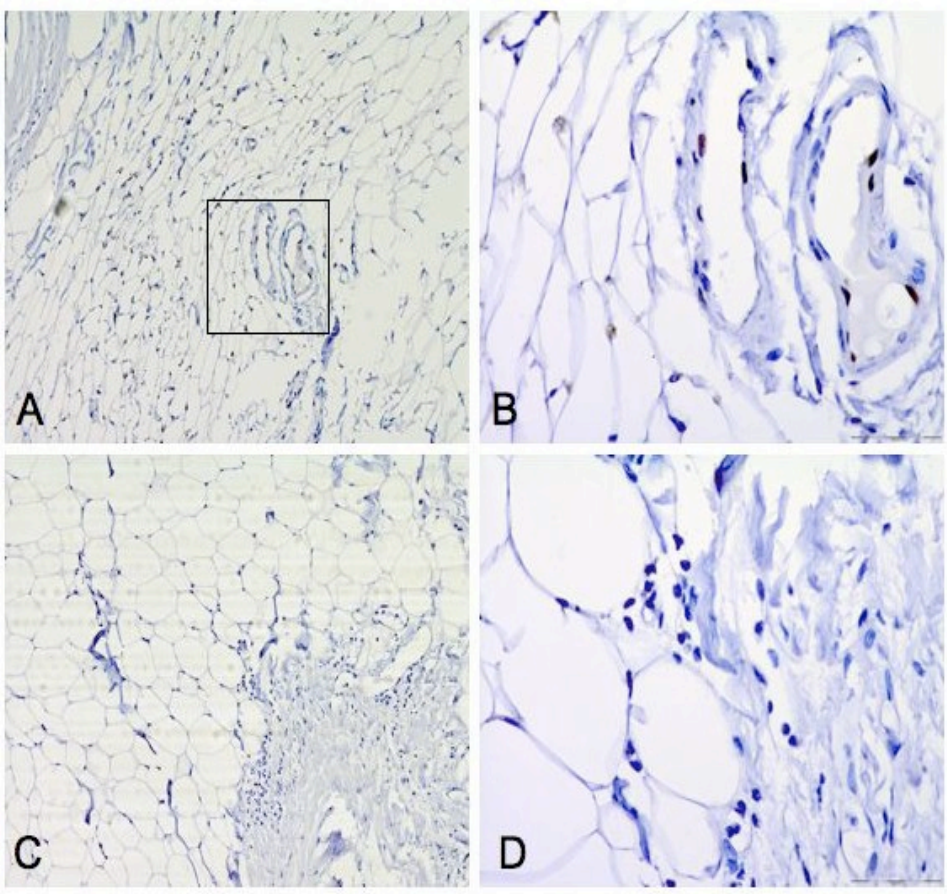

Figure 4.1 IL-33 expressed by vasa vasorum of aortic adventitia

Paraffin embedded aortic adventitial sections underwent deparaffination, antigen retrieval and were stained with either an anti-IL-33 antibody 5μg/ml (A & B) or an isotype control antibody (C&D) and localized with DAB (brown. A & B, illustrate that the monolayer of vascular endothelial cells of vasa vasorum are positive for IL-33 staining and that this staining is predominately nuclear. No positive staining was observed in the isotype control sections (C & D). Original magnification 10x (A & C) and 40x (B & D)

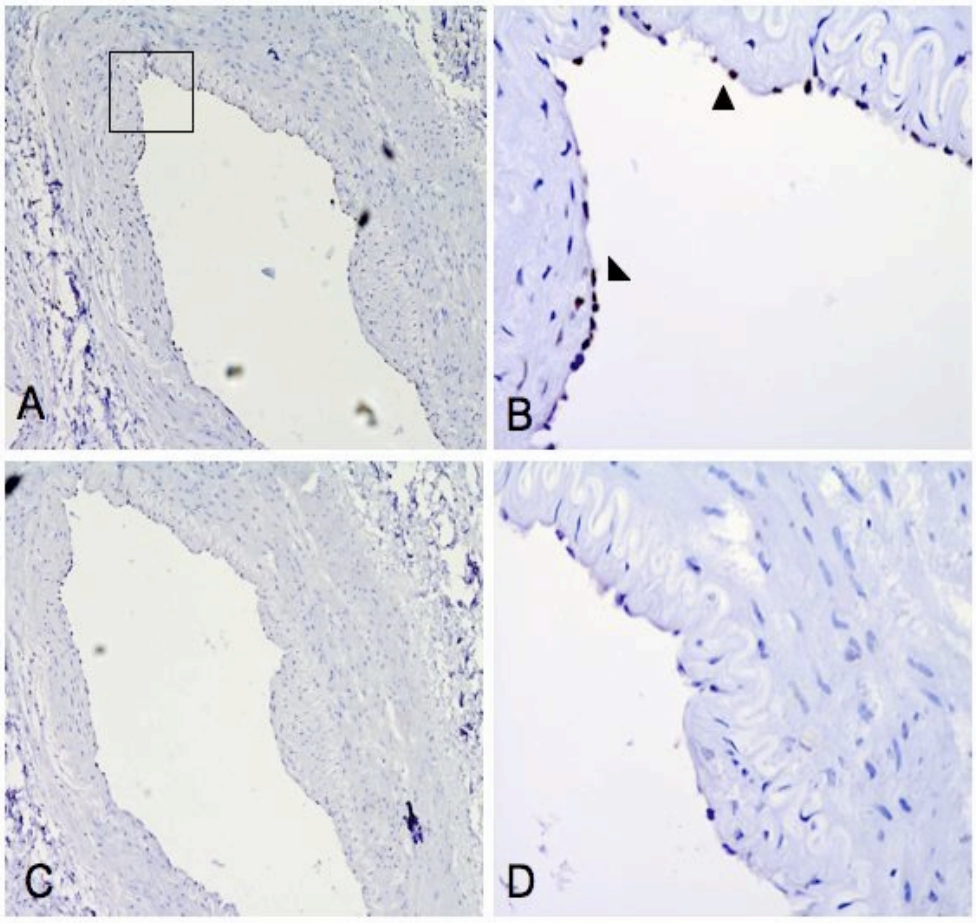

Figure 4.2 IL-33 expressed by vascular endothelial cells of IMA.
IMA tissue section showing lining layer and the adjacent interstitium were stained with either an anti-IL-33 antibody 5μg/ml (A & B) or an isotype control antibody (C&D) and localized with DAB (brown. A & B, illustrate that the monolayer of vascular endothelial cells lining IMA are positive for IL-33 staining (arrows) and that this staining is predominately nuclear. Original magnification 10x (A & C) and 40x (B & D)

4.3.1.1 IL-33 is down regulated in aortic adventitia of smokers

Previous studies have shown that cardiovascular disease is associated with many risk factors including; diabetes mellitus, smoking, dyslipidemia, high blood pressure, advanced age and genetic abnormalities [95]. Our study cohort of patients with advanced atherosclerosis could be sub-divided into smokers (n=21) and non-smokers (n=14). In addition, patients had co-morbidity (RA with CVD, n=20) and only CVD (n=20).

The expression of IL-33 in aortic adventitia of smokers (n=21) and non-smoking patients (n=14) showed that smokers had a significantly reduced level of IL-33 expression than non-smoking patients (p=0.03, t test, Figure 4.3, A). To confirm if this was specific to AA, the IMA tissues were also analyzed for IL-33 expression in smokers (n=19) vs. non-smokers (n=9), and there was no significant difference seen (Figures 4.3, B).

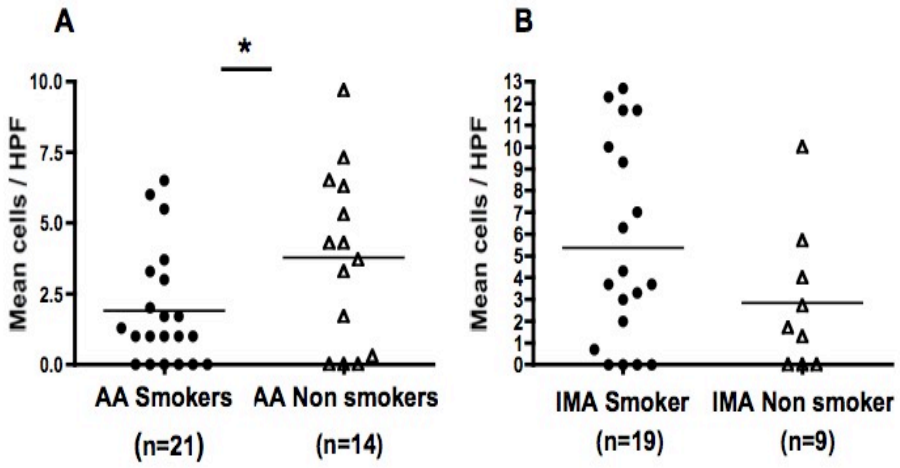

Figure 4.3 IL-33 expression reduced in smokers AA
IL-33 staining was specifically observed in endothelial cells of vasa vasorum. Analysis was performed using mean cells per high power field to demonstrate differences between the subgroups. The circles and triangles represents groups compared A) AA of smoking patients had significantly less IL-33 expression than non-smoking patients (p=0.03, T test). B) The staining scores for (IL-33) in control vessel IMA as mean cells (per HPF) between smokers vs. non-smokers was found to be insignificant.

The results for IL-33 expression in AA of smokers were quite intriguing. To validate if this observation that smoking affects IL-33 expression is specific to diseased vessel (AA) we compared the scores between AA and IMA. There was a marked reduction observed in IL-33 expression in AA (n=21) of smoking patients (p=0.0036, Figure 4.4, A). As smoking is a well know risk factor in cardiovascular diseases; we anticipated no effects on IL-33 expression in vascular adventitia of

non-smoking patients, this was confirmed by analysis shown in graph (Figure 4.4, B).

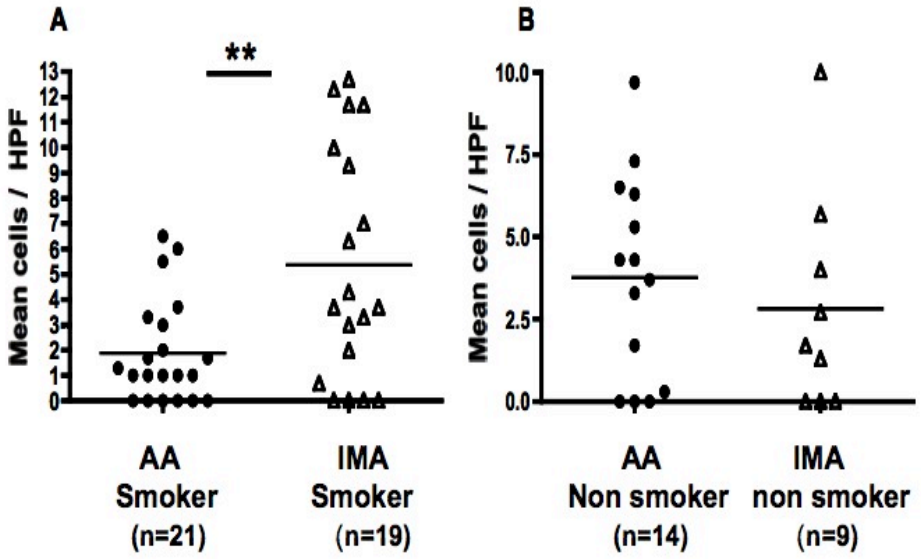

Figure 4.4 IL-33 expressions in Aortic adventitia and IMA
The staining score were quantified using light microscopy and mean cells per (HPF) were used to analyse differences between the groups. The circles and triangles represent the groups compared. A) IL-33 staining scores in smoking patients AA (n=21) compared with IMA (n=19) demonstrated significant reduction (p=0.0036, paired t-test), whereas, B) Non smokers AA (n=14) and IMA (n=9) showed no significant difference.

In addition, the sub-division of patients into those with or without RA co-morbidity demonstrated that RA did not affect the levels of IL-33 in either endothelial cells of vasa vasorum (AA) or lining layer of IMA (figure 4.5).

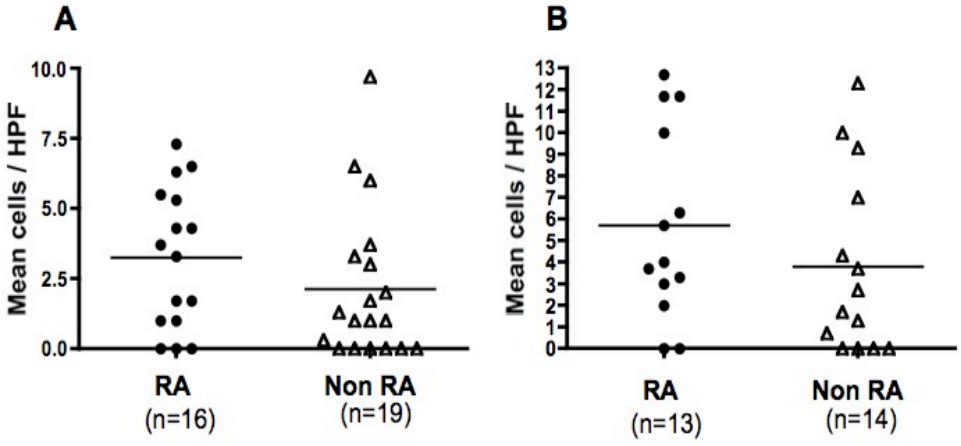

Figure 4.5 IL-33 expressions in RA and non-RA patients
IL-33 staining was specifically observed in endothelial cells of vasa vasorum. Analysis was performed using mean cells (per field) to demonstrate differences between the groups. The circles and triangles represents groups compared A) AA of RA patients (n=16) had a similar IL-33 expression as non-RA patients (n=19). B) The staining for IL-33 was specifically seen in endothelial lining layer of control vessel (IMA) and no significant difference was observed between RA (n=13) vs. non-RA (n=14) patients.

These data clearly suggest that in the vasculature IL-33 is expressed primarily in endothelial cells and that smoking can contribute to decreased cellular expression/nuclear localisation of IL-33 in small vessels in an inflammatory environment. Subsequent experiments addressed the possible functional significance of this observation.

4.3.2 IL-33/sST2 mRNA transcript under oxLDL and Hypoxic conditions

Previous studies have demonstrated that IL-33 is expressed in vascular endothelial cells of chronically inflammed tissues [182]. Whilst other studies have shown factors such as oxLDL and hypoxia can induce endothelial dysfunction or damage. It has been previously shown that in vivo effects of IL-33 can be altered by the use of decoy receptor sST2. Interestingly we looked at these two transcripts in parallel because the vascular endothelial cells express them so if one goes up then the other is down regulated. It was therefore important to look at these two transcripts in parallel to demonstrate the impact of different

treatments (oxLDL, hypoxia) on their transcript levels. To test this hypothesis we established a culture system to examine the mRNA expression of IL-33 under the influence of oxLDL and hypoxia. Our initial experiments were performed to demonstrate that mouse vascular endothelial cells (SVEC4-10) expressed detectable levels of IL-33 and sST2 transcripts. A PCR was designed and optimised to evaluate the expression of IL-33 and sST2. An example of the PCR can be seen in Figure 4.6. This illustrates that the IL-33 transcript (270bp) is expressed in SVEC4-10, where smooth muscle cells were used as a positive control (Figure 4.6, A). In addition, sST2 (600bp) was also detectable in SVEC4-10 cells (Figure 4.6, B). Studies have shown that non-haemopoietic cells like fibroblasts, retinal cells and mammary tissue express the inducible isoform sST2 (reviewed [188]). However, the expression sST2 by vascular endothelial cells have not previously been reported. Our experiment demonstrates that mouse vascular endothelial cells express sST2 transcript.

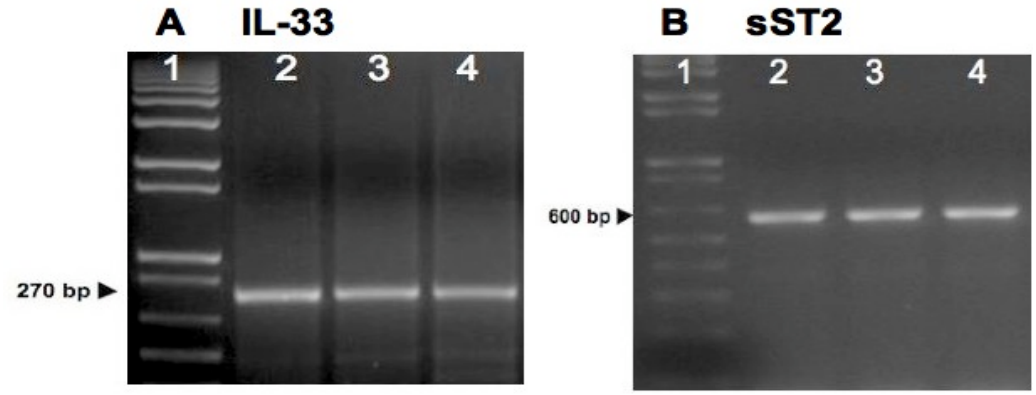

Figure 4.6 PCR for IL-33 and sST2 in vascular endothelial cell line (SVEC4-10) PCR was performed to detect mouse IL-33 and sST2 mRNA expression in vascular endothelial cell line. A) Lane 1 is 1 kb ladder, lane 2-3 represents vascular endothelial cells and lane 4 is positive control (mouse smooth muscle cells); whereas, B) is sST2 PCR, lane 2-3 represents vascular endothelial cells and lane 4 is positive control (mouse Fibroblast)

Having established that both IL-33 and sST2 are expressed in the murine vascular endothelial cell line SVEC4-10, we designed a quantitative PCR procedure to evaluate the specific levels of both IL-33 and sST2. Using primers for IL-33/sST2 QPCR was performed and the data was normalized with the house-keeping gene GAPDH, we generated gene specific standards (purified products) using an outer

set of primers. Inner primers were then used to detect the specific gene in the samples and in the generation of a standard curve for quantification. A QPCR was performed to evaluate the standard curves, generated from outer primers, for the housekeeping GAPDH (ct 19) and IL-33 (ct 24, Figure 4.7, B & C). A melting curve was performed to ensure product specificity, which can be seen as single peaks for both the genes. (Figure 4.7, A)

This data shows that mouse vascular endothelial cells (SVEC4-10) express IL-33 that can be quantified using the method explained for evaluating changes in transcript levels under different conditions (oxLDL or hypoxia).

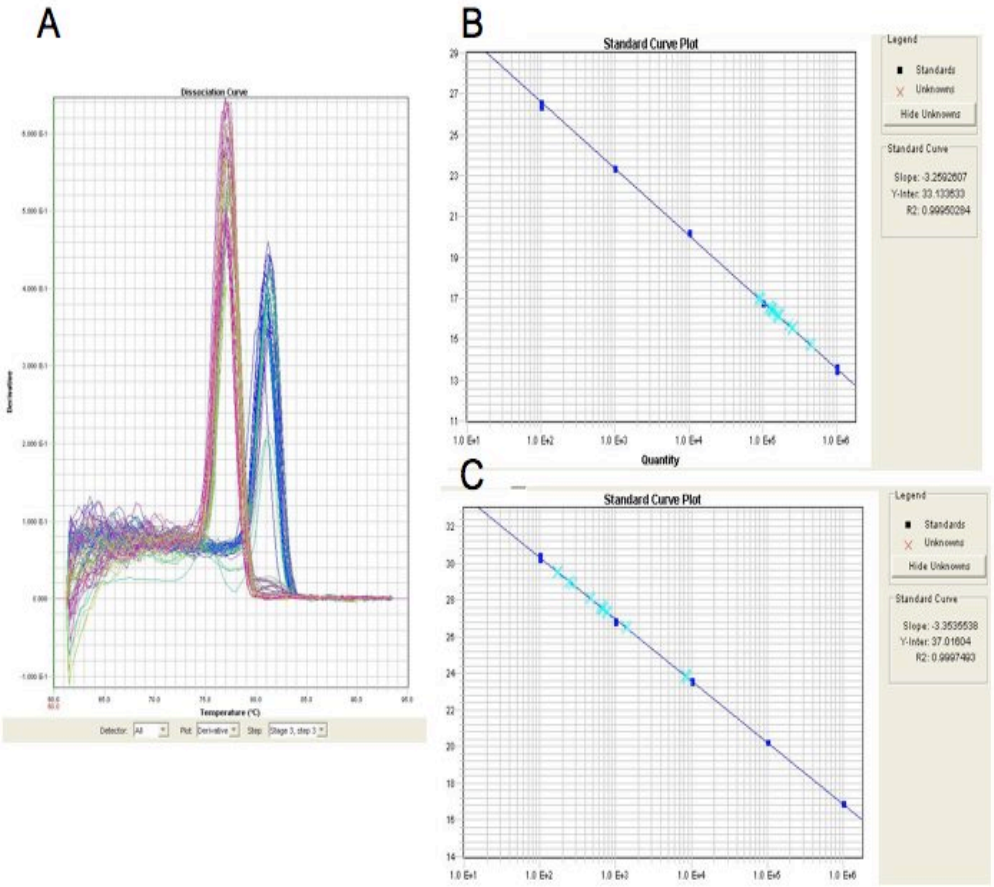

Figure 4.7 QPCR for IL-33 and house keeping gene (GAPDH)
This QPCR was performed using SYBR green; (A) The product specificity was confirmed by dissociation curve showing two peaks one for the housekeeping gene GAPDH (Red) and other for IL-33 (blue). (B) The graph represents the standard curve for IL-33 using the outer primers; this is to extrapolate the number of copies of the sample gene. (C) Using the outer primer, the product of house

keeping gene (GAPDH) is serially diluted to generate the standard curve; which helps to normalize the number of copies of the sample gene (IL-33).

4.3.2.1 Lipoprotein isolation and oxidative modification

To investigate the effect of oxLDL on IL-33 and sST2 transcript levels in SVEC4-10 we used the method of Binder et al to generate native LDL from fasting human serum collected from healthy individuals. This involved the isolation of LDL lipoproteins by consecutive ultracentrifugation of fasting human serum. After isolating native LDL, it was quantified using the modified Lowry protein assay, a standard curve was generated using bovine serum albumin (BSA) and the concentration of LDL samples was determined by extrapolation from the standard curve. The OD value for LDL was 0.14, which was used to calculate the LDL concentration (12.4 mg/ml) using the formula shown in the graph (Figure 4.8). The modification of native LDL to an oxidised LDL was achieved by the addition of copper sulphate using a previously published protocol [224]. To stop the oxidization of native LDL and additional oxidization of oxLDL the lipoproteins were stored in PBS containing 0.25mM EDTA.

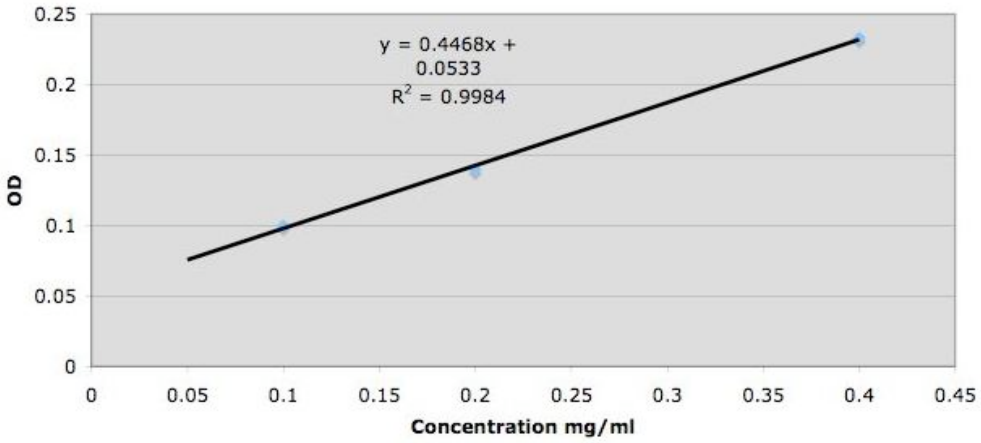

Figure 4.8 Modified Lowry assay

This standard curve was generated using known concentration of BSA; which was used to extrapolate the LDL concentration in mg/ml.

4.3.2.2 The effect of ox-LDL on the level of IL-33 transcript in SVEC4-10

Thus far, the IL-33 transcript is confirmed in endothelial cell line and to investigate the hypothesis that danger signals (oxLDL or hypoxia) could affect IL-33 transcript levels. We treated SVEC4-10 cells at 75% confluence, as confirmed by light microscope, with either, oxLDL (80μg/ml) and native LDL at the same concentration, or vehicle (PBS-EDTA). The freshly isolated modified LDL and oxLDL were prevented form oxidation by adding 0.25mM EDTA. Therefore, because of the addition of EDTA to our low-density lipoprotein samples a vehicle (PBS) containing EDTA was included as a control treatment. Cells were treated for 24 or 48h and RNA harvested for determining IL-33 transcript level. To establish a baseline value for IL-33 transcript cells were harvested when the treatment was started at time (0hr). As can be seen in (Figure 4.9), at 24hr both native LDL and vehicle resulted in an increase (<2 fold) in IL-33 transcript, while oxLDL did not affect the IL-33 transcript.

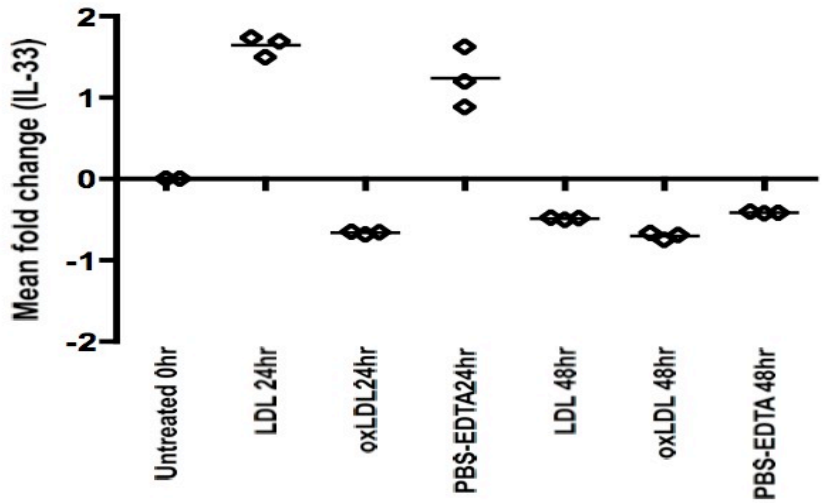

Figure 4.9 QPCR analysis of IL-33 expression in mouse endothelial cell line (SVEC4-10).
Cells were treated for 24hrs with LDL, oxLDL and PBS-EDTA (in triplicate) and every single square represents a treated sample. Transcript levels are represented as mean fold change relative to base line levels (untreated 0hr). DNA-free RNA was extracted from mouse cell line, which was reverse transcribed and used in a quantitative PCR (SYBR Green chemistry). A trend was observed in IL-33 expression (up regulated) at 24hr with LDL and PBS-EDTA treatment as compared to the untreated (0hr) levels. However, the expression is close to the

base line (untreated 0hr), and was almost similar for all the treatments after 48hours.

As these findings show a trend at 24hr time point in the level of IL-33 transcript and not at 48hr, it was important to investigate the change in IL-33 transcript prior to 24hr. The treatment groups were kept same as the pervious experiment. Unfortunately, in this experiment there was no difference seen within the groups at any time points. However, there was a fluctuation observed for all the samples at three different time points, At 6hr IL-33 baseline levels were below baseline and at 12hr and 24hr remained above the base line. However, all the values were very close to base line and hence nothing significant (Figure 4.10).

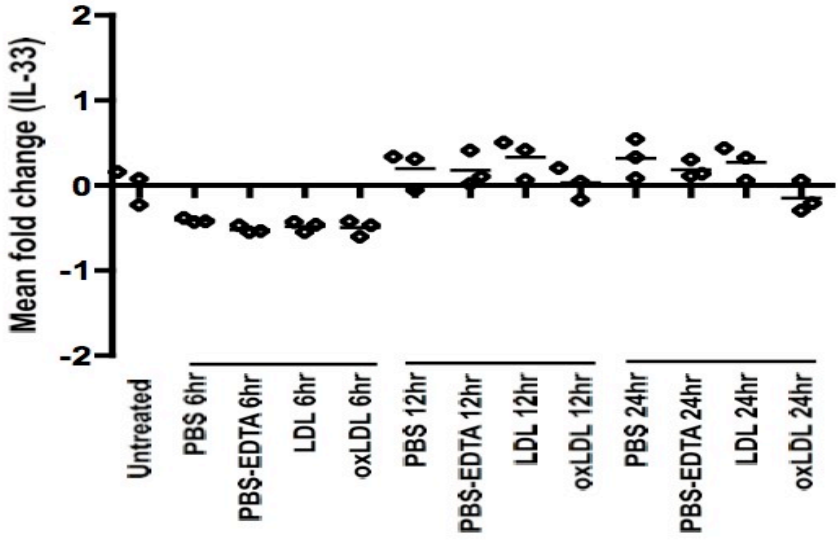

Figure 4.10 IL-33 expression at earlier time points (6hr, 12hr, 24hr)
The IL-33 transcript were looked under different treatments at earlier time points like 6hr, 12hr and 24hrs; cells were treated with (PBS-EDTA, PBS, LDL, and OxLDL) at each time point; each treatment was in triplicate and every single square represents a sample. Transcript levels are represented as mean fold change relative to base line levels (untreated 0hr). None of the treatment showed any significant differences within the groups.

To verify that oxLDL did not affect IL-33 transcript levels another experiment was set, this time apart from the three different treatment groups an additional group of untreated cells was added at each time point. This was to confirm if the baseline level of IL-33 transcript remains consistent for the untreated cells.

In addition this time we also looked at the sST2 expression in the same settings as explained above.

There was no difference seen in IL-33 mRNA fold change with or without treatment within the groups at any time point. (Figure 4.11, A). Moreover, the sST2 transcript levels were not significantly affected at any time point (6hr, 12hr, 24hr), and no considerable changes were observed within the groups with any treatment (Figure 4.11, B).

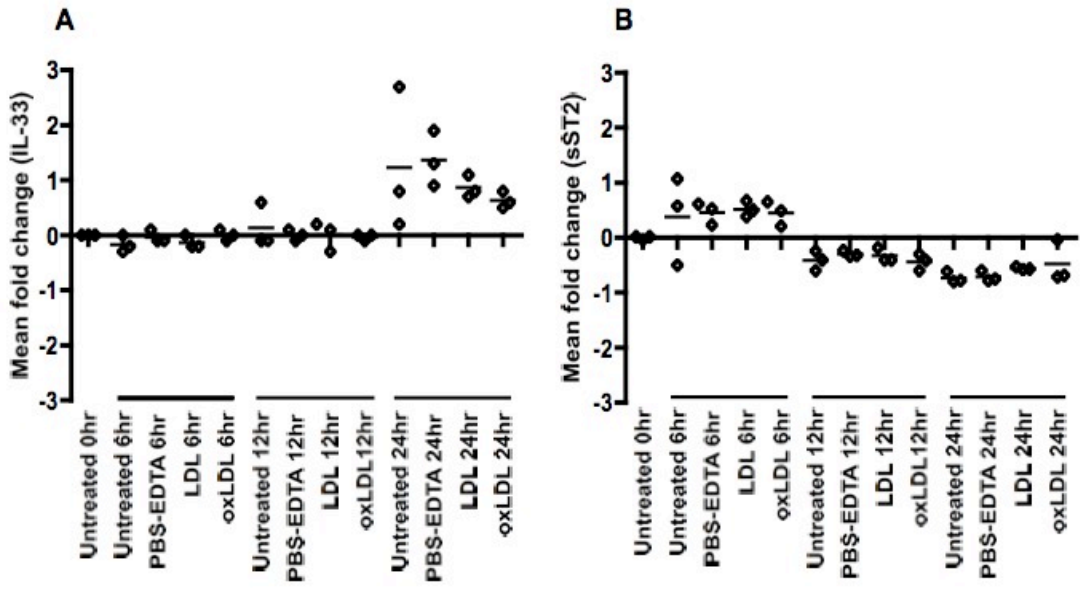

Figure 4.11 A) IL-33 mRNA expression at 6hr, 12hr and 24hr time point
The gene expression was looked under different conditions at earlier time points; 6, 12 and 24hr; The cells were treated with (PBS-EDTA, LDL, OxLDL and an untreated group was also included) at every time point; each treatment was in triplicate and every single dot represents a mean fold change relative to baseline line level. None of the treatment showed any significant differences within the group; however, IL-33 showed slight increase at 24hr in comparison with cells harvested at any other time point. B) sST2 mRNA expression shows a trend at 6hr time point in vascular endothelial cells

4.3.2.3 Synchronized SVEC4-10 and IL-33/sST2 mRNA

In the experiments performed to this point it was not clear whether the IL-33 transcript level fluctuation at different time points were because of cell cycle or

any other factor. Previous studies have shown that serum starvation synchronize cells cycle of the cultured cells. Therefore, mouse vascular endothelial were serum starved (0.2% FCS) [225], as this would result in synchronization of the cells in culture. After 12hr of serum starvation with 0.2% FCS; fully confluent cells were harvested at 0hr, 6hr, 12hr and 24hr. The semi quantitative PCR (Semi QPCR) showed consistent levels of IL-33 transcript levels at all time point as demonstrated (Figure 4.12), indicative of no effects of cell cycle on the IL-33 expression.

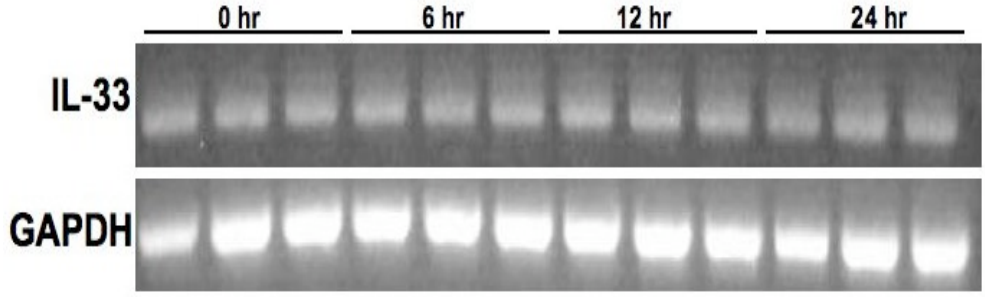

Figure 4.12 IL-33 mRNA expression in synchronized mouse vascular endothelial cells
Murine vascular endothelial cells were serum starved with (0.2% FCS) for 6hr, 12hr and 24hr. Top panel is IL -33 level at 4 different time points (in triplicate); which were analyzed relative to the house keeping gene (GAPDH). IL-33 transcript levels were consistent across all time points.

4.3.2.4 Confluence of cultured cells and IL-33 expression

As there was no effect seen with serum starvation, which suggest that cell cycle is not affecting IL-33 gene expression; another interesting factor to examine was confluence of the cultured cells. To investigate the impact of confluence on cultured cells, an experiment was set with fully confluent cells, which were treated with oxLDL and native LDL. When cells were fully confluent untreated cells were harvested to confirm baseline levels and also at each time point (6hr, 12hr, 24hr) to see the impact of different treatments. This demonstrated that the IL-33 baseline levels were increased with confluence because this time the mean fold change relative to baseline levels dropped for all treatment close to

zero. Therefore, in these settings IL-33 transcript levels are almost same (Figure 4.13, A).

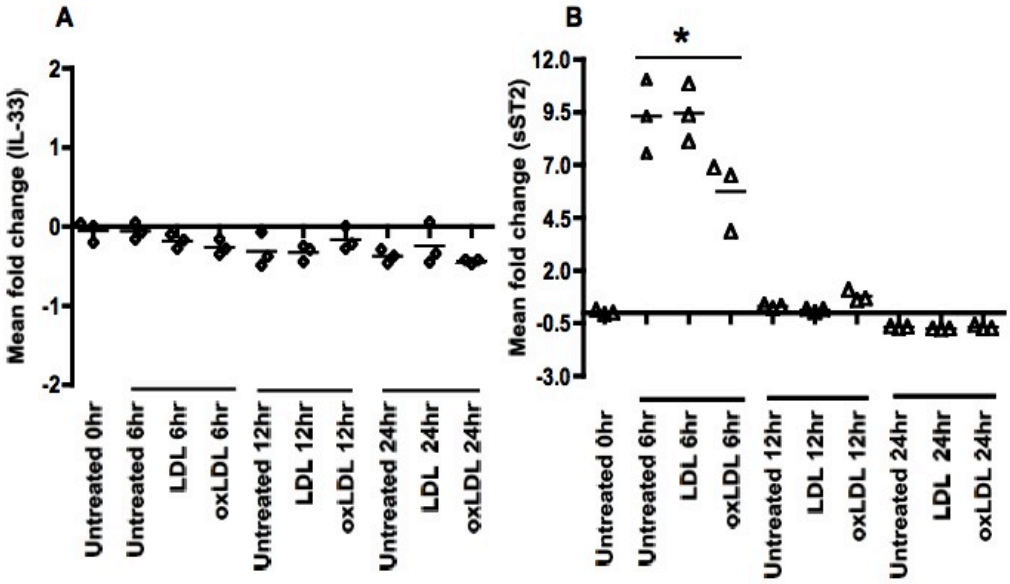

Figure 4.13 IL-33 mRNA upregulated with confluence
Fully confluent cells were treated for different time points (6hr, 12hr, and 24hr) with oxLDL and native LDL. Every treatment was performed in triplicate. Each single sample is represented with a square. A) There were no significant change observed in IL-33 transcript with different treatments within each individual group relative to the expression of untreated cells at 0hr. B) The base line expression level of sST2 with full confluence was quite low and this got significantly upregulated at 6hr ($p<0.05$, Mann-Whitney) for all the treatments. However, this was followed by a decrease in the expression level at later time points of 12hr and 24hr.

In this experiment with fully confluent cells in culture assuming that the IL-33 transcripts would be stable for untreated (0hr) These confluent cells were treated with oxLDL and native LDL for 3 different time points. Interestingly the same exact triplicate was also analyzed for sST2 transcript to confirm IL-33/sST2 relationship under the influence of stress factors in cells expressing both these transcripts together. IL-33 transcripts did not show a change with any treatment within the groups at 6hr, 12hr and 24hr (Figure 4.13, A). However, the transcript levels of sST2 were looked at in parallel and there was a significant up

regulation seen at the 6hr time point with all the different treatments ($p<0.05$, Mann-Whitney).

Thus far, it was observed that fluctuations seen in IL-33 mRNA was due to change in confluence and this was confirmed by a recent study, where resting confluent vascular endothelial were shown to have high IL-33 expression and it was lost upon angiogenic proliferation [220].

4.3.2.5 Validation of generated lipoproteins

In our culture system oxLDL treatment did not alter the levels of IL-33 transcript. To validate whether lipoproteins generated from fasting human serum were properly oxidized with copper, we ran a lipogel (Beckman coulter) for different batches of both oxLDL and native LDL. To our surprise all the batches of modified and non-modified LDL used in the present study were found to be oxidized, which seemed a spontaneously oxidation (Figure, 4.14), despite the fact that they were kept in dark in a buffer containing EDTA to prevent spontaneous oxidation.

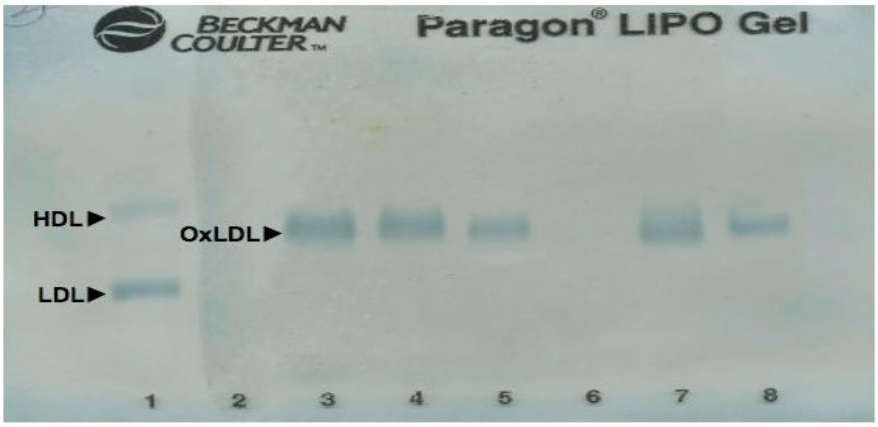

Figure 4.14 Gel electrophoresis for lipoproteins
The native LDL and oxLDL isolated from healthy donors were confirmed for their oxidation status on the lipogels. Lane 1 is serum from fasting donor (a positive control for LDL and HDL) that shows two bands top one is HDL and the bottom one is LDL. Lane 3 is OxLDL (Batch 1), Lane 4 is native LDL (batch 1). Lane 5 is also oxLDL; thereafter lane 7 is oxLDL (Batch 2) and lane 8 is native LDL (Batch 2) This gel, therefore, confirms that both batches of native and modified LDL are

oxidized, which implies a spontaneous oxidation despite the fact that they were stored in dark at 4^0C.

Henceforth, fasting serum from healthy donors was used again to generate fresh native LDL. After 4 days of ultracentrifugation a fresh batch of LDL was produced, which was oxidized using copper sulphate. This time samples were immediately run on a lipogel with human serum as a control that contains both LDL and HDL. Surprisingly, the freshly prepared LDL was not oxidized using the published protocol (Figure 4.15)[224]. Therefore, all the experiments

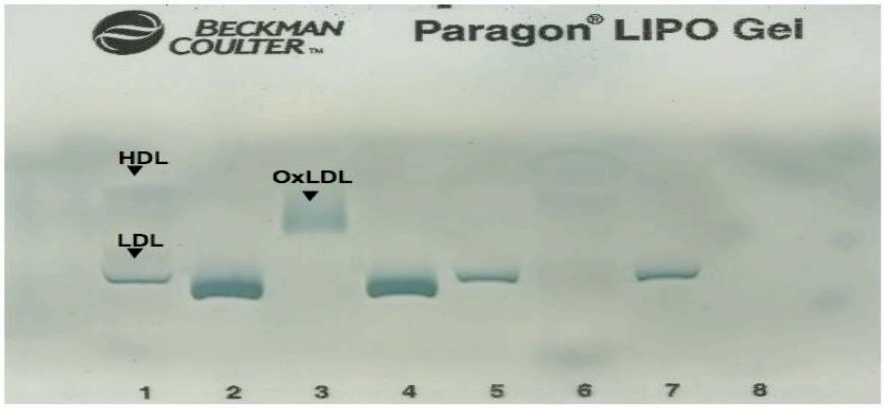

Figure 4.15 Gel electrophoresis for lipoproteins
Lane 1 is human fasting serum (positive control) that has two bands a top faint one is HLD and the bottom one is LDL. Lane 2 is native LDL. Lane 3 is spontaneously oxidized LDL (positive control, previous batch). Lane 4 is fresh LDL. Lane 5 is new oxidized LDL, which is not oxidized. Lane 6 is HDL extracted from fasting serum. Lane 7 is native LDL.

Performed in the present study to examine the impact of oxLDL on IL-33/sST2 system are inconclusive and needs to be repeated with properly oxidized LDL.

4.3.2.6 Hypoxia and IL-33/sST2

Previous studies have shown that smoking can cause vasoconstriction of nutrient vessels (vasa vasorum) of aortic adventitia, resulting in hypoxia of vascular endothelium. Together both smoking and hypoxia are implicated in the underlying disease mechanism of atherosclerosis [226]. In addition, this present study confirms that IL-33 expression in vascular endothelial cells of AA was down

regulated in smoking patients. Therefore, it was important to investigate the expression of IL-33 and sST2 under the influence of hypoxia.

As we were unaware of the fact that oxLDL used in the system was not properly oxidized, we initiated a parallel set of experiments to investigate the impact of hypoxia and/or oxLDL on IL-33/sST2 transcript levels. Murine vascular endothelial cells in the established culture system were kept under hypoxia (1% oxygen) and normoxic conditions at 75% confluence. No significant difference was seen in comparison to cells at normoxia at both 6hr and 12hr (Figure 4.16, A). The IL-33 fluctuation observed with full confluence in the earlier experiments was not seen this time. sST2 transcript levels were also same for all the samples. (Figure 4.16, B)

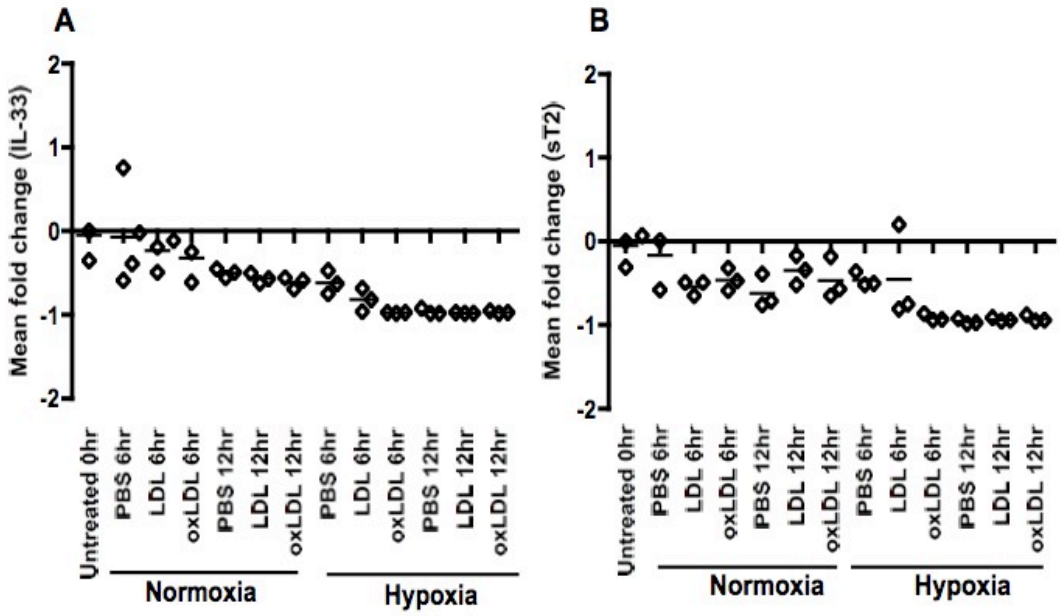

Figure 4.16 QPCR for IL-33 & sST2 gene expression under hypoxia
A) IL-33 mRNA in murine SVEC4-10 treated with PBS, oxLDL, LDL in triplicate under normoxia and hypoxia (1%) for 6hr and 12hrs. No significant effects were seen in the expression level of IL-33 at both 6hr and 12hrs. B) Soluble ST2 transcript levels in similar settings showed a trend of reduction in transcript level, which was not significant.

It came to our attention at this point that a published study has demonstrated in the past that the house-keeping gene (GAPDH) was affected by hypoxia. This was

particularly relevant, as all of our previous studies had used GAPDH as a house-keeping gene to normalise our specific genes. We, therefore, investigated the effect of hypoxia on GAPDH in our culture system. We designed a new set of primers for beta actin gene to perform QPCR. The data with beta actin showed a clear 5 fold up regulation of GAPDH level at 6hr and a 9-fold up-regulation at 12hr. The reoxygenation of the cells at 6h resulted in stabilisation of the GAPDH levels, as can be seen in Figure 4.17. These finding were consistent with the data published for GAPDH up regulation under hypoxia [227]. Therefore in all subsequent hypoxic experiment beta actin was used as the house-keeping gene.

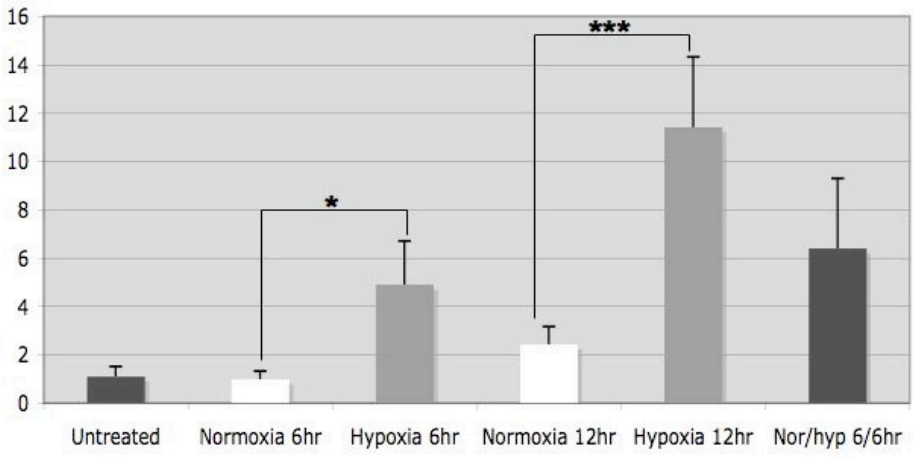

Figure 4.17 Hypoxia upregulates expression of house keeping gene GAPDH Mouse vascular endothelial cell line (SVEC4-10) was looked for GAPDH expression under hypoxic conditions; the white columns represents cells exposed to normoxia; whereas, the grey column show expression of cells under hypoxia. The GAPDH expression is significantly up regulated after 6hr treatment (5 fold) and it further increases to around 10 fold ($p<0.0001$, T test) after 12 hours of exposure to hypoxic conditions in comparison to cells exposed to normoxia. The last column shows that cells that were kept in normoxia for 6hr and then in hypoxia for 6hr had an up rise as well.

To investigate the effect of hypoxia on IL-33 transcript levels in murine vascular endothelial cells line. Cultured cells were exposed to normoxia; hypoxia (1% oxygen) and one group of cells were reoxygenated by incubation in hypoxia for 6hr and then in normoxia for another 6hr. The data was analyzed with both

GAPDH and Beta actin (Figure 4.18 A, B) respectively; which look completely different and knowing that it is the house keeping gene GAPDH that gets up regulated under hypoxia. In this experiment again the expression levels increased at 12hr time point and no important variation seen with the different treatment; which is consistent with previous results for IL-33/sST2.

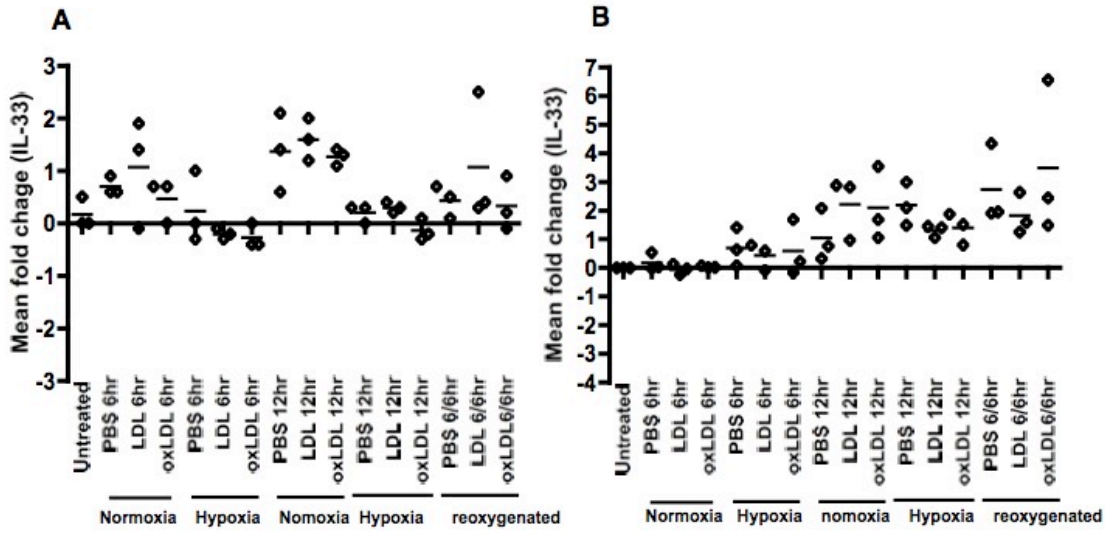

Figure 4.18 IL-33 transcript levels, hypoxia and house keeping genes. Mouse vascular endothelial cells were treated with vehicle (PBS), LDL and oxLDL under hypoxia (1% oxygen) and normoxia for 6hr and 12hr. Another group was added where treatments were carried out for 6hr under hypoxia and then the cultured cells were reoxygenated for the last 6hrs. The IL-33 transcript levels were normalized with two different house keeping genes GAPDH and beta actin. A) QPCR data for IL-33 transcript levels normalized with GAPDH show some random variation that are due to changes in the house keeping gene (GAPDH) B) The transcript levels normalized with beta actin as house keeping gene shows a trend of up-regulation at 12hr.

As we understand from the results so far, that IL-33 transcript levels have fluctuation in baseline level depending on cells confluence at the time of harvest. Moreover, the effects of oxLDL cannot be investigated because the modification of LDL did not yield oxLDL form. Therefore, a Final experiment was designed to determine the impact of hypoxia on IL-33/sST2 transcript levels.

Murine cells were cultured and once fully confluent SVEC4-10, exposed to hypoxia (1% oxygen) for 6hr and 12hr. Cell were also kept in normoxia as a control group for the same length of time, lastly a group of cells were kept under hypoxia for 6hr and then brought back to normoxia for the last 6hr to examine the affects of reoxygenation on IL-33/sST2 expression. The QPCR data was normalized with beta actin as a house keeping genes. IL-33 transcript level at 0hr was considered as baseline therefore all the other treatment are presented as mean fold change calculated relative to the baseline, which showed that all treatment samples had almost similar transcript levels (Figure 4.19, A). Whereas, the sST2 transcript levels up regulated at 12hrs under both normoxia and hypoxia, which were not significant (<2.5 fold), Figure 4.19, B)

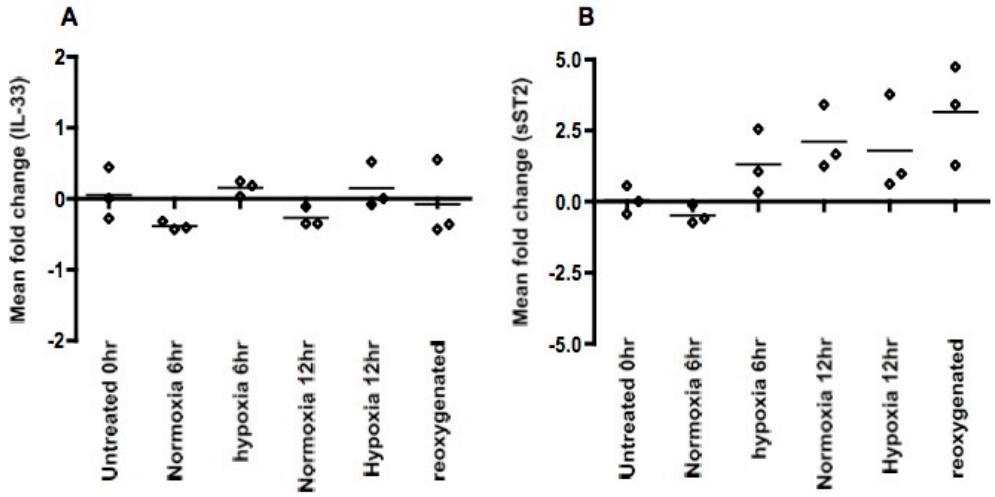

Figure 4.19 Fully confluent SVEC4-10 under hypoxia
Murine endothelial cells were exposed to normoxia, hypoxia (1% oxygen) and reoxygenation for 6hr and 12hr. Cell were harvested when fully confluent at 0hr and IL-33 ct was normalized with β actin and fold change was calculated. A) IL-33 expression at 0hr is base line and it was used to calculate relative fold change for all the samples treated under different conditions. B) sST2 fold change at 12hr show an increase of (<2.5), which is not significantly different.

4.4 Discussion

It has been shown previously that IL-33/sST2 is important in cardiovascular system. The protective effects of IL-33 in the murine model of atherosclerosis are shown to exist through Th2 cytokines IL-5 and IL-13. Importantly, the blockade of IL-5 results in augmented plaque size despite IL-33 treatment [199]. Moreover, IL-5 is known to exert its anti atherosclerotic response through natural antibodies against oxLDL [139]. This suggests that IL-33 has an atheroprotective role through B-lymphocytes and antibodies.

The salient findings of this study are that there is down regulation of IL-33 expression in vascular endothelial cells of human AA of smokers. In non-smoking patients the level of IL-33 was comparable between the AA and IMA, and it was similar for both the vessels. It can be hypothesized that IL-33 is released with damage to vascular endothelium, which then stimulates the production of natural antibodies against oxLDL through IL-5; the antibodies then perhaps block the uptake of oxLDL by macrophages. Most likely this smoking associated down regulation of IL-33 expression is suggestive of failed protective mechanisms of this Th2 cytokine, however, this could be an indirect effect of smoking on IL-33 expression in AA.

A culture system was established to confirm the impact of hypoxia and reoxygenation on IL-33/sST2 transcripts in vascular endothelial cells. Initially the expression of IL-33/sST2 was confirmed in vascular endothelial cell line. In the process of optimization of the culture system for gene quantification, it was observed that GAPDH (house-keeping gene) is significantly up regulated with hypoxia at 6h and 12hrs. It was also established that other house keeping gene, Beta actin is not affected by hypoxia. Therefore, in the experiments towards the end, the data was normalized with Beta actin, which confirmed that IL-33/sST2 is not affected under hypoxia or reoxygenation. Interestingly, it was observed that IL-33 transcript fluctuate with proliferation/confluence of cells; whereas fully confluent cells in culture resulted in stable level of IL-33 transcripts [220]. Therefore, fully confluent cells were treated under hypoxia and reoxygenation, which confirmed insignificant changes in IL-33/sST2 transcripts. In addition a recent study showed that IL-33 is lost by endothelial cells during wound healing and angiogenesis [220]. While optimizing the culture system it was shown that IL-33

expression fluctuates with confluence of cells. To ensure stable base line IL-33 transcripts at 0hr in the culture, fully confluent cells should be used in the future experiments. This would certainly help in consistent results, and add to the reliability of data in addressing the impact of hypoxia on IL-33/sST2 transcripts in vascular endothelial cells.

The present study also aimed to investigate the impact of oxLDL on IL-33/sST2 expression. The effects of oxLDL could not be demonstrated because the copper sulphate induced modification of LDL did not result in oxidation for us. In addition, the time limitation does not allow for establishing a new protocol for LDL modification and more experiments in our culture system.

In summary IL-33 is expressed by vascular endothelial cells of human AA and IMA. The protein expression is down regulated in smoking patients AA. In a culture system IL-33/sST2 are not affected under hypoxia. Therefore the formal explanation for the down regulation of IL-33 in smokers remains unclear. It does not however appear to be a direct smoking related phenomenon

5 The impact of B cell depletion therapy on Atherosclerosis

5.1 Introduction

Rheumatoid arthritis (RA) is a chronic progressive debilitating disease that primarily involves the joints. If the treatment is started early in the course of disease with DMRDs (methotrexate, sulfasalazine, hydroxychloroquine, leflunomide and glucocorticoids)[41] this can delay the onset of cartilage and bone erosion associated with excruciating pain and joint deformity. Moreover, RA patients have a strong association with cardiovascular morbidity and mortality [89, 90, 99].

RA patients require lifelong treatment including medications, exercise and even surgery in advanced cases. Different treatments are available and the first line is primarily DMARDs with or without prednisolone. If upon clinical assessment the disease seems to have progressed then either a second DMARD is added or an alternate DMARD in combination with anti-TNF (Infliximab, Etanercept or Adalimumab) together with methotrexate is started. To prevent further deterioration methotrexate can be used in combination with different anti TNF therapies. However, patient's refractory to treatment with anti TNF can respond effectively to B cell depletion therapy [205]. The only FDA approved B cell depleting agent is Rituximab, a chimeric monoclonal antibody to CD20, which is specifically expressed on human B cells [45, 228, 229], which has a transmembrane protein with 4 domains [230]. The antibody started out as a murine antibody and was then engineered to contain parts of the human antibody. This resulted in a chimeric antibody a combination of constant portion from humans and the antigen binding variable portion of a murine origin. The standard Rituximab therapy in patients results in more than 95% reduction of detectable circulating B-lymphocytes [231]. The clinical responses suggest a proinflammatory role of B cells in RA pathogenesis. Importantly, RA patients are strongly linked with cardiovascular morbidity and mortality and studies suggest that B cells have an anti-inflammatory role in atherosclerosis [232]. Keeping this in view it becomes very important to address the implications of B cell depletion therapy on atherosclerosis. Especially when rituximab is used in refractory cases of rheumatoid arthritis. One would assume that the majority of the patients would be more than 50 years of age at the time this B cell targeted therapy is started

and it becomes important to validate the effects of rituximab therapy on atherosclerosis.

To investigate this we decided to use the ApoE-/- mice, an experimental model of atherosclerosis. These mice develop atherosclerosis as they age, however, if these mice are given a high fat diet then the process of atherosclerosis is accelerated [233-235]. The human CD20 transgenic mice express the human CD20 receptor and are therefore susceptible to Rituximab induced B cell depletion [203]. We crossed these two murine strains to generate the huCD20^{+}/ApoE$^{-/-}$ murine line. These mice were fed on a high fat diet and treated with Rituximab to deplete B cell. The effect of B cell depletion on atherogenesis was evaluated in these mice.

5.1.1 Aims of the study

This study was performed using huCD20^{+}/ApoE$^{-/-}$ mice, allowing us to combine the induction of atherosclerosis (by high fat diet) and B cells depletion. The aims of this study were

1. To investigate the impact of B cell depletion therapy on plaque formation in atherosclerotic prone mice.

2. To monitor B cell depletion and recovery during the course of the study.

3. Examine the outcome of the treatment in relation to different B cell subsets in various areas (peripheral blood, spleen and bone marrow).

4. Validation of the total serum lipids of mice and correlate these lipid levels to different B cell subsets and aortic lesions.

5.2 Result

5.2.1 Model system and plan of the study

To determine the safety of B cell depletion therapy in RA patients, who are prone to atherosclerosis, we developed a model system to mimic the cardiovascular clinical situation and thus bred the huCD20^{+}/ApoE$^{-/-}$ mice. The rationale for using these mice is that whilst being prone to hyperlipidemia, which leads to plaque formation in their blood vessels, they also express the human CD20 receptor and therefore render the B cells susceptible to anti-CD20 antibody mediated depletion.

5.2.2 Generating huCD20^{+}/ApoE$^{-/-}$ mice

The huCD20tg were generated using a 168kb human bacterial artificial chromosome and maintained as heterozygous [203]. To generate the huCD20^{+}/ApoE$^{-/-}$ mice, human CD20 mice were crossed with ApoE$^{-/-}$mice. These mice on a C57BL6 background, initially from Professor Mark Shlomchik at Yale, came via the University of Southampton in Professor Glennie laboratory. Unfortunately, on arrival it was observed that these mice had several pathogens. To clean the mice so that they were allowed access to our animal facility the mice underwent embryo re-derivation prior to initiating the ApoE$^{-/-}$ huCD20tg crossing. In addition, due to the poor breeding nature of the ApoE$^{-/-}$ mice it took a considerable time to get to a point where we had the required genotype to set up productive breeding pairs. During the breeding of these mice the presence of the huCD20 and the lack of the ApoE gene was confirmed using tail samples. Blood was used to document the expression of the huCD20 molecule on the surface of B-lymphocytes. The PCR to detect the huCD20 molecule was performed using 4 sets of primers for different regions of the BAC (used to derive transgenic CD20 mice) these include huCD20 exon 2, 3UTR, 5 region BAC and 3 region BAC. Whereas, the absence of the ApoE gene was confirmed with a set of 3 primers. Sequences for all genotyping primers are in appendix 7.

After two years of breeding we started to get huCD20^{+}/ApoE$^{-/-}$ mice that we could use in experiments. Owing to time limitation, we had to start the study

with a limited number of mice (n=4) in the first group. The PCR analysis of tail samples demonstrate that in this set of pups 3 out of 4 mice were positive for the expression of huCD20 as shown by exon 2 (464bp) in 3 out of 4 mice and this was confirmed by positive signal seen for the 5' BAC region (100bp) (Figure 5.1, A). Whereas, the PCR for the ApoE gene results in a band of 245bp for the knocked-out gene ApoE$^{-/-}$, while one mouse with two bands of both 155bp and 245bp was a heterozygous represented as ApoE$^{+/-}$ (Figure 5.1, B). The genotyping confirmed three of the mice as huCD20^{+}/ApoE$^{-/-}$. Blood samples were also taken from these mice and PBMCs were extracted for FACS analysis to confirm protein expression of human CD20 on B-lymphocytes. PBMCs were stained for CD19 and huCD20; the FACS plot demonstrates huCD20 positive cells (44.9%) out of the gated population (Figure 5.1, C).

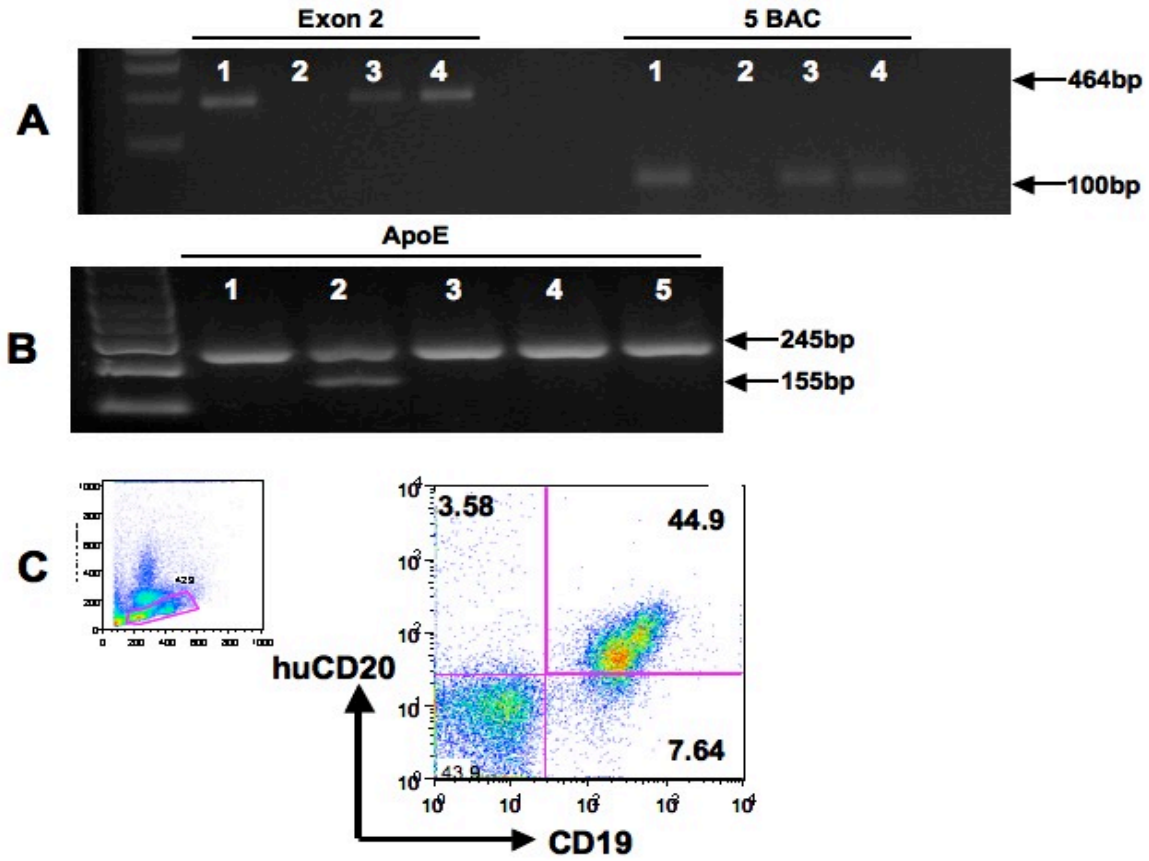

Figure 5.1 Confirmation of hCD20^{+}/ApoE$^{-/-}$ mice

(A) Genotyping of huCD20/ApoE mice using tail samples show 3 out of 4 mice positive for huCD20 receptor as bands are seen for Exon 2 and 5' BAC. (B) The PCR for the ApoE gene show 4 out of 5 pups as ApoE$^{-/-}$, whereas, the mouse in

lane 2 was a ApoE$^{+/-}$ (C) The FACS analysis of PBMCs to determine expression of the huCD20 receptor revealed that in a mouse, who was previously genotyped as being huCD20^{+} had expression of the receptor on all CD19^{+} B cells. C) Pseudocolour dot plot were gated on mononuclear cells as shown in the small panel. The huCD20 vs. CD19 plot shows 44.9% CD20 positive B cells.

5.2.3 Four huCD20^{+}/ApoE$^{-/-}$ mice on high fat diet

Mice were fed on high fat diet, which was started around 6 weeks of age. Two mice were treated with iv rituximab (100μg) every 4 weeks for a total of 3 treatments. Control mice (n=2) were treated with 100μg of chromopure human IgG. To monitor B cells depletion in these mice, they were bled a week before and after each systemic treatment (Figure 5.2). Blood samples were used to extract sera and PBMCs. The peripheral blood mononuclear cells were stained with fluorescent antibodies for flow cytometric analysis. Mice were weighed every time they were injected or bled. This was to ensure that mice gained weight during the course of study and if they did not then it can indicate that they have overgrown teeth, which impairs their feeding.

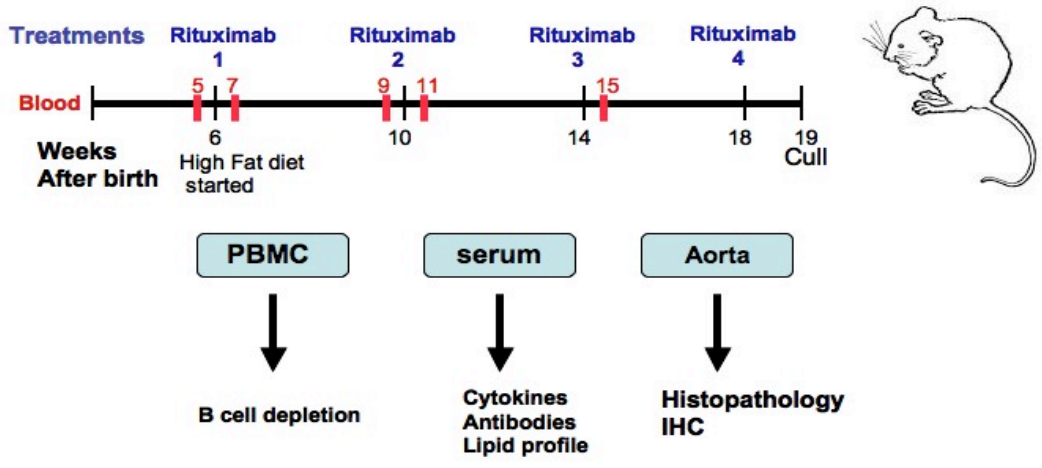

Figure 5.2 Model system planed for the study
To investigate the impact of B cell depletion therapy (rituximab), huCD20^{+}/ApoE$^{-/-}$ mice were fed on high fat diet from 6 weeks onwards. Mice were treated with (rituximab 100μg) every 4 weeks, with the first treatment started at 6 weeks of age. Mice were bled, a week before and after every single treatment shown with red

lines. To follow B cell depletion and recovery mice were serially bled to extract PBMCs for flow cytometric analysis. Finally, mice were sacrificed at 19 weeks of age (14 weeks on HFD). Heart, aorta, spleen, lymph nodes, bone marrow and blood were harvested for various analyses.

The model was set up to sacrifice mice after 4 treatments around the age of 19 weeks (14 weeks on HFD). At the end of the study, heart and aortas are to be analyzed for lesions. Spleen, lymph nodes, bone marrow and blood were harvested to examine B cells and their subsets. Sera were harvested for subsequent lipid analysis.

5.2.3.1 Monitoring of body weight

At the age of 6 weeks mice were shifted on to a high fat diet (HFD) to induce atherosclerosis. These (huCD20^{+}/ApoE$^{-/-}$) mice with a genetic susceptibility are expected to develop hyperlipidemia and weight gain. Therefore, during the course of study weights of these mice (n=4) was recorded at the time of every systemic treatment and a week before and after the treatment when the mice were bled, which is 3 times a month. All the mice at 6 week of age were between 19-23gm, after 1 week on HFD all the mice gained weight a max weight gain of 2.5gm was seen in one of the IgG treated mice represented with green line. After 4 weeks on HFD one of the rituximab treated mouse died having gained 5gm (pink line), the other rituximab treated mouse gained 4gm. However, the mice that received IgG showed more increase in their weight they started at 23gm and in 4 weeks time reached a maximum of 30gm shown with red and green. A week later we saw an unexplained drop in the body weight of both the IgG treated mice. However, the only rituximab treated mouse showed a rapid increase with a body weight of 28.5gm. In the last 4 weeks mice on systemic IgG gained more weight and their final body weight were 30gm and 33gms. Whereas, the rituximab treated mice ended up 26gms (Figure 5.3).

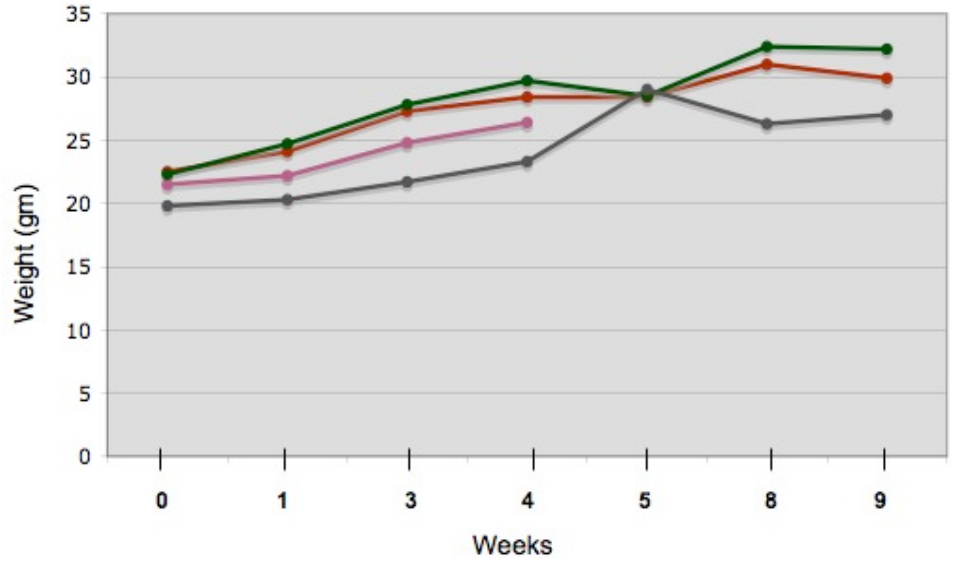

Figure 5.3 Body weight chart

Body weight was monitored of the mice in study three times a month till the end of the study. Each line represents single mouse; Red and pink are the mice treated with rituximab and the mouse represented with (pink) line was found dead (week 4) of study therefore no more weight recordings. The rest of the mice (n=3) had a gradual increase in their weight roughly between 6-10 grams in 9 weeks.

5.2.3.2 Circulating B lymphocytes and rituximab

Mice were treated intravenously (iv) with either rituximab (100μg, n=2) or IgG (100μg, n=2). To examine the impact of treatment on circulating B-lymphocytes, mice were bled a week before and a week after the treatment. To determine the baseline level of B-lymphocytes in the blood, PBMCs were extracted from the blood at week (0) and were stained for CD19, human CD20. FACS analysis showed that rituximab treated mice (n=2) had 44.6% ± 0.3 (mean ± SD) huCD20 positive B cells while human IgG treated mice (n=2) had 43.4% ± 7.3 (Figure 5.4).

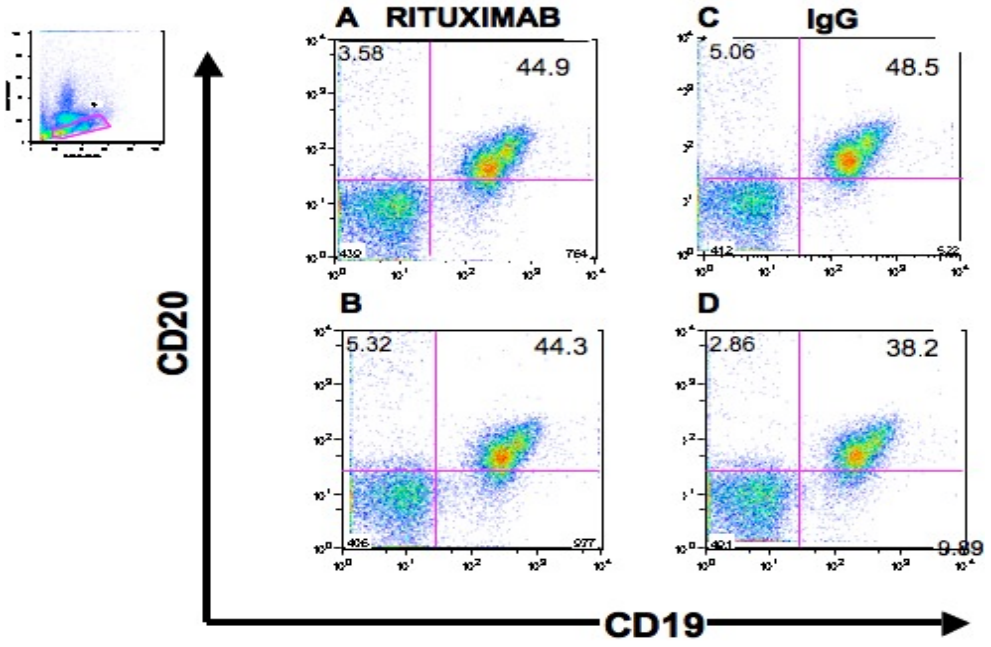

Figure 5.4 Circulating huCD20^{+} cell at first week
Blood samples were taken at the time of first treatment (week 0) from rituximab and control mice, PBMCs were isolated from the blood and stained for FACS analysis. Pseudocolour dot plots were gated on lymphocytes as shown in the smaller panel in the left corner. CD19 vs. CD20 plots showed that all four mice had human CD20 positive cells. The percentages of huCD20 positive cells for rituximab treated (A & B) mice were 44.9% and 44.3%, and IgG mice (C & D) had 48.5% and 38.2% respectively as indicated in each quadrant.

One week after systemic treatment of all the mice (n=4) they were bled and the percentage of B cells present in the blood was analysed by FACS. The analysis showed significant depletion of B cells in rituximab treated mice. In specific, rituximab treated mice had 0.45% ± 0.4 (mean ± SD) B cells, representing a 98% reduction (Figure 5.5, A, B). The huCD20 positive cells were not affected by the treatment, as the B cells in the control mice a week after the systemic (100μg, IgG) were 45.6% ± 1 (mean ± SD) of the gated lymphocytes (Figure 5.5, C, D)

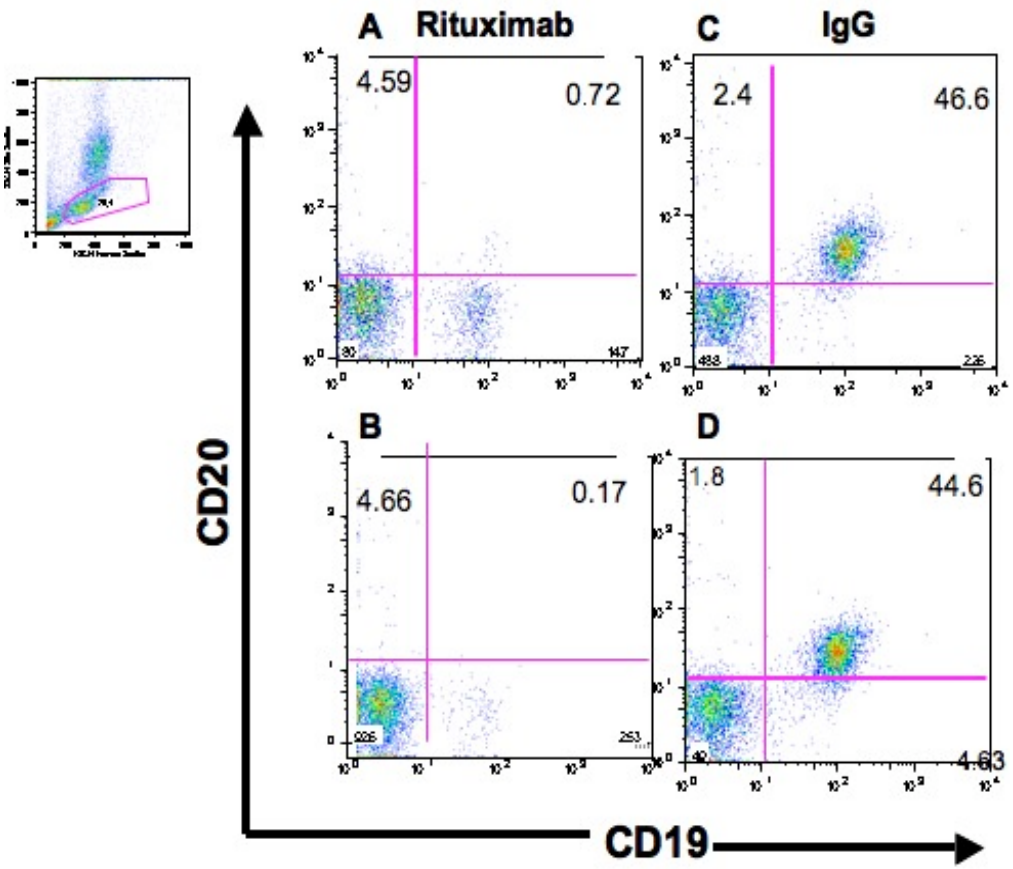

Figure 5.5 Circulating B cells (huCD20^{+}) a week after the systemic treatment Mice were bled one week after first treatment. (A & B) are rituximab treated mice and (C & D) are the control mice; PBMCs were isolated from the blood and stained for 4 colours Flow cytometric analysis. Pseudocolour dot plots were gated on lymphocytes as shown in the smaller panel. Then (CD19 vs. CD20) showed 98% reduction in CD20^{+} B cells in the rituximab treated mice as the depletion resulted in (0.72% and 0.17%); whereas, the IgG treatment did not affect the CD20 expressing population. The percentages are shown in each quadrant.

Thereafter, the mice were bled again a week before the second treatment to see if the huCD20 positive cells were replenished in the rituximab treated mice (n=2) during the two weeks time. There was a rapid recovery of huCD20 positive B cells in rituximab treated mice as a 77% increase was observed evident from B cells percentages 34.7% ± 5.2 mean ± SD. In fact B cell percentage increased further in the IgG treated mice n=2, 51.75% ± 4.35 (mean ± SD, Figure 5.6).

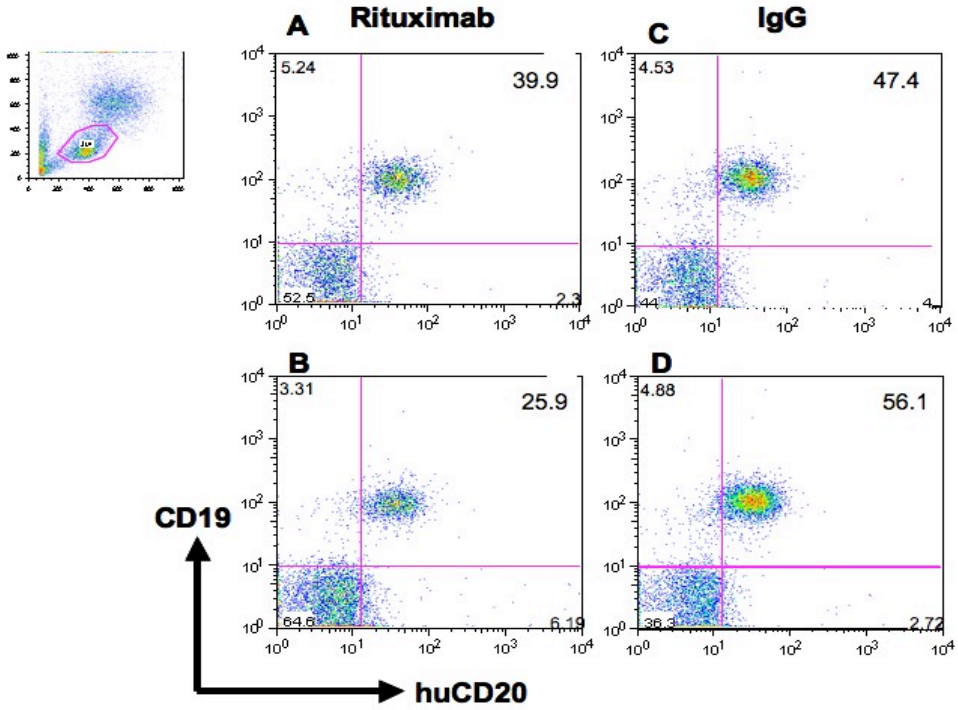

Figure 5.6 B cells (huCD20$^+$) percentages one week before second treatment Mice were bled one week before second treatment, rituximab (A & B), and control mice IgG (C & D). PBMCs were isolated from the blood and stained for 4 colours FACS analysis. Pseudocolour dot plots were gated on lymphocytes as shown in the smaller panel. The (CD19 vs. CD20) showed that there is recovery of CD20 positive B cells in the two rituximab treated mice 39.9% and 25.9% respectively; whereas, the IgG treated mice huCD20$^+$ cells percentage had a small increase 47.4% and 56.1%.

Unfortunately, during the course of study one of the rituximab treated mouse was found dead a week before second treatment (week 5), which seems one of those unexplained deaths. Later, the second rituximab treated mouse developed a skin condition probably xanthomas (these are fatty deposits under the skin or around nerve endings and can cause irritation) because of this we decided to terminate the study around the age (15 weeks) with (9 weeks) of study. Therefore, after second treatment mice (n=3) were analyzed for B cells (huCD20$^+$) depletion in the peripheral blood. Interestingly, rituximab treated mouse showed resistance to treatment with a modest depletion 9% compared to the B cells percentage a week before second treatment, whereas, IgG treated control mice (n=2) had further 15% increase in their B cells 60.3% ± 0.2 (mean ± SD, Figure 5.7).

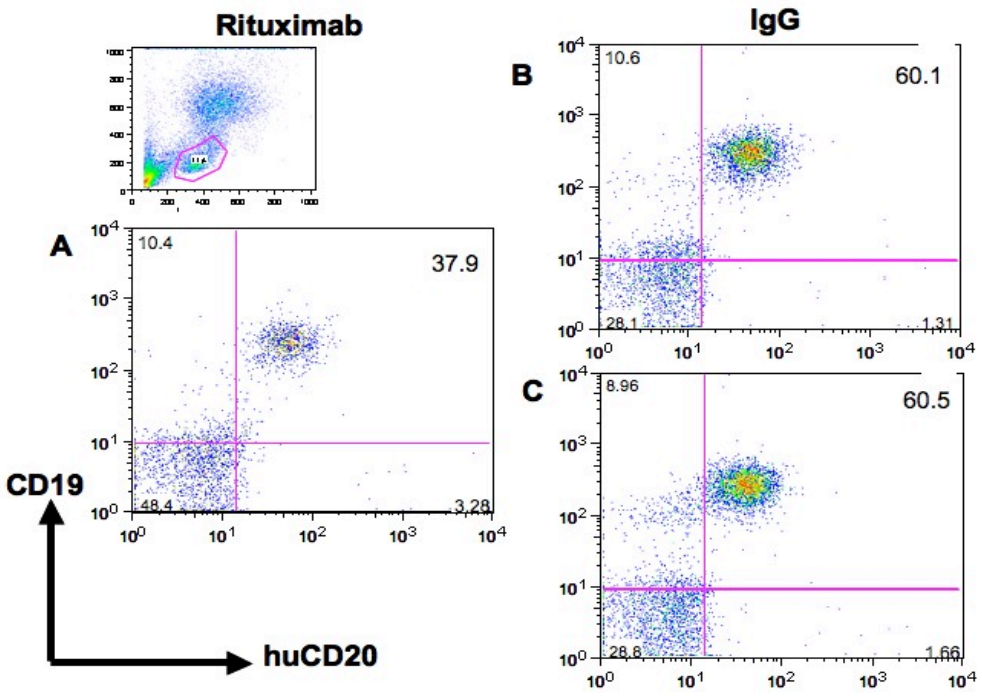

Figure 5.7 B cells (huCD20$^+$) one week after second treatment
Mice were bled one week after second treatment. A) Rituximab treated mouse and (B & C) are the control mice; PBMCs were isolated from the blood and stained for 4 colours FACS analysis. The (CD19 vs. CD20) analysis showed that huCD20$^+$ cells showed resistance to second treatment with B cells percentage as 37.9%; whereas, the IgG treatment did not reduce the huCD20 expressing population, in fact the B cells increased 60.1% and 60.5% respectively. The percentages of cells are shown in each quadrant.

As all the mice were bled a week before and after every treatment, and the circulating B cells numbers were assessed with FACS (CD19 vs. huCD20) staining of peripheral blood lymphocytes. The results are expressed as B cells percentages of the gated lymphocytes. Rituximab was able to rapidly and extensively deplete 98% of B cells after a single dose of rituximab (100μg, iv), compared with IgG treated control mice with huCD20$^+$ cells percentage as high as 50%. FACS analysis of B cells (huCD20$^+$) percentage a week before second treatment confirmed 77% recovery of B cells in rituximab mice (n=2). However, a week after the second treatment a modest depletion of 9% was observed in peripheral blood in these mice. Whereas, a week after the second treatment with IgG, mice had a further 15% increase in there circulating B cells. Moreover, one week after third treatment the only rituximab treated mouse had a modest

drop of 20% in the circulating B cells and the IgG treated mice had consistent levels of circulating B cells (Figure 5.8)

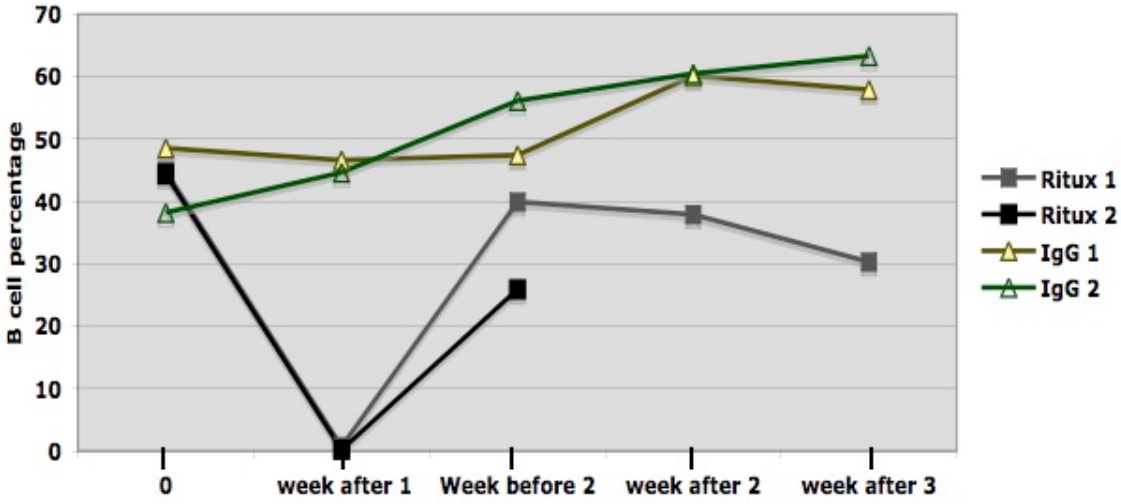

Figure 5.8 Trend of Circulating B cells (huCD20^{+}) during the course of study Mice (huCD20/ApoE$^{-/-}$) received 100μg of rituximab (black and grey line) and the control mice treated with IgG (yellow and green line) at different time points (day 0, one week after first treatment, a week before second treatment, a week after second treatment and finally a week after third treatment) . Rituximab treated mice (n=2) show a sharp drop in B cell percentage after first treatment. Then a week after second and third treatment B cells resisted depletion and showed modest changes 37.9% and 30.3% respectively. Whereas, the IgG treated controls showed a consistent rise in B cells percentages (represented with green and brown lines)

5.2.3.3 Effects of B cell directed therapy on lymphocytes of spleen and lymph nodes

As previously stated the original plan was to harvest different organs from mice after 14 weeks on HFD, but because of the skin problem of the rituximab treated mouse in study we had to terminate the study at week 9. Having established that depletion of circulating B cells is massive (98%) after 1 treatment and later on they resisted depletion, even than at least 9% depletion was seen in the

replenished B cells in 3 weeks time prior to treatment. Mice were sacrificed and heart, aorta, spleen, bone marrow, lymph nodes and blood were all harvested from the remaining mice (n=3). Aortas were analyzed for atherosclerotic lesions (section 2.5.4.8). Bone marrow and secondary lymphoid organs were assessed for B cells depletion.

At the end of the study, spleen and lymph nodes were harvested from sacrificed mice. Single cell suspensions from these tissues were examined for lymphocytes content by flow cytometry. The ratios of B to T lymphocytes in the spleen of rituximab vs. IgG treated mice were (1.85: 1.6) respectively. Whereas, the percentages of lymphocytes (B and T) in the lymph nodes of rituximab and IgG treated mice were (0.58: 0.68) respectively. This shows that both spleen and lymph nodes had similar ratio of lymphocytes, suggestive of the fact that spleen and lymph node huCD20 positive B cells were not affected by rituximab therapy (Figure 5.9).

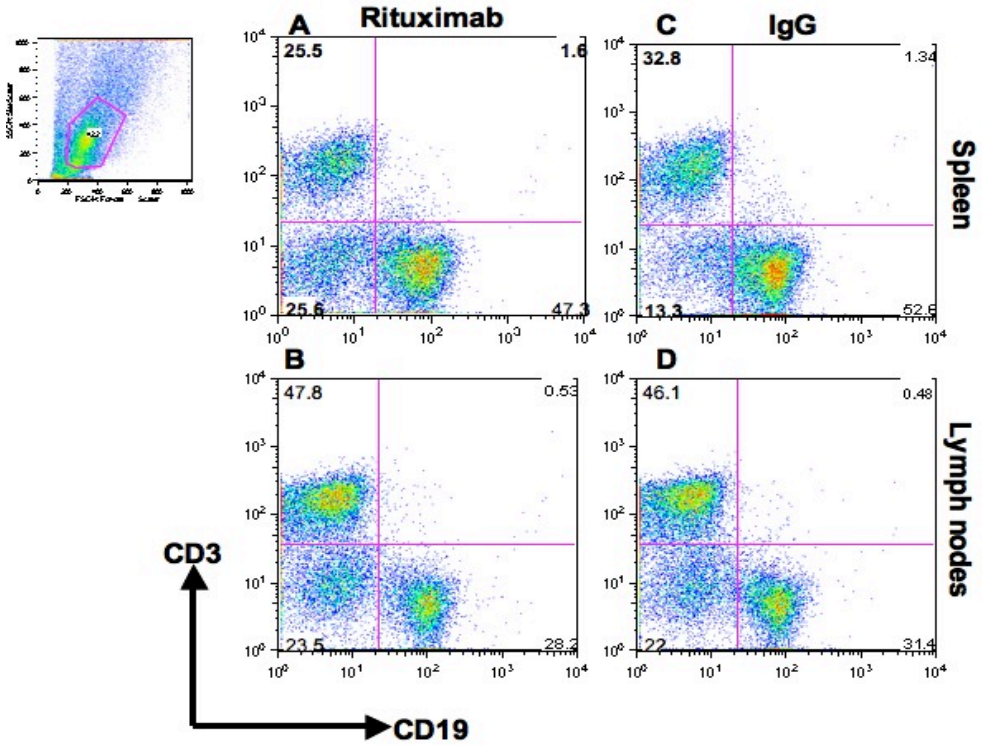

Figure 5.9 Depletion therapy and lymphocytes in spleen and lymph nodes Single cell suspension of lymphocytes were extracted from spleen (A & C) and lymph nodes (B & D) of mice and were examined by 4 colour staining for flow

cytometry. Pseudocolour dot plots were gated on lymphocytes as shown in the smaller panel on left corner. B and T lymphocyte percentages in spleen of rituximab treated mouse were 47.3% and 25.5% and lymph nodes 28.2% and 47.8% respectively. Whereas, the B and T lymphocytes in spleen of IgG treated mouse were 52.6% and 32.8% and in lymph nodes 31.4% and 46.1% respectively. The percentages are indicated in corner of each quadrant.

5.2.3.4 Effects of rituximab on B cell subsets in spleen

Transitional type 2 (T2), Marginal zone (MZ) and Follicular (Fo) B cells

Rituximab treatment in (huCD20^{+}/ApoE$^{-/-}$) mice did not demonstrate B cells depletion in spleen and lymph nodes. We further wanted to validate if the treatment affected different B cells subsets in secondary lymphoid organs. Harvested spleen cells were stained for different B cells subsets. The identification of transitional (T2), marginal zone (Mz) and follicular (Fo) B cells in the spleen was possible through combination of several markers, which are expressed during development. The combination used includes CD19, CD21 and CD23; a plot of forward scatter (FSC) vs. CD19 can be used to separate (CD21^{+}CD23^{+}) cells. This population was subdivided into Fo (CD21^{+}CD23^{+}lo), T2 (CD21^{+}CD23^{+}hi) and Mz (CD21^{+}CD23^{+}dull) B cells. There was a difference noted in marginal zone B cells between rituximab treated (4.18%) and control mice (2.84%). This altered representation of B cells subset percentage could be a response of decreased follicular B cells (Figure 5.10).

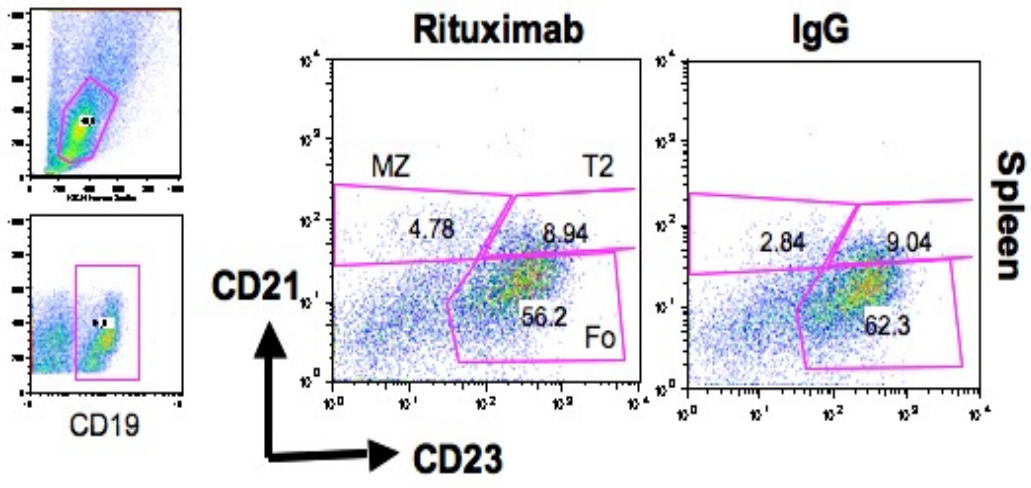

Figure 5.10 Marginal zone (MZ), follicular (Fo) and transitional type 2 (T2) B cells The single cell suspension was isolated from rituximab and IgG treated mice. These cells were stained for FACS analysis. A plot of forward scatter (FSC) can be used to separate out lymphocytes as shown in the top small panel on the left. These cells are further gated on to CD19$^+$ cells to separate CD21$^+$CD23$^+$ B cells. The CD21$^+$CD23$^+$ fraction can be further subdivided into CD21$^+$CD23$^+$lo Fo cells and CD21$^+$CD23$^+$hi T2 and Mz B cells. The percentages of (Fo, T2 and Mz) cells are written besides the gated factions.

Transitional type 1 and 2, marginal zone and follicular B lymphocytes

Harvested cells from spleen and lymph nodes were stained for T1, T2, Mz and Fo B cells. This was possible through combination of several markers, which are expressed during development. The combination used includes CD19, CD21 and CD24; a plot of forward scatter (FSC) vs. CD19 was used to separate CD21$^+$ and CD24$^+$ cells. This population was subdivided into T 1 (CD21$^+$CD24$^+$lo), the T2, Mz (CD21$^+$CD24$^+$hi) but this does not allow the discrimination of Mz and T2 cells and Fo cells are an intermediate population (CD21$^+$CD24$^+$). The response of the rituximab treatment on splenocytes B cells (T1, Mz and Fo) is (31.5%, 8.01%, 49.6%) vs. IgG treated mice (T1, Mz and Fo) is (16.3%, 5.56%, 63.6%) respectively. These demonstrate that rituximab result in an increase in the T1 31.5% in rituximab treated mice than the IgG, which was a 16.3% B cell (Figure 5.11).

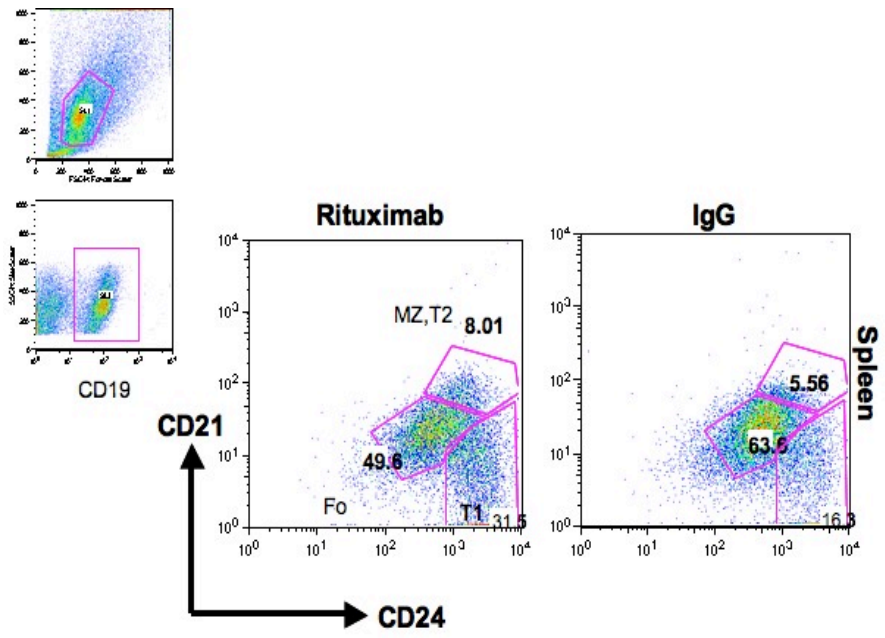

Figure 5.11 B cells subsets in spleen and lymph nodes
The single cell suspension of spleen and lymph node was isolated from rituximab and IgG treated mice. A plot of forward scatter (FSC) was used to separate out lymphocytes as shown in the top small panel on the left. A plot of forward scatter vs. CD19 was used to separate ($CD21^+CD24^+$) B cells. The $CD21^+CD24^+$ fraction can be further subdivided into T 1 ($CD21^+CD24^+$lo), the T2+Mz ($CD21^+CD24^+$hi) and Fo ($CD21^+CD24^+$ intermediate population). The CD21 and CD24 staining does not allow discrimination of MZ & T2 cells. The percentage in rituximab treated mice in spleen as compared to control mice. The percentages of these cells are written besides the gated factions

B1a cells in spleen and lymph nodes

Previous studies have shown that generation of natural antibodies IgM (T15) can be atheroprotective, which imply a role for B1 cells in atherosclerosis. Therefore we validated the percentages of B1 cells in spleen and lymph nodes of treated mice (n=3). Harvested cells from spleen and lymph nodes were stained for flow cytometric analysis of B cell subset (B1a). A plot of forward scatter (FSC) vs. side scatter was used to gate lymphocytes. This was then used to gate $CD19^+IgD^+$ intermediate population. This population was used to separate ($CD5^+CD43^+$ Hi) population recognised as B1a cells. The response of the rituximab treatment on splenocytes B1a cells (4.51%) vs. IgG treated mice (6.64%) show similar percentage. In fact a similar observation was made for the percentage of B1a subset in the lymph nodes of rituximab treated mice (14.1%) compared to IgG treated mice 11.6% (Figure 5.12).

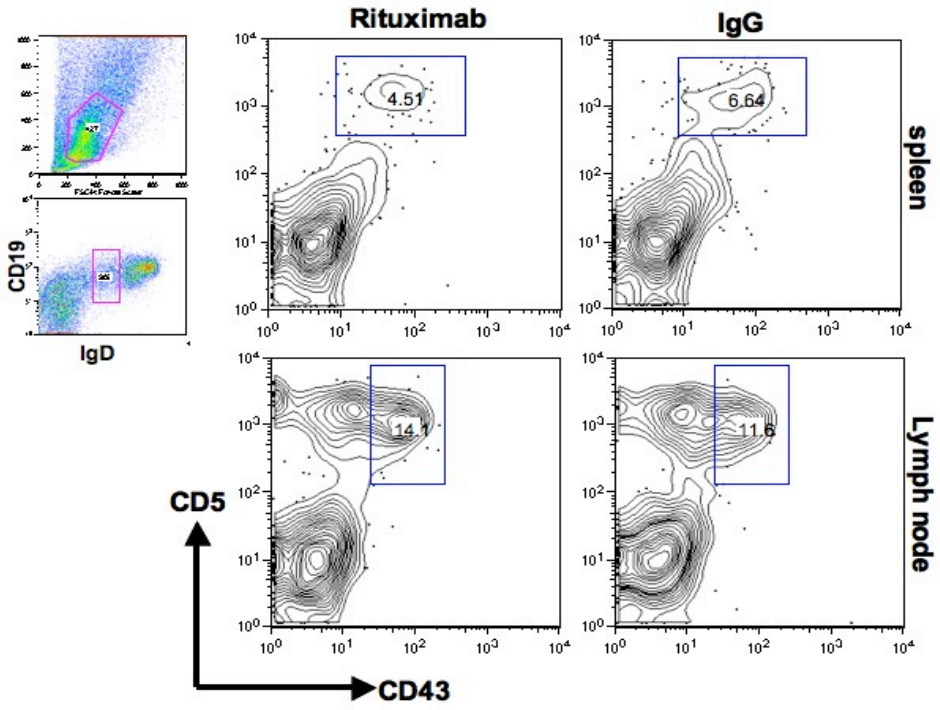

Figure 5.12 B1a cells in spleen and lymph nodes
The single cell suspension of spleen and lymph nodes were isolated from rituximab and IgG treated mice. A plot of forward scatter (FSC) was used to separate out lymphocytes as shown in the top small panel on the left. These cells are further gated on to ($CD19^{+}$ IgD^{+}) intermediate population to separate ($CD43^{+}CD5^{+}$)^{Hi} B1a cells. The percentage of B1a cells in spleen and lymph nodes are shown within the gated population.

5.2.3.5 Analysis of Aortic lesions

Blood was collected from the mice through the vena cava, followed by removal of lymph node, spleen and hind legs. After this the mice were perfused and fixed through the vena cava so the heart was not touched. Heart and aorta were carefully dissected out. To compare the lesions between different mice it is very important to cut the heart at the right plane and place. As shown (Figure 5.13, A) the heart was separated form the ascending aorta just above the aortic root, perpendicular to the longitudinal axis of aorta. After this paraffin embedded sections were cut and stained as explained (section 2.5.5). It is important to note that aortic valves are important landmarks to identify the aortic level. Once we had established the correct slides to be used for lesion analysis, based

on the position of the aortic valves, both lesional and luminal areas were recorded (Figure 5.13, B).

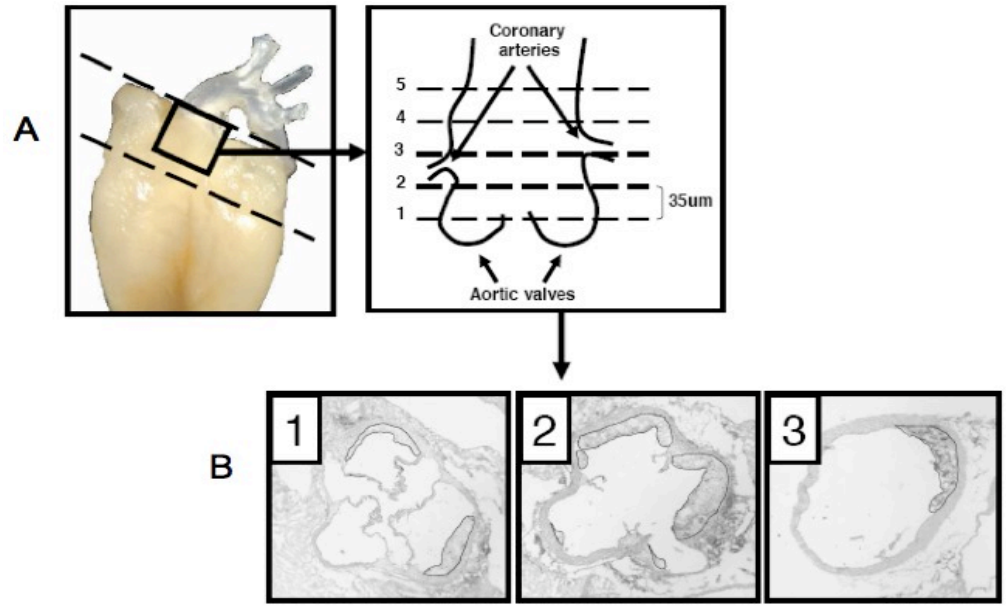

Figure 5.13 Schematic for dissection of mouse heart and aorta
The atherosclerotic lesions are mostly seen in the aortic root, where the aortic valves end. A) Show the plane at which the cut is made to separate the atria from the ventricles and ascending aorta from the root of aorta. This was to ensure a horizontal plane perpendicular to the aortic lumen. Whereas, a gradual shift can be seen as the aorta is cut B) shows aortic lumen with valves visible in (1) to a point where aortic lumen is round and valve are not seen. (3) a lesion is marked to show the measured area of the lesion and it is next to the tunica intima of blood vessel.

All the aortic samples from the 3 mice were cut to generate 7μm thick sections and 2 consecutive sections were placed on one slide. Sections were stained with H & E and slides numbered 1, 3, 6, 9, 12, 15, 18, 21, 24, 27, 30 were visualised to confirm the position of the aortic heart valves. Once the aortic valves were determined 5 sections were measured for atherosclerotic lesions, one from each slide. The representative H and E stained sections from the mice (n=3) demonstrate atherosclerotic lesions in the aorta. The lesions seen in the rituximab treated mouse are small as compared to the lesions in control mice. Cholesterol cleft can be seen as white holes or clefts in the areas of maximum elevation of the lesion into the lumen (Figure 5.14).

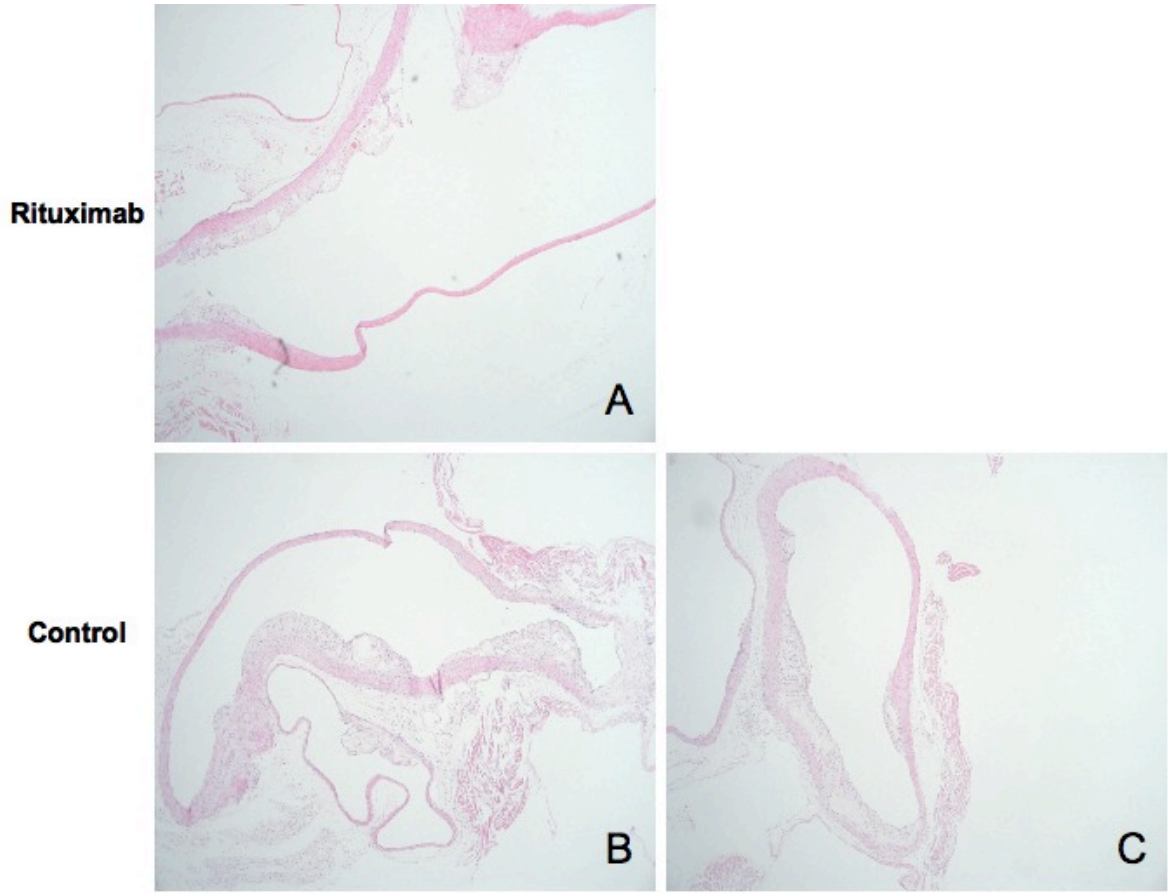

Figure 5.14 Aortic lesions in huCD20^{+}/ApoE$^{-/-}$ mice
Mice were treated every four weeks with iv rituximab or IgG (control), and were sacrificed around 9 weeks on HFD and the aortic lesions were examined by H & E staining. The Rituximab treated mouse (A) has small lesions, whereas, both of the IgG treated mice (B & C) have much larger lesions that cover more area of the lining layer.

The aortic lesions and the luminal area were measured in μm^2 using the imaging software (Axiovision version 4). The mean of lesion area for 5 sections 7μm thick and each section 7μm apart, in a rituximab treated mice was compared with the mean lesion area of IgG treated controls. This showed an almost 2 fold reduction in lesion area of rituximab treated mice (Figure 5.15). As the sections used for measuring the lesions were from 5 consecutive slides, this means the lesions extended longitudinally over 70μm.

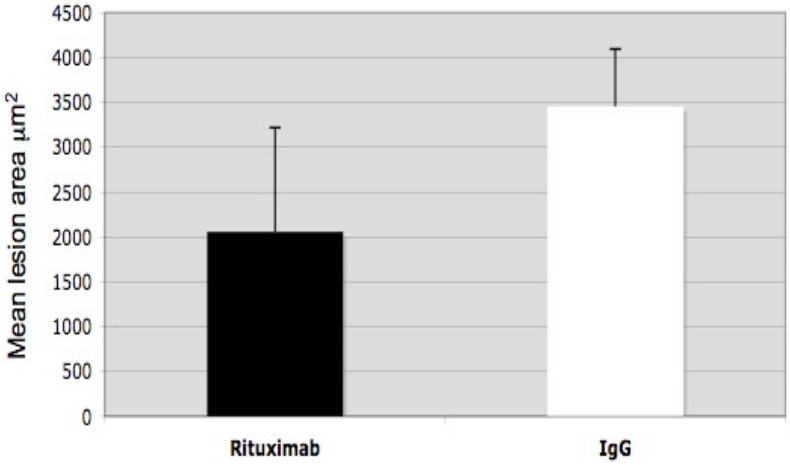

Figure 5.15 Atherosclerotic lesion areas in rituximab and IgG treated $CD20^{+}/ApoE^{-/-}$ mice

Lesion area in aorta of ($CD20^{+}/ApoE^{-/-}$) mice fed on atherogenic diet (n=3). The average lesion size measured in cross section through the aortic origin is indicated in μm^2. The rituximab (black bar) treated mice have almost half the lesion area as compared to IgG treated mice (white bar), these lesions extended longitudinally over 70μm.

We observed a variation in luminal area of the aorta between these mice, so to ensure that the results reflect the absolute lesion area compared to vessel size we determined the percentage area of the lesion relative to luminal area. We calculated the percentage area for all 5 sections per mice by (lesion area / luminal area × 100) for each section of the mice (n=3), which revealed the percentage of aortic lumen obliterated with lesion, and there was reduction seen in the percentage area of aortic lumen obliterated with lesion in the rituximab treated compared to IgG treated control mice (n=2). The lesion of rituximab treated mouse had small plaques on 1-3 sections. In fact the 2 remaining section had no lesions at all (blue line, Figure 5.16). On the other hand the IgG treated mice (red and yellow) had lesions bigger then rituximab treated mice. This demonstrates that not only there is at least 2-fold difference in the lesion area between rituximab and IgG treated mice; in fact this difference is seen longitudinally for around 35μm from root of aorta towards ascending aorta. Moreover, there is a 100% difference seen in the lesions size in the last 2 sections. Which imply that the plaque formation has extended upwards

from the root of aorta into the ascending aorta for at least 70μm in the IgG treated mice, whereas the longitudinal extension of these lesions in the rituximab treated mouse is limited to around 35μm as shown by the blue line (Figure, 5.16).

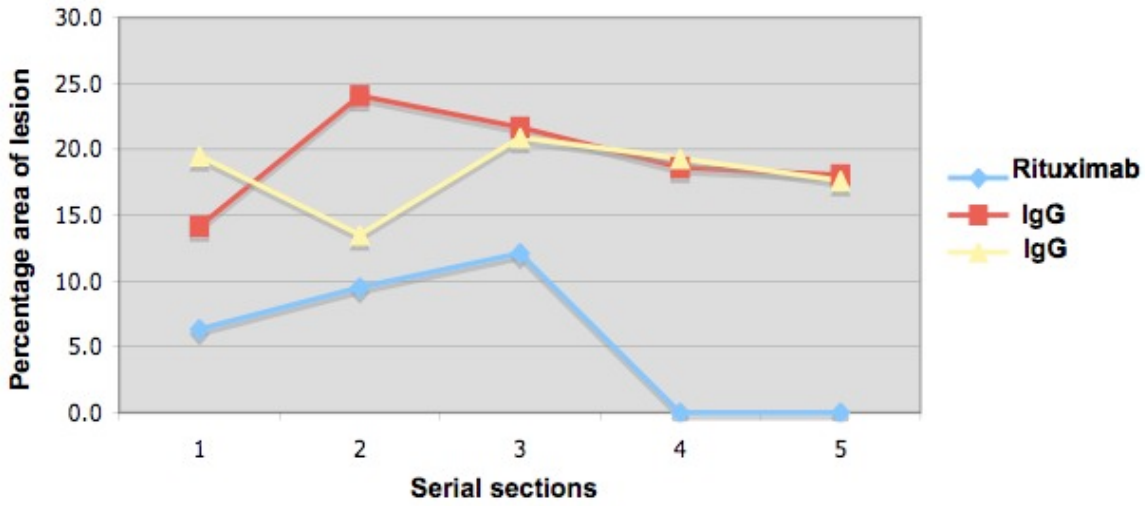

Figure 5.16 Percentage area of Aortic lesion in (huCD20^{+}/ApoE$^{-/-}$) mice
The aorta from (huCD20/ApoE$^{-/-}$) mice were analysed for the lesion area measured in um^{2} for all 5 sections per mouse, and the luminal area was also measured for all the mice. This graph represents the percentages of the aortic lesions relative to the aortic lumen. The mice treated with IgG (red & yellow) show a reasonable overlap in the lesion size. However, the mice treated (blue) with rituximab (100μg) showed reduction in percentage area of aortic lumen obliterated with lesion.

5.3 Discussion

This initial data to address the safety of B cells depletion therapy (Rituximab) is interesting for patient management, especially in the late stages of the disease. RA patients are vulnerable to cardiovascular morbidity and mortality, we hypothesised depletion of B-lymphocytes (atheroprotective cells)[232] in the experimental model of atherosclerosis might result in aggravation of lesion formation in the mice. However, this preliminary data from a limited number of mice (n=3) is surely not enough to draw conclusions but it gives us the clue what to expect from a full study with a reasonable number of (huCD20^{+}/ApoE$^{-/-}$) mice.

The current data shows a 2-fold reduction in lesion size in response to rituximab treatment in comparison with the IgG treated control mice. Variation was observed in size of aortic lumen and arterial wall thickness in these genetically engineered mice. Therefore not only aortic lesion area was measured but we also calculated the percentage area of the aortic lumen obliterated with the plaque. Importantly, the measures of aortic lesion area and percentage area of the aortic lumen obliterated have both shown that B cell depletion resulted in at least 2-fold reduction in atherosclerotic lesions. Importantly, these lesions extend vertically from root of aorta towards the ascending aorta. Whereas, the overall reduction in the arterial wall thickness of these (huCD20^{+}/ApoE$^{-/-}$) mice needs to be validated in the future studies.

The B cells depletion every four-week with rituximab (100μg) was monitored through out the course of study, and a massive (>90%) reduction was observed in the B cell percentage after the first treatment, which was followed by rapid recovery of the B-lymphocytes in a three weeks time. Interestingly, the systemic treatments (second and third) resulted in modest depletion of 9-20% B cells percentage. In a study Rituximab (type I) has been shown to be 5 times less potent then tositumomab (type II), the return of B cells was reported 30-35 days after the treatment [236]. In addition comparison of B cell depletion with a single dose of rituximab (250μg) in two different strains of mice was performed, and it was demonstrated that C57BL/6 mice are more resistant than BALB/c, in fact the analysis of B cells depletion in peripheral lymphoid organ (bone marrow and lymph nodes) was resistant to rituximab therapy [236]. Although in the present

study the rituximab dose (100μg) is less than half the dose used in the study mentioned but a massive depletion was confirmed in our mice C57BL/6 background. However, the spleen and lymph nodes harvested at the end of the study showed resistance to rituximab therapy.

The B cells subsets Mz and B1 cells are potent responders to TLR activation, which has resulted in them being referred as innate B cells [237-239]. Moreover, pneumococcal vaccination in $Ldlr^{-/-}$ mouse have been demonstrated to reduce the atherosclerotic burden in mice, which was shown to be a result of oxLDL specific IgM antibodies produced by spleenic B cells [135]. In the present study we observed an increase in the T1 B cells in spleen of rituximab treated mice. Even though this subpopulation is small but there is a fold increase in this population, which might be because they escape depletion or because of some stimulatory response. Moreover, the B1 B cells are mainly found in the peritoneal cavity [240]. A modest population of B1 B cells was identified in spleen and lymph nodes, which was not affected by rituximab treatment.

Limitation of mice number was not the only factor, in fact due to time constraints sera from mice at every bled and at the time of sacrifice could not be evaluated to determine the lipid profile. This is very important to confirm if this ($CD20^{+}$/$ApoE^{-/-}$) mouse model has a normal lipid profile and that the affects observed were of B cell directed therapy (rituximab) and not as a result of changes in serum lipids.

6 General Discussion

Rheumatoid arthritis (RA) is a chronic progressive autoimmune disease that primarily affects the joints and cause severe deformity and loss of function. The aetiology of the disease is not known but epidemiological data has identified many genes (HLA-DR, PTPN22, PADI-4) and environmental factor (smoking) that could be involved in RA pathogenesis [10]. RA diagnosis is based on a criteria put forward by the ACR, which include clinical symptoms, radiological features and serological marker (RF). A new addition to this diagnostic arsenal is serum titre of ACPA (antibodies to citrullinated proteins); a highly specific biomarker for diagnosing RA patients even at early stages[217]. RA patients quality of life is severely affected; moreover, RA patients are at increased risk (1.5 fold to 2 fold) of developing cardiovascular events [88, 95, 97]. It is unclear how the underlying disease mechanism of RA, influences the vascular environment in atherosclerosis.

Atherosclerosis is asymmetrical intimal thickening of arterial wall, with an inflammatory mechanism involving cells of innate and adaptive immunity [241-243]. The underlying cause of the disease is not completely understood neither its link to RA. However, strong genetic associations with smoking have been identified for both the diseases. Klareskog et al has proposed an etiological model for RA centred on smoking [10]. This was primarily based on presence of ACPA antibodies generated in response to smoking and can target CP in the joints. The expression of CP an inflammation specific protein is demonstrated in RA synovium [206] and RA synovial fluid [27].

The biopsy cohort of aortic adventitia from patients, with well-established CVD and coexisting RA were investigated for the presence of CP. This inflammation specific protein was seen in the AA of all the patients but was expressed significantly more in CVD patients with comorbid RA. Previous studies have shown that the conversion of arginine to citrulline is a PADI dependent enzymatic process; which is activated under high calcium concentration; physiological calcium level does not support this enzymatic conversion [36]. However, under stress full conditions like apoptosis, terminal differentiation of

cells (stratified skin) and inflammatory responses can cause an increase in the calcium concentrations to levels that support citrullination. This was an interesting finding and the ACPA levels from sera of RA patients strengthened the rationale for citrullinated proteins presence in RA patients. To examine the impact of both CP and ACPA in these CVD patient subsets were identified. RA patients were subdivided on the basis of maximum CP staining scores in non-RA patients, which was (CP=5.5) and therefore it was made the cut off. As a result a subset of RA patients (CP>5.5) was identified and their ACPA titre was correlated with an inflammatory marker (CRP levels). Importantly, we confirmed that ACPA in the subset of patients (CP>5.5) was strongly correlated with raised CRP levels. This implies that raised CP and ACPA could be critical in the progress of atherosclerosis and hence cardiovascular events seen in ACPA positive patients. As the patients with susceptible genetic background when exposed to environmental factors like smoking might generate ACPA; In addition dyslipidemia in the same patients initiate inflammation in the blood vessels that results in CP formation within the blood vessels. Once there is increased titre of ACPA in the circulation and expression of CP in the vessel wall they might result in immune complex formation. Henceforth, the progress of atherosclerotic plaque might be affected by this immune complexes formation in the vascular adventitia.

This is the first time presence of CP is demonstrated in the Aortic adventitia. CP expression is significantly more in RA aortic adventitia but a reasonable number of non-RA vessels demonstrated CP expression as well. Which confirms the fact that citrullination is an inflammation associated phenomenon rather than a disease specific [206]. This suggests that atherosclerosis might be initiated by risk factors (dyslipidemia, hypertension, cigarette smoking or diabetes mellitus), which in turn generates citrullinated proteins in aortic adventitia. In fact citrullination of adipocytes in aortic adventitia is interesting because adipocytes are the major cellular component of the adventitia; with their ability to produce cytokines, adipokines and angiogenic molecules one would expect a change in their functional ability that might affect the pathogenesis of atherosclerosis; which needs to be investigated in the future studies.

Our findings were broadened by the analysis of ACPA levels in sera of patients with CVD and co existing RA. We confirmed that all non-RA patients were negative for ACPA and most of RA patients had high ACPA titre. There is increasing evidence to support the fact that cigarette smoking is an individual risk factor for both atherosclerosis and rheumatoid arthritis. Moreover, accumulating data from the past decade has indicated that citrullination is strongly associated with smoking and rheumatoid arthritis (RA)[10]. However, we could not observe any association between CP and smoking in patients of rheumatoid arthritis. Perhaps this effect of smoking on citrullination is limited to lungs.

In the past B cells were demonstrated in human aortic adventitia and in addition the experimental model of atherosclerosis ($ApoE^{-/-}$) was shown to have B cell follicles in the adventitia of abdominal aorta [142, 144]. We established B-lymphocytes presence only in diseased aortic adventitia from CVD patients. None of the adventitia of the internal control (IMA) had B-lymphocytes. This confirmed the previous observation by researchers regarding B lymphocyte presence in human aortic adventitia.[210 144 213]. In an environment where different cells have to be efficient and survive longer, cells require factors especially during chronic inflammatory responses. Here we show for the first time that a B cell survival niche exist in the aortic adventitia that provide the microenvironment for B cell survival and maturation. B cell activating factor (BAFF or Blys) is a TNF like ligand and its close member a proliferation inducing ligand (APRIL) are members of tumor necrosis factor (TNF) superfamily. These two factors can mediate B-lymphocytes behaviour through their interaction with the receptors on B cells. Aortic adventitia and IMA express BAFF (adipocytes, monocytes and vascular endothelial cells), which was found to be significantly more among smoking patients. Furthermore, smoking induced vasoconstriction can result in hypoxia of the end arteries like vasa vasorum; which means hypoxia of vascular endothelial cells that can result in endothelial dysfunction. To investigate this hypothesis we looked at BAFF and APRIL expression under hypoxia in murine vascular endothelial cells. Nevertheless, hypoxia or reoxygenation of vascular endothelial cells does not affect the transcript level of neither BAFF nor APRIL. This suggests

that smoking might be affecting BAFF through another way in aortic adventitia of diseased CVD patients.

B-lymphocytes have been shown to have proinflammatory role in the settings of RA, evident from the fact that B cell depletion therapy (rituximab) is an approved drug for refractory cases of RA. Whereas, B lymphocytes are demonstrated as atheroprotective in atherosclerosis [232]. To investigate the impact of B cell depletion therapy on atherosclerosis, huCD20^{+}/ApoE$^{-/-}$ mice were generated and a small group of mice n=4 were treated every four weeks with rituximab and IgG (100μg). The circulating B-lymphocytes were efficiently depleted and before the next treatment they were repopulated. The rituximab treated mice showed a 2-fold reduction in lesions area as compared to control mice treated with IgG. This preliminary data is suggestive of the fact that the reduction in atherosclerotic lesion, as a result of B cell targeted depletion could be due to removal of B cell influence, resulting in impaired cell-to-cell interaction and suppression of antigen presentation induced T cell stimulation [244]. Studies in murine model of RA and diabetes have shown that B cell depletion impairs the antigen specific activation of CD4 (+) cells, despite the fact that lymphoid tissue B cells resist this target killing [245].

There is in vitro data that confirms release of B cell survival factor (Blys) by neutrophils [246]. In fact Blys protein and APRIL are also found in synovial fluid of patients with inflammatory arthritis [247]. These survival factors promote expansion and survival of B cells and therefore are implicated as protective factors for synovial B cells. This is further supported by the evidence that patients synovial expression of APRIL, BAFF and SDF-1 was unaltered following rituximab therapy [248]. Importantly, in this thesis we have established BAFF and APRIL in aortic adventitia from patients with advanced atherosclerosis. Moreover, we have also validated their expression by mouse vascular endothelial cells. If the protective role of survival factors (BAFF & APRIL) is shielding the synovial B cells from rituximab, it could be hypothesized that proinflammatory environment within the blood vessels might be promoting B cell survival factors.

These aggregates of B cells might represent sites where B cell selection and maturation takes place; presumably high affinity antibodies are raised against locally delivered citrullinated protein. The presence of two different subsets of

RA patients on account of autoantibodies, the ACPA positive and negative subset reduced the possibility of identifying autoantibodies in our samples [217]. It is interesting to note that when we screened all the samples for autoantibody presence five patients were positive for plasma cells and only one of these was a RA patient. Our attempt to characterize citrulline reactive antibody secreting plasma cells was ineffective, perhaps because of the distribution of plasma cells. Whereas, the fact that our samples were quite variable in size. The distribution pattern is vital in interpreting this set of data. Besides this it is quite difficult to confirm this in only one RA patient positive for plasma cells.

The RA patients that received systemic treatment with rituximab are shown to have 97% decrease in CD19+ but around 80% of the remaining cells were memory B cells or plasma cells. An other study showed a small fraction of T lymphocytes (3%) and natural killer cells (2%) to express CD20; this was also associated with an increase in the immature B cells like CD19+, IgD+, CD38 (high), CD10 (low), CD24 (high) cells [249]. This would imply that antibody producing plasma cells resist depletion and could continue to produce protective antibodies.

Interestingly, dyslipidemia (high LDL) is an important factor in initiating atherosclerosis; due to time limitation we could not validate the lipid profile of mice in study. Surely that would have added vital information and more depth to the understanding of our model. As for now we do not know whether these huCD20^{+}/ApoE$^{-/-}$ mice have a normal lipid profile.

Our study does have limitations as we have shown all the differences by comparing diseased aortic adventitia and matched IMA (internal control); which is not the best option to compare with aortic adventitia. Replacement of aortic adventitia with coronary artery with dimensions similar to IMA would have been a good internal control. In addition, matched saphenous vein adventitia is closer to aorta in size and calibre, so as a negative control it would have provided a better comparison. Moreover, the severity of inflammation in these atherosclerotic plaques would have been underestimated as the specimens were selectively taken (for some surgical reasons) from areas with less severe disease.

The characteristic of IMA to resist atherosclerosis is established but it is not fully understood why it behaves different. However, Ferro et al showed that the

lesions are ten times greater in coronary artery then the IMA. This was seen in the inner most layer i.e. intima but not in the tunica media [218]. The IMA have high antioxidant capacity compared to coronary artery SMC; IMA smooth muscle cells also express low tenascin and decorin that are involved in the LDL binding and SMC migration. Apart from these factors there are extrinsic features like axial stretch, sheer stress and small number of side branches that might play a role in the IMA resistance to atherosclerosis [219]. The underlying mechanism for resisting atherosclerosis might not be unfolded yet but there is some unknown attribute that makes IMA unique.

It has been shown previously that IL-33/sST2 is important in cardiovascular system. The protective effects of IL-33 in the murine model of atherosclerosis are shown to exist through Th2 cytokines IL-5 and IL-13. Importantly, the blockade of IL-5 results in augmented plaque size despite IL-33 treatment [199]. Moreover, IL-5 is know to exert its anti atherosclerotic response through natural antibodies against oxLDL [139]. This might suggest that IL-33 has a link with B-lymphocytes.

The salient finding of this study is that expression of IL-33 is down regulated in vascular endothelial cells of smokers (AA); the IL-33 levels of non smoking patients in the AA were indifferent to IMA suggestive of an indirect association of smoking resulting in failure of IL-33 induce protection in AA specifically. Smoking is as a danger signal that could be creating an inflammatory environment through oxLDL; which is known to cause endothelial dysfunction and damage; depending on the duration and severity of the insult.

We hypothesized that IL-33 could be released with damage to the vascular endothelium; which may stimulate the production of natural antibodies against oxLDL through IL-5, these antibodies then perhaps block the uptake of oxLDL by macrophages. However, the increase in the reactive oxygen species production and the inflammatory environment cause damage to endothelial cells. To confirm the impact of hypoxia and reoxygenation on IL-33/sST2 in vascular endothelial cells a culture system was established; which revealed that hypoxia has no effect on IL-33/sST2 message. A recent study showed that IL-33 is lost by endothelial cells during wound healing and angiogenesis [220]. While optimizing the

culture system it was shown that IL-33 expression is stable when cells are fully confluent.

This thesis has shown that RA associated antigen CP is seen in patient's aorta and is strongly associated with ACPA and CRP, suggestive of their significance in atherosclerosis seen in RA patients. Moreover, presence of B cells and their survival niche in aortic adventitia imply an important role in the vascular environment. In fact B cell depletion in mouse model resulted in reduction of atherosclerotic plaques, indicative of depletion of proatherogenic B cell subset, perhaps it' s supportive function towards T cell is impaired that caused the reduction in lesion size. However, this needs to be addressed in future studies, In fact in a large sample size with rituximab treatments. In addition investigation of the lipid profile and antibody titre would be more helpful in understanding the underlying mechanism of the impact of B cell depletion in atherosclerosis.

References

1. Majithia V, Geraci SA. Rheumatoid arthritis: diagnosis and management. *Am J Med*. Nov 2007;120(11):936-939.
2. Arnett FC, Edworthy SM, Bloch DA, et al. The American Rheumatism Association 1987 revised criteria for the classification of rheumatoid arthritis. *Arthritis Rheum*. Mar 1988;31(3):315-324.
3. Tarkowski A, Czerkinsky C, Nilsson LA. Simultaneous induction of rheumatoid factor- and antigen-specific antibody-secreting cells during the secondary immune response in man. *Clin Exp Immunol*. Aug 1985;61(2):379-387.
4. Stastny P. Association of the B-cell alloantigen DRw4 with rheumatoid arthritis. *N Engl J Med*. Apr 20 1978;298(16):869-871.
5. Klareskog L, Forsum U, Scheynius A, et al. Evidence in support of a self-perpetuating HLA-DR-dependent delayed-type cell reaction in rheumatoid arthritis. *Proc Natl Acad Sci U S A*. Jun 1982;79(11):3632-3636.
6. Gregersen PK, Silver J, Winchester RJ. The shared epitope hypothesis. An approach to understanding the molecular genetics of susceptibility to rheumatoid arthritis. *Arthritis Rheum*. Nov 1987;30(11):1205-1213.
7. Lorentzen JC, Flornes L, Eklow C, et al. Association of arthritis with a gene complex encoding C-type lectin-like receptors. *Arthritis Rheum*. Aug 2007;56(8):2620-2632.
8. Johansson M, Arlestig L, Hallmans G, et al. PTPN22 polymorphism and anti-cyclic citrullinated peptide antibodies in combination strongly predicts future onset of rheumatoid arthritis and has a specificity of 100% for the disease. *Arthritis Res Ther*. 2006;8(1):R19.
9. Sigurdsson S, Padyukov L, Kurreeman FA, et al. Association of a haplotype in the promoter region of the interferon regulatory factor 5 gene with rheumatoid arthritis. *Arthritis Rheum*. Jul 2007;56(7):2202-2210.
10. Klareskog L, Stolt P, Lundberg K, et al. A new model for an etiology of rheumatoid arthritis. *Arthritis and Rheumatism*. 2006;54(1):38-46.
11. Pedersen M, Jacobsen S, Garred P, et al. Strong combined gene-environment effects in anti-cyclic citrullinated peptide-positive

rheumatoid arthritis: a nationwide case-control study in Denmark. *Arthritis Rheum*. May 2007;56(5):1446-1453.

12. Van Boxel JA, Paget SA. Predominantly T-cell infiltrate in rheumatoid synovial membranes. *N Engl J Med*. Sep 11 1975;293(11):517-520.

13. Brennan FM, Chantry D, Jackson A, et al. Inhibitory effect of TNF alpha antibodies on synovial cell interleukin-1 production in rheumatoid arthritis. *Lancet*. Jul 29 1989;2(8657):244-247.

14. Nishimoto N, Kishimoto T. Interleukin 6: from bench to bedside. *Nat Clin Pract Rheumatol*. Nov 2006;2(11):619-626.

15. Burger D, Dayer JM, Palmer G, et al. Is IL-1 a good therapeutic target in the treatment of arthritis? *Best Pract Res Clin Rheumatol*. Oct 2006;20(5):879-896.

16. Jimenez-Boj E, Redlich K, Turk B, et al. Interaction between synovial inflammatory tissue and bone marrow in rheumatoid arthritis. *J Immunol*. Aug 15 2005;175(4):2579-2588.

17. Maini RN, Taylor PC. Anti-cytokine therapy for rheumatoid arthritis. *Annu Rev Med*. 2000;51:207-229.

18. Klareskog L, Widhe M, Hermansson M, et al. Antibodies to citrullinated proteins in arthritis: pathology and promise. *Curr Opin Rheumatol*. May 2008;20(3):300-305.

19. Vander Cruyssen B, Peene I, Cantaert T, et al. Anti-citrullinated protein/peptide antibodies (ACPA) in rheumatoid arthritis: specificity and relation with rheumatoid factor. *Autoimmun Rev*. Sep 2005;4(7):468-474.

20. Huizinga TW, Amos CI, van der Helm-van Mil AH, et al. Refining the complex rheumatoid arthritis phenotype based on specificity of the HLA-DRB1 shared epitope for antibodies to citrullinated proteins. *Arthritis Rheum*. Nov 2005;52(11):3433-3438.

21. van der Helm-van Mil AH, Verpoort KN, le Cessie S, et al. The HLA-DRB1 shared epitope alleles differ in the interaction with smoking and predisposition to antibodies to cyclic citrullinated peptide. *Arthritis Rheum*. Feb 2007;56(2):425-432.

22. van der Helm-van Mil AH, Verpoort KN, Breedveld FC, et al. The HLA-DRB1 shared epitope alleles are primarily a risk factor for anti-cyclic citrullinated peptide antibodies and are not an independent risk factor for

development of rheumatoid arthritis. *Arthritis Rheum.* Apr 2006;54(4):1117-1121.

23. Masson-Bessiere C, Sebbag M, Girbal-Neuhauser E, et al. The major synovial targets of the rheumatoid arthritis-specific antifilaggrin autoantibodies are deiminated forms of the alpha- and beta-chains of fibrin. *J Immunol.* Mar 15 2001;166(6):4177-4184.

24. Vossenaar ER, Despres N, Lapointe E, et al. Rheumatoid arthritis specific anti-Sa antibodies target citrullinated vimentin. *Arthritis Res Ther.* 2004;6(2):R142-150.

25. Burkhardt H, Sehnert B, Bockermann R, et al. Humoral immune response to citrullinated collagen type II determinants in early rheumatoid arthritis. *Eur J Immunol.* May 2005;35(5):1643-1652.

26. Pratesi F, Tommasi C, Anzilotti C, et al. Deiminated Epstein-Barr virus nuclear antigen 1 is a target of anti-citrullinated protein antibodies in rheumatoid arthritis. *Arthritis Rheum.* Mar 2006;54(3):733-741.

27. Kinloch A, Lundberg K, Wait R, et al. Synovial fluid is a site of citrullination of autoantigens in inflammatory arthritis. *Arthritis Rheum.* Aug 2008;58(8):2287-2295.

28. Vossenaar ER, Zendman AJ, van Venrooij WJ, et al. PAD, a growing family of citrullinating enzymes: genes, features and involvement in disease. *Bioessays.* Nov 2003;25(11):1106-1118.

29. Chavanas S, Mechin MC, Takahara H, et al. Comparative analysis of the mouse and human peptidylarginine deiminase gene clusters reveals highly conserved non-coding segments and a new human gene, PADI6. *Gene.* Apr 14 2004;330:19-27.

30. Gyorgy B, Toth E, Tarcsa E, et al. Citrullination: a posttranslational modification in health and disease. *Int J Biochem Cell Biol.* 2006;38(10):1662-1677.

31. Baeten D, Peene I, Union A, et al. Specific presence of intracellular citrullinated proteins in rheumatoid arthritis synovium: relevance to antifilaggrin autoantibodies. *Arthritis Rheum.* Oct 2001;44(10):2255-2262.

32. Kubilus J, Waitkus RW, Baden HP. The presence of citrulline in epidermal proteins. *Biochim Biophys Acta.* Nov 23 1979;581(1):114-121.

33. Senshu T, Kan S, Ogawa H, et al. Preferential deimination of keratin K1 and filaggrin during the terminal differentiation of human epidermis. *Biochem Biophys Res Commun.* Aug 23 1996;225(3):712-719.

34. Nicholas AP, Whitaker JN. Preparation of a monoclonal antibody to citrullinated epitopes: its characterization and some applications to immunohistochemistry in human brain. *Glia.* Mar 15 2002;37(4):328-336.

35. Pritzker LB, Joshi S, Gowan JJ, et al. Deimination of myelin basic protein. 1. Effect of deimination of arginyl residues of myelin basic protein on its structure and susceptibility to digestion by cathepsin D. *Biochemistry.* May 9 2000;39(18):5374-5381.

36. Mechin MC, Enji M, Nachat R, et al. The peptidylarginine deiminases expressed in human epidermis differ in their substrate specificities and subcellular locations. *Cell Mol Life Sci.* Sep 2005;62(17):1984-1995.

37. Chang X, Yamada R, Suzuki A, et al. Localization of peptidylarginine deiminase 4 (PADI4) and citrullinated protein in synovial tissue of rheumatoid arthritis. *Rheumatology (Oxford).* Jan 2005;44(1):40-50.

38. Foulquier C, Sebbag M, Clavel C, et al. Peptidyl arginine deiminase type 2 (PAD-2) and PAD-4 but not PAD-1, PAD-3, and PAD-6 are expressed in rheumatoid arthritis synovium in close association with tissue inflammation. *Arthritis Rheum.* Nov 2007;56(11):3541-3553.

39. Yamada R, Suzuki A, Chang X, et al. Citrullinated proteins in rheumatoid arthritis. *Front Biosci.* Jan 1 2005;10:54-64.

40. Makrygiannakis D, af Klint E, Lundberg IE, et al. Citrullination is an inflammation-dependent process. *Ann Rheum Dis.* Sep 2006;65(9):1219-1222.

41. O'Dell JR, Haire CE, Erikson N, et al. Treatment of rheumatoid arthritis with methotrexate alone, sulfasalazine and hydroxychloroquine, or a combination of all three medications. *N Engl J Med.* May 16 1996;334(20):1287-1291.

42. Elliott MJ, Maini RN, Feldmann M, et al. Randomised double-blind comparison of chimeric monoclonal antibody to tumour necrosis factor alpha (cA2) versus placebo in rheumatoid arthritis. *Lancet.* Oct 22 1994;344(8930):1105-1110.

43. Smolen JS, Aletaha D, Koeller M, et al. New therapies for treatment of rheumatoid arthritis. *Lancet.* Dec 1 2007;370(9602):1861-1874.

44. Smolen JS, Beaulieu A, Rubbert-Roth A, et al. Effect of interleukin-6 receptor inhibition with tocilizumab in patients with rheumatoid arthritis (OPTION study): a double-blind, placebo-controlled, randomised trial. *Lancet*. Mar 22 2008;371(9617):987-997.

45. Edwards JC, Szczepanski L, Szechinski J, et al. Efficacy of B-cell-targeted therapy with rituximab in patients with rheumatoid arthritis. *N Engl J Med*. Jun 17 2004;350(25):2572-2581.

46. Martinez-Gamboa L, Brezinschek HP, Burmester GR, et al. Immunopathologic role of B lymphocytes in rheumatoid arthritis: rationale of B cell-directed therapy. *Autoimmun Rev*. Aug 2006;5(7):437-442.

47. Viau M, Zouali M. B-lymphocytes, innate immunity, and autoimmunity. *Clin Immunol*. Jan 2005;114(1):17-26.

48. Firestein GS, Zvaifler NJ. How important are T cells in chronic rheumatoid synovitis?: II. T cell-independent mechanisms from beginning to end. *Arthritis Rheum*. Feb 2002;46(2):298-308.

49. Protheroe A, Edwards JC, Simmons A, et al. Remission of inflammatory arthropathy in association with anti-CD20 therapy for non-Hodgkin's lymphoma. *Rheumatology (Oxford)*. Nov 1999;38(11):1150-1152.

50. Stewart M, Malkovska V, Krishnan J, et al. Lymphoma in a patient with rheumatoid arthritis receiving methotrexate treatment: successful treatment with rituximab. *Ann Rheum Dis*. Sep 2001;60(9):892-893.

51. Lefebvre ML, Krause SW, Salcedo M, et al. Ex vivo-activated human macrophages kill chronic lymphocytic leukemia cells in the presence of rituximab: mechanism of antibody-dependent cellular cytotoxicity and impact of human serum. *J Immunother*. Jul-Aug 2006;29(4):388-397.

52. Cragg MS, Walshe CA, Ivanov AO, et al. The biology of CD20 and its potential as a target for mAb therapy. *Curr Dir Autoimmun*. 2005;8:140-174.

53. Kennedy AD, Beum PV, Solga MD, et al. Rituximab infusion promotes rapid complement depletion and acute CD20 loss in chronic lymphocytic leukemia. *J Immunol*. Mar 1 2004;172(5):3280-3288.

54. Reff ME, Carner K, Chambers KS, et al. Depletion of B cells in vivo by a chimeric mouse human monoclonal antibody to CD20. *Blood*. Jan 15 1994;83(2):435-445.

55. Taylor RP, Lindorfer MA. Drug insight: the mechanism of action of rituximab in autoimmune disease--the immune complex decoy hypothesis. *Nat Clin Pract Rheumatol*. Feb 2007;3(2):86-95.

56. Schellekens GA, de Jong BA, van den Hoogen FH, et al. Citrulline is an essential constituent of antigenic determinants recognized by rheumatoid arthritis-specific autoantibodies. *J Clin Invest*. Jan 1 1998;101(1):273-281.

57. Carroll MC. The complement system in regulation of adaptive immunity. *Nat Immunol*. Oct 2004;5(10):981-986.

58. Dorner T, Burmester GR. The role of B cells in rheumatoid arthritis: mechanisms and therapeutic targets. *Curr Opin Rheumatol*. May 2003;15(3):246-252.

59. Takemura S, Klimiuk PA, Braun A, et al. T cell activation in rheumatoid synovium is B cell dependent. *J Immunol*. Oct 15 2001;167(8):4710-4718.

60. Schroder AE, Greiner A, Seyfert C, et al. Differentiation of B cells in the nonlymphoid tissue of the synovial membrane of patients with rheumatoid arthritis. *Proc Natl Acad Sci U S A*. Jan 9 1996;93(1):221-225.

61. Humby F, Bombardieri M, Manzo A, et al. Ectopic lymphoid structures support ongoing production of class-switched autoantibodies in rheumatoid synovium. *PLoS Med*. Jan 13 2009;6(1):e1.

62. Ohata J, Zvaifler NJ, Nishio M, et al. Fibroblast-like synoviocytes of mesenchymal origin express functional B cell-activating factor of the TNF family in response to proinflammatory cytokines. *J Immunol*. Jan 15 2005;174(2):864-870.

63. Gross JA, Johnston J, Mudri S, et al. TACI and BCMA are receptors for a TNF homologue implicated in B-cell autoimmune disease. *Nature*. Apr 27 2000;404(6781):995-999.

64. Shu HB, Hu WH, Johnson H. TALL-1 is a novel member of the TNF family that is down-regulated by mitogens. *J Leukoc Biol*. May 1999;65(5):680-683.

65. Mukhopadhyay A, Ni J, Zhai Y, et al. Identification and characterization of a novel cytokine, THANK, a TNF homologue that activates apoptosis, nuclear factor-kappaB, and c-Jun NH2-terminal kinase. *J Biol Chem*. Jun 4 1999;274(23):15978-15981.

66. Jiang Y, Ohtsuji M, Abe M, et al. Polymorphism and chromosomal mapping of the mouse gene for B-cell activating factor belonging to the tumor

necrosis factor family (Baff) and association with the autoimmune phenotype. *Immunogenetics*. Dec 2001;53(9):810-813.

67. Pelekanou V, Kampa M, Kafousi M, et al. Expression of TNF-superfamily members BAFF and APRIL in breast cancer: immunohistochemical study in 52 invasive ductal breast carcinomas. *BMC Cancer*. 2008;8:76.

68. Dillon SR, Gross JA, Ansell SM, et al. An APRIL to remember: novel TNF ligands as therapeutic targets. *Nat Rev Drug Discov*. Mar 2006;5(3):235-246.

69. Bossen C, Schneider P. BAFF, APRIL and their receptors: structure, function and signaling. *Semin Immunol*. Oct 2006;18(5):263-275.

70. Karpusas M, Cachero TG, Qian F, et al. Crystal structure of extracellular human BAFF, a TNF family member that stimulates B lymphocytes. *J Mol Biol*. Feb 1 2002;315(5):1145-1154.

71. Oren DA, Li Y, Volovik Y, et al. Structural basis of BLyS receptor recognition. *Nat Struct Biol*. Apr 2002;9(4):288-292.

72. Cachero TG, Schwartz IM, Qian F, et al. Formation of virus-like clusters is an intrinsic property of the tumor necrosis factor family member BAFF (B cell activating factor). *Biochemistry*. Feb 21 2006;45(7):2006-2013.

73. Thompson JS, Bixler SA, Qian F, et al. BAFF-R, a newly identified TNF receptor that specifically interacts with BAFF. *Science*. Sep 14 2001;293(5537):2108-2111.

74. Gras MP, Laabi Y, Linares-Cruz G, et al. BCMAp: an integral membrane protein in the Golgi apparatus of human mature B lymphocytes. *Int Immunol*. Jul 1995;7(7):1093-1106.

75. Laabi Y, Gras MP, Carbonnel F, et al. A new gene, BCM, on chromosome 16 is fused to the interleukin 2 gene by a t(4;16)(q26;p13) translocation in a malignant T cell lymphoma. *Embo J*. Nov 1992;11(11):3897-3904.

76. von Bulow GU, Bram RJ. NF-AT activation induced by a CAML-interacting member of the tumor necrosis factor receptor superfamily. *Science*. Oct 3 1997;278(5335):138-141.

77. Lopez-Fraga M, Fernandez R, Albar JP, et al. Biologically active APRIL is secreted following intracellular processing in the Golgi apparatus by furin convertase. *EMBO Rep*. Oct 2001;2(10):945-951.

78. Mackay F, Schneider P, Rennert P, et al. BAFF AND APRIL: a tutorial on B cell survival. *Annu Rev Immunol*. 2003;21:231-264.

79. Ingold K, Zumsteg A, Tardivel A, et al. Identification of proteoglycans as the APRIL-specific binding partners. *J Exp Med*. May 2 2005;201(9):1375-1383.

80. Rennert P, Schneider P, Cachero TG, et al. A soluble form of B cell maturation antigen, a receptor for the tumor necrosis factor family member APRIL, inhibits tumor cell growth. *J Exp Med*. Dec 4 2000;192(11):1677-1684.

81. Ng LG, Sutherland AP, Newton R, et al. B cell-activating factor belonging to the TNF family (BAFF)-R is the principal BAFF receptor facilitating BAFF costimulation of circulating T and B cells. *J Immunol*. Jul 15 2004;173(2):807-817.

82. Schiemann B, Gommerman JL, Vora K, et al. An essential role for BAFF in the normal development of B cells through a BCMA-independent pathway. *Science*. Sep 14 2001;293(5537):2111-2114.

83. Tardivel A, Tinel A, Lens S, et al. The anti-apoptotic factor Bcl-2 can functionally substitute for the B cell survival but not for the marginal zone B cell differentiation activity of BAFF. *Eur J Immunol*. Feb 2004;34(2):509-518.

84. Yang M, Hase H, Legarda-Addison D, et al. B cell maturation antigen, the receptor for a proliferation-inducing ligand and B cell-activating factor of the TNF family, induces antigen presentation in B cells. *J Immunol*. Sep 1 2005;175(5):2814-2824.

85. Castigli E, Scott S, Dedeoglu F, et al. Impaired IgA class switching in APRIL-deficient mice. *Proc Natl Acad Sci U S A*. Mar 16 2004;101(11):3903-3908.

86. Bonci D, Hahne M, Felli N, et al. Potential role of APRIL as autocrine growth factor for megakaryocytopoiesis. *Blood*. Nov 15 2004;104(10):3169-3172.

87. Planelles L, Carvalho-Pinto CE, Hardenberg G, et al. APRIL promotes B-1 cell-associated neoplasm. *Cancer Cell*. Oct 2004;6(4):399-408.

88. Turesson C, O'Fallon WM, Crowson CS, et al. Extra-articular disease manifestations in rheumatoid arthritis: incidence trends and risk factors over 46 years. *Ann Rheum Dis*. Aug 2003;62(8):722-727.

89. Wallberg-Jonsson S, Johansson H, Ohman ML, et al. Extent of inflammation predicts cardiovascular disease and overall mortality in

seropositive rheumatoid arthritis. A retrospective cohort study from disease onset. *J Rheumatol*. Dec 1999;26(12):2562-2571.

90. Maradit-Kremers H, Crowson CS, Nicola PJ, et al. Increased unrecognized coronary heart disease and sudden deaths in rheumatoid arthritis: a population-based cohort study. *Arthritis Rheum*. Feb 2005;52(2):402-411.

91. Farragher TM, Goodson NJ, Naseem H, et al. Association of the HLA-DRB1 gene with premature death, particularly from cardiovascular disease, in patients with rheumatoid arthritis and inflammatory polyarthritis. *Arthritis Rheum*. Feb 2008;58(2):359-369.

92. Shoenfeld Y, Gerli R, Doria A, et al. Accelerated atherosclerosis in autoimmune rheumatic diseases. *Circulation*. Nov 22 2005;112(21):3337-3347.

93. Stevens RJ, Douglas KM, Saratzis AN, et al. Inflammation and atherosclerosis in rheumatoid arthritis. *Expert Rev Mol Med*. May 6 2005;7(7):1-24.

94. Metsios GS, Stavropoulos-Kalinoglou A, Panoulas VF, et al. Association of physical inactivity with increased cardiovascular risk in patients with rheumatoid arthritis. *Eur J Cardiovasc Prev Rehabil*. Apr 2009;16(2):188-194.

95. Van Doornum S, McColl G, Wicks IP. Accelerated atherosclerosis: an extraarticular feature of rheumatoid arthritis? *Arthritis Rheum*. Apr 2002;46(4):862-873.

96. Capell H, McCarey D, Madhok R, et al. "5D" Outcome in 52 patients with rheumatoid arthritis surviving 20 years after initial disease modifying antirheumatic drug therapy. *J Rheumatol*. Oct 2002;29(10):2099-2105.

97. Solomon DH, Karlson EW, Rimm EB, et al. Cardiovascular morbidity and mortality in women diagnosed with rheumatoid arthritis. *Circulation*. Mar 11 2003;107(9):1303-1307.

98. Kitas GD, Erb N. Tackling ischaemic heart disease in rheumatoid arthritis. *Rheumatology (Oxford)*. May 2003;42(5):607-613.

99. Wallberg-Jonsson S, Ohman ML, Dahlqvist SR. Cardiovascular morbidity and mortality in patients with seropositive rheumatoid arthritis in Northern Sweden. *J Rheumatol*. Mar 1997;24(3):445-451.

100. del Rincon ID, Williams K, Stern MP, et al. High incidence of cardiovascular events in a rheumatoid arthritis cohort not explained by

traditional cardiac risk factors. *Arthritis Rheum*. Dec 2001;44(12):2737-2745.

101. Gonzalez-Gay MA, Gonzalez-Juanatey C, Lopez-Diaz MJ, et al. HLA-DRB1 and persistent chronic inflammation contribute to cardiovascular events and cardiovascular mortality in patients with rheumatoid arthritis. *Arthritis Rheum*. Feb 15 2007;57(1):125-132.

102. Sattar N, McCarey DW, Capell H, et al. Explaining how "high-grade" systemic inflammation accelerates vascular risk in rheumatoid arthritis. *Circulation*. Dec 16 2003;108(24):2957-2963.

103. Avina-Zubieta JA, Choi HK, Sadatsafavi M, et al. Risk of cardiovascular mortality in patients with rheumatoid arthritis: a meta-analysis of observational studies. *Arthritis Rheum*. Dec 15 2008;59(12):1690-1697.

104. Hannawi S, Haluska B, Marwick TH, et al. Atherosclerotic disease is increased in recent-onset rheumatoid arthritis: a critical role for inflammation. *Arthritis Res Ther*. 2007;9(6):R116.

105. Cuomo G, Di Micco P, Niglio A, et al. [Atherosclerosis and rheumatoid arthritis: relationships between intima-media thickness of the common carotid arteries and disease activity and disability]. *Reumatismo*. Oct-Dec 2004;56(4):242-246.

106. Pasceri V, Yeh ET. A tale of two diseases: atherosclerosis and rheumatoid arthritis. *Circulation*. Nov 23 1999;100(21):2124-2126.

107. Murray CJ, Lopez AD. Global mortality, disability, and the contribution of risk factors: Global Burden of Disease Study. *Lancet*. May 17 1997;349(9063):1436-1442.

108. Plump A. Cardiovascular medicine at the turn of the millennium. *N Engl J Med*. Mar 26 1998;338(13):919-920.

109. Breslow JL. Cardiovascular disease burden increases, NIH funding decreases. *Nat Med*. Jun 1997;3(6):600-601.

110. Stary HC, Chandler AB, Glagov S, et al. A definition of initial, fatty streak, and intermediate lesions of atherosclerosis. A report from the Committee on Vascular Lesions of the Council on Arteriosclerosis, American Heart Association. *Circulation*. May 1994;89(5):2462-2478.

111. Hansson GK, Libby P. The immune response in atherosclerosis: a double-edged sword. *Nat Rev Immunol*. Jul 2006;6(7):508-519.

112. Ross R. Atherosclerosis--an inflammatory disease. *N Engl J Med*. Jan 14 1999;340(2):115-126.

113. Mayerl C, Lukasser M, Sedivy R, et al. Atherosclerosis research from past to present--on the track of two pathologists with opposing views, Carl von Rokitansky and Rudolf Virchow. *Virchows Arch*. Jul 2006;449(1):96-103.

114. Stary HC. Macrophages, macrophage foam cells, and eccentric intimal thickening in the coronary arteries of young children. *Atherosclerosis*. Apr 1987;64(2-3):91-108.

115. Ross R. The pathogenesis of atherosclerosis: a perspective for the 1990s. *Nature*. Apr 29 1993;362(6423):801-809.

116. Maiellaro K, Taylor WR. The role of the adventitia in vascular inflammation. *Cardiovasc Res*. Sep 1 2007;75(4):640-648.

117. Newby AC. An overview of the vascular response to injury: a tribute to the late Russell Ross. *Toxicol Lett*. Mar 15 2000;112-113:519-529.

118. Acton SL, Scherer PE, Lodish HF, et al. Expression cloning of SR-BI, a CD36-related class B scavenger receptor. *J Biol Chem*. Aug 19 1994;269(33):21003-21009.

119. Ramprasad MP, Terpstra V, Kondratenko N, et al. Cell surface expression of mouse macrosialin and human CD68 and their role as macrophage receptors for oxidized low density lipoprotein. *Proc Natl Acad Sci U S A*. Dec 10 1996;93(25):14833-14838.

120. Sambrano GR, Parthasarathy S, Steinberg D. Recognition of oxidatively damaged erythrocytes by a macrophage receptor with specificity for oxidized low density lipoprotein. *Proc Natl Acad Sci U S A*. Apr 12 1994;91(8):3265-3269.

121. Edfeldt K, Swedenborg J, Hansson GK, et al. Expression of toll-like receptors in human atherosclerotic lesions: a possible pathway for plaque activation. *Circulation*. Mar 12 2002;105(10):1158-1161.

122. Liuzzo G, Biasucci LM, Gallimore JR, et al. The prognostic value of C-reactive protein and serum amyloid a protein in severe unstable angina. *N Engl J Med*. Aug 18 1994;331(7):417-424.

123. Tracy RP, Lemaitre RN, Psaty BM, et al. Relationship of C-reactive protein to risk of cardiovascular disease in the elderly. Results from the Cardiovascular Health Study and the Rural Health Promotion Project. *Arterioscler Thromb Vasc Biol*. Jun 1997;17(6):1121-1127.

124. Ridker PM, Hennekens CH, Buring JE, et al. C-reactive protein and other markers of inflammation in the prediction of cardiovascular disease in women. *N Engl J Med*. Mar 23 2000;342(12):836-843.

125. Palinski W, Rosenfeld ME, Yla-Herttuala S, et al. Low density lipoprotein undergoes oxidative modification in vivo. *Proc Natl Acad Sci U S A*. Feb 1989;86(4):1372-1376.

126. Nakashima Y, Raines EW, Plump AS, et al. Upregulation of VCAM-1 and ICAM-1 at atherosclerosis-prone sites on the endothelium in the ApoE-deficient mouse. *Arterioscler Thromb Vasc Biol*. May 1998;18(5):842-851.

127. Gerrity RG, Naito HK, Richardson M, et al. Dietary induced atherogenesis in swine. Morphology of the intima in prelesion stages. *Am J Pathol*. Jun 1979;95(3):775-792.

128. Smith JD, Trogan E, Ginsberg M, et al. Decreased atherosclerosis in mice deficient in both macrophage colony-stimulating factor (op) and apolipoprotein E. *Proc Natl Acad Sci U S A*. Aug 29 1995;92(18):8264-8268.

129. Janeway CA, Jr., Medzhitov R. Innate immune recognition. *Annu Rev Immunol*. 2002;20:197-216.

130. Bobryshev YV, Lord RS. Ultrastructural recognition of cells with dendritic cell morphology in human aortic intima. Contacting interactions of Vascular Dendritic Cells in athero-resistant and athero-prone areas of the normal aorta. *Arch Histol Cytol*. Aug 1995;58(3):307-322.

131. Galkina E, Ley K. Immune and inflammatory mechanisms of atherosclerosis (*). *Annu Rev Immunol*. 2009;27:165-197.

132. Zhou X, Hansson GK. Detection of B cells and proinflammatory cytokines in atherosclerotic plaques of hypercholesterolaemic apolipoprotein E knockout mice. *Scand J Immunol*. Jul 1999;50(1):25-30.

133. Major AS, Fazio S, Linton MF. B-lymphocyte deficiency increases atherosclerosis in LDL receptor-null mice. *Arterioscler Thromb Vasc Biol*. Nov 1 2002;22(11):1892-1898.

134. Caligiuri G, Nicoletti A, Poirier B, et al. Protective immunity against atherosclerosis carried by B cells of hypercholesterolemic mice. *J Clin Invest*. Mar 2002;109(6):745-753.

135. Binder CJ, Horkko S, Dewan A, et al. Pneumococcal vaccination decreases atherosclerotic lesion formation: molecular mimicry between

Streptococcus pneumoniae and oxidized LDL. *Nat Med.* Jun 2003;9(6):736-743.

136. Shaw PX, Goodyear CS, Chang MK, et al. The autoreactivity of anti-phosphorylcholine antibodies for atherosclerosis-associated neo-antigens and apoptotic cells. *J Immunol.* Jun 15 2003;170(12):6151-6157.

137. Binder CJ, Shaw PX, Chang MK, et al. The role of natural antibodies in atherogenesis. *J Lipid Res.* Jul 2005;46(7):1353-1363.

138. Shaw PX, Horkko S, Chang MK, et al. Natural antibodies with the T15 idiotype may act in atherosclerosis, apoptotic clearance, and protective immunity. *J Clin Invest.* Jun 2000;105(12):1731-1740.

139. Binder CJ, Hartvigsen K, Chang MK, et al. IL-5 links adaptive and natural immunity specific for epitopes of oxidized LDL and protects from atherosclerosis. *J Clin Invest.* Aug 2004;114(3):427-437.

140. Zhou X, Paulsson G, Stemme S, et al. Hypercholesterolemia is associated with a T helper (Th) 1/Th2 switch of the autoimmune response in atherosclerotic apo E-knockout mice. *J Clin Invest.* Apr 15 1998;101(8):1717-1725.

141. Robertson AK, Zhou X, Strandvik B, et al. Severe hypercholesterolaemia leads to strong Th2 responses to an exogenous antigen. *Scand J Immunol.* Mar 2004;59(3):285-293.

142. Moos MP, John N, Grabner R, et al. The lamina adventitia is the major site of immune cell accumulation in standard chow-fed apolipoprotein E-deficient mice. *Arterioscler Thromb Vasc Biol.* Nov 2005;25(11):2386-2391.

143. Scott NA, Cipolla GD, Ross CE, et al. Identification of a potential role for the adventitia in vascular lesion formation after balloon overstretch injury of porcine coronary arteries. *Circulation.* Jun 15 1996;93(12):2178-2187.

144. Houtkamp MA, de Boer OJ, van der Loos CM, et al. Adventitial infiltrates associated with advanced atherosclerotic plaques: structural organization suggests generation of local humoral immune responses. *J Pathol.* Feb 2001;193(2):263-269.

145. Higuchi ML, Gutierrez PS, Bezerra HG, et al. Comparison between adventitial and intimal inflammation of ruptured and nonruptured atherosclerotic plaques in human coronary arteries. *Arq Bras Cardiol.* Jul 2002;79(1):20-24.

146. Zhou X, Nicoletti A, Elhage R, et al. Transfer of CD4(+) T cells aggravates atherosclerosis in immunodeficient apolipoprotein E knockout mice. *Circulation.* Dec 12 2000;102(24):2919-2922.

147. Zhou X, Robertson AK, Hjerpe C, et al. Adoptive transfer of CD4+ T cells reactive to modified low-density lipoprotein aggravates atherosclerosis. *Arterioscler Thromb Vasc Biol.* Apr 2006;26(4):864-870.

148. Stemme S, Faber B, Holm J, et al. T lymphocytes from human atherosclerotic plaques recognize oxidized low density lipoprotein. *Proc Natl Acad Sci U S A.* Apr 25 1995;92(9):3893-3897.

149. Frostegard J, Ulfgren AK, Nyberg P, et al. Cytokine expression in advanced human atherosclerotic plaques: dominance of pro-inflammatory (Th1) and macrophage-stimulating cytokines. *Atherosclerosis.* Jul 1999;145(1):33-43.

150. Hansson GK, Holm J, Jonasson L. Detection of activated T lymphocytes in the human atherosclerotic plaque. *Am J Pathol.* Jul 1989;135(1):169-175.

151. Whitman SC, Ravisankar P, Daugherty A. IFN-gamma deficiency exerts gender-specific effects on atherogenesis in apolipoprotein E-/- mice. *J Interferon Cytokine Res.* Jun 2002;22(6):661-670.

152. Whitman SC, Ravisankar P, Elam H, et al. Exogenous interferon-gamma enhances atherosclerosis in apolipoprotein E-/- mice. *Am J Pathol.* Dec 2000;157(6):1819-1824.

153. Laurat E, Poirier B, Tupin E, et al. In vivo downregulation of T helper cell 1 immune responses reduces atherogenesis in apolipoprotein E-knockout mice. *Circulation.* Jul 10 2001;104(2):197-202.

154. Karvonen J, Paivansalo M, Kesaniemi YA, et al. Immunoglobulin M type of autoantibodies to oxidized low-density lipoprotein has an inverse relation to carotid artery atherosclerosis. *Circulation.* Oct 28 2003;108(17):2107-2112.

155. Robinette CD, Fraumeni JF, Jr. Splenectomy and subsequent mortality in veterans of the 1939-45 war. *Lancet.* Jul 16 1977;2(8029):127-129.

156. Lindstedt KA, Mayranpaa MI, Kovanen PT. Mast cells in vulnerable atherosclerotic plaques--a view to a kill. *J Cell Mol Med.* Jul-Aug 2007;11(4):739-758.

157. Bot I, de Jager SC, Zernecke A, et al. Perivascular mast cells promote atherogenesis and induce plaque destabilization in apolipoprotein E-deficient mice. *Circulation*. May 15 2007;115(19):2516-2525.

158. Sun J, Sukhova GK, Wolters PJ, et al. Mast cells promote atherosclerosis by releasing proinflammatory cytokines. *Nat Med*. Jun 2007;13(6):719-724.

159. Lee M, Calabresi L, Chiesa G, et al. Mast cell chymase degrades apoE and apoA-II in apoA-I-knockout mouse plasma and reduces its ability to promote cellular cholesterol efflux. *Arterioscler Thromb Vasc Biol*. Sep 1 2002;22(9):1475-1481.

160. Barksby HE, Lea SR, Preshaw PM, et al. The expanding family of interleukin-1 cytokines and their role in destructive inflammatory disorders. *Clin Exp Immunol*. Aug 2007;149(2):217-225.

161. Arend WP, Palmer G, Gabay C. IL-1, IL-18, and IL-33 families of cytokines. *Immunol Rev*. Jun 2008;223:20-38.

162. Gracie JA, Forsey RJ, Chan WL, et al. A proinflammatory role for IL-18 in rheumatoid arthritis. *J Clin Invest*. Nov 1999;104(10):1393-1401.

163. Matsui K, Yoshimoto T, Tsutsui H, et al. Propionibacterium acnes treatment diminishes CD4+ NK1.1+ T cells but induces type I T cells in the liver by induction of IL-12 and IL-18 production from Kupffer cells. *J Immunol*. Jul 1 1997;159(1):97-106.

164. Pizarro TT, Michie MH, Bentz M, et al. IL-18, a novel immunoregulatory cytokine, is up-regulated in Crohn's disease: expression and localization in intestinal mucosal cells. *J Immunol*. Jun 1 1999;162(11):6829-6835.

165. Prinz M, Hanisch UK. Murine microglial cells produce and respond to interleukin-18. *J Neurochem*. May 1999;72(5):2215-2218.

166. Stoll S, Jonuleit H, Schmitt E, et al. Production of functional IL-18 by different subtypes of murine and human dendritic cells (DC): DC-derived IL-18 enhances IL-12-dependent Th1 development. *Eur J Immunol*. Oct 1998;28(10):3231-3239.

167. Gu Y, Kuida K, Tsutsui H, et al. Activation of interferon-gamma inducing factor mediated by interleukin-1beta converting enzyme. *Science*. Jan 10 1997;275(5297):206-209.

168. Cheung H, Chen NJ, Cao Z, et al. Accessory protein-like is essential for IL-18-mediated signaling. *J Immunol*. May 1 2005;174(9):5351-5357.

169. Rooney T, Murphy E, Benito M, et al. Synovial tissue interleukin-18 expression and the response to treatment in patients with inflammatory arthritis. *Ann Rheum Dis.* Nov 2004;63(11):1393-1398.

170. Yamada N, Niwa S, Tsujimura T, et al. Interleukin-18 and interleukin-12 synergistically inhibit osteoclastic bone-resorbing activity. *Bone.* Jun 2002;30(6):901-908.

171. Tak PP, Bacchi M, Bertolino M. Pharmacokinetics of IL-18 binding protein in healthy volunteers and subjects with rheumatoid arthritis or plaque psoriasis. *Eur J Drug Metab Pharmacokinet.* Apr-Jun 2006;31(2):109-116.

172. Tedgui A, Mallat Z. Cytokines in atherosclerosis: pathogenic and regulatory pathways. *Physiol Rev.* Apr 2006;86(2):515-581.

173. Elhage R, Jawien J, Rudling M, et al. Reduced atherosclerosis in interleukin-18 deficient apolipoprotein E-knockout mice. *Cardiovasc Res.* Jul 1 2003;59(1):234-240.

174. Whitman SC, Ravisankar P, Daugherty A. Interleukin-18 enhances atherosclerosis in apolipoprotein E(-/-) mice through release of interferon-gamma. *Circ Res.* Feb 8 2002;90(2):E34-38.

175. Schmitz J, Owyang A, Oldham E, et al. IL-33, an interleukin-1-like cytokine that signals via the IL-1 receptor-related protein ST2 and induces T helper type 2-associated cytokines. *Immunity.* Nov 2005;23(5):479-490.

176. Cayrol C, Girard JP. The IL-1-like cytokine IL-33 is inactivated after maturation by caspase-1. *Proc Natl Acad Sci U S A.* Jun 2 2009;106(22):9021-9026.

177. Talabot-Ayer D, Lamacchia C, Gabay C, et al. Interleukin-33 is biologically active independently of caspase-1 cleavage. *J Biol Chem.* Jul 17 2009;284(29):19420-19426.

178. Luthi AU, Cullen SP, McNeela EA, et al. Suppression of interleukin-33 bioactivity through proteolysis by apoptotic caspases. *Immunity.* Jul 17 2009;31(1):84-98.

179. Chackerian AA, Oldham ER, Murphy EE, et al. IL-1 receptor accessory protein and ST2 comprise the IL-33 receptor complex. *J Immunol.* Aug 15 2007;179(4):2551-2555.

180. Towne JE, Garka KE, Renshaw BR, et al. Interleukin (IL)-1F6, IL-1F8, and IL-1F9 signal through IL-1Rrp2 and IL-1RAcP to activate the pathway

leading to NF-kappaB and MAPKs. *J Biol Chem*. Apr 2 2004;279(14):13677-13688.

181. Brint EK, Fitzgerald KA, Smith P, et al. Characterization of signaling pathways activated by the interleukin 1 (IL-1) receptor homologue T1/ST2. A role for Jun N-terminal kinase in IL-4 induction. *J Biol Chem*. Dec 20 2002;277(51):49205-49211.

182. Carriere V, Roussel L, Ortega N, et al. IL-33, the IL-1-like cytokine ligand for ST2 receptor, is a chromatin-associated nuclear factor in vivo. *Proc Natl Acad Sci U S A*. Jan 2 2007;104(1):282-287.

183. Iwahana H, Yanagisawa K, Ito-Kosaka A, et al. Different promoter usage and multiple transcription initiation sites of the interleukin-1 receptor-related human ST2 gene in UT-7 and TM12 cells. *Eur J Biochem*. Sep 1999;264(2):397-406.

184. Bergers G, Reikerstorfer A, Braselmann S, et al. Alternative promoter usage of the Fos-responsive gene Fit-1 generates mRNA isoforms coding for either secreted or membrane-bound proteins related to the IL-1 receptor. *Embo J*. Mar 1 1994;13(5):1176-1188.

185. Thomassen E, Kothny G, Haas S, et al. Role of cell type-specific promoters in the developmental regulation of T1, an interleukin 1 receptor homologue. *Cell Growth Differ*. Feb 1995;6(2):179-184.

186. Tominaga S, Kuroiwa K, Tago K, et al. Presence and expression of a novel variant form of ST2 gene product in human leukemic cell line UT-7/GM. *Biochem Biophys Res Commun*. Oct 14 1999;264(1):14-18.

187. Iwahana H, Hayakawa M, Kuroiwa K, et al. Molecular cloning of the chicken ST2 gene and a novel variant form of the ST2 gene product, ST2LV. *Biochim Biophys Acta*. Nov 24 2004;1681(1):1-14.

188. Kakkar R, Lee RT. The IL-33/ST2 pathway: therapeutic target and novel biomarker. *Nat Rev Drug Discov*. Oct 2008;7(10):827-840.

189. Gachter T, Werenskiold AK, Klemenz R. Transcription of the interleukin-1 receptor-related T1 gene is initiated at different promoters in mast cells and fibroblasts. *J Biol Chem*. Jan 5 1996;271(1):124-129.

190. Sweet MJ, Leung BP, Kang D, et al. A novel pathway regulating lipopolysaccharide-induced shock by ST2/T1 via inhibition of Toll-like receptor 4 expression. *J Immunol*. Jun 1 2001;166(11):6633-6639.

191. Yin H, Huang BJ, Yang H, et al. Pretreatment with soluble ST2 reduces warm hepatic ischemia/reperfusion injury. *Biochem Biophys Res Commun*. Dec 29 2006;351(4):940-946.

192. Leung BP, Xu D, Culshaw S, et al. A novel therapy of murine collagen-induced arthritis with soluble T1/ST2. *J Immunol*. Jul 1 2004;173(1):145-150.

193. Xu D, Jiang HR, Kewin P, et al. IL-33 exacerbates antigen-induced arthritis by activating mast cells. *Proc Natl Acad Sci U S A*. Aug 5 2008;105(31):10913-10918.

194. Lee DM, Friend DS, Gurish MF, et al. Mast cells: a cellular link between autoantibodies and inflammatory arthritis. *Science*. Sep 6 2002;297(5587):1689-1692.

195. Januzzi JL, Jr., Peacock WF, Maisel AS, et al. Measurement of the interleukin family member ST2 in patients with acute dyspnea: results from the PRIDE (Pro-Brain Natriuretic Peptide Investigation of Dyspnea in the Emergency Department) study. *J Am Coll Cardiol*. Aug 14 2007;50(7):607-613.

196. Mueller T, Dieplinger B, Gegenhuber A, et al. Increased plasma concentrations of soluble ST2 are predictive for 1-year mortality in patients with acute destabilized heart failure. *Clin Chem*. Apr 2008;54(4):752-756.

197. Weinberg EO, Shimpo M, De Keulenaer GW, et al. Expression and regulation of ST2, an interleukin-1 receptor family member, in cardiomyocytes and myocardial infarction. *Circulation*. Dec 3 2002;106(23):2961-2966.

198. Shimpo M, Morrow DA, Weinberg EO, et al. Serum levels of the interleukin-1 receptor family member ST2 predict mortality and clinical outcome in acute myocardial infarction. *Circulation*. May 11 2004;109(18):2186-2190.

199. Miller AM, Xu D, Asquith DL, et al. IL-33 reduces the development of atherosclerosis. *J Exp Med*. Feb 11 2008.

200. Sanada S, Hakuno D, Higgins LJ, et al. IL-33 and ST2 comprise a critical biomechanically induced and cardioprotective signaling system. *J Clin Invest*. Jun 2007;117(6):1538-1549.

201. Rangel-Moreno J, Hartson L, Navarro C, et al. Inducible bronchus-associated lymphoid tissue (iBALT) in patients with pulmonary complications of rheumatoid arthritis. *J Clin Invest*. Dec 2006;116(12):3183-3194.

202. O'Connell KA, Edidin M. A mouse lymphoid endothelial cell line immortalized by simian virus 40 binds lymphocytes and retains functional characteristics of normal endothelial cells. *J Immunol*. Jan 15 1990;144(2):521-525.

203. Ahuja A, Shupe J, Dunn R, et al. Depletion of B cells in murine lupus: efficacy and resistance. *J Immunol*. Sep 1 2007;179(5):3351-3361.

204. Wolfe F, Freundlich B, Straus WL. Increase in cardiovascular and cerebrovascular disease prevalence in rheumatoid arthritis. *J Rheumatol*. Jan 2003;30(1):36-40.

205. Klareskog L, Catrina AI, Paget S. Rheumatoid arthritis. *Lancet*. 2009;373(9664):659-672.

206. Vossenaar ER, Smeets TJ, Kraan MC, et al. The presence of citrullinated proteins is not specific for rheumatoid synovial tissue. *Arthritis Rheum*. Nov 2004;50(11):3485-3494.

207. Nakayama-Hamada M, Suzuki A, Kubota K, et al. Comparison of enzymatic properties between hPADI2 and hPADI4. *Biochem Biophys Res Commun*. Feb 4 2005;327(1):192-200.

208. Hollan I, Scott H, Saatvedt K, et al. Inflammatory rheumatic disease and smoking are predictors of aortic inflammation: a controlled study of biopsy specimens obtained at coronary artery surgery. *Arthritis Rheum*. Jun 2007;56(6):2072-2079.

209. Schwartz CJ, Mitchell JR. Cellular infiltration of the human arterial adventitia associated with atheromatous plaques. *Circulation*. Jul 1962;26:73-78.

210. Parums D, Mitchinson MJ. Demonstration of immunoglobulin in the neighbourhood of advanced atherosclerotic plaques. *Atherosclerosis*. Jan-Feb 1981;38(1-2):211-216.

211. Galkina E, Kadl A, Sanders J, et al. Lymphocyte recruitment into the aortic wall before and during development of atherosclerosis is partially L-selectin dependent. *J Exp Med*. May 15 2006;203(5):1273-1282.

212. Grabner R, Lotzer K, Dopping S, et al. Lymphotoxin beta receptor signaling promotes tertiary lymphoid organogenesis in the aorta adventitia of aged ApoE-/- mice. *J Exp Med*. Jan 16 2009;206(1):233-248.

213. Aubry MC, Riehle DL, Edwards WD, et al. B-Lymphocytes in plaque and adventitia of coronary arteries in two patients with rheumatoid arthritis and coronary atherosclerosis: preliminary observations. *Cardiovasc Pathol*. Jul-Aug 2004;13(4):233-236.

214. Hollan I, Prayson R, Saatvedt K, et al. Inflammatory cell infiltrates in vessels with different susceptibility to atherosclerosis in rheumatic and non-rheumatic patients: a controlled study of biopsy specimens obtained at coronary artery surgery. *Circ J*. Dec 2008;72(12):1986-1992.

215. Watanabe M, Sangawa A, Sasaki Y, et al. Distribution of inflammatory cells in adventitia changed with advancing atherosclerosis of human coronary artery. *J Atheroscler Thromb*. Dec 2007;14(6):325-331.

216. Danesh J, Wheeler JG, Hirschfield GM, et al. C-reactive protein and other circulating markers of inflammation in the prediction of coronary heart disease. *N Engl J Med*. Apr 1 2004;350(14):1387-1397.

217. Klareskog L, Ronnelid J, Lundberg K, et al. Immunity to citrullinated proteins in rheumatoid arthritis. *Annu Rev Immunol*. 2008;26:651-675.

218. Ferro M, Conti M, Novero D, et al. [Incidence of atherosclerosis of the internal mammary artery compared with the coronary artery. A study of 22 non-selected autopsy cases]. *Minerva Cardioangiol*. Jul-Aug 1990;38(7-8):325-330.

219. Molin DG, Post MJ. Do intrinsic arterial wall features determine atherosclerosis susceptibility? *Cardiovasc Res*. Oct 1 2006;72(1):3-4.

220. Kuchler AM, Pollheimer J, Balogh J, et al. Nuclear interleukin-33 is generally expressed in resting endothelium but rapidly lost upon angiogenic or proinflammatory activation. *Am J Pathol*. Oct 2008;173(4):1229-1242.

221. Ribatti D, Levi-Schaffer F, Kovanen PT. Inflammatory angiogenesis in atherogenesis--a double-edged sword. *Ann Med*. 2008;40(8):606-621.

222. Lorelius LE. Arterial vasoconstriction: a possible pathogenetic factor in the process of atherosclerosis. *Med Hypotheses*. Mar 1980;6(3):297-302.

223. Haraldsen G, Balogh J, Pollheimer J, et al. Interleukin-33 - cytokine of dual function or novel alarmin? *Trends Immunol*. May 2009;30(5):227-233.

224. Palinski W, Yla-Herttuala S, Rosenfeld ME, et al. Antisera and monoclonal antibodies specific for epitopes generated during oxidative modification of low density lipoprotein. *Arteriosclerosis*. May-Jun 1990;10(3):325-335.

225. Kues WA, Anger M, Carnwath JW, et al. Cell cycle synchronization of porcine fetal fibroblasts: effects of serum deprivation and reversible cell cycle inhibitors. *Biol Reprod*. Feb 2000;62(2):412-419.

226. Jarvilehto M, Tuohimaa P. Vasa vasorum hypoxia: initiation of atherosclerosis. *Med Hypotheses*. Jul 2009;73(1):40-41.

227. Graven KK, Troxler RF, Kornfeld H, et al. Regulation of endothelial cell glyceraldehyde-3-phosphate dehydrogenase expression by hypoxia. *J Biol Chem*. Sep 30 1994;269(39):24446-24453.

228. Emery P, Fleischmann R, Filipowicz-Sosnowska A, et al. The efficacy and safety of rituximab in patients with active rheumatoid arthritis despite methotrexate treatment: results of a phase IIB randomized, double-blind, placebo-controlled, dose-ranging trial. *Arthritis Rheum*. May 2006;54(5):1390-1400.

229. Cohen SB, Emery P, Greenwald MW, et al. Rituximab for rheumatoid arthritis refractory to anti-tumor necrosis factor therapy: Results of a multicenter, randomized, double-blind, placebo-controlled, phase III trial evaluating primary efficacy and safety at twenty-four weeks. *Arthritis Rheum*. Sep 2006;54(9):2793-2806.

230. Tedder TF, Engel P. CD20: a regulator of cell-cycle progression of B lymphocytes. *Immunol Today*. Sep 1994;15(9):450-454.

231. Breedveld F, Agarwal S, Yin M, et al. Rituximab pharmacokinetics in patients with rheumatoid arthritis: B-cell levels do not correlate with clinical response. *J Clin Pharmacol*. Sep 2007;47(9):1119-1128.

232. Hansson GK. The B cell: a good guy in vascular disease? *Arterioscler Thromb Vasc Biol*. Apr 1 2002;22(4):523-524.

233. Zhang SH, Reddick RL, Piedrahita JA, et al. Spontaneous hypercholesterolemia and arterial lesions in mice lacking apolipoprotein E. *Science*. Oct 16 1992;258(5081):468-471.

234. Plump AS, Breslow JL. Apolipoprotein E and the apolipoprotein E-deficient mouse. *Annu Rev Nutr*. 1995;15:495-518.

235. Nakashima Y, Plump AS, Raines EW, et al. ApoE-deficient mice develop lesions of all phases of atherosclerosis throughout the arterial tree. *Arterioscler Thromb*. Jan 1994;14(1):133-140.

236. Beers SA, Chan CH, James S, et al. Type II (tositumomab) anti-CD20 monoclonal antibody out performs type I (rituximab-like) reagents in B-cell depletion regardless of complement activation. *Blood*. Nov 15 2008;112(10):4170-4177.

237. Brummel R, Lenert P. Activation of marginal zone B cells from lupus mice with type A(D) CpG-oligodeoxynucleotides. *J Immunol*. Feb 15 2005;174(4):2429-2434.

238. Lenert P, Brummel R, Field EH, et al. TLR-9 activation of marginal zone B cells in lupus mice regulates immunity through increased IL-10 production. *J Clin Immunol*. Jan 2005;25(1):29-40.

239. Ng LG, Ng CH, Woehl B, et al. BAFF costimulation of Toll-like receptor-activated B-1 cells. *Eur J Immunol*. Jul 2006;36(7):1837-1846.

240. Martin F, Oliver AM, Kearney JF. Marginal zone and B1 B cells unite in the early response against T-independent blood-borne particulate antigens. *Immunity*. May 2001;14(5):617-629.

241. Ross R. Atherosclerosis is an inflammatory disease. *Am Heart J*. Nov 1999;138(5 Pt 2):S419-420.

242. Hansson GK, Libby P, Schonbeck U, et al. Innate and adaptive immunity in the pathogenesis of atherosclerosis. *Circ Res*. Aug 23 2002;91(4):281-291.

243. Binder CJ, Chang MK, Shaw PX, et al. Innate and acquired immunity in atherogenesis. *Nat Med*. Nov 2002;8(11):1218-1226.

244. Sfikakis PP, Souliotis VL, Fragiadaki KG, et al. Increased expression of the FoxP3 functional marker of regulatory T cells following B cell depletion with rituximab in patients with lupus nephritis. *Clin Immunol*. Apr 2007;123(1):66-73.

245. Bouaziz JD, Yanaba K, Venturi GM, et al. Therapeutic B cell depletion impairs adaptive and autoreactive CD4+ T cell activation in mice. *Proc Natl Acad Sci U S A*. Dec 26 2007;104(52):20878-20883.

246. Scapini P, Nardelli B, Nadali G, et al. G-CSF-stimulated neutrophils are a prominent source of functional BLyS. *J Exp Med*. Feb 3 2003;197(3):297-302.

247. Tan SM, Xu D, Roschke V, et al. Local production of B lymphocyte stimulator protein and APRIL in arthritic joints of patients with inflammatory arthritis. *Arthritis Rheum*. Apr 2003;48(4):982-992.

248. Kavanaugh A, Rosengren S, Lee SJ, et al. Assessment of rituximab's immunomodulatory synovial effects (ARISE trial). 1: clinical and synovial biomarker results. *Ann Rheum Dis*. Mar 2008;67(3):402-408.

249. Leandro MJ, Cambridge G, Ehrenstein MR, et al. Reconstitution of peripheral blood B cells after depletion with rituximab in patients with rheumatoid arthritis. *Arthritis Rheum*. Feb 2006;54(2):613-620.

Appendix

1. Immunohistochemistry reagents

a) Peroxidase block:	5 ml 30% Hydrogen peroxide (H_2O_2) in 295 ml of methanol
b) Citrate buffer:	2.1 g Citric acid monohydrate dissolved in 1000 ml of distilled water (pH 6)
c) Tris buffered saline (TBS)	6.05 g Tris base (50 mM), 8.76 g sodium chloride (150 mM) to 800 ml of distilled water. Adjust pH to 7.5 with HCl. Adjust to 1 litre with distilled water. Add Tween-20 to 0.1% (v/v). Stored for up to 3 months at room temperature.
d) 10x Phosphate buffered saline	80 g NaCl, 2 g KCl, 11.5 g$Na_2HPO_4 7H_2O$ and 2 g KH_2PO_4 to 1 litre distilled water (pH 7.4) 10x stock.
e) Trypsin solution:	Trypsin 0.5%, 1% calcium chloride solution and pH adjusted to 7.8 with 1N NaOH.
f) SDS-PAGE Lysis buffer	62.5 mM Tris-HCl (pH 6.8), 2% SDS, 5% 2-mecaptoethanol, 10% glycerol.
g) FACS buffer	3% BSA and 0.05% NaN_3 in 1x PBS

2. Western blotting reagents

a) 20x MES SDS running buffer:	The 500 ml contains 97.6 g of MES, 60.6 g Tris Base, 10 g SDS and 3 g of EDTA.

b) 20x NuPAGE transfer buffer:	The 125 ml contains 10.2 g of Bicine, 13.1 g Bis-Tris (free base) and 0.75 g EDTA
c) 4x LDS sample buffer:	10 ml contains 0.66 g of Tris HCl, 0.62 g Tris Base, 0.8 g LDS, 0.006 g EDTA, 4 g Glycerol, 0.75 ml 1% bromophenol and 0.25 ml of Phenol red.
d) Fixative solution:	60% reagent alcohol (95% ethanol, 5% methanol) 30% glacial acetic acid.

3. Lipoprotein isolation reagents.

a) 1.006 density solution	10.07 g/L NaBr, 0.37 g EDTA in distilled water pH 7.4
b) 1.020 density solution	28.31 g/L NaBr, 0.37 g EDTA in distilled water pH 7.4
c) 1.063 density solution	84.98 g/L NaBr, 0.37 g EDTA in distilled water pH 7.4
d) 1.21 density solution	283.32 g/L NaBr, 0.37 g EDTA in distilled water pH 7.4
e) Copper reagent	20 gm sodium carbonate, 0.4 gm cupric sulphate pentahydrate and 0.2 gm sodium

4. Lipoprotien (Lipo) Electrophoresis reagents

a) LIPO gel	0.5% Agarose gel.
b) B-2 Barbital buffer:	18.2 g (5, 5-Diethylbarbituric Acid), 10mmol/L reconstituted; 5, 5-Diethylbarbituric Acid sodium salt 50mmol/L.
c) Paragon lipostain:	Sudan Black B stain, 7% (W/W). The working Lipo stain was prepared by adding 3 ml of Lipostain to 165 ml of reagent alcohol.
d) Reagent alcohol:	95% ethanol denatured with methanol.
e) Fixative solution:	180 ml reagent alcohol, 90 ml deionised water, 30 ml of Glacial acetic acid.
f) Destain solution:	450 ml of reagent alcohol, 550 ml of deionised water.

5. **Mouse genotyping buffers**

a) Alkaline lysis buffer:	25 mMol sodium hydroxide (NaOH), 0.2 mMol EDTA (pH 12).
b) Neutralizing buffer:	40 mMol Tris (pH 5).

6. Primers for quantitative PCR

a) Human Primers:

Human GAPDH	Forward 5’ ACAGTCAGCCGCATCTTCTT 3’
(Annealing Temp: 55^0C)	Reverse 5’ AAATGAGCCCCAGCCTTCT 3’

Human IL-33	Forward 5’ CCATTACTTTTGCTTTGGAGGA 3’
(Annealing Temp: 56^0C)	Reverse 5’ TTACCATCAACACCGTCACC 3’
Human sST2	Forward 5’ AGCTGACGTGAAGGAAGAGG 3’
(Annealing Temp: 58^0C)	Reverse 5’ GCCATTCCCATTGTCTTGATG 3’

b) Mouse Primer:

Murine GAPDH (inner)	Forward 5’ CAGCAAGGACACTGAGCAAG 3’
	Reverse 5’ TATTATGGGGGTCTGGGATG 3’
Murine GAPDH (outer)	Forward 5’ TGTCTCCTGCGACTTCAA 3’
(Annealing Temp: 55^0C)	Reverse 5’ TGCAGCGAACTTTATTGATG 3’
Murine β Actin (inner)	Forward 5’ CGTTGACATCCGTAAAGACC 3’
	Reverse 5’ CTGGAAGGTGGACAGTGAG 3’
Murine β Actin (outer)	Forward 5’ GCTCTTTTCCAGCCTTCCTT 3’
(Annealing Temp: 55^0C)	Reverse 5’ GCTCAGTAACAGTCCGCCTA 3’
Murine IL-33 (inner)	Forward 5’ CCTGGTCTTGCTCTTGGTCT 3’
	Reverse 5’ AGTCTCCTGCCTCCCTGAGT 3’
Murine IL-33 (outer)	Forward 5’ CAGCACCGCAGGCGAAGCCC 3’
(Annealing Temp: 59^0C)	Reverse 5’ TATGTACTCAGGGAGGCAGG 3’
Murine sST2 (inner)	Forward 5’ GACCCCCTTCTCTCTTTTCC 3’

	Reverse 5’ TGCTCTGAACCCACTACCAA 3’
Murine sST2 (outer)	Forward 5’ TGGCATGATAAGGCACACCATAAGGCT
(Annealing Temp: 55^0C)	Reverse 5’ GTTAGTGTCTCTCTCCCTCCCATGC 3’
Murine APRIL (inner)	Forward 5’ ATGCCAGCCTCATCTCCA 3’
	Reverse 5’ GCGACAGCACAAGTCACAG 3’
Murine APRIL (outer)	Forward 5’ GTAACCCGCTCTTCCCTTCT 3’
(Annealing Temp: 62^0C)	Reverse 5’ CAGGACATCAGGACTCTGCTC 3’
Murine BAFF (outer)	Forward 5’ TGCCTTGGAGGAGAAAGAGA 3’
(Annealing Temp: 60^0C)	Reverse 5’ GGAATTGTTGGGCAGTGTTT 3’
Murine SK-1 (outer)	Forward 5’ AGGTGGTGAATGGGCTAATG 3’
(Annealing Temp: 60^0C)	Reverse 5’ CCAGAGGAACAAGGTGTGTG 3’
Murine SK-1 (inner)	Forward 5’ CGAGCAGGTGACTAATGAAGA 3’
	Reverse 5’ GCAGCCCAGAAGCAGTGT 3’

7) Murine Primers for genotyping:

Four sets of primers were used for genotyping of HumanCD20 (hCD20) transgenic mice.

1) **hCd20 Exon2 region**	Forward 5’ CACAAGGTAAGACTGCCAAAAATC 3’
	Reverse 5’ ATATACAAGCCCCAAAACCAAAAG 3’

2) **hCD20 3'UTR region** Forward 5' GGCCTTTGCATGGAGTGAC 3'

Reverse 5' AGCCCTGTAGAAAGATAAATGGA 3'

3) **hCD20 5' region BAC** Forward 5' ATTGTTTGAGTGCTCAGCATG 3'

Reverse 5' GGGAAAAACAATATTGCCTCC 3'

4) **hCD20 3' region BAC** Forward 5' GTTGGAGGTTCTGGTTGCAT 3'

Reverse 5' AATTGGCTTAGGATTGGGCT 3'

Three sets of primers were used for genotyping of **Apo E knock out mice**.

1) **ApoE IMR0180** Forward 5' GCCTAGCCGAGGGAGAGCCG 3'

2) **ApoE IMR0181** Reverse 5' TGTGACTTGGGAGCTCTGCAGC 3'

3) **ApoE IMR0182** Reverse 5' GCCGCCCCGACTGCATCT 3'